

Dudley Knox Library, NPS
Monterey, CA 93943

NAVAL POSTGRADUATE SCHOOL

Monterey, California



THESIS

BANK-TO-TURN CRUISE MISSILE TERMINAL
GUIDANCE AND CONTROL LAW COMPARISON

by

Kent B. Watterson

June 1983

Thesis Advisor:

Marle D. Hewett

Approved for public release, distribution unlimited

T208979

REPORT DOCUMENTATION PAGE		READ INSTRUCTIONS BEFORE COMPLETING FORM
1. REPORT NUMBER	2. GOVT ACCESSION NO.	3. RECIPIENT'S CATALOG NUMBER
4. TITLE (and Subtitle) Bank-To-Turn Cruise Missile Terminal Guidance and Control Law Comparison		5. TYPE OF REPORT & PERIOD COVERED Master's Thesis June 1983
		6. PERFORMING ORG. REPORT NUMBER
7. AUTHOR(s) Kent B. Watterson		8. CONTRACT OR GRANT NUMBER(s)
9. PERFORMING ORGANIZATION NAME AND ADDRESS Naval Postgraduate School Monterey, California 93940		10. PROGRAM ELEMENT, PROJECT, TASK AREA & WORK UNIT NUMBERS
11. CONTROLLING OFFICE NAME AND ADDRESS Naval Postgraduate School Monterey, California 93940		12. REPORT DATE June 1983
		13. NUMBER OF PAGES 189
14. MONITORING AGENCY NAME & ADDRESS (if different from Controlling Office)		15. SECURITY CLASS. (of this report)
		15a. DECLASSIFICATION/DOWNGRADING SCHEDULE
16. DISTRIBUTION STATEMENT (of this Report) Approved for public release, distribution unlimited		
17. DISTRIBUTION STATEMENT (of the abstract entered in Block 20, if different from Report)		
18. SUPPLEMENTARY NOTES		
19. KEY WORDS (Continue on reverse side if necessary and identify by block number) Bank-To-Turn Terminal Homing Proportional Navigation Guidance and Control		
20. ABSTRACT (Continue on reverse side if necessary and identify by block number) This work consists of the development of the six degree of freedom non-linear model of a sea launched generic bank-to-turn cruise missile attacking a medium sized combatant ship. Two guidance and control schemes are compared in the terminal phase. The first, or baseline guidance scheme (pop out maneuver), uses a 50-foot altitude hold for an ingress phase, followed by a pop out maneuver, and then an attack phase which uses proportional		

20. ABSTRACT (cont'd)

navigation in elevation and azimuth planes along with bank-to-turn maneuvering. The second scheme (sea skimmer) uses identical ingress and attack phases but eliminates the pop out maneuver. Miss distances for both schemes are compared while varying missile roll rate limit, ECM blinking frequency, and burn through ranges.

Approved for public release, distribution unlimited

Bank-To-Turn Cruise Missile Terminal
Guidance and Control Law Comparison

by

Kent B. Watterson
Lieutenant Commander, United States Navy
B.S., Findlay College, 1969

Submitted in partial fulfillment of the
requirements for the degree of

MASTER OF SCIENCE IN ENGINEERING SCIENCE

from the

NAVAL POSTGRADUATE SCHOOL
June 1983

ABSTRACT

This work consists of the development of the six degree of freedom non linear model of a sea launched generic bank-to-turn cruise missile attacking a medium sized combatant ship. Two guidance and control schemes are compared in the terminal phase. The first, or baseline guidance scheme (pop out maneuver), uses a 50-foot altitude hold for an ingress phase, followed by a pop out maneuver, and then an attack phase which uses proportional navigation in elevation and azimuth planes along with bank-to-turn maneuvering. The second scheme (sea skimmer) uses identical ingress and attack phases but eliminates the pop out maneuver. Miss distances for both schemes are compared while varying missile roll rate limit, ECM blinking frequency, and burn through ranges.

TABLE OF CONTENTS

I.	INTRODUCTION	17
II.	DEVELOPMENT AND SIMULATION OF MISSILE DYNAMICS . . .	20
A.	MISSILE EQUATIONS OF MOTION	20
1.	Assumptions	21
2.	Coordinate System	23
3.	The Equations of Motion	23
4.	Trim Equations	26
5.	Other Useful Relations	27
6.	Definition of Controls and Control Limits .	27
B.	AERODYNAMIC COEFFICIENT BUILD UP	29
1.	Definition of Coefficients	29
2.	Coefficient Build Up	30
C.	MISSILE LINEARIZED EQUATIONS OF MOTION	32
1.	Additional Assumptions for Linearized Equations	32
2.	Linearized Equations Summarized	33
3.	Definition of Stability Derivatives	34
4.	Trim Equations	36
III.	DEVELOPMENT AND SIMULATION OF THE MISSILE AUTOPILOT.	37
A.	AUTOPILOT INNER LOOP REQUIREMENTS AND DESIGNS .	37
1.	Description of the Autopilot Inner Loops . .	37
2.	Normal Acceleration Command System	39
3.	Bank Angle Command System	44
4.	Turn Coordinator	49
B.	AUTOPILOT OUTER LOOP REQUIREMENTS AND DESIGNS .	57

1.	Description	57
2.	Vertical Flight Path Angle System	57
3.	Altitude Hold System	58
IV.	DEVELOPMENT AND SIMULATION OF MISSILE GUIDANCE	
	SYSTEM	63
A.	MISSION DESCRIPTION	64
1.	Baseline Guidance Scheme (Pop Out Maneuver)	64
2.	Alternate Guidance Scheme (Sea Skimmer)	65
3.	Electronic Counter Measures (ECM)	65
4.	Glint	68
B.	SEEKER EQUATIONS AND SIMULATION	68
1.	Line of Sight Rates	68
2.	Missile Dynamic Filters	73
C.	BASELINE GUIDANCE LAW DESIGN (POP OUT MANEUVER)	73
1.	Attack Phase	73
2.	Ingress Phase	78
3.	Offset Phase	80
4.	Pop Up Phase	81
5.	Guidance Summary (Baseline)	83
D.	ALTERNATE GUIDANCE LAW DESIGN (SEA SKIMMER)	83
1.	Ingress Phase	83
2.	Attack Phase	84
3.	Guidance Summary (Sea Skimmer)	85
V.	PROBLEM SIMULATION, RESULTS, CONCLUSIONS AND	
	RECOMMENDATIONS	86
A.	CSMP SIMULATION	86
B.	RESULTS	88

1. Analysis of Base Line Scheme Results	92
2. Analysis of Sea Skimmer Scheme Results . . .	129
3. Analysis of Glint Simulation Results	129
4. Proportional Navigation Ratio Selection . .	132
C. CONCLUSIONS AND RECOMMENDATIONS	132
APPENDIX A: AERODYNAMIC COEFFICIENTS	134
APPENDIX B: STEADY STATE DATA	151
APPENDIX C: AUTOPILOT ROOT LOCUS PLOTS	153
APPENDIX D: BASELINE GUIDANCE LAW SIMULATION	166
APPENDIX E: SEA SKIMMER GUIDANCE LAW SIMULATION	176
LIST OF REFERENCES	187
INITIAL DISTRIBUTION LIST	188

LIST OF TABLES

2-1 Longitudinal Equations (Perturbed Variables)	34
2-2 Lateral Directional Equations (Perturbed Variables).	34
3-1 Autopilot Inner Loop Description	38
5-1 Baseline Guidance and Control Scheme	90
5-2 Sea Skimmer Guidance and Control Scheme	91

LIST OF FIGURES

2-1	Missile System Flow Diagram	22
2-2	Body Coordinate System Description	25
3-1	Normal Acceleration Command Autopilot Description .	40
3-2	Normal Acceleration Command Autopilot Block Diagram (Analysis)	42
3-3	NAC Autopilot Response to 1g Commanded Load Factor.	45
3-4	Bank Angle Command Autopilot Description	46
3-5	BAC Autopilot Response to 60° Commanded Bank Angle (PHI Response)	50
3-6	BAC Autopilot Response to 60° Commanded Bank Angle (Altitude Response)	51
3-7	Turn Coordinator Autopilot Description	52
3-8	Turn Coordinator Autopilot Block Diagram (Analysis)	55
3-9	System Response to 8.6° Commanded Vertical Flight Path Angle	59
3-10	System Response to 50 Ft. Altitude Hold Command .	62
4-1	Baseline Guidance Scheme Flight Profile	66
4-2	Sea Skimmer Guidance Scheme Flight Profile	67
4-3	Seeker Simulation Flow Chart	69
4-4	Azimuth Line of Sight Description	71
4-5	Elevation Line of Sight Description	72
4-6	Baseline Guidance Law Flow Diagram	74
4-7	Load Factor and Bank Angle Description	76
5-1a	Baseline Response for No ECM, Roll Rate Limit 100 deg/sec (PHICMD, PHI vs TIME)	93

5-1b	Baseline Response for No ECM, Roll Rate Limit 100 deg/sec (PCMD, P vs TIME)	94
5-1c	Baseline Response for No ECM, Roll Rate Limit 100 deg/sec (RANGE, XRANGE, YRANGE, ZRANGE vs TIME)	95
5-1d	Baseline Response for No ECM, Roll Rate Limit 100 deg/sec (L STAB, R STAB vs TIME)	96
5-1e	Baseline Response for No ECM, Roll Rate Limit 100 deg/sec (RUDDER vs TIME)	97
5-1f	Baseline Response for No ECM, Roll Rate Limit 100 deg/sec (YMISLE, HMISLE vs XMISLE).	98
5-2a	Baseline Response for ECM 1 CPS, Roll Rate Limit 100 deg/sec (PCMD,P vs TIME)	99
5-2b	Baseline Response for ECM 1 CPS, Roll Rate Limit 100 deg/sec (PHICMD, PHI vs TIME)	100
5-2c	Baseline Response for ECM 1 CPS, Roll Rate Limit 100 deg/sec (RANGE, XRANGE, YRANGE, ZRANGE, vs TIME)	101
5-2d	Baseline Response for ECM 1 CPS, Roll Rate Limit 100 deg/sec (L STAB, R STAB vs TIME)	102
5-2e	Baseline Response for ECM 1 CPS, Roll Rate Limit 100 deg/sec (RUDDER vs TIME)	103
5-2f	Baseline Response for ECM 1 CPS, Roll Rate Limit 100 deg/sec (YMISLE, HMISLE vs XMISLE)	104
5-3a	Baseline Response for ECM 1 CPS, Roll Rate Limit 50 deg/sec (PCMD,P vs TIME)	105

5-3b	Baseline Response for ECM 1 CPS, Roll Rate Limit 50 deg/sec (PHICMD, PHI vs TIME)	106
5-3c	Baseline Response for ECM 1 CPS, Roll Rate Limit 50 deg/sec (RANGE, XRANGE, YRANGE, ZRANGE vs TIME)	107
5-3d	Baseline Response for ECM 1 CPS, Roll Rate Limit 50 deg/sec (L STAB, R STAB vs TIME)	108
5-3e	Baseline Response for ECM 1 CPS, Roll Rate Limit 50 deg/sec (RUDDER vs TIME)	109
5-3f	Baseline Response for ECM 1 CPS, Roll Rate Limit 50 deg/sec (YMISLE, HMISLE, vs. XMISLE)	110
5-4a	Baseline Response for ECM 1 CPS, Roll Rate Limit 200 deg/sec (PCMD, P vs TIME)	111
5-4b	Baseline Response for ECM 1 CPS, Roll Rate Limit 200 deg/sec (PHICMD, PHI vs TIME)	112
5-4c	Baseline Response for ECM 1 CPS, Roll Rate Limit 200 deg/sec (RANGE, XRANGE, YRANGE, ZRANGE vs TIME)	113
5-4d	Baseline Response for ECM 1 CPS, Roll Rate Limit 200 deg/sec (L STAB, R STAB vs TIME)	114
5-4e	Baseline Response for ECM 1 CPS, Roll Rate Limit 200 deg/sec (RUDDER vs TIME)	115
5-4f	Baseline Response for ECM 1 CPS, Roll Rate Limit 200 deg/sec (YMISLE, HMISLE vs XMISLE)	116
5-5a	Sea Skimmer Response for No ECM, Roll Rate Limit 100 deg/sec (PCMD, P vs TIME)	117

5-5b	Sea Skimmer Response for No ECM, Roll Rate Limit 100 deg/sec (PHICMD, PHI vs TIME)	118
5-5c	Sea Skimmer Response for No ECM, Roll Rate Limit 100 deg/sec (RANGE, XRANGE, YRANGE, ZRANGE vs TIME)	119
5-5d	Sea Skimmer Response for No ECM, Roll Rate Limit 100 deg/sec (L STAB, R STAB vs TIME)	120
5-5e	Sea Skimmer Response for No ECM, Roll Rate Limit 100 deg/sec (RUDDER vs TIME)	121
5-5f	Sea Skimmer Response for No ECM, Roll Rate Limit 100 deg/sec (YMISLE, HMISLE vs XMISLE)	122
5-6a	Sea Skimmer Response for ECM 1 CPS, Roll Rate Limit 100 deg/sec (PCMD,P vs TIME)	123
5-6b	Sea Skimmer Response for ECM 1 CPS, Roll Rate Limit 100 deg/sec (PHICMD,PHI vs TIME)	124
5-6c	Sea Skimmer Response for ECM 1 CPS, Roll Rate Limit 100 deg/sec (RANGE, XRANGE, YRANGE, ZRANGE vs TIME)	125
5-6d	Sea Skimmer Response for ECM 1 CPS, Roll Rate Limit 100 deg/sec (L STAB, R STAB vs TIME)	126
5-6e	Sea Skimmer Response for ECM 1 CPS, Roll Rate Limit 100 deg/sec (RUDDER vs TIME)	127
5-6f	Sea Skimmer Response for ECM 1 CPS, Roll Rate Limit 100 deg/sec (YMISLE, HMISLE vs X MISLE)	128
5-7a	Baseline Response with Glint (SYT,THETAT vs TIME)	130
5-7b	Baseline Response with Glint (XT,YT vs TIME)	131

SYMBOLS AND ABBREVIATIONS

U	Linear Velocity along body x axis
V	Linear Velocity along body y axis
W	Linear Velocity along body z axis
P	Roll rate
Q	Pitch rate
R	Yaw rate
X	Aerodynamic force in body x direction
Y	Aerodynamic force in body y direction
Z	Aerodynamic force in body z direction
Φ	Bank angle
Θ	Pitch angle
Ψ	Yaw angle
X_E	Earth coordinate of missile (Latitude)
Y_E	Earth coordinate of missile (-Longitude)
$-Z_E = H_E$	Earth coordinate of missile (Altitude)
L_A	Rolling Moment about x axis (Aerodynamic)
M_A	Pitching moment about y axis (Aerodynamic)
N_A	Pitching moment about z axis (Aerodynamic)
V_T	Total missile velocity
T	Thrust
\bar{q}	Dynamic pressure ($\frac{1}{2} \rho V_T^2$)
α	Angle of attack
β	Side slip angle

γ	Flight path angle ($\theta + \alpha$)
ρ	Air density (0.002377) <i>slug/ft³</i>
S	Wing area (12 ft. ²)
b	Wing span (8.485 ft.)
\bar{c}	Mean aerodynamic chord (1.414 ft.)
η	Elevator Deflection
ξ	Aileron Deflection
ζ	Rudder Deflection
η_L	Left Stabilator Deflection
η_R	Right Stabilator Deflection
L	Lift force
D	Drag force
N	Normal force
C	Chord wise force
m	Missile mass (68.38 slugs)
g	Acceleration due to gravity (32.17 ft/sec ²)
ST	Static coefficient
DYN	Dynamic coefficient
n_z	Normal load factor (body fixed axis system)*
n_y	Lateral load factor (body fixed axis system)*
n_z	Vertical load factor (earth fixed axis system)*
n_y	Horizontal load factor (earth fixed axis system)*
u	Perturbed linear velocity x axis *
v	Perturbed linear velocity y axis *
w	Perturbed linear velocity z axis *

p	Perturbed angular velocity about x axis *
q	Perturbed angular velocity about y axis *
r	Perturbed angular velocity about z axis *
ϕ	Perturbed Euler angle Φ *
θ	Perturbed Euler Angle Θ *
ψ	Perturbed Euler Angle Ψ *
*	Laplace transforms of these variables are shown in capital letters

SUBSCRIPTS

SS	Steady State
E	Earth
B	Body
x,y,z	In body fixed axes
X,Y,Z	In earth fixed axes
T	Due to thrust/Target
A	Due to Aerodynamic Forces
xx,yy,zz	About the axis specified
ST	Steady State
DYN	Dynamic
EL	Elevation
AZ	Azimuth
c	Commanded

ACKNOWLEDGMENT

The author wishes to express his sincere appreciation to Professor M. D. Hewett for his guidance, direction and understanding in completing this work.

I. INTRODUCTION

The relative merits of bank-to-turn versus skid-to-turn missiles have been argued for years. Bank-to-turn missiles which must roll to a commanded bank angle before a lateral acceleration can be commanded in the appropriate direction are inherently slower to respond to target maneuvering than skin-to-turn missiles of comparable lateral acceleration capabilities. This is particularly true if the bank-to-turn missile has limited roll authority or limited roll rate capability. On the other hand, as discussed in Gonzalez, {Ref. 1}, it is sometimes difficult to build a skid-to-turn missile which meets certain operational goals and performance criteria and also has sufficient control authority in both the y and z directions to generate the large lateral accelerations required to perform skid-to-turn.

In this thesis the terminal guidance accuracy of a bank-to-turn cruise missile is studied for a sea launched, sea target cruise missile of conventional wing-tail configuration. It is assumed that roll authority is extremely limited due to operational design restrictions which impose the use of low authority ailerons or differential stabilator (no ailerons) for rolling. Lateral acceleration is also assumed to be extremely limited in the y direction due to the presence of only a small vertical surface at the tail (vertical stabilizer and rudder).

Two bank-to-turn guidance schemes are compared for accuracy against a medium sized combatant ship employing electronic countermeasures (an ECM blinker mounted aft on the ship). The first baseline scheme employs a pop-out maneuver consisting of a low altitude run in, azimuth offset, pop-up and roll into the target using proportional navigation in azimuth and elevation. The second, or sea-skimmer scheme, employs a straight-in low altitude attack. Miss distances for both schemes are compared while varying missile roll rate limit, ECM blinking frequency and burn through ranges.

A CSMP III simulation was coded to perform the study. Missile dynamics were represented by 6 degree of freedom nonlinear equations of motion with table look-up aerodynamic coefficients. These coefficients are representative of a generic cruise missile with a conventional wing-tail configuration of limited roll authority. Inner loop augmentation and autopilot modes were designed to improve missile damping in all axes, provide commanded load factor, commanded bank angle, and turn coordination. Autopilot outer loops were designed to provide altitude hold, and vertical flight path angle hold. Guidance loops were designed to provide proportional navigation in elevation and azimuth.

Since this study involves the influence of flight dynamic parameters (roll rate limits) on terminal guidance accuracy, no extensive tracker modeling is employed in the simulation. It is assumed that the seeker always tracks

the point target perfectly. The point target is, however, moved by an ECM blinker and contaminated with a glint model.

In Chapter II the equations used to represent missile dynamics are presented along with the methodology used to build up aerodynamic forces and moments. In Chapter III the development, design and simulation of the missile autopilot modes are presented. In Chapter IV the design of the guidance systems and a complete description of the two guidance schemes is presented. In Chapter V the CSMP simulation is presented followed by the results and conclusions of this study.

II. DEVELOPMENT AND SIMULATION OF MISSILE DYNAMICS

In this chapter the linear and nonlinear mathematical models are developed which are used to describe the flight dynamics of a generic bank-to-turn cruise missile. The linearized mathematical model of missile dynamics is used to design the missile autopilot control laws and guidance laws. The nonlinear mathematical model is used to accurately represent missile dynamics in a CSMP computer simulation of a sea launched generic cruise missile attacking a medium sized combatant ship. Since the purpose of this investigation is to perform a detailed evaluation of terminal control laws, it was decided that a linear dynamic simulation would not adequately represent missile motion; hence a full six degree of freedom (6 DOF) nonlinear dynamic simulation was encoded. The overall system that is modeled in this study is depicted in block diagram format in Figure 2-1 and will be developed in this thesis.

A. MISSILE EQUATIONS OF MOTION

The full nonlinear six degree of freedom rigid body, dynamic equations of motion are used to represent the motion of a generic bank-to-turn cruise missile. The aerodynamic forces and moments are built up from representative tabular coefficient data for the generic missile. These tabular

data are given in Appendix A in graphical form along with the generic missile's physical and geometric characteristics.

1. Assumptions

The assumptions used in the development of the equations of motion are given below.

- a. The earth is flat, does not rotate, and is fixed in inertial space.
- b. The mass of the missile is constant.
- c. The missile is a rigid body.
- d. The mass distribution of the missile is constant.
- e. Engine angular momentum is neglected.
- f. The missile is symmetric about the body's xy plane. Therefore, the products of inertia I_{xy} and I_{yz} are zero.
- g. The engine thrust line is parallel to the missile body x axis. Thus, the thrust components T_y and T_z are zero.
- h. The density of the atmosphere is constant.
- i. The engine thrust line passes through the missile center of mass. Therefore, the moments due to thrust L_T , M_T and N_T are zero.
- j. The wind is calm.
- k. Right aileron trailing edge down is positive deflection. Negative elevator deflection yields nose up pitching moment (positive).

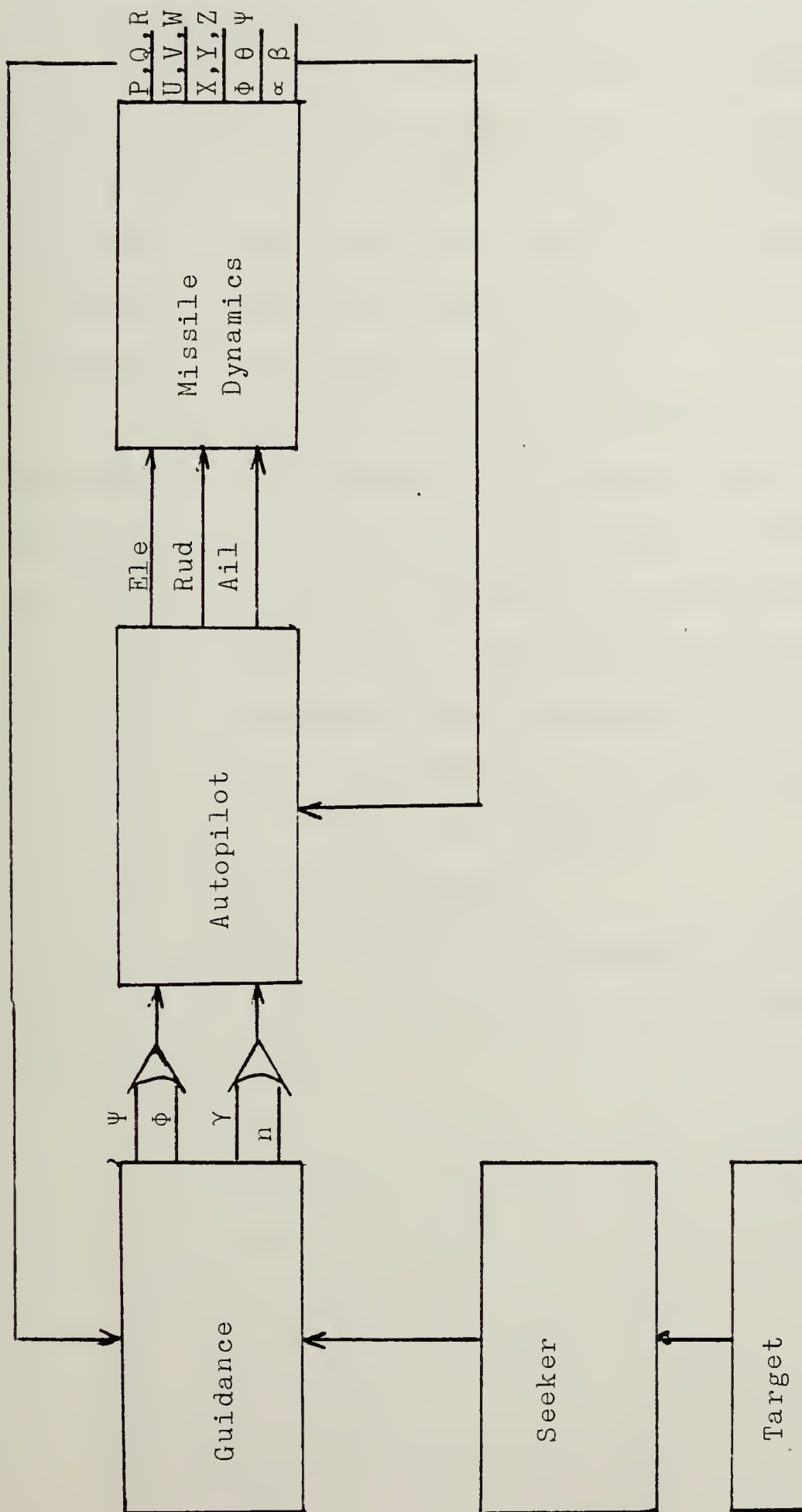


Figure 2-1 Missile System Flow Diagram

2. Coordinate System

An earth fixed coordinate system is established with its origin fixed at the initial position of the missile. The X_E axis points to true north, the Y_E axis points east, and the Z_E axis points toward the center of the earth. Altitude (H) therefore equals the negative of Z_E . The system is considered to be an inertial system.

A stability axis coordinate system is used with coordinates x, y, z fixed at the missile center of mass and oriented such that the x axis lies along the vehicle's forward velocity vector in steady state balanced cruise flight at 0.75 Mach number. The y axis is chosen perpendicular to the plane of symmetry and is oriented out the right wing. The z axis is chosen perpendicular to the x axis in the down direction and in the plane of symmetry.

3. The Equations of Motion

The following nonlinear equations as developed by Hewett {Ref. 2} describe the motion of the missile in 6 degrees of freedom.

$$m (\dot{U} - VR + WQ) = -mg \sin \theta + X + T \quad (1a)$$

$$m (\dot{V} + UR - WP) = mg \sin \phi \cos \theta + Y \quad (1b)$$

$$m (\dot{W} - UQ + VP) = mg \cos \phi \cos \theta + Z \quad (1c)$$

$$\dot{P}I_{xx} - (\dot{R} + PQ)I_{xz} + RQ(I_{zz} - I_{yy}) = L_A \quad (2a)$$

$$\dot{Q}I_{yy} + PR(I_{xx} - I_{zz}) + (P^2 - R^2)I_{xy} = M_A \quad (2b)$$

$$\dot{R}I_{zz} - \dot{P}I_{xz} + PQ(I_{yy} - I_{xx}) + QR I_{xz} = N_A \quad (2c)$$

$$\dot{\Phi} = P + (Q \sin \Phi + R \cos \Phi) \tan \theta \quad (3a)$$

$$\dot{\theta} = Q \sin \Phi - R \cos \Phi \quad (3b)$$

$$\dot{\Psi} = (Q \sin \Phi + R \cos \Phi) \sec \theta \quad (3c)$$

Equations (1a), (1b) and (1c) describe the translational motion of the missile. Equations (2a), (2b), and (2c) represent the rotational motion. Equations (3a), (3b) and (3c) are the Euler relations for bank, pitch and yaw angles.

Equations (4a), (4b), and (4c) describe the missile's position referenced to the earth fixed system (X_E, Y_E, Z_E).

$$\begin{aligned} \dot{X}_E = U \cos \Psi \cos \theta + V(\cos \Psi \sin \theta \sin \Phi - \sin \Psi \cos \Phi) \\ + W(\cos \Psi \sin \theta \cos \Phi + \sin \Psi \sin \Phi) \end{aligned} \quad (4a)$$

$$\begin{aligned} \dot{Y}_E = U \sin \Psi \cos \theta + V(\sin \Psi \sin \theta \sin \Phi + \cos \Psi \cos \Phi) \\ + W(\sin \Psi \sin \theta \cos \Phi - \cos \Psi \sin \Phi) \end{aligned} \quad (4b)$$

$$\dot{Z}_E = U \sin \theta - V \cos \theta \sin \Phi - W \cos \theta \cos \Phi \quad (4c)$$

Equations (5), (6) and (7) are also required.

Equations (5) and (6) yield angle of attack and side slip angle respectively in terms of velocity components U, V and W . Equation (7) represents the total velocity of the missile.

$$\alpha = \arctan \frac{W}{U} = \arcsin \frac{W}{(U^2 + W^2)^{\frac{1}{2}}} \quad (5)$$

$$\beta = \arctan \frac{V}{U^2 + W^2} = \arcsin \frac{V}{(U^2 + V^2 + W^2)^{\frac{1}{2}}} \quad (6)$$

$$V_T = (U^2 + V^2 + W^2)^{\frac{1}{2}} \quad (7)$$

Figure 2-2 illustrates the positive directions and locations of forces, moments and velocities in the body coordinate system (x, y, z).

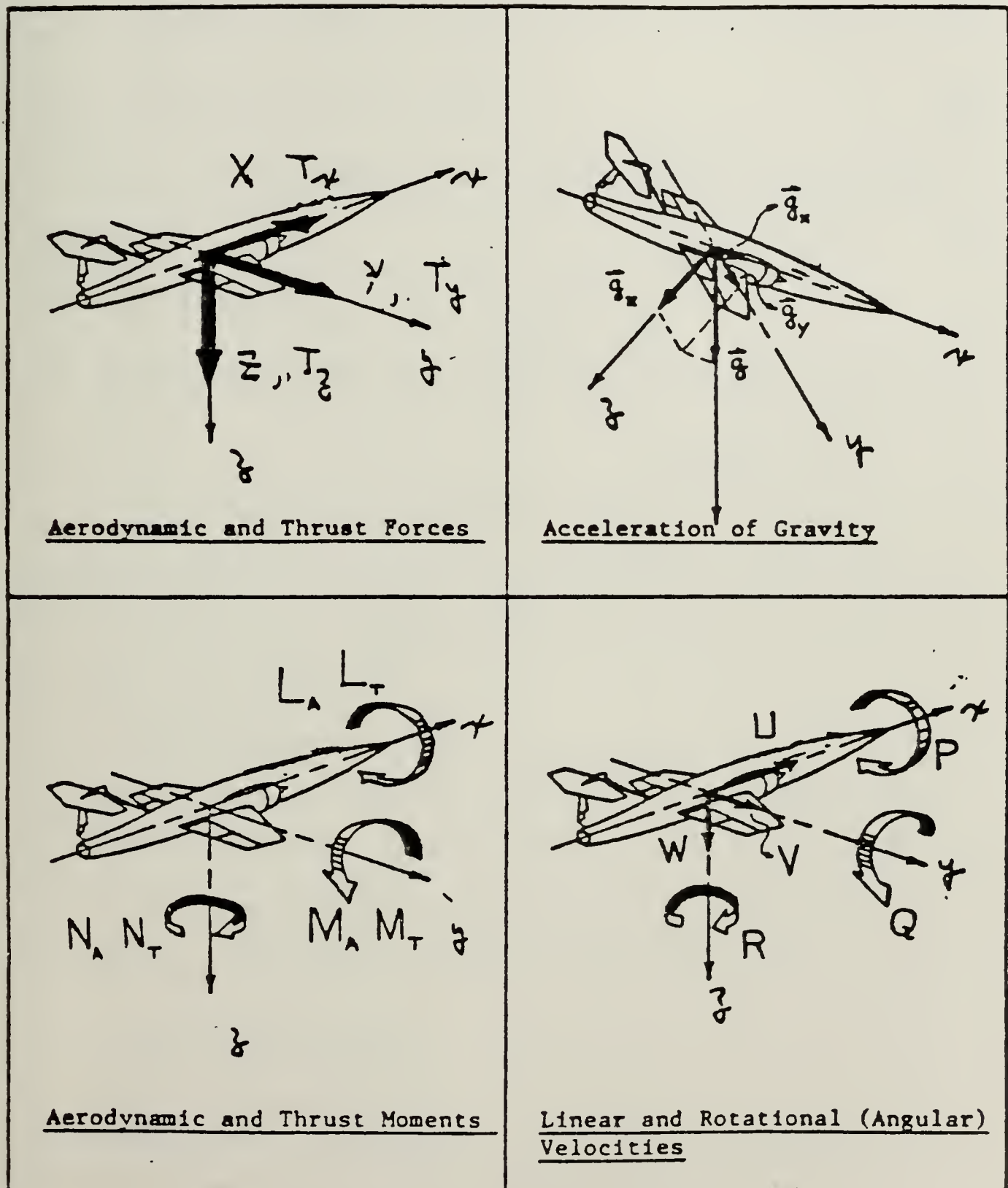


Figure 2-2 Body Coordinate System Description

Equations (1a), (1b), (1c) and (2a), (2b), (2c) can be rewritten in state format as follows:

$$\dot{U} = -g \sin \theta + VR - WQ + \frac{X}{m} + \frac{T}{m} \quad (8a)$$

$$\dot{V} = g \sin \phi \cos \theta - UR + WP + \frac{Y}{m} \quad (8b)$$

$$\dot{W} = g \cos \phi \cos \theta + UQ - VP + \frac{Z}{m} \quad (8c)$$

$$\dot{P} = \left[L_A I_{zz} + N_A I_{xz} - PQ(I_{yy} - I_{xx} - I_{zz})I_{xz} - RQ(I_{zz}^2 - I_{yy}I_{zz} + I_{xz}^2) \right] / (I_{xx}I_{zz} - I_{xz}^2) \quad (9a)$$

$$\dot{Q} = \left[M_A - PR(I_{xx} - I_{zz}) - (P^2 - R^2)I_{xz} \right] / I_{yy} \quad (9b)$$

$$\dot{R} = \left[L_A I_{xz} + N_A I_{xx} - PQ(I_{yy}I_{xx} - I_{xx}^2 - I_{xz}^2) - RQ(I_{xx} + I_{zz} - I_{yy})I_{xz} \right] / (I_{xx}I_{zz} - I_{xz}^2) \quad (9c)$$

Now integrating equations (3), (4), (8) and (9) results in U , V , W , P , Q , R , ϕ , θ , ψ , X_E , Y_E and Z_E (-H). The missile's velocities, angular rates, and angles and positions have thus been described.

4. Trim Equations

For straight and level flight at constant velocity the following variables are all zero: \dot{U} , \dot{V} , \dot{W} , \dot{P} , \dot{Q} , \dot{R} , $\dot{\phi}$, $\dot{\theta}$, $\dot{\psi}$, \dot{Z}_E , P_{SS} , Q_{SS} , R_{SS} , ϕ_{SS} , L_{ASS} , N_{ASS} , Y_{SS} , γ_{SS} , β_{SS} , V_{SS} , M_{ASS} . Thus the trim equations reduce to:

$$X_{SS} + T_x = mg \sin \theta_{SS}$$

$$Z_{SS} = -mg \cos \theta_{SS}$$

$$\dot{X}_{ESS} = U_{SS} \cos \psi_{SS} \cos \theta_{SS} - V_{SS} \sin \psi_{SS} + W_{SS} \cos \psi_{SS} \sin \theta_{SS}$$

$$\dot{Y}_{ESS} = U_{SS} \sin \psi_{SS} \cos \theta_{SS} + V_{SS} \cos \psi_{SS} + W_{SS} \sin \psi_{SS} \sin \theta_{SS}$$

$$\tan \theta_{SS} = W_{SS} / U_{SS}$$

$$V_{TSS} = (U_{SS}^2 + W_{SS}^2)^{\frac{1}{2}}$$

Since bank angle equals zero and the sum of flight path angle and angle of attack equal the pitch angle, then in steady state pitch angle equals angle of attack.

$$\theta_{SS} = \alpha_{SS}$$

These equations are used to define the initial cruise condition of the missile which is low level straight and level cruise flight at 0.75 Mach number. The precise initial flight condition and initial target position is described in Appendix B.

5. Other Useful Relations

Components of load factor at the missile center of mass in the y and -z directions are given below:

$$n_z = \frac{-Z}{mg} = \frac{V_T}{g} (Q - \dot{\alpha}) \quad (10a)$$

$$n_y = \frac{Y}{mg} = \frac{V_T}{g} (\dot{\beta} + R) \quad (10b)$$

6. Definition of Controls and Control Limits

The control configuration considered in the thesis is a conventional wing and tail with conventional rudder (ζ), aileron (ξ) and elevator (η) control surfaces. In addition, to cover a missile configuration which uses

differential horizontal stabilizer (stabilator) for roll control as opposed to aileron, the quantities left stabilator deflection (η_L) and right stabilator deflection (η_R) are defined and calculated.

Limits are imposed on rudder, elevator, and aileron travel. Limits are not imposed on differential stabilator travel but stabilator travel is presented for all simulations to show the stabilator travel required if indeed that were the control configuration. The aileron power coefficient data presented in Appendix A reflects the limited control authority in roll typical of a missile configured with differential stabilator for roll control as opposed to aileron.

The following control definitions and limits are applied:

a) Thrust (T) is a constant and is oriented along the x axis.

$$T = T_x = \text{constant}$$

b) Rudder deflection (ζ) is defined as positive trailing edge left from the rear and is limited to

$$-15^\circ \leq \zeta \leq 15^\circ$$

c) Elevator deflection (η) is defined as positive trailing edge down (produces a nose down moment) and is limited to

$$-15^\circ \leq \eta \leq 15^\circ$$

d) Aileron deflection (ξ) is defined as positive with trailing edge of the right aileron up (produces a positive (clockwise from the rear) roll) and is limited to

$$-15 \leq \xi \leq 15^\circ$$

e) Left horizontal stabilizer deflection (η_L) is positive trailing edge down.

$$\eta_L = \eta + \xi$$

f) Right horizontal stabilizer deflection (η_R) is positive trailing edge down.

$$\eta_R = \eta - \xi$$

B. AERODYNAMIC COEFFICIENT BUILD UP

Aerodynamic forces and moments are built up from coefficient data in standard fashion using the following relations:

$$D = C_D \bar{q} S$$

$$L = C_L \bar{q} S$$

$$Y = C_Y \bar{q} S$$

$$M_A = C_M \bar{q} S \bar{c}$$

$$L_A = C_{L_A} \bar{q} S \bar{b}$$

$$N_A = C_{N_A} \bar{q} S \bar{b}$$

1. Definition of Coefficients

Each coefficient is partitioned into two parts; a static term and a dynamic term as follows:

$$C_D = C_{D_{ST}} + C_{D_{DYN}}$$

$$C_L = C_{L_{ST}} + C_{L_{DYN}}$$

$$C_Y = C_{Y_{ST}} + C_{Y_{DYN}}$$

$$C_m = C_{m_{ST}} + C_{m_{DYN}}$$

$$C_{l_1} = C_{l_{1_{ST}}} + C_{l_{1_{DYN}}}$$

$$C_n = C_{n_{ST}} + C_{n_{DYN}}$$

2. Coefficient Build Up

The static terms are constructed from coefficient data stored in tables (Appendix A) as functions of two or three variables (either α , β , M , η , ζ , ξ) as follows:

$$C_{L_{basic}} = f(\alpha, \beta, M)$$

$$\Delta C_{L_{ST}}(\eta) = f(\alpha, \beta, \eta)$$

$$C_{D_{basic}} = f(\alpha, \beta, M)$$

$$\Delta C_{D_{ST}}(\eta) = f(\alpha, \beta, \eta)$$

$$\Delta C_{D_{ST}}(\xi) = f(\alpha, \beta, \xi)$$

$$\Delta C_{D_{ST}}(\zeta) = f(\alpha, \beta, \zeta)$$

$$C_{Y_{basic}} = f(\alpha, \beta)$$

$$\Delta C_{Y_{ST}}(\zeta) = f(\alpha, \beta, \zeta)$$

$$\Delta C_{Y_{ST}}(\xi) = f(\alpha, \beta, \xi)$$

$$C_{m_{basic}} = f(\alpha, \beta, M)$$

$$\Delta C_{m_{ST}}(\eta) = f(\alpha, \beta, \eta)$$

$$C_{n_{basic}} = f(\alpha, \beta)$$

$$\Delta C_{n_{ST}}(\zeta) = f(\alpha, \beta, \zeta)$$

$$\Delta C_{n_{ST}}(\xi) = f(\alpha, \beta, \xi)$$

η : elevator

ζ : rudder

ξ : aileron

$$C_{L_{\text{basic}}} = f(\alpha, \beta)$$

$$C_{L_{\text{ST}}}(\xi) = f(\alpha, \beta, \xi)$$

$$C_{L_{\text{ST}}}(\zeta) = f(\alpha, \beta, \zeta)$$

The static coefficients are formed as:

$$C_{L_{\text{ST}}} = C_{L_{\text{basic}}} + \Delta C_L(\eta)$$

$$C_{D_{\text{ST}}} = C_{D_{\text{basic}}} + \Delta C_{D_{\text{ST}}}(\eta) + \Delta C_{D_{\text{ST}}}(\xi) + \Delta C_{D_{\text{ST}}}(\zeta)$$

$$C_{Y_{\text{ST}}} = C_{Y_{\text{basic}}} + \Delta C_{Y_{\text{ST}}}(\zeta) + \Delta C_{Y_{\text{ST}}}(\xi)$$

$$C_{m_{\text{ST}}} = C_{m_{\text{basic}}} + \Delta C_{m_{\text{ST}}}(\eta)$$

$$C_{n_{\text{ST}}} = C_{n_{\text{basic}}} + \Delta C_{n_{\text{ST}}}(\xi) + \Delta C_{n_{\text{ST}}}(\zeta)$$

$$C_{l_{\text{ST}}} = C_{l_{\text{basic}}} + \Delta C_{l_{\text{ST}}}(\xi) + \Delta C_{l_{\text{ST}}}(\zeta)$$

The dynamic terms are constructed from dynamic coefficient data stored in tables (Appendix A) as a function of angle of attack and Mach number $f(\alpha, M)$. They are

$$C_{L_{\dot{\alpha}}}, C_{L_q}, C_{D_{\dot{\alpha}}}, C_{D_q}, C_{Y_{\dot{\beta}}}, C_{Y_r}, C_{Y_p}, C_{m_{\dot{\alpha}}}, C_{m_q}, C_{n_{\dot{\beta}}}, C_{n_r}, C_{n_p},$$

$$C_{l_r}, \text{ and } C_{l_p}.$$

The dynamic coefficients are formed as:

$$C_{L_{\text{DYN}}} = \frac{\bar{c}}{2V_T} (C_{L_{\dot{\alpha}}} + C_{L_q})$$

$$C_{D_{\text{DYN}}} = \frac{\bar{c}}{2V_T} (C_{D_{\dot{\alpha}}} + C_{D_q})$$

$$C_{Y_{\text{DYN}}} = \frac{b}{2V_T} (C_{Y_r} + C_{Y_p} + C_{Y_{\dot{\beta}}})$$

$$C_{m_{DYN}} = \frac{\bar{c}}{2V_T} (C_{m_{\dot{\alpha}}} + C_{m_q} q)$$

$$C_{n_{DYN}} = \frac{b}{2V_T} (C_{n_{\dot{\beta}}} + C_{n_r} r + C_{n_p} p)$$

$$C_{l_{DYN}} = \frac{b}{2V_T} (C_{l_r} r + C_{l_p} p)$$

The total coefficient build up is summarized below.

$$C_L = C_{L_{basic}} + \Delta C_{L_{ST}}(\eta) + \frac{\bar{c}}{2V_T} (C_{L_{\dot{\alpha}}} + C_{L_q} q)$$

$$C_D = C_{D_{basic}} + \Delta C_{D_{ST}}(\eta) + \Delta C_{D_{ST}}(\xi) + \Delta C_{D_{ST}}(\zeta) + \frac{\bar{c}}{2V_T} (C_{D_{\dot{\alpha}}} + C_{D_q} q)$$

$$C_Y = C_{Y_{basic}} + \Delta C_{Y_{ST}}(\zeta) + \Delta C_{Y_{ST}}(\xi) + \frac{\bar{b}}{2V_T} (C_{Y_r} r + C_{Y_p} p + C_{Y_{\dot{\beta}}} \dot{\beta})$$

$$C_m = C_{m_{basic}} + \Delta C_{m_{ST}}(\eta) + \frac{\bar{c}}{2V_T} (C_{m_{\dot{\alpha}}} + C_{m_q} q)$$

$$C_n = C_{n_{basic}} + \Delta C_{n_{ST}}(\eta) + \Delta C_{n_{ST}}(\xi) + \frac{\bar{b}}{2V_T} (C_{n_{\dot{\beta}}} + C_{n_r} r + C_{n_p} p)$$

$$C_l = C_{l_{basic}} + \Delta C_{l_{ST}}(\zeta) + \Delta C_{l_{ST}}(\xi) + \frac{b}{2V_T} (C_{l_r} r + C_{l_p} p)$$

C. MISSILE LINEARIZED EQUATIONS OF MOTION

The linearized equations of motion used to design the missile autopilot are presented in this section. The equations are linearized about the cruise flight condition.

1. Additional Assumptions for Linearized Equations

The additional assumptions required for linearized equations are as follows:

a) Derivatives are given in stability axes which are fixed for the missile low level cruise condition.

b) Standard small perturbation assumptions apply.

1) Perturbed angles are small.

2) Products of perturbed variables are neglected.

3) There is no coupling between longitudinal and lateral directional motions.

c) Thrust derivatives are neglected.

d) The steady state condition is chosen as low level straight and level cruise.

2. Linearized Equations Summarized

The linear equations of motion in state variable form are shown in Tables 2-1 and 2-2. The following coefficients are defined as used in Table 2-2.

$$A = \frac{I_{zz}I_{xz}}{I_{zz}I_{xx} - I_{xz}^2}$$

$$B = \frac{I_{xx}}{I_{xz}}$$

$$C = \frac{I_{xx}I_{xz}}{I_{zz}I_{xx} - I_{xz}^2}$$

$$D = \frac{I_{zz}}{I_{xz}}$$

3. Definition of Stability Derivatives

The dimensional aerodynamic stability derivatives used in the equations of motion are defined by the following relations.

a. Longitudinal Dimensional Stability Derivatives

$$X_U = -\bar{q}_{SS} S (C_{D_U} + 2C_{D_{SS}}) / m U_{SS} \quad 1/\text{sec}$$

$$X_\alpha = \bar{q}_{SS} S (C_{L_{SS}} - C_{D_\alpha}) / m \quad \text{ft/sec}$$

$$X_\eta = -\bar{q}_{SS} S C_{D_\eta} / m \quad \text{ft/sec}^2$$

$$Z_U = -\bar{q}_{SS} S (C_{L_U} + 2C_{L_{SS}}) / m U_{SS} \quad 1/\text{sec}$$

TABLE 2-1

Longitudinal Equations (Perturbed Variables)

(11)

$$\begin{bmatrix} \dot{U} \\ \dot{\alpha} \\ \dot{q} \\ \dot{\theta} \end{bmatrix} = \begin{bmatrix} X_U & X_\alpha & 0 & -g \cos \gamma_{SS} \\ \frac{Z_U}{U_{SS} - Z_{\dot{\alpha}}} & \frac{Z_\alpha}{U_{SS} - Z_{\dot{\alpha}}} & \frac{U_{SS} + Z_q}{U_{SS} - Z_{\dot{\alpha}}} & \frac{-g \sin \gamma_{SS}}{U_{SS} - Z_{\dot{\alpha}}} \\ \frac{M_U + M_\alpha Z_U}{U_{SS} - Z_{\dot{\alpha}}} & \frac{M_\alpha + M_\alpha Z_\alpha}{U_{SS} - Z_{\dot{\alpha}}} & \frac{M_q + M_\alpha (U_{SS} + Z_q)}{U_{SS} - Z_{\dot{\alpha}}} & \frac{-M_\alpha g \sin \gamma_{SS}}{U_{SS} - Z_{\dot{\alpha}}} \\ 0 & 0 & 1 & 0 \end{bmatrix} \begin{bmatrix} U \\ \alpha \\ q \\ \theta \end{bmatrix} + \begin{bmatrix} X_\eta \\ \frac{Z_\eta}{U_{SS} - Z_{\dot{\alpha}}} \\ \frac{M_\eta + M_\alpha Z_\eta}{U_{SS} - Z_{\dot{\alpha}}} \\ 0 \end{bmatrix} \eta$$

TABLE 2-2

Lateral Directional Equations (Perturbed Variables)

(12)

$$\begin{bmatrix} \dot{\beta} \\ \dot{\phi} \\ \dot{p} \\ \dot{r} \end{bmatrix} = \begin{bmatrix} \frac{Y_\beta}{U_{SS}} & \frac{g \cos \gamma_{SS}}{U_{SS}} & \frac{Y_p}{U_{SS}} & \frac{Y_r - U_{SS}}{U_{SS}} \\ 0 & 0 & 1 & 0 \\ A(N_\beta + BL_\beta) & 0 & A(N_p + BL_p) & A(N_r + BL_r) \\ C(L_\beta + DN_\beta) & 0 & C(L_p + DN_p) & C(L_r + DN_r) \end{bmatrix} \begin{bmatrix} \beta \\ \phi \\ p \\ r \end{bmatrix} + \begin{bmatrix} \frac{Y_\xi}{U_{SS}} & 0 & A(N_\xi + BL_\xi) & A(N_\zeta + BL_\zeta) \\ 0 & 0 & C(L_\xi + DN_\xi) & C(L_\zeta + DN_\zeta) \end{bmatrix} \begin{bmatrix} \xi \\ \zeta \end{bmatrix}$$

$$Z_{\alpha} = -\bar{q}_{SS} S (C_L + C_{D_{SS}}) / m \quad \text{ft/sec}^2$$

$$Z_{\dot{\alpha}} = -\bar{q}_{SS} S \bar{c} C_{L_{\dot{\alpha}}} / 2mU_{SS} \quad \text{ft/sec}$$

$$Z_q = -\bar{q}_{SS} S \bar{c} C_{L_q} / 2mU_{SS} \quad \text{ft/sec}$$

$$\overset{Mfe}{Z_{\eta}} = -\bar{q}_{SS} S C_{L_{\eta}} / m \quad \text{ft/sec}$$

$$M_U = \bar{q}_{SS} S \bar{c} (C_{M_U} + 2C_{M_{SS}}) / I_{yy} U_{SS} \quad 1/\text{ft sec}$$

$$M_{\alpha} = \bar{q}_{SS} S \bar{c} C_{M_{\alpha}} / I_{yy} \quad 1/\text{sec}^2$$

$$M_{\dot{\alpha}} = \bar{q}_{SS} S \bar{c}^2 C_{m_{\dot{\alpha}}} / 2I_{yy} U_{SS} \quad 1/\text{sec}$$

$$M_q = \bar{q}_{SS} S \bar{c}^2 C_{m_q} / 2I_{yy} U_{SS} \quad 1/\text{sec}$$

$$\overset{Mfe}{M_{\eta}} = \bar{q}_{SS} S \bar{c} C_{m_{\eta}} / I_{yy} \quad 1/\text{sec}^2$$

b. Lateral Directional Dimensional Stability

Derivatives

$$Y_{\beta} = \bar{q}_{SS} S C_{y_{\beta}} / m \quad \text{ft/sec}^2$$

$$Y_p = \bar{q}_{SS} S b C_{y_p} / 2mU_{SS} \quad \text{ft/sec}$$

$$Y_r = \bar{q}_{SS} S b C_{y_r} / 2mU_{SS} \quad \text{ft/sec}$$

$$Y_{\xi} = \bar{q}_{SS} S C_{y_{\xi}} / m \quad \overset{Y_{\xi a}}{\text{ft/sec}^2}$$

$$Y_{\zeta} = \bar{q}_{SS} S C_{y_{\zeta}} / m \quad \overset{Y_{\zeta r}}{\text{ft/sec}^2}$$

$$L_{\beta} = \bar{q}_{SS} S b C_{l_{\beta}} / I_{xx} \quad 1/\text{sec}^2$$

$$L_p = \bar{q}_{SS} S b^2 C_{l_p} / 2I_{xx} U_{SS} \quad 1/\text{sec}$$

$$L_r = \bar{q}_{SS} S b^2 C_{l_r} / 2I_{xx} U_{SS} \quad 1/\text{sec}$$

$$L_{\xi} = \bar{q}_{SS} S b C_{l_{\xi}} / I_{xx} \quad 1/\text{sec}^2$$

$$L_{\zeta} = \bar{q}_{SS} S b C_{l_{\zeta}} / I_{xx} \quad 1/\text{sec}^2$$

$$N_{\beta} = \bar{q}_{SS} S b C_{n_{\beta}} / I_{zz} \quad 1/\text{sec}^2$$

$$N_p = \bar{q}_{SS} S b^2 C_{n_p} / 2 I_{zz} U_{SS} \quad 1/\text{sec}$$

$$N_r = \bar{q}_{SS} S b^2 C_{n_r} / 2 I_{zz} U_{SS} \quad 1/\text{sec}$$

$$N_{\xi} = \bar{q}_{SS} S b C_{n_{\xi}} / I_{zz} \quad 1/\text{sec}^2$$

$$N_{\zeta} = \bar{q}_{SS} S b C_{n_{\zeta}} / I_{zz} \quad 1/\text{sec}^2$$

4. Trim Equations

For straight and level flight at constant velocity the following variables are all zero: $\dot{U}=\dot{V}=\dot{W}=\dot{P}=\dot{Q}=\dot{R}=\dot{\theta}=\dot{\psi}=\dot{\phi}$

$$\dot{Z}_E=0 \quad Q_{SS}=P_{SS}=R_{SS}=\phi_{SS}=L_{A_{SS}}=M_{A_{SS}}=N_{A_{SS}}=Y_{SS}=\gamma_{SS}=\beta_{SS}=V_{SS}=$$

$$W_{SS}=\zeta_{SS}=\zeta_{SS}=0$$

The trim equations reduce to:

$$T \sin \alpha_{SS} = mg - (C_{L_o} + C_{L_{\alpha}} \alpha_{SS} + C_{L_{\eta}} \eta_{SS}) \bar{q}_{SS} S$$

$$T \cos \alpha_{SS} = (C_{D_o} + C_{D_{\alpha}} \alpha_{SS} + C_{D_{\eta}} \eta_{SS}) \bar{q}_{SS} S$$

$$0 = (C_{m_o} + C_{m_{\alpha}} \alpha_{SS} + C_{m_{\eta}} \eta_{SS}) \bar{q}_{SS} S \bar{c}$$

III. DEVELOPMENT AND SIMULATION OF THE MISSILE AUTOPILOT

The missile is assumed to be equipped with an autopilot capable of providing closed loop control which consists of the following:

- a) normal acceleration (n_z)
- b) lateral acceleration (n_y)
- c) bank angle (ϕ).

In addition, an outer closed loop control, which serves as the outer autopilot, is as follows:

- a) altitude (H)
- b) vertical flight path angle (γ)

These two outer loops are employed as required during certain phases of the attack mission.

It is assumed that the missile possesses accelerometer sensors in the y and z body axes located at the missile center of gravity, rate gyros and rate integrating gyros about the x, y, and z axes, and a radar altimeter. Sensor noise is neglected in this simulation.

A. AUTOPILOT INNER LOOP REQUIREMENTS AND DESIGNS

1. Description of the Autopilot Inner Loops

The autopilot is assumed to employ three inner loops as depicted in Table 3-1.

TABLE 3-1

Autopilot Inner Loop Description

LOOP	COMMANDED VARIABLE	CONTROL	CONSTRAINTS
1 Normal Acceleration Command	n_z (normal acceleration)	η Elevator	$-15^\circ \leq \eta \leq 15^\circ$ $-2 \leq N_z \leq 4$
2 Bank Angle Command	ϕ (Bank Angle)	ξ Aileron	$-15^\circ \leq \xi \leq 15^\circ$ $\phi \leq 60^\circ*$ $p \leq 50, 100, 200^\circ/\text{sec}$
3 Turn Coordinator	n_y (Lateral Acceleration)	ζ Rudder	$-15^\circ \leq \zeta \leq 15^\circ$ $N_y = 0$

* Applies in certain mission phases only

2. Normal Acceleration Command System

The purpose of normal acceleration command (NAC) system is to provide a vertical load factor (n_z) response to a commanded load factor (n_{z_c}). An accelerometer is used to provide the primary feedback and a rate gyro is used to provide inner loop pitch rate feedback for improved damping.

a. Block Diagram

The block diagram of the normal acceleration command autopilot is shown in Figure 3-1. Limiter a allows the commanded acceleration to a range from -2.0 to +4.0 g's. Limiter b allows the elevator control to vary from -15 degrees to +15 degrees.

b. Assumptions

1) The rate gyro and accelerometer dynamic lags are negligible.

2) The accelerometer is mounted at the center of gravity. Therefore the moment arm is zero and the feedback load factor is totally n_z . ($C=0$)

3) The fix servo can be represented by a first order lag.

4) The missile dynamics can be represented by a short period approximation.

5) Commanded normal acceleration is limited from -2.0 to +4.0 g's.

c. Design

The following transfer function was developed from equation (11):

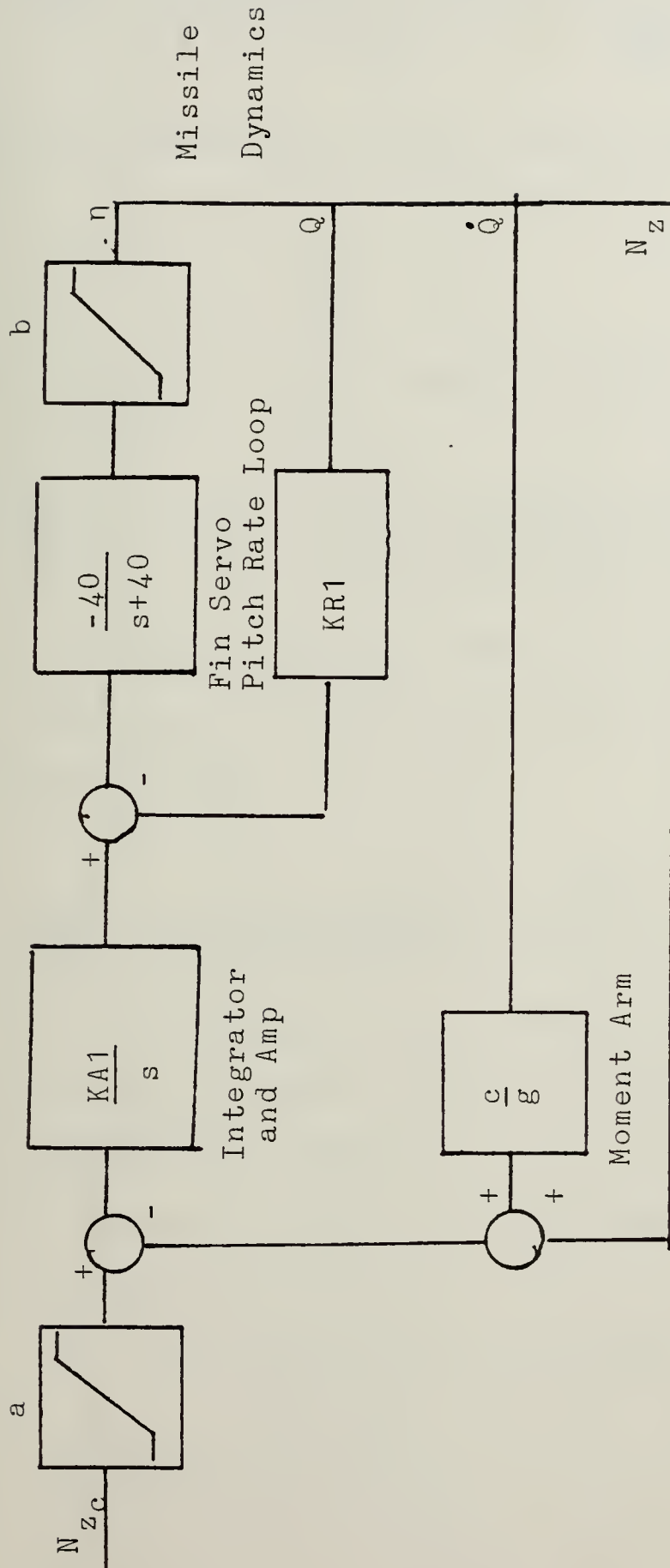


Figure 3-1 Normal Acceleration Command Autopilot Description

$$\frac{Q(s)}{\eta(s)} = \frac{V_T M_{\eta} + Z_{\eta} \dot{M}_{\alpha}) s + (M_{\alpha} Z_{\eta} - Z_{\alpha} M_{\eta})}{V_T \{ s^2 - (M_q + Z_{\frac{\alpha}{q}} + \dot{M}_{\alpha}) s + (Z_{\frac{\alpha}{q}} M_q - M_{\alpha}) \}}$$

From this transfer function and equation (10a)

$$n_z = \frac{V_T}{g} (Q - \dot{\alpha})$$

the following θ to n_z transfer function was obtained.

$$\frac{N_z(s)}{Q(s)} = \frac{V_T}{g} \frac{-Z_{\eta} s^2 + (M_q Z_{\eta} + Z_{\eta} \dot{M}_{\alpha}) s + (M_{\alpha} Z_{\eta} - Z_{\alpha} M_{\eta})}{(V_T M_{\eta} + Z_{\eta} \dot{M}_{\alpha}) s + (M_{\alpha} Z_{\eta} - Z_{\alpha} M_{\eta})}$$

Utilizing the characteristics listed in Appendix A for this cruise missile at 0.75 Mach number, the above transfer functions become

$$\frac{Q(s)}{\eta(s)} = \frac{-26.99(s+1.009)}{s^2+1.289s+27.13} \quad \text{and} \quad \frac{N_z(s)}{Q(s)} = \frac{-0.08(s^2+0.1985s-328.9)}{(s+1.009)}$$

Evaluating the characteristic polynomial of the $Q(s)/\eta(s)$ transfer function yields the natural frequency of 0.829 Hz and a damping ratio of 0.1237. The resulting block diagram for the normal acceleration command inner loop autopilot for analysis purposes is shown in Figure 3-2.

(1) Root Locus Evaluation.

(a) Pitch Rate Loop. The transfer function for the pitch rate loop is:

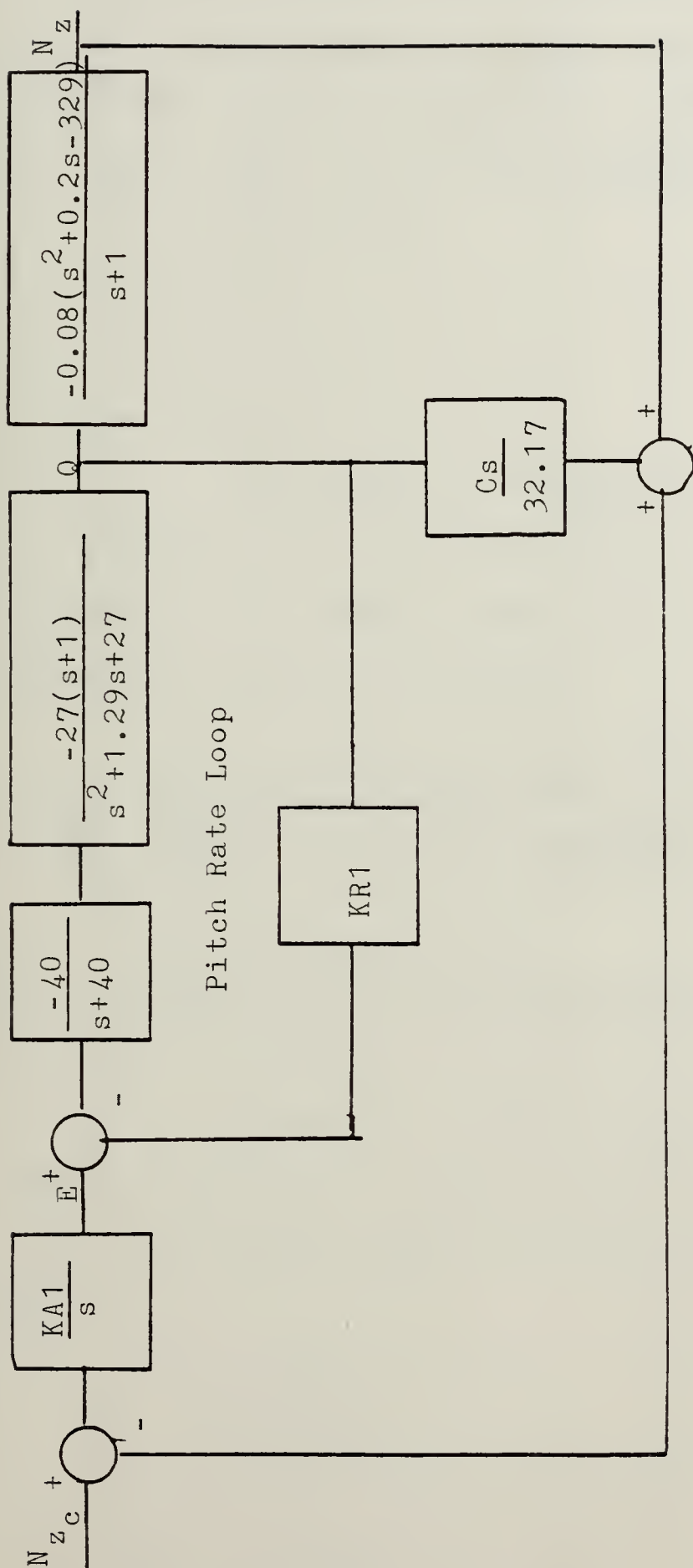


Figure 3-2 Normal Acceleration Command Autopilot Block Diagram (Analysis)

$$\frac{Q(s)}{E(s)} = \frac{1080(s+1)}{(s^3 + 41.29s^2 + (78.7 + 1080KR1)s + (1084 + 1080KR1))}$$

Appendix C contains the root locus plot of the pitch rate loop for ranging KR1. A KR1 of 0.28 is chosen which yields the following characteristics:

$$s = -5.600 \pm 3.844 j$$

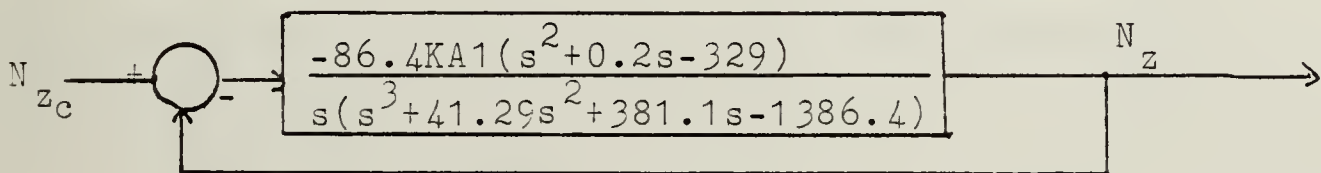
$$\phi = 55.53^\circ$$

$$\zeta = 0.82$$

$$\omega_n = 1.08 \text{ Hz}$$

(b) Normal Acceleration Command Loop.

Using a KR1 of 0.28 in the pitch rate loop, and locating the acceleration at the missile center of mass (C=0), the normal acceleration command loop becomes:



$$\frac{N_z(s)}{N_{zc}(s)} = \frac{-86.4KA1(s^2 + 0.2s - 329)}{s(s^3 + 41.29s^2 + 381.1s - 1386.4) - 86.4KA1(s^2 + 0.2s - 329)}$$

Appendix C contains the root locus plot of the normal acceleration command system for varying KA1. A KA1 of 0.05 is chosen which yields the following characteristics:

$$s = -1.981 \pm 3.317 j$$

$$\phi = 30.85^\circ$$

$$\zeta = 0.513$$

$$\omega_n = 0.615 \text{ Hz}$$

With a KR1 of 0.28 and a KA1 of 0.05 the system transfer function relating n_{z_c} to n_z is:

$$\frac{N_z(s)}{N_{z_c}(s)} = \frac{-4.32(s^2 - 0.2s - 329)}{s^4 + 41.29s^3 + 376.78s^2 - 1387.26s - 1421.28}$$

The normal acceleration command autopilot has zero steady state error for a step input as it is a type 1 system. The system response to a 1g commanded load factor is shown in Figure 3-3.

3. Bank Angle Command System

The purpose of the bank angle command (BAC) autopilot is to command missile bank angle. Limits are applied to commanded roll rate and in certain mission phases commanded bank angle. A rate integrating gyro feeds back bank angle and a roll rate gyro provides feedback as a roll rate damper.

a. Block Diagram

The bank angle command autopilot is presented in block diagram in Figure 3-4. Limiter a allows the commanded bank angle to vary from 0 to 60 degrees and is active in certain flight phases. Limiter b limits the roll rate to either 50, 100, or 200 degrees/second. Limiter c limits aileron deflections to range from -15 to +15 degrees.

b. Assumptions

1) The rate gyro and displacement dynamic lags are negligible.

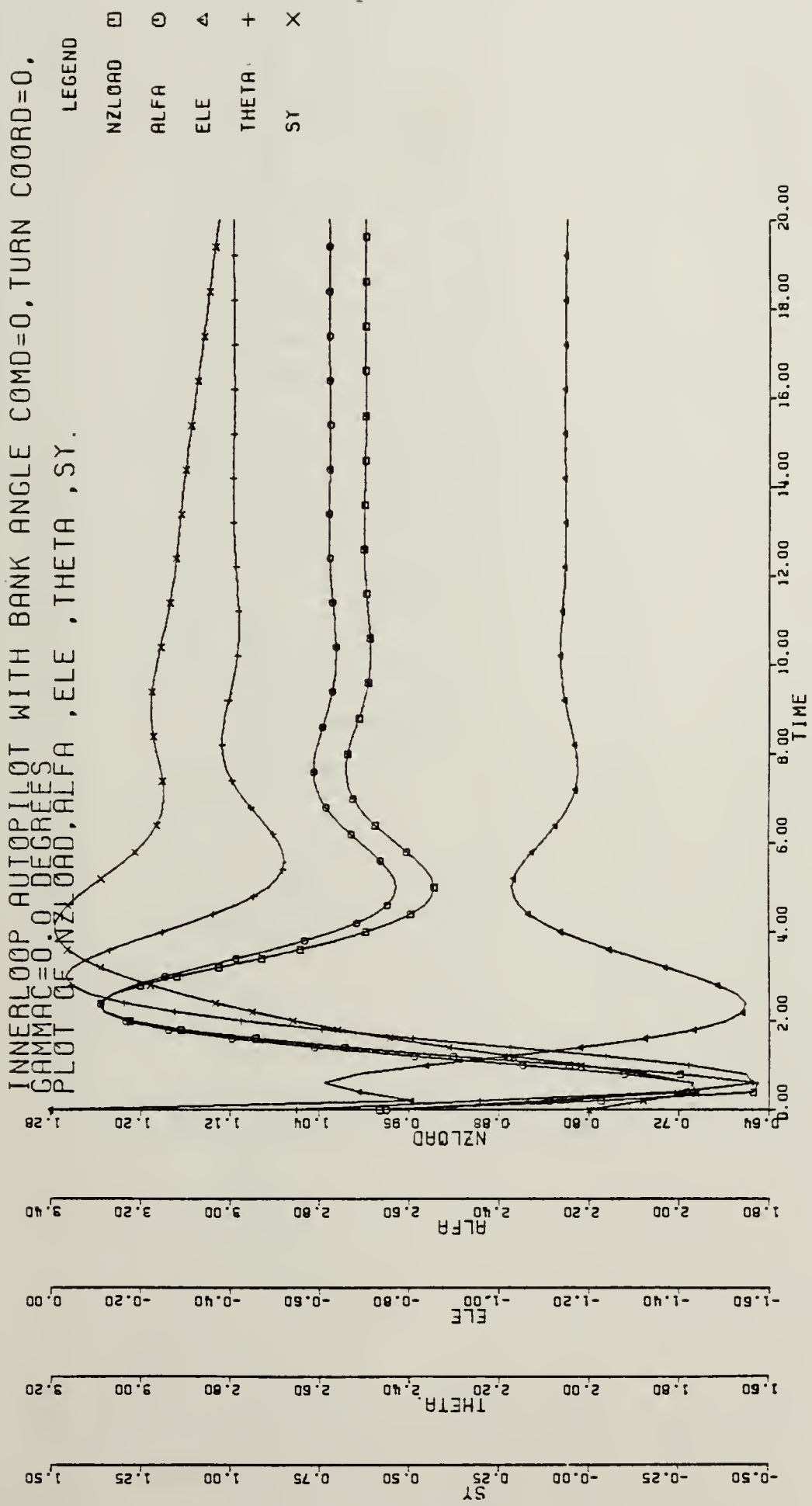


Figure 3-3 NAC Autopilot Response to 1g Commanded Load Factor

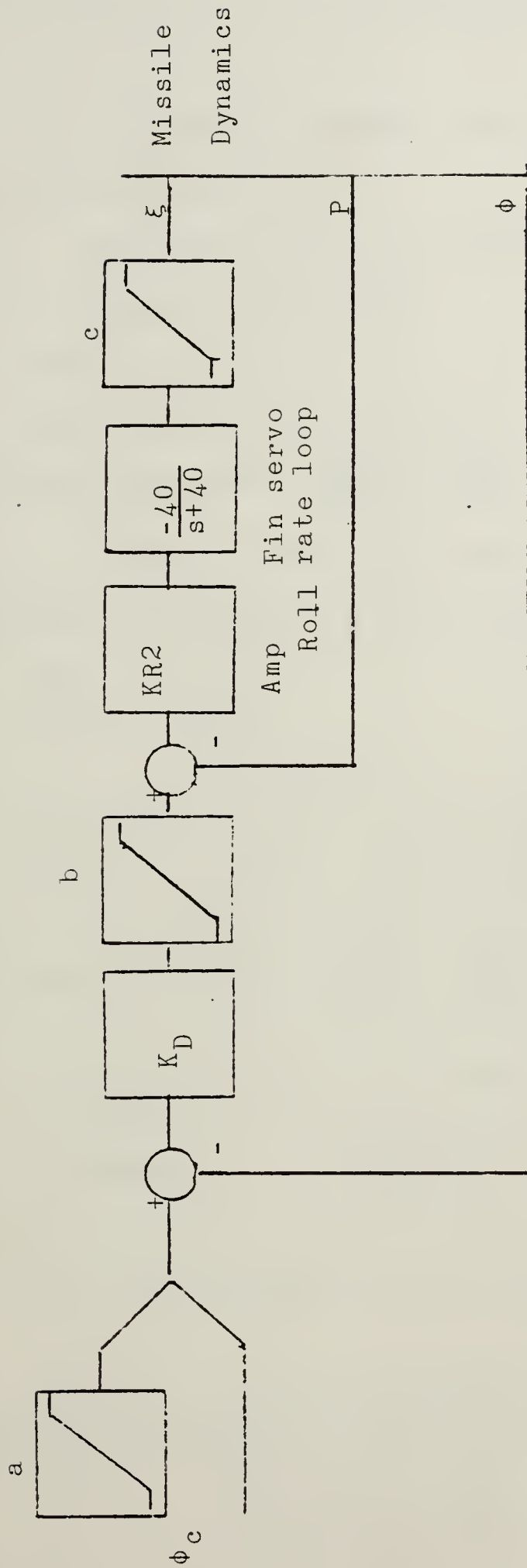


Figure 3-4 BANK ANGLE COMMAND AUTOPILOT DESCRIPTION

2) The fin servo can be represented by a first order lag.

3) The missile dynamics can be represented by a roll mode approximation.

4) There are limits on commanded bank angle and commanded roll rate as noted above.

c. Design

Equation (12) can be written to find the lateral transfer functions $\frac{\beta(s)}{\zeta(s)}$, $\frac{\phi(s)}{\zeta(s)}$, and $\frac{\psi(s)}{\zeta(s)}$,

where $\delta = \xi$ or ζ . By allowing a roll approximation the transfer function relating aileron and bank angle becomes:

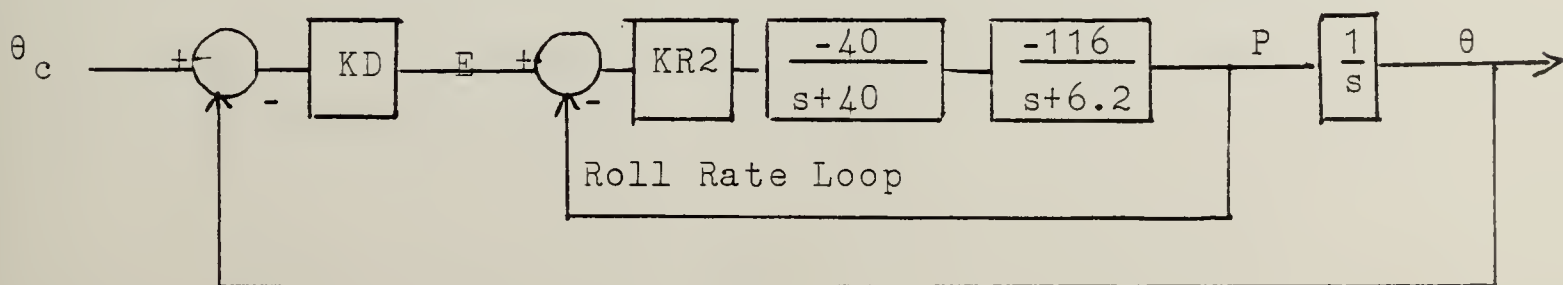
$$\frac{\phi(s)}{\xi(s)} = \frac{L_{\xi}}{s(s-L_p)}$$

The root at the origin indicates the missile does not have bank angle stability without autopilot stabilization.

Evaluation of the transfer function coefficients results in the transfer functions $\frac{\phi(s)}{\xi(s)} = \frac{-116}{s(s+6.2)}$ and $\frac{p(s)}{\xi} =$

$\frac{-116}{s+6.2}$. The maximum missile roll rate can be approximated by $P_{\max} = \left[\frac{L_{\xi} \xi_{\max}}{L_p} \right] = \frac{(116)(15)}{6.2} = 280.6 \text{ degrees/second.}$

The block diagram of the bank angle command system is:



(1) Root Locus Evaluation.

(a) Roll Rate Loop. The transfer function for the roll rate loop is:

$$\frac{P(s)}{E(s)} = \frac{4640 \text{ KR2}}{s^2 + 46.2s + 248 + 4640\text{KR2}}$$

Appendix C contains the root locus plot of the roll rate loop for varying KR2. A gain KR2 of 0.10 yields the following characteristics.

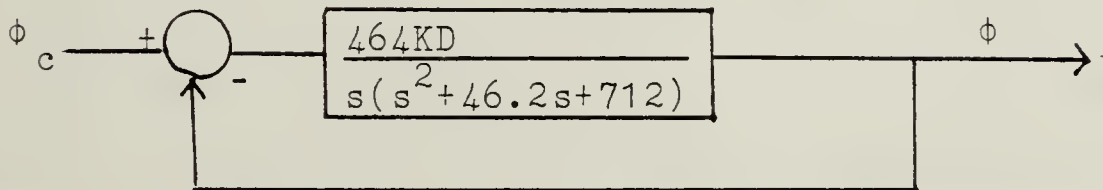
$$s = -23.10 \pm 13.36 s$$

$$\phi = 59.96^\circ$$

$$\zeta = 0.8656$$

$$\omega_n = 4.247 \text{ Hz}$$

(b) Bank Angle Command Loop. With a KR2 of 0.10 the bank angle command loop becomes:



The transfer function is:

$$\frac{\phi(s)}{\phi_c(s)} = \frac{464KD}{s^3 + 46.2s^2 + 712s + 464KD}$$

The root locus plot is shown in Appendix C for varying KD. Choosing a KD gain of 10.8 yields the following characteristics:

$$s = -9.98 \pm 9.58j$$

$$\phi = 45.056^\circ$$

$$\zeta = 0.718$$

$$\omega_n = 2.19 \text{ Hz}$$

Using gains of 0.10 for the inner loop and 10.8 for the outer loop of the bank angle command system, the system transfer function $G(s)$ becomes

$$\frac{\phi(s)}{\phi_c(s)} = \frac{5011.2}{s^3 + 46.2s^2 + 712s + 5011.2}$$

and the system is a type 1 system for a step input. The transient response is demonstrated in Figures 3-5 and 3-6 for a commanded bank angle of 60 degrees.

4. Turn Coordinator

The turn coordinator (TC) is a lateral autopilot which provides a body directional load factor, n_y , to a commanded load factor, n_{y_c} . Like the normal acceleration command autopilot it employs an inner loop yaw rate damper. The outer loop uses unity accelerometer feedback and has the capability of moment arm feedback if the accelerometer is located at a different position than the missile center of mass.

a. Block Diagram

The block diagram representing the turn coordinator autopilot is shown in Figure 3-7. Limiter a limits the rudder deflection (ζ) from -15 to +15 degrees.

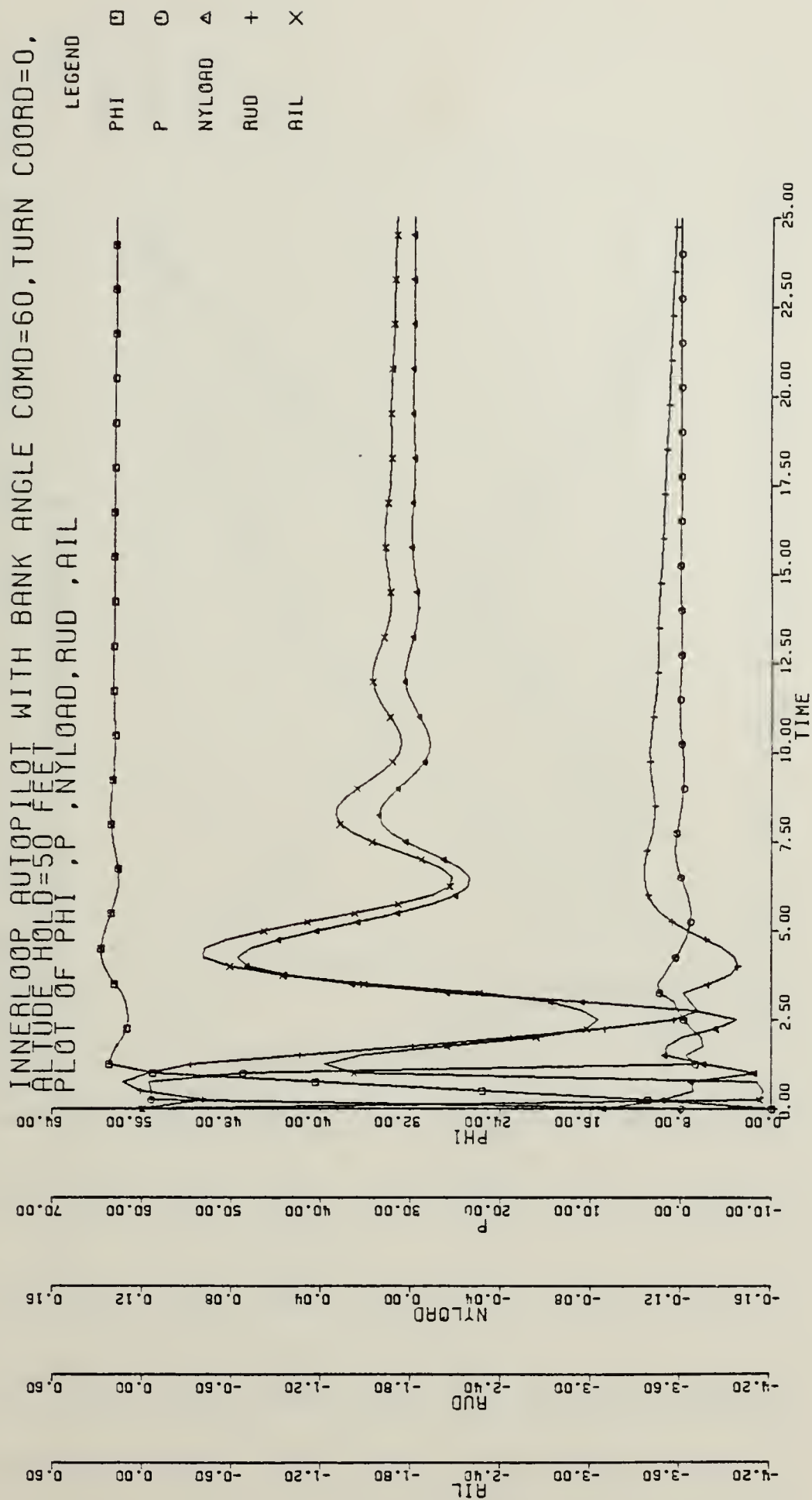


Figure 3-5 BAC Autopilot Response to 60° Commanded Bank Angle (PHI Response)

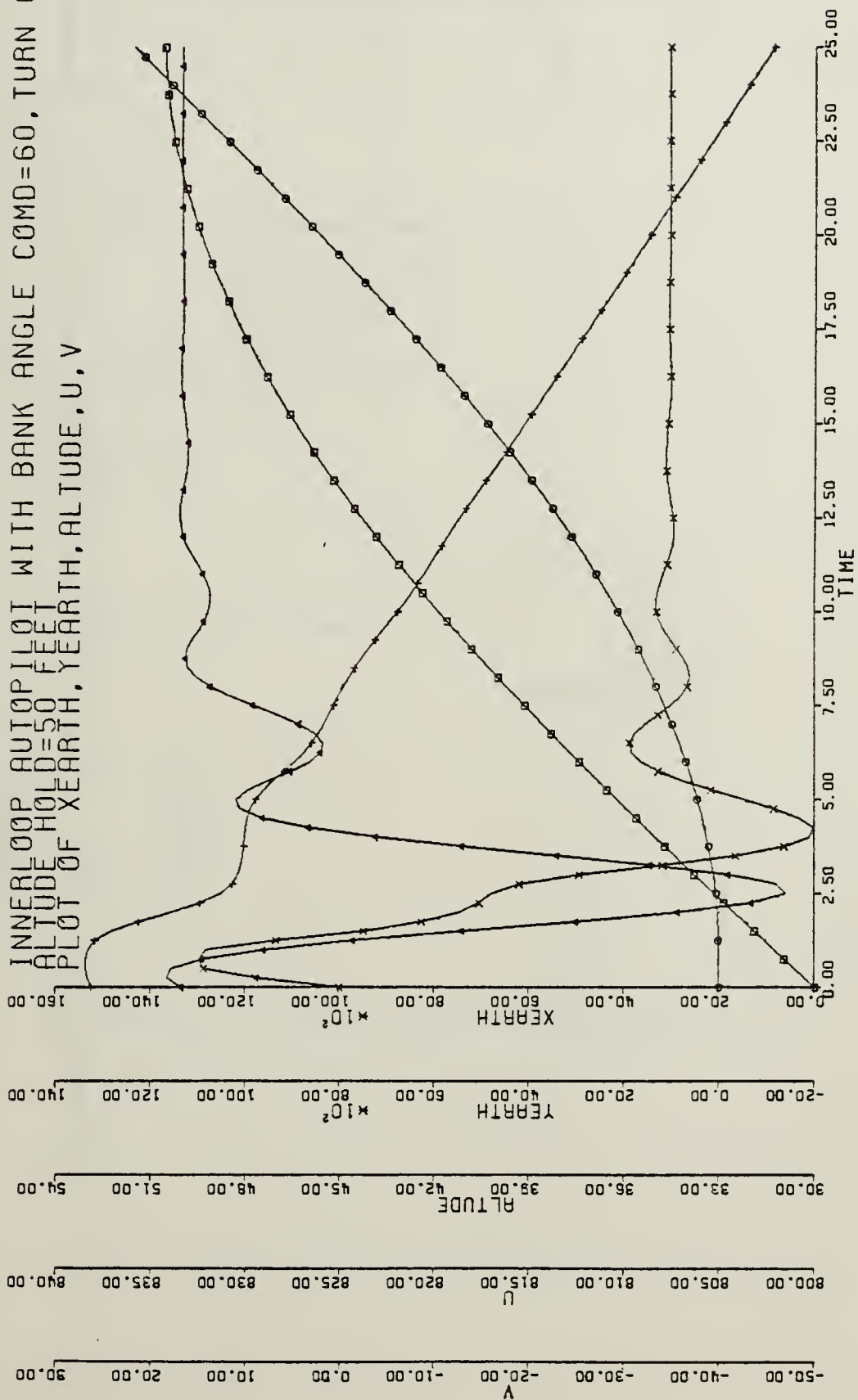


Figure 3-6 BAC Autopilot Response to 60° Commanded Bank Angle (Altitude Response)

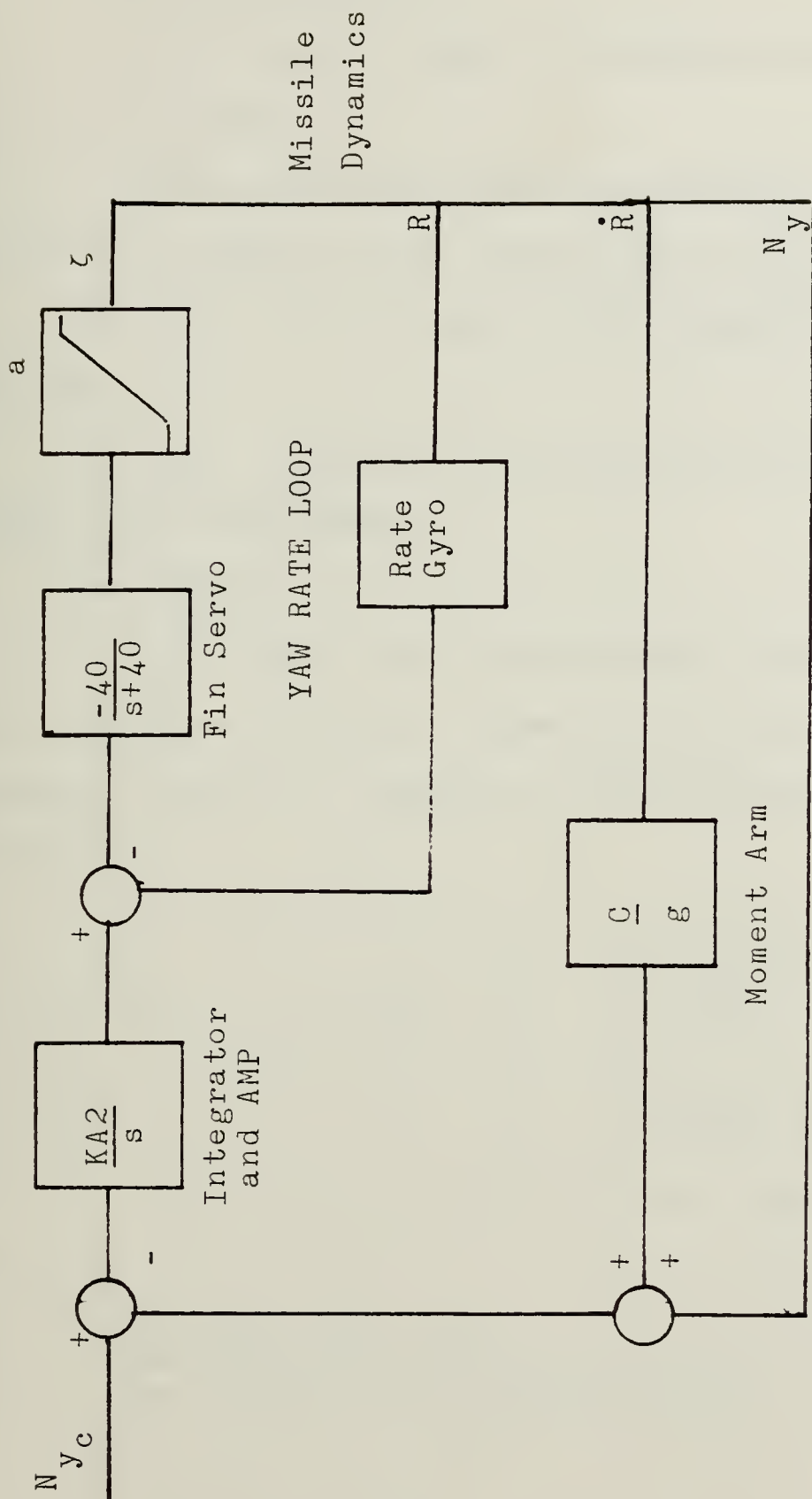


Figure 3-7 Turn Coordinator Autopilot Description

b. Assumptions

- 1) The rate gyro and accelerometer dynamic lags are negligible.
- 2) An accelerometer is mounted at the center of gravity. Therefore the moment arm is zero. $C=0$
- 3) The fin servo can be represented by a first order lag.
- 4) The missile dynamics can be represented by a dutch roll approximation.

c. Design

The dutch roll approximation involves side slip angle β , and yaw angle Ψ . Equation (12) with ϕ neglected (assuming a small $C_{l\beta}$ results in the following set of equations:

$$\begin{bmatrix} sV_T - Y_\beta & s(V_T - Y_r) \\ -N_\beta & s^2 - sN_r \end{bmatrix} \begin{bmatrix} \frac{\beta(s)}{\zeta(s)} \\ \frac{\Psi(s)}{\zeta(s)} \end{bmatrix} = \begin{bmatrix} Y_\zeta \\ N_\zeta \end{bmatrix}$$

The following transfer functions can be

extracted:

$$\frac{\beta(s)}{\zeta(s)} = \frac{Y_\zeta s + (Y_r N_\zeta - V_T N_\zeta - Y_\zeta N_r)}{V_T s^2 - (Y_\beta + V_T N_r) s + (Y_\beta N_r + V_T N_\beta - Y_r N_\beta)}$$

$$\frac{\Psi(s)}{\zeta(s)} = \frac{V_T N_\zeta s + (Y_\zeta N_\beta - Y_\beta N_\zeta)}{s \{ V_T s^2 - (Y_\beta + V_T N_r) s + (Y_\beta N_r + V_T N_\beta - Y_r N_\beta) \}}$$

$$\frac{R(s)}{\zeta(s)} = \frac{V_T N_\zeta s + (Y_\zeta N_\beta - Y_\beta N_\zeta)}{V_T s^2 - Y_\beta + V_T N_r) s + (Y_\beta N_r + V_T N_\beta - Y_r N_\beta)}$$

Using the equation (10b) in Chapter I the transfer function for yaw rate to n_y is

$$\frac{N_y(s)}{R(s)} = \frac{V_T}{g} \frac{Y_\zeta s^2 + (Y_r N_\zeta - Y_\zeta N_r) s + (Y_\zeta N_\beta - Y_\beta N_\zeta)}{V_T N_\zeta s + (Y_\zeta N_\beta - Y_\beta N_\zeta)}$$

Substituting coefficient data obtained from Appendix A results in the transfer functions as:

$$\frac{R(s)}{\zeta(s)} = \frac{-14.5(s+0.11)}{s^2 + 0.245s + 14.5}$$

$$\frac{N_y(s)}{R(s)} = \frac{-0.14(s^2 - 0.01s - 20.9)}{s + 0.11}$$

The resulting turn coordinator block diagram for analysis purposes is given in Figure 3-8.

(1) Root Locus Evaluation.

(a) Yaw Rate Loop. The loop transfer function is

$$\frac{R(s)}{E(s)} = \frac{580(s+0.11)}{s^3 + 40.25s^2 + (24.3 + 580KR_3)s + (580 + 63.8KR_3)}$$

Appendix C shows the root locus plot of the yaw rate loop for varying KR_3 . Selecting a gain KR_3 of 0.40 results in the following characteristics:

$$s = -3.581 \pm 2.339j$$

$$\phi = 56.85^\circ$$

$$\zeta = 0.8372$$

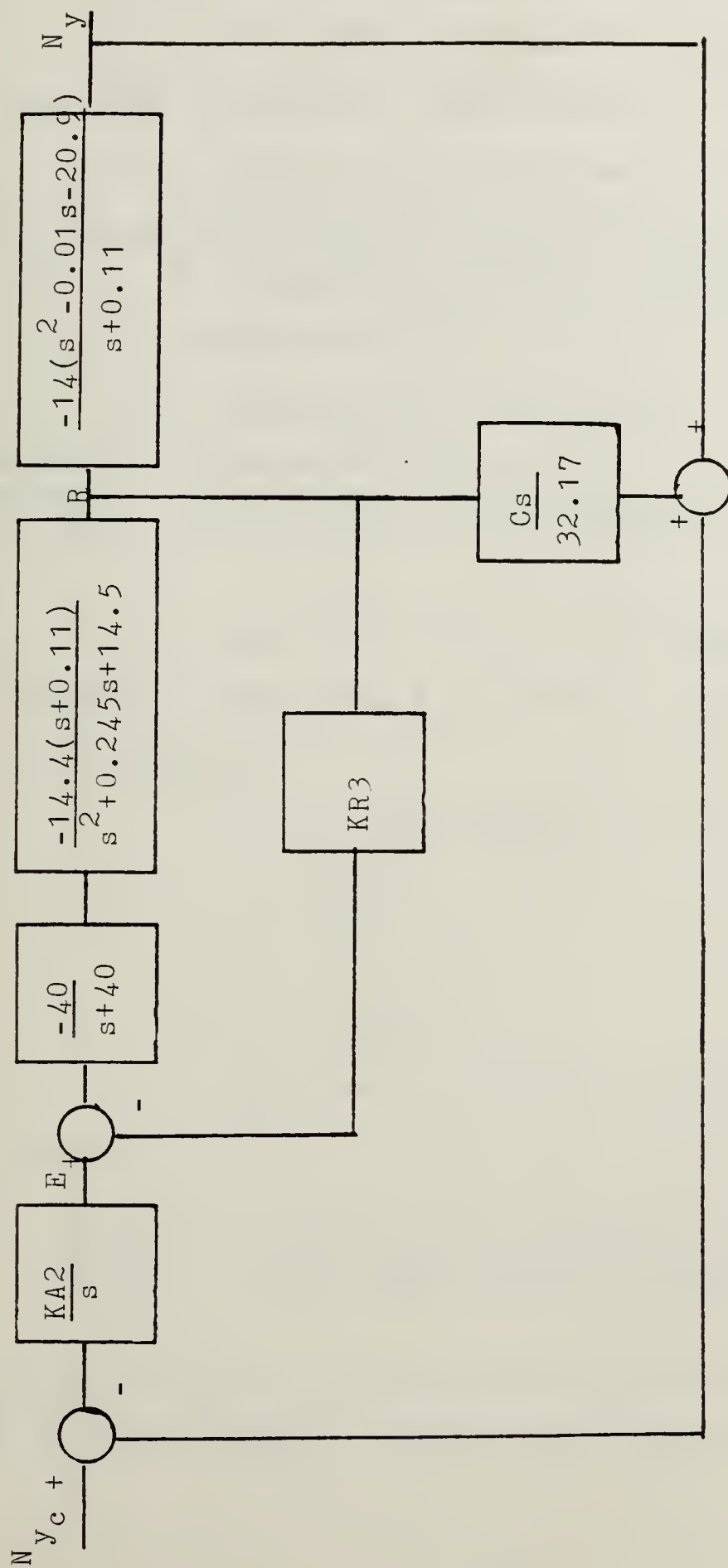
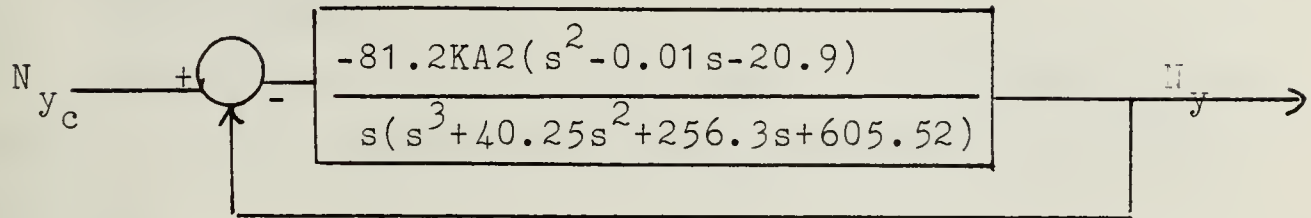


Figure 3-8 Turn Coordinator Autopilot Block Diagram (Analysis)

$$\omega_n = 0.6807 \text{ Hz}$$

$$\phi = 56.85 \text{ degrees}$$

(b) Turn Coordinator Loop. With a KR3 of 0.40 the turn coordinator loop becomes:



The transfer function is:

$$\frac{N_y(s)}{N_{y_c}(s)} = \frac{-81.2KA2(s^2 - 0.01s - 20.9)}{s^4 + 40.25s^3 + (244.7 - 81.2KA2)s^2 + (604.2 + 81.2KA2)s + 1697KA2}$$

The root locus plot for varying KA2 is shown in Appendix C. Selecting a gain KA2 of 0.25 yields characteristics as follows:

$$s = -2.206 \pm 2.807j$$

$$\phi = 38.16^\circ$$

$$\zeta = 0.618$$

$$\omega_n = 0.5682 \text{ Hz}$$

The turn coordinator system transfer function $G(s)$ becomes:

$$\frac{N_y(s)}{N_{y_c}(s)} = \frac{-32.48(s^2 - 0.01s - 20.9)}{s^4 + 40.25s^3 + 212.2s^2 + 604.5s + 678.8}$$

The system is type 1 and therefore has zero steady state error to a step input. Figure 2-5a shows the response

of the turn coordinator for a step aileron input. Note that an n_{y_c} of zero results in a coordinated turn.

B. AUTOPILOT OUTER LOOP REQUIREMENTS AND DESIGNS

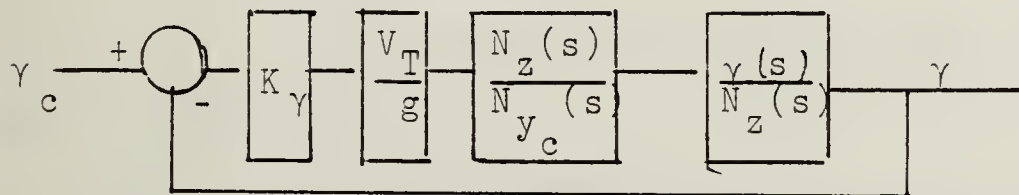
1. Description

The outer loop auto pilot has two functional loops consisting of an altitude hold and a vertical flight path angle hold.

2. Vertical Flight Path Angle System

The purpose of the vertical flight path angle hold loop or gamma command loop is to provide missile reponse to a command of 8.6 degrees during a specified phase in the terminal profile.

a. Block Diagram



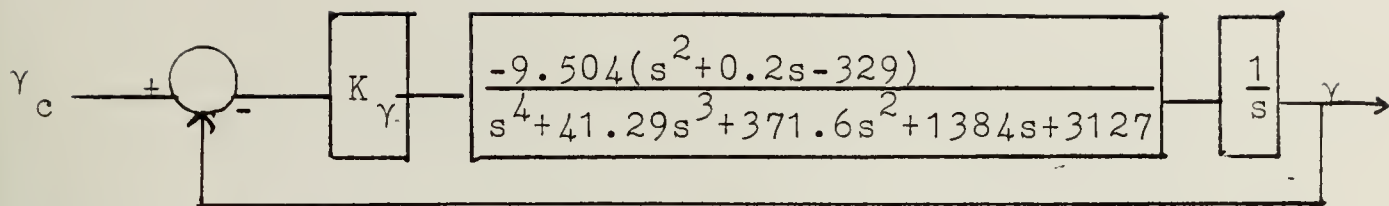
b. Assumption

- 1) Bank angle is zero.

c. Design

Starting with equation (10a) $n_z = \frac{V_T(Q - \dot{\alpha})}{g} = \frac{V_T}{g} \dot{\gamma}$

the transfer function $\frac{\gamma(s)}{N_z(s)} = \frac{g}{V_T(s)}$ can be derived. Using the inner loop design previously for load factor the vertical flight path angle block diagram becomes:



The transfer function $\frac{\gamma(s)}{\gamma_c(s)}$ is:

$$\frac{\gamma(s)}{\gamma_c(s)} = \frac{-9.504K (s^2 + 0.2s - 329)}{s^5 + 41.29s^4 + 37.6s^3 + (1384 - 9.504K)s^2 + (3127 - 1.9K_{\gamma})s + 3127K_{\gamma}}$$

(1) Root-Locus Evaluation. Appendix C shows the root locus plot of the vertical flight path angle loop for varying gain K_{γ} . A gain K_{γ} of 1.0 yields the following characteristics:

$$s = 1.2725 \pm 2.5407j$$

$$\phi = 26.6^\circ$$

$$\zeta = 0.4478$$

$$\omega_n = 0.45 \text{ Hz}$$

The system transfer function $G(s)$ with a gain of 1.0 becomes:

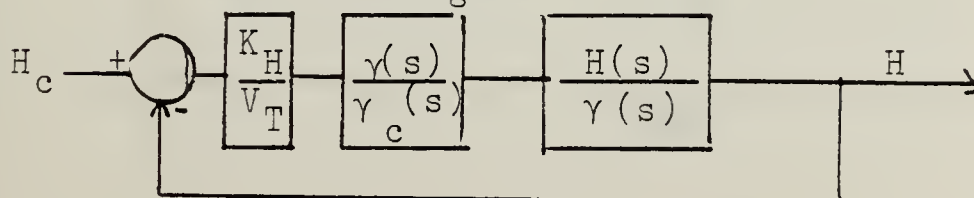
$$\frac{\gamma(s)}{\gamma_c(s)} = \frac{-9.504(s^2 + 0.2s - 329)}{s^5 + 41.29s^4 + 371.6s^3 + 1374.5s^2 + 3125.1s + 3127}$$

Figure 3-9 depicts the system response to a commanded vertical flight path angle of 8.6 degrees.

3. Altitude Hold System

The purpose of the altitude hold autopilot is to hold altitude at 50 feet during specified flight phases.

a. Block Diagram



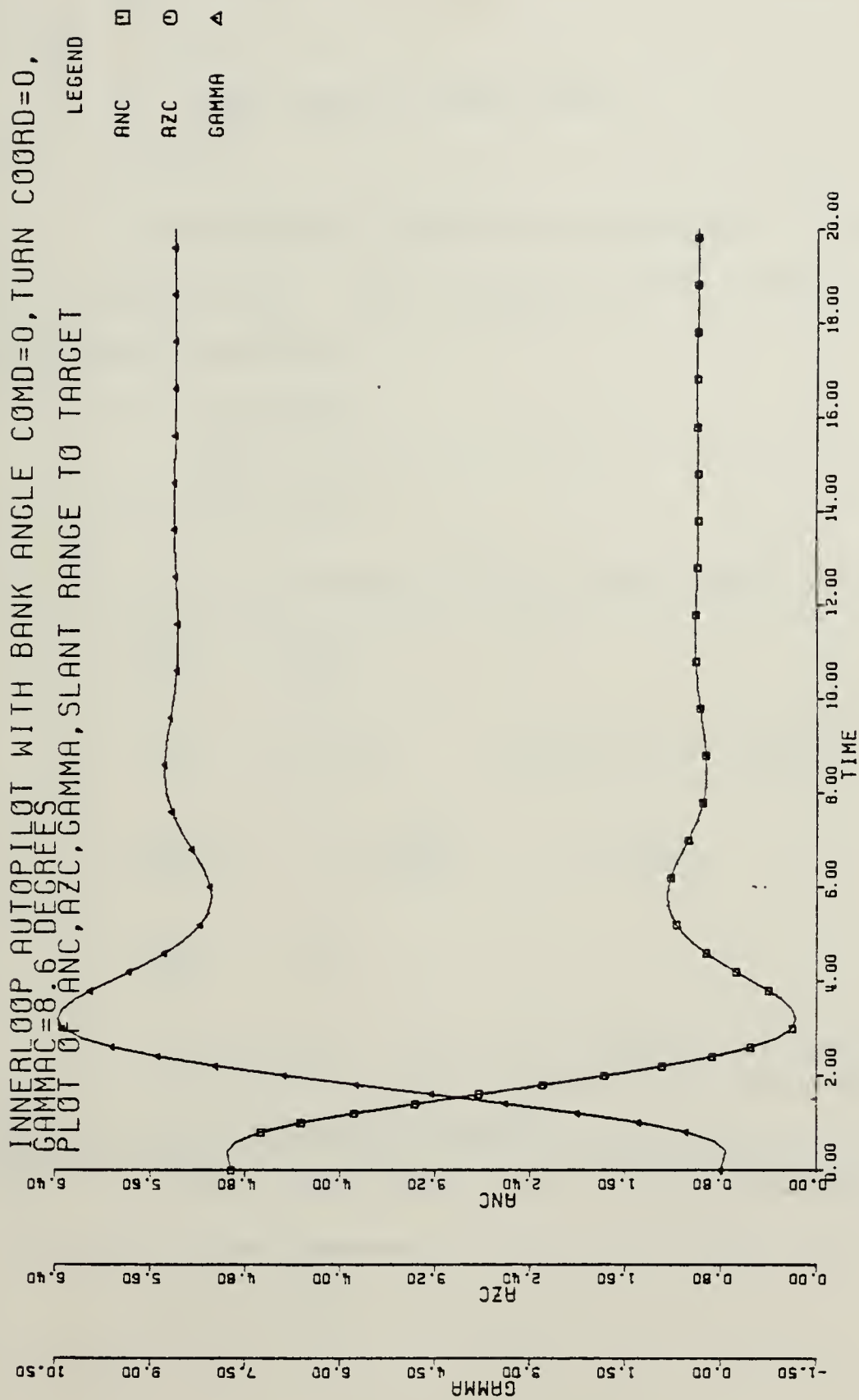


Figure 3-9 System Response to Commanded 8.6° Vertical Flight Path Angle

b. Assumptions

1) Vertical rate of climb (or descent)

subtends a small angle (γ is less than 20°), therefore

$$H = V_T \sin \gamma = V_T \gamma.$$

2) Bank angle equals zero.

c. Design

Let altitude command and altitude be designated H_c and H respectfully. The design is based upon the following two relations:

$$H = K_H (H_c - H)$$

$$\gamma_c = \frac{K_H}{V_T} (H_c - H)$$

From the vertical flight path angle development,

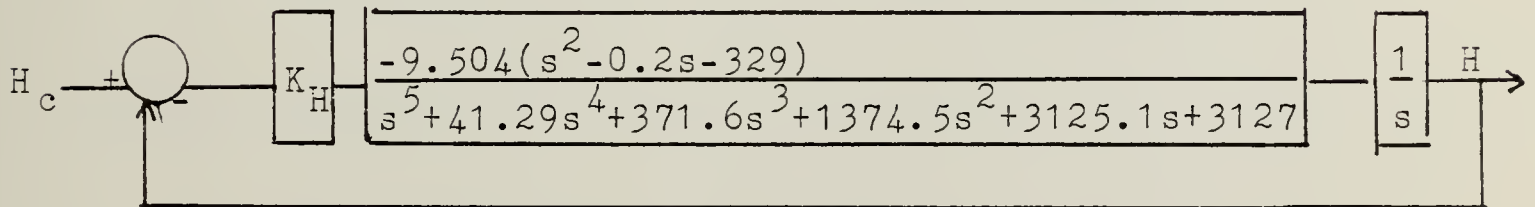
$$\frac{\gamma(s)}{N_z(s)} = \frac{g}{V_T s}$$

$$sH(s) = V_T \gamma(s) \quad (\text{Divide both sides by } a_n(s))$$

$$\frac{sH(s)}{N_z(s)} = V_T \frac{\gamma(s)}{N_z(s)} = V_T \frac{g}{V_T s}$$

$$\frac{H(s)}{\gamma(s)} = \frac{V_T}{s}$$

The altitude hold block diagram becomes:



The transfer function $H(s)/H_c(s)$ is:

$$\frac{H(s)}{H_c(s)} = \frac{-9.504KH(s^2+0.2s-329)}{s^6+41.29s^5+371.6s^4+1374.5s^3+(3125.1-9.504KH)s^2+(3127-1.9KH)s+3127KH}$$

(1) Root Locus Evaluation. Appendix C contains the root locus plot of the altitude hold loop for a varying gain KH. Again KH of 0.3 results in characteristics:

$$s = -1.4045 \pm 2.424j$$

$$\phi = 30.08^\circ$$

$$\zeta = 0.501$$

$$\omega_n = 0.445 \text{ Hz}$$

The altitude hold loop transfer function

G(s) with KH of 0.3 is:

$$\frac{H(s)}{H_c(s)} = \frac{2.8512(s^2+0.2s-329)}{s^6+41.29s^5+371.6s^4+1374.5s^3+3122.25s^2+3126.4s+938.1}$$

and Figure 3-10 shows the response to a γ_c of 50 feet.

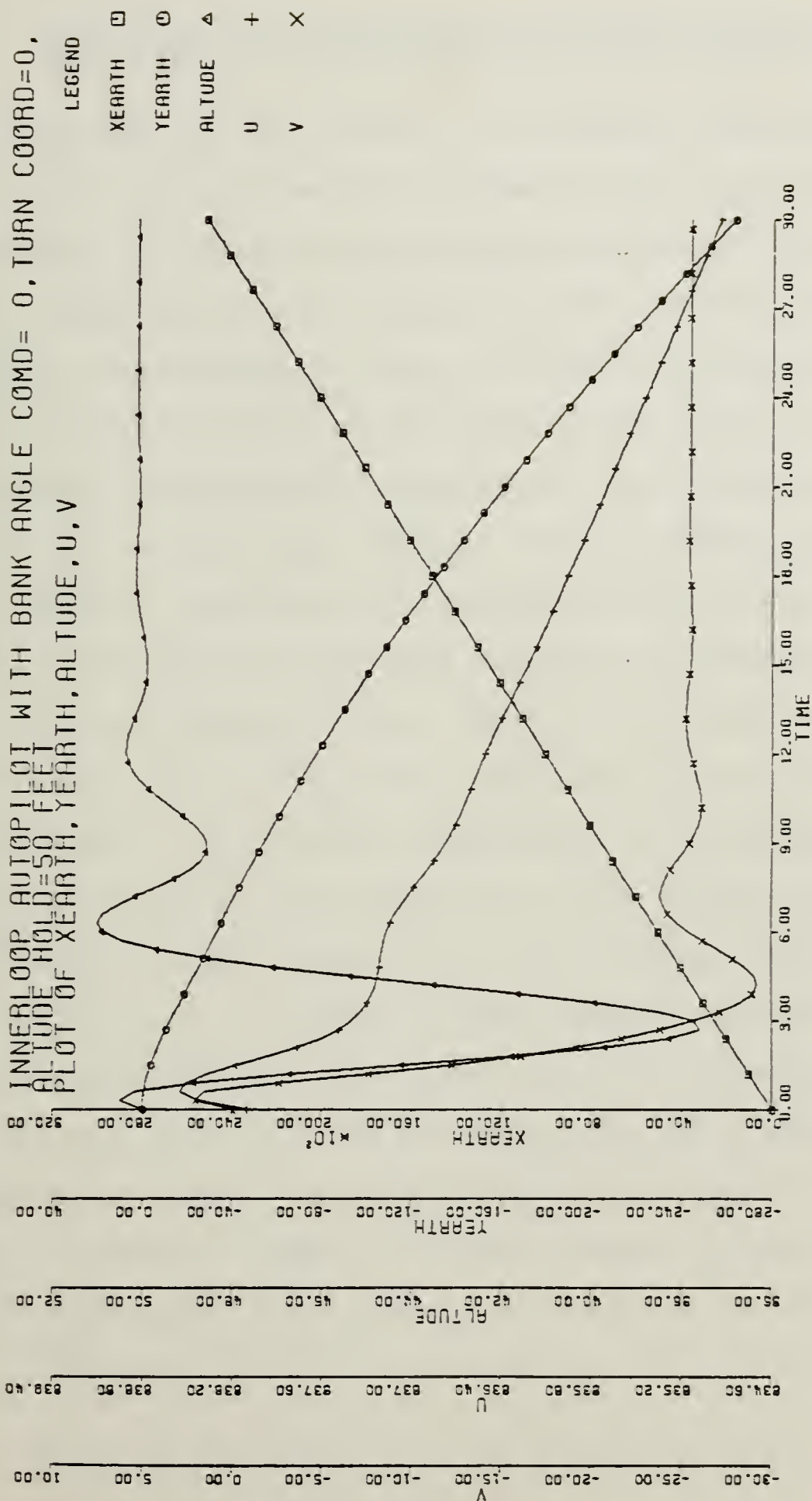


Figure 3-10 System Response to 50 ft. Altitude Hold Command

IV. DEVELOPMENT AND SIMULATION OF MISSILE GUIDANCE SYSTEM

The purpose of this study is to evaluate the effect of limited roll rate and various guidance laws on the terminal performance of a bank-to-turn cruise missile using proportional navigation in the terminal (attack) phase against a medium to large combatant ship. A baseline guidance and control scheme is designed and studied which uses a pop out maneuver, proportional navigation, and bank-to-turn maneuvering in the attack phase. The trajectory parameters and navigation constants are optimized for best performance against a moving ship utilizing blinking countermeasures. The missile is assumed to have limited roll performance due to the use of differential stabilizer for roll control vice ailerons. The terminal performance of this baseline system is evaluated for varying roll rate limits, electronic countermeasure blinking rates and burn through ranges.

A second control scheme is also designed and evaluated for the attack phase. This mode uses a sea skimming scheme in which a 50 foot altitude is maintained and proportional navigation is used in azimuth during ingress until a specified range is reached at which time proportional navigation is used in both azimuth and elevation to attack the target.

A. MISSION DESCRIPTION

1. Baseline Guidance Scheme (Pop Out Maneuver)

The mission is divided into four phases:

- a) ingress
- b) offset
- c) popup
- d) attack

The mission commences with target ship located 25,000 feet north of the missile and moving east at 21 knots. The missile initial heading is north.

The ingress phase commences with the missile flying at an altitude of 50 feet on altitude hold and utilizing proportional navigation in azimuth to home in on the target. At a given range the offset phase is initiated with a turn to the right of approximately 12 degrees followed by a commanded bank angle of zero degrees. No proportional navigation is used in this phase. At another given range a pop up maneuver is initiated which generates a low angle climb in preparation for the attack phase. During the pop up maneuver, proportional navigation is used to begin turning the missile toward the target. Finally the missile enters the attack phase at a specified range where proportional navigation is used in both vertical and azimuth planes. In this phase the bank angle is unlimited but roll rates are limited and used as one of the parameters in studying miss distances. The second parameter under study is the electronic

counter measure blinking rate frequency which is initiated at the start at the start of the attack phase and allowed to remain activated until a specified burn through range which is the third miss distance study parameter. Figure 4-1 is a geometric depiction of the missile flight path.

2. Alternate Guidance Scheme (Sea Skimmer)

The mission for this guidance scheme is divided into two phases:

- a. ingress
- b. attack

This mission begins with the same initial scenario as the baseline scheme, however, the pop out maneuvers (turn and pop up phases) is eliminated.

The missile flies at 50 foot altitude during the ingress phase and utilizes proportional navigation in azimuth until a range of 3000 feet at which point the missile enters the attack phase and dives in on the target using proportional navigation in both azimuth and elevation. This low altitude approach essentially resembles a sea skimming effect. Figure 4-2 shows the geometric flight profile of this scheme.

3. Electronic Counter Measures (ECM)

It is assumed that the target has the ECM capability of simultaneously shifting the aim point of the missile 75 feet aft and 10 feet vertically. The simulation is tested for ECM blinking frequencies of 0.5, 1.0, and 2.0 cycles

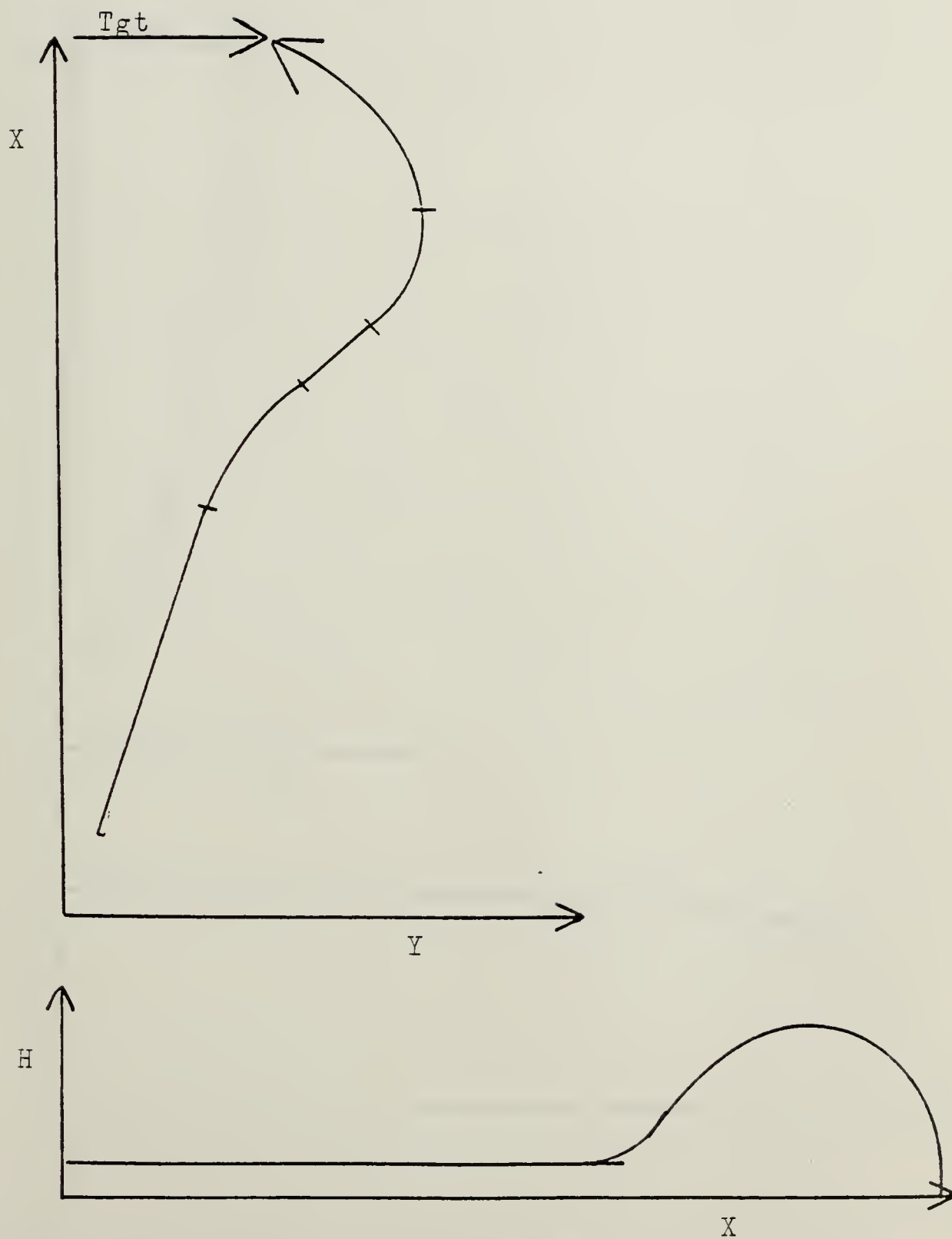


Figure 4-1 Baseline Guidance Scheme Flight Profile

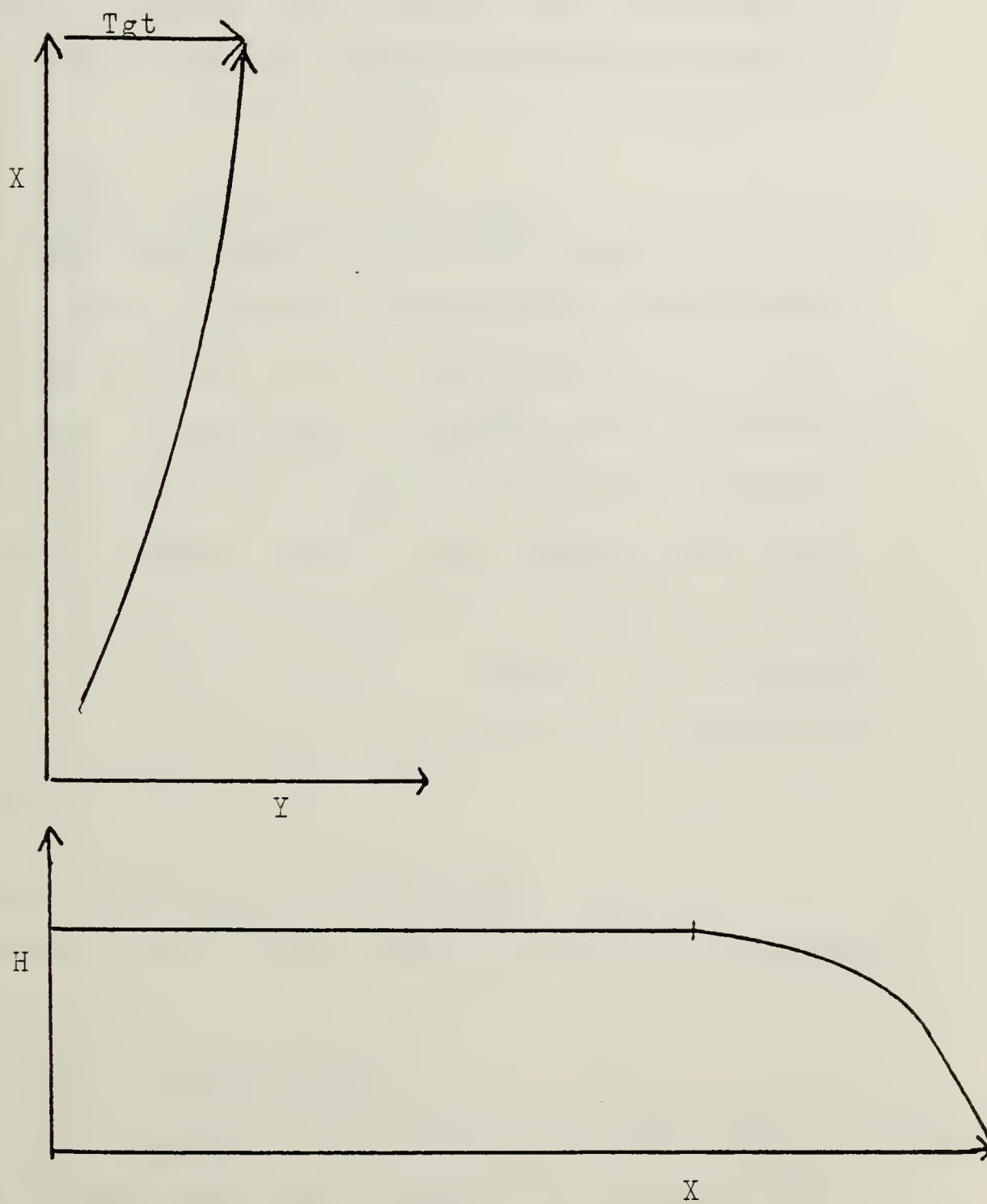


Figure 4-2 Sea Skimmer Guidance Scheme Flight Profile

per second. Blinking is commenced during the attack phase and continues until jammer burn through occurs when the target signal power can be seen over jammer power. Although 3800 feet (as calculated using Hosington, {Ref. 3}) is considered a typical burn through range the missile is tested for burn through ranges from 3800 feet down to 400 feet.

4. Glint

This study models glint with a gaussian function that gives the aim point a random shift effect with a variance of 25 feet in the Y axis and 4 feet in both the X and Z axes. Since glint is imposed as a fluctuation in target coordinates and target coordinates are used to calculate the target line of sight angles then glint is modeled as inversely proportional to range as required. For ease in simulation glint is imposed only during the attack phase. Results for runs with glint included are presented in Chapter IV.

B. SEEKER EQUATIONS AND SIMULATION

A flow diagram of the seeker simulation is presented in Figure 4-3.

1. Line of Sight Rates

It is assumed that the missile seeker has the ability to sense target range and target line of sight rates in azimuth and elevation ($\dot{\sigma}_{AZ_B}$ and $\dot{\sigma}_{EL_B}$) in the body coordinate system out to a range of 25,000 feet.

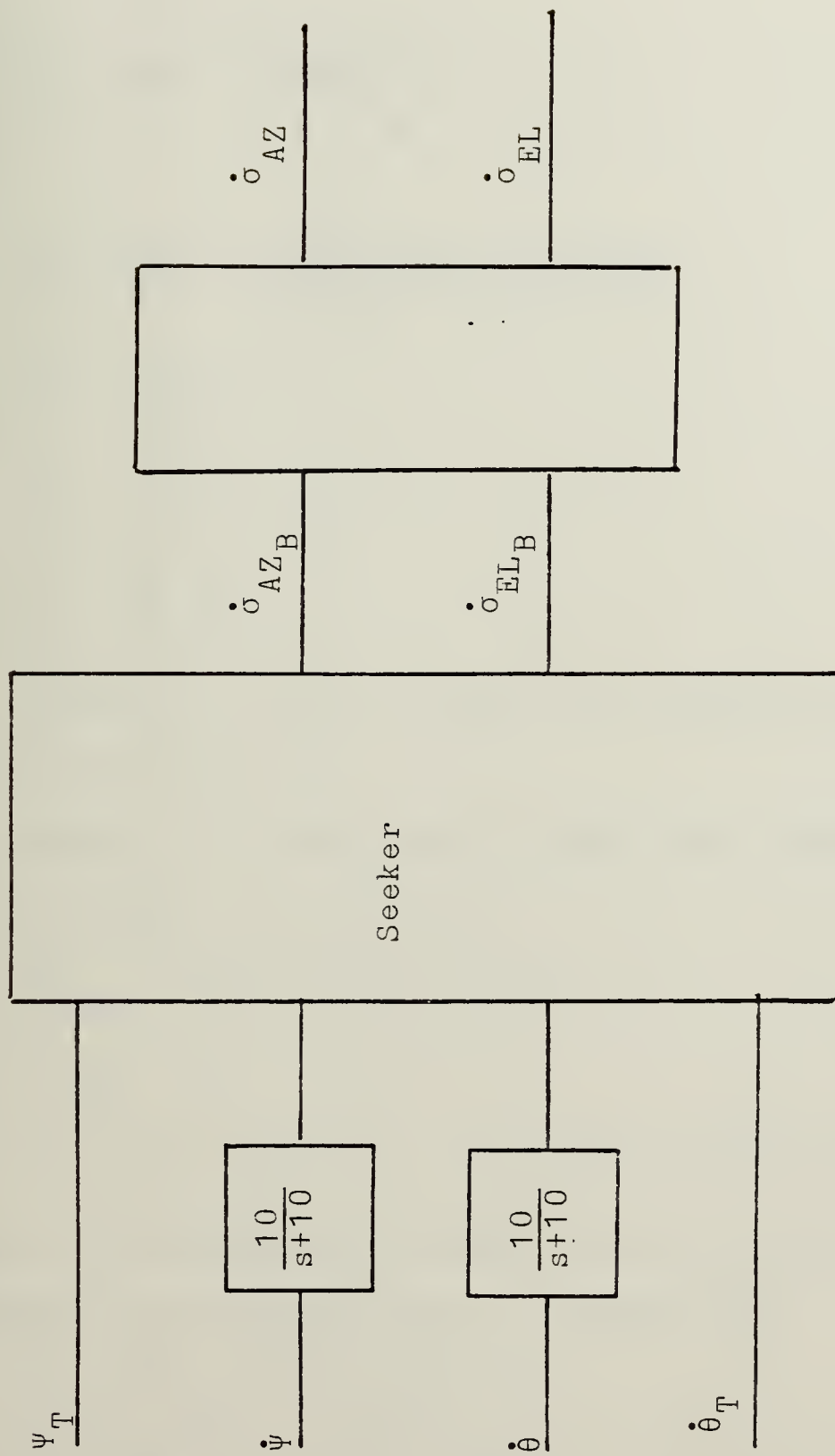


Figure 4-3 Seeker Simulation Flow Chart

These line of sight rates are generated in simulation by a two step procedure. First, the line of sight rates in earth referenced azimuth and elevation ($\dot{\sigma}_{AZ}$ and $\dot{\sigma}_{EL}$) are constructed by using the following relations:

$$\psi_T = \tan^{-1} \frac{Y_T - Y_E}{X_T - X_E}$$

$$\theta_T = \tan^{-1} \frac{-H}{((X_T - X_E)^2 + (Y_T - Y_E)^2)^{\frac{1}{2}}}$$

$$\sigma_{AZ} = \psi_T - \psi$$

$$\dot{\sigma}_{AZ} = \dot{\psi}_T - \dot{\psi}$$

$$\sigma_{EL} = \theta_T - \theta$$

$$\dot{\sigma}_{EL} = \dot{\theta}_T - \dot{\theta}$$

Figures 4-4 and 4-5 depict the geometry represented by the above equations.

Second, the body line of sight rates are calculated from the following transformation.

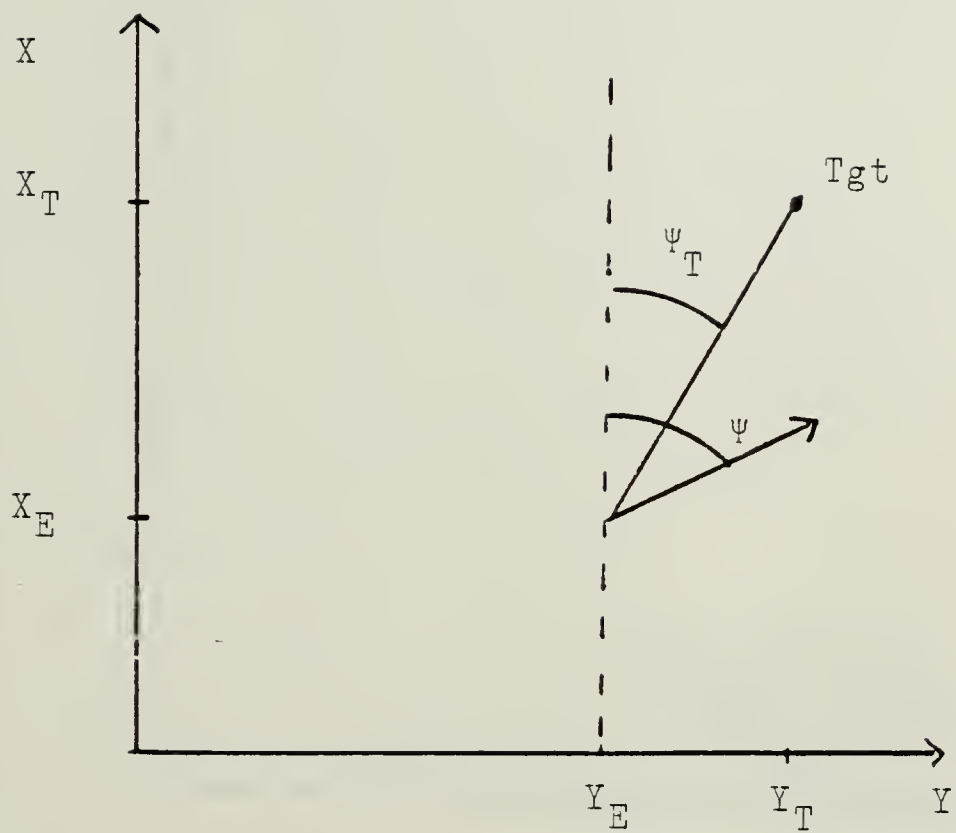
$$\dot{\sigma}_{AZ_B} = -\dot{\sigma}_{EL} \sin \phi + \dot{\sigma}_{AZ} \cos \theta \cos \phi$$

$$\dot{\sigma}_{EL_B} = \dot{\sigma}_{EL} \cos \phi + \dot{\sigma}_{AZ} \cos \theta \sin \phi$$

Once the body rates have been simulated ($\dot{\sigma}_{AZ_B}$, $\dot{\sigma}_{EL_B}$) they are transformed to earth horizontal and vertical rates through the transformation T_ϕ , defined by:

$$\dot{\sigma}_{EL} = \dot{\sigma}_{EL_B} \cos \phi - \dot{\sigma}_{AZ_B} \sin \phi$$

$$\dot{\sigma}_{AZ} = \dot{\sigma}_{EL_B} \sin \phi + \dot{\sigma}_{AZ_B} \cos \phi$$



$$\sigma_{AZ} = \psi_T - \psi$$

Figure 4-4 Azimuth Line of Sight Description

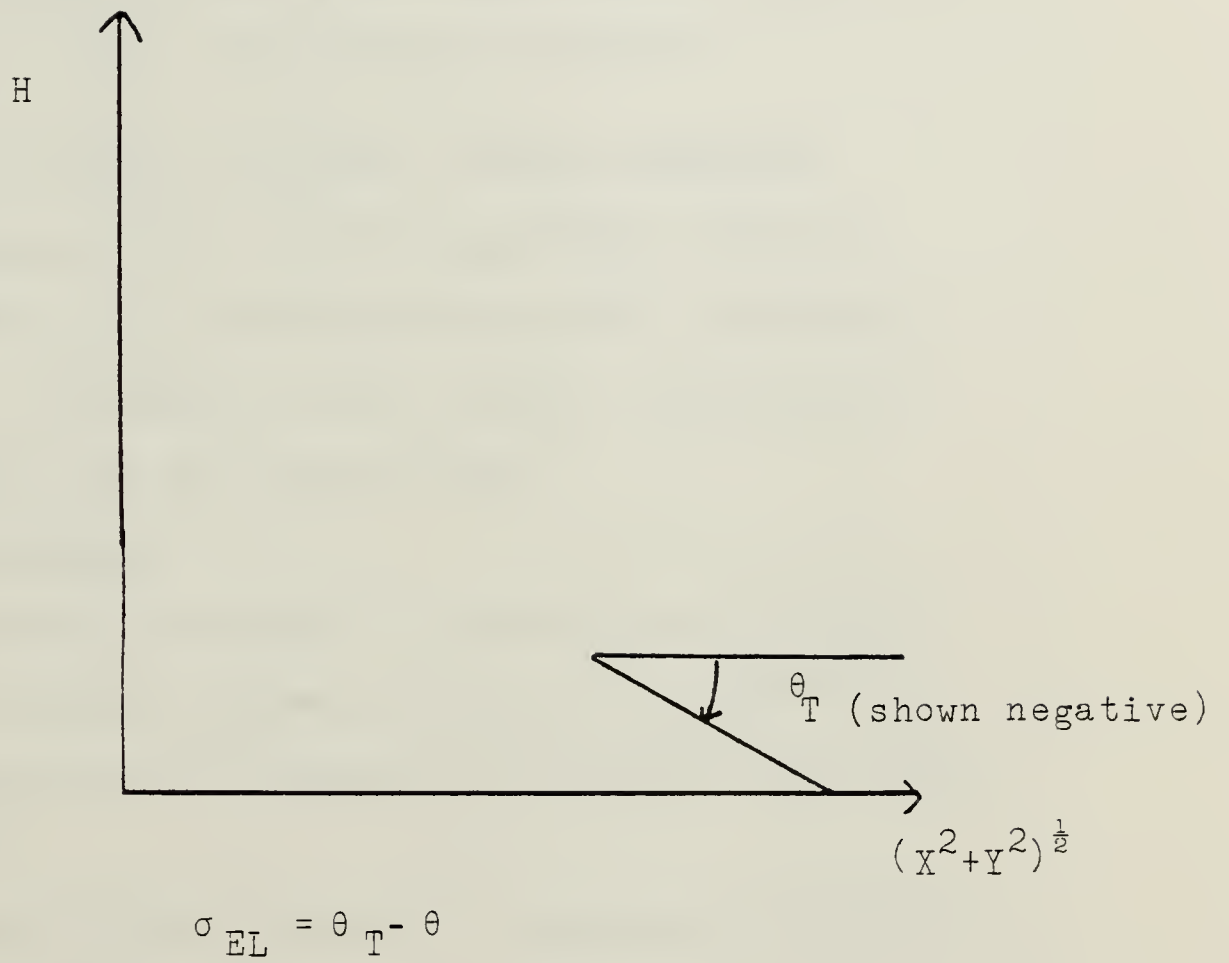


Figure 4-5 Elevation Line of Sight Description

This transformation includes the assumption that θ is small throughout the mission. The earth horizontal and vertical line of sight rates ($\dot{\sigma}_{EL}$ and $\dot{\sigma}_{AZ}$) are then used in the appropriate guidance laws for proportional navigation.

2. Missile Dynamic Filters

In order to filter out missile dynamics from the seeker line of sight rates, a low pass filter, $10/(S+10)$, is used at the input to the seeker on $\dot{\theta}$ and $\dot{\psi}$.

C. BASELINE GUIDANCE LAW DESIGN (POPOUT MANEUVER)

A flow diagram of the baseline guidance scheme is shown in Figure 4-6. Switch positions are a function of mission phase. Each phase of the mission is described below beginning with the attack phase.

1. Attack Phase

Proportional navigation is used in azimuth and elevation to construct guidance commands to the missile autopilot commencing at a range of 9100 feet in the manner described below.

a. Proportional Navigation Constants and Guidance Commands

The earth horizontal and vertical line of sight rates ($\dot{\sigma}_{AZ}$ and $\dot{\sigma}_{EL}$) which are generated from the body rates $\dot{\sigma}_{AZ_B}$ and $\dot{\sigma}_{EL_B}$ by the transformation T_ϕ are multiplied by a navigation constant and V_T/g to generate commanded lateral accelerations in the earth vertical and horizontal planes.

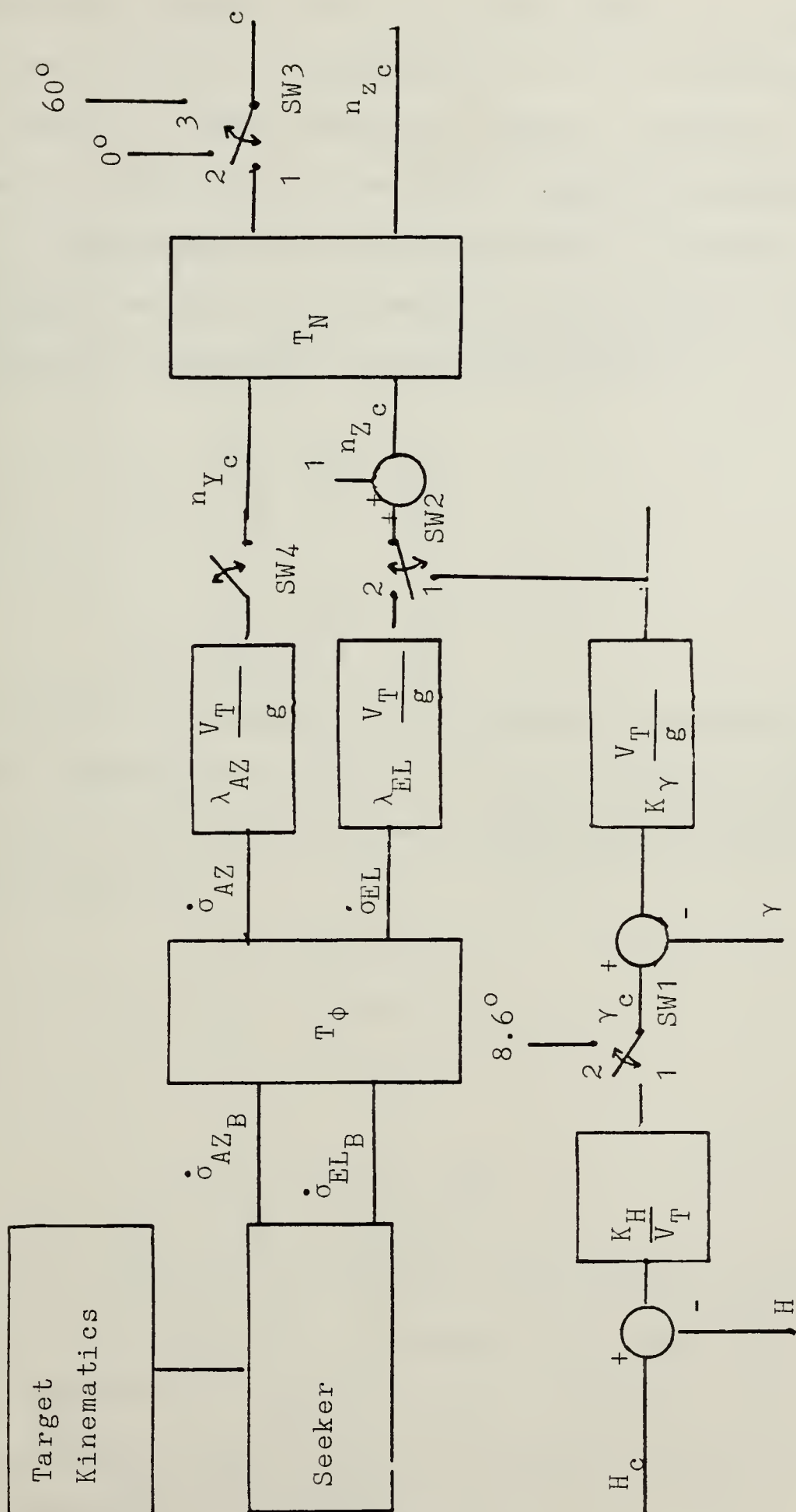


Figure 4-6 Baseline Guidance Law Flow Diagram

A navigation constant of 4.0 in each plane was found to yield best results. Values from 3.0 to 4.5 were evaluated with results of that evaluation shown in Chapter V. A one g bias is applied to the vertical commanded lateral acceleration to compensate for acceleration due to gravity. Thus two lateral acceleration commands (n_{Y_c} and n_{Z_c}) are computed in the earth horizontal and vertical planes.

$$n_{Y_c} = \lambda_{AZ} \frac{V_T}{g} \dot{\sigma}_{AZ} \quad (13)$$

$$n_{Z_c} = \lambda_{EL} \frac{V_T}{g} \dot{\sigma}_{EL} + 1 \quad (14)$$

These commanded lateral accelerations are subjected to a further transformation (T_N) in order to generate commanded bank angle and normal load factor which are required by the missile autopilot.

$$\phi_c = \tan^{-1} \frac{n_{Y_c}}{n_{Z_c}}$$

$$n_{z_c} = n_{Z_c} \cos \phi + n_{Y_c} \sin \phi$$

Figure 4-7 depicts the geometric relationship described by the above two equations. Commanded bank angle (ϕ_c) and normal load factor (n_{z_c}) are used as inputs to the appropriate autopilot outer command loops to provide closed loop bank angle and load factor responses.

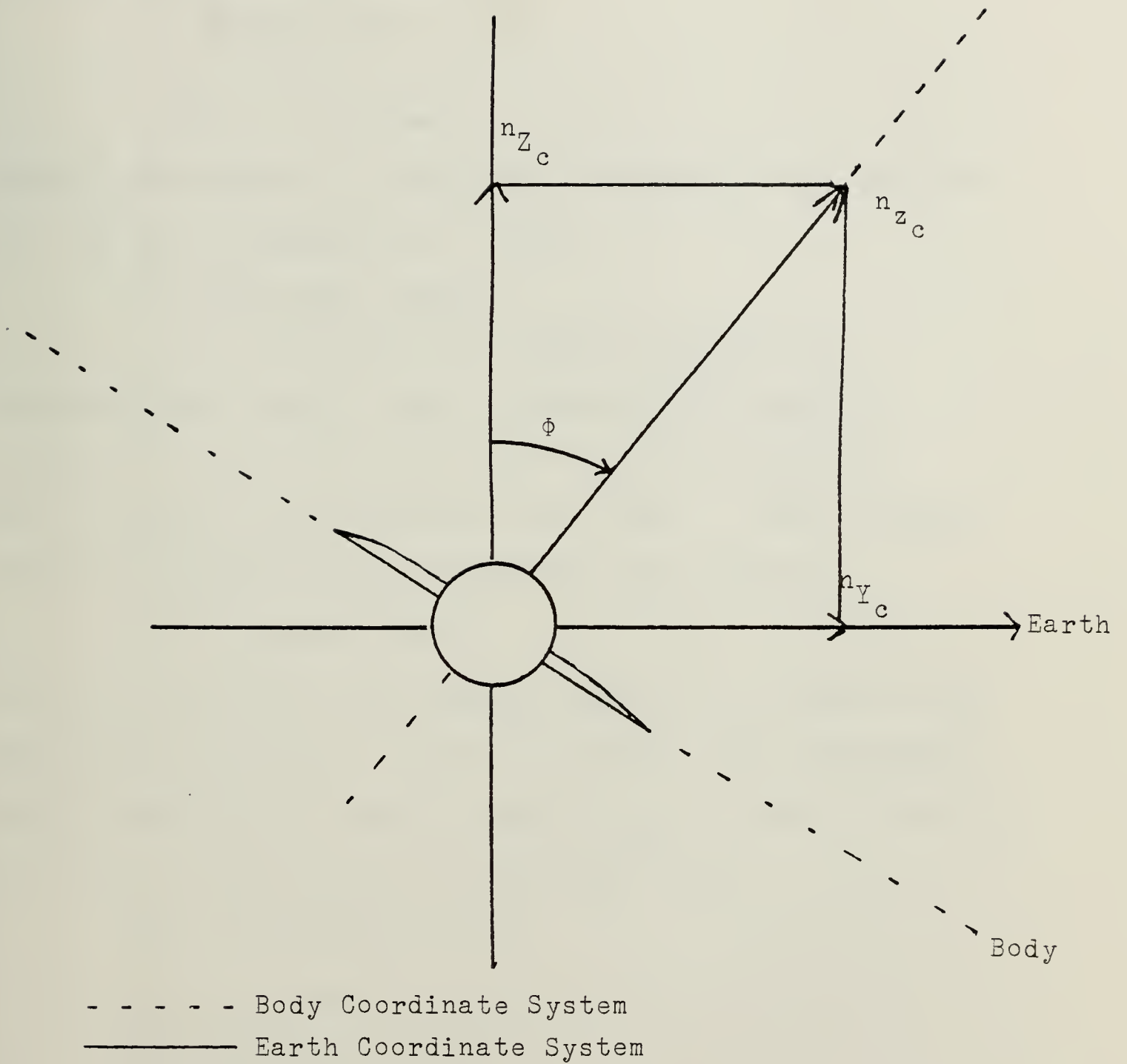


Figure 4-7 Load Factor and Bank Angle Description

b. Limits on Guidance Commands

In the attack phase, the following limits are applied to commanded variables:

$$-2 \leq n_{z_c} \leq 4$$

$$|\dot{\phi}_c| \leq \dot{\phi}_{\max}$$

Missile performance is evaluated for maximum roll rates of 50, 100 and 200 degrees per second.

c. Bank Angle Anomaly

In the attack mode there is no limit on commanded bank angle. Thus a computational scheme is required to insure that the missile always rolls the shortest way to a new commanded bank angle. This is accomplished by continuously calculating the quantity:

$$\Delta(t) = |\phi_c(t) - \phi(t)|$$

If $\Delta(t)$ is less than 180 degrees then $\phi_c(t)$ is sent to the bank angle autopilot. If $\Delta(t)$ is greater than 180 degrees then a modified bank angle command (ϕ_{c_M}) is sent to the autopilot in accordance with the following logic:

$$\phi_{c_M} = \phi_c + 360^\circ \text{ for } \phi_c < 0$$

$$\phi_{c_M} = \phi_c - 360^\circ \text{ for } \phi_c > 0$$

d. Switch Positions

The switches shown in figure 4-6 are in the following positions for the attack phase:

SW1 Either position

SW2 Position 2

SW3 Position 1

SW4 Closed

e. Attack Phase Summary

In the attack phase proportional navigation is used in both azimuth and elevation to generate bank angle and normal load factor commands to the missile autopilot. The phase is commenced at a range of 9100 feet with missile offset in heading from the target at an altitude of approximately 250 feet. Roll rate is limited to ϕ_{\max} . Bank angle is not limited. Normal load factor is limited from -2 to 4 g's.

2. Ingress Phase

The ingress phase commences with the beginning of the problem simulation when the missile is 25,000 feet from the target and initially heading north. The missile's Mach number is 0.75 and the ship's velocity is 21 knots to the east.

a. Altitude Hold Methodology and Guidance Commands

The missile is required to maintain altitude of 50 feet above sea level during this phase. It accomplishes this by comparing present altitude with 50 feet and multiplying the error by $\frac{K_H}{V_T}$ to establish a flight path angle command.

K_H is assigned a value of 0.3. This calculated flight path angle command is compared with the present flight path angle

and the difference or error is multiplied by K_H and $\frac{V_T}{g}$ to give an elevation line of sight rate, $\dot{\sigma}_{EL}$. A value of 0.3 is assigned for K_H . Thus n_{Z_c} is computed as follows:

$$n_{Z_c} = K_H \frac{V_T}{g} (\dot{\gamma}_c - \dot{\gamma}) + 1$$

The lateral acceleration command n_{Y_c} is computed exactly as described in the attack phase with bank angle and roll rates limited.

The second transformation for the ingress phase (T_N) remains the same form as the attack phase.

$$\phi_c = \tan^{-1} \frac{n_{Y_c}}{n_{Z_c}}$$

$$n_{Z_c} = n_{Z_c} \cos \phi + n_{Y_c} \sin \phi$$

b. Limits on Guidance Commands

In the ingress phase the following limits are applied to commanded variables:

$$-2 \leq n_{Z_c} \leq 4$$

$$|\phi_c| \leq |\phi_{\max}|$$

$$|\dot{\phi}_c| \leq |\dot{\phi}_{\max}|$$

The maximum bank angle allowed is 60 degrees and roll rate is limited to 50, 100 or 200 degrees per second.

c. Switch Positions

The switch positions as shown in Figure 4-6 are as follows during the ingress phase:

SW1, SW2, SW3 Position 1

SW4 Closed

3. Offset Phase

The missile initiates the offset phase at 17,800 feet. The offset phase is subdivided into two sub-phases -- turn and level.

a. Turn and Level Sub-Phases

The missile maintains an altitude of 50 feet throughout the offset phase in the same manner as described during the ingress phase. Thus

$$n_{Z_c} = K_{\gamma} \frac{V_T}{g} (\gamma_c - \gamma) + 1$$

The missile performs the coordinated turn by using a commanded bank angle and computing a normal load factor as follows:

$$\begin{aligned} \phi_C &= 60^\circ \\ n_{Z_c} &= \frac{n_{Z_c}}{\cos \phi} \end{aligned}$$

At a range of 15800 feet from the target a turn of approximately 12 degrees is accomplished. The missile then performs a straight and level maneuver by commanding zero bank angle along with the same normal load factor as follows:

$$\begin{aligned} \phi_C &= 0^\circ \\ n_{Z_c} &= \frac{n_{Z_c}}{\cos \phi} \end{aligned}$$

b. Limits on Guidance Commands

For the offset phase normal load factor is limited as follows:

$$-2 \leq n_{z_c} \leq 4$$

Commanded bank angle is fixed at 60 degrees during the turn sub-phase and 0 degrees during the level sub-phase.

c. Switch Positions

The switch position, as shown in Figure 4-6, are as follows during the offset phase:

1) Turn sub-phase

SW1, SW2 Position 1

SW3 Position 3

SW4 Open

2) Level sub-phase

SW1, SW2 Position 1

SW3 Position 2

SW4 Open

4. Pop Up Phase

The missile enters the pop up phase when the range becomes 10,200 feet. The purpose of this phase is to pop up the missile to an altitude of approximately 250 feet so that a dive into the target will give acceptable deck penetration.

a. Vertical Flight Path Angle Methodology and Guidance Commands

The missile achieves the pop up effect by commanding a vertical flight path angle of 8.6 degrees.

This commanded climb angle is compared with the actual γ and the error is multiplied by K_γ and $\frac{V_T}{g}$ to give an elevation line of sight rate. A value of 1.0 is assigned for K_γ in this simulation. Thus n_{Z_c} is computed as follows:

$$n_{Z_c} = K_\gamma \frac{V_T}{g} (\gamma_{\text{climb}} - \gamma) + 1$$

The lateral acceleration commanded n_{y_c} is computed exactly as described in the ingress phase.

The second transformation T_N is as follows:

$$\phi_c = \tan^{-1} \frac{n_{y_c}}{n_{Z_c}}$$

$$n_{z_c} = n_{Z_c} \cos \phi + n_{y_c} \sin \phi$$

The missile is free to start rolling into the target using proportional navigation during the pop up phase and thus aids in the attack phase which follows the pop up phase.

b. Limits on Guidance Commands

In the pop up phase the following limits are applied to commanded variables:

$$-2 \leq n_{z_c} \leq 4$$

$$|\phi_c| \leq |\phi_{\text{max}}|$$

$$|\phi_c| \leq |\phi_{\text{max}}|$$

The maximum bank angle is limited to 60 degrees and the maximum roll rate is limited to 50, 100 or 200 degrees per second.

c. Switch Positions

The switch positions as shown in Figure 4-6 are as follows during the pop up phase:

SW1	Position 2
SW2, SW3	Position 1
SW4	Closed

5. Guidance Summary (Baseline)

The following matrix indicates the horizontal and vertical controls during each phase of missile flight.

<u>PHASE</u>	<u>AZIMUTH CONTROL</u>	<u>ELEVATION CONTROL</u>
Ingress	PN*	Altitude Hold
Offset	ϕ Command	Altitude Hold
Popup	PN	Flight Path Angle Hold
Attack	PN	PN

*Proportional Navigation

D. ALTERNATE GUIDANCE LAW DESIGN SEA-SKIMMER

The sea skimmer scheme differs only from the baseline guidance scheme in that the offset and popup phases are eliminated. In essence this scheme is composed of an ingress phase and an attack phase.

1. Ingress Phase

The ingress phase commences with problem initialization which locates the missile 25,000 feet from the target with

identical initial conditions as the baseline guidance scheme.

The vertical load factor is computed as

$$n_{Z_c} = K_H \frac{V_T}{g} (\gamma_c - \gamma) + 1$$

The lateral acceleration command is computed as

$$n_{Y_c} = \lambda_{AZ} \frac{V_T}{g} \dot{\sigma}_{AZ}$$

The second transformation (T_N) is as follows:

$$\phi_c = \tan^{-1} \frac{n_{Y_c}}{n_{Z_c}}$$

and

$$n_{z_c} = n_{Z_c} \cos \phi + n_{Y_c} \sin \phi$$

Limits on guidance commands and switch positions for the ingress phase are identical to the ingress phase for the baseline scheme.

2. Attack Phase

The attack phase commences at 3000 feet range and uses proportional navigation in both elevation and azimuth. The missile dives into the target from 50 foot altitude.

The bank angle command and normal load factor are computed exactly as in the baseline scheme attack phase and are:

$$\phi_c = \tan^{-1} \frac{n_{Y_c}}{n_{Z_c}}$$

$$n_{z_c} = n_{z_c} \cos \phi + n_{y_c} \sin \phi$$

Limits on guidance commands and switch positions are also identical to the attack phase in the baseline guidance scheme.

3. Guidance Summary (Sea Skimmer)

The following matrix shows the horizontal and vertical controls during each phase of the sea skimmer guidance scheme.

PHASE	AZIMUTH CONTROL	VERTICAL CONTROL
Ingress	PN	Altitude Hold
Attack	PN	PN

V. PROBLEM SIMULATION, RESULTS, CONCLUSIONS AND RECOMMENDATIONS

This chapter describes the computer simulation special language used and presents the results of test runs in which roll rate, ECM blinking rate and burn through range are all varied in both the baseline guidance scheme and the sea skimming guidance scheme. From these results optimum parameters are chosen to yield minimum miss distance for each guidance scheme. Miss distance ranges are also presented for the baseline scheme with Glint imposed.

A. CSMP SIMULATION

The Continuous System Modeling Program III (CSMP III), an IBM developed system, is the modeling technique chosen for this study. CSMP, as discussed in Speclchart and Green {Ref. 4}, is compatable with the Fortran IV language, has six selectable integration methods (fourth order Runge-Kutta is used for this simulation), and has multiple special function codes that can solve a large variety of control engineering problems.

The special functions used for this simulation are:

a. FUNGEN - This function extracts the value of a function of one variable from a stored table in memory. It is used for aerodynamic coefficients.

b. TWOVAR - This function extracts the value of a function of two variables from a stored table in memory. It is used for aerodynamic coefficients.

c. INSW - $Y = \text{INSW}(X_1, X_2, X_3)$ assigns $Y = X_2$ for $X_1 < 0$, $Y = X_3$ for $X_1 \geq 0$. It is used to accomplish ECM blinking action.

d. GAUSS - This function is a random number generator with normal distribution. It is used to realize glint.

e. REALPL - This function simulates a first order lag $1/(\tau S + 1)$ filter. It is used in autopilot and seeker equations as low pass filters.

f. DEBUG - This is a computer program aid that evaluates all output parameters and variables at requested times.

In addition to the special functions, trigonometric, integral, derivative and square root functions are used to perform necessary steps with one invocation. CSMP also has the ability to perform calculations in either a sort section, where the order of computation is not considered, or a nosort section, where ordered sequential fortran statements are required. The program is structured as shows below:

MISSILE SIMULATION PROGRAM

INITIAL

CONSTANTS
AERODYNAMIC COEFFICIENT TABLES

DYNAMIC
NOSORT

MISSION PHASE LOGIC
GUIDANCE EQUATIONS
ECM (BLINKING) EQUATIONS

SORT

6 DOF MISSILE DYNAMIC EQUATIONS

INNER LOOP AUTOPILOTS SEEKER EQUATIONS

TERMINAL

OUTPUT GRAPHS

The CSMP initially sets up the two and three variable coefficients in tabular form in memory. The run commences with the missile in steady state flight with steady state variables established. These steady state variables are used to enter the tables in memory and extract coefficients which are used to calculate aerodynamic derivatives, forces, moments, and other relations. From the steady state flight condition small perturbations are made and new table entries produced. This process is repeated for all phases of flight.

B. RESULTS

Both the baseline guidance scheme and the sea skim guidance scheme were tested under the same conditions and quantitative results obtained. All scenarios started from the following initial conditions:

1. Target position - 25,000 feet north of the missile.
2. Target speed - east at 21 knots.
3. Missile speed - north at 0.75 Mach number
4. Missile altitude - 50 feet above sea level.

The simulation was run for 31 seconds. Miss distance data was obtained for varying roll rate limits, ECM blinking frequencies, and burn through ranges. The following matrix of parameters was tested:

Burn through range (feet)

2000
1500
1200
800
400

Roll rate limit (degrees per second)

200
100
50

ECM blinking frequency (Hertz)

2
1
0.5

The resulting miss distances are shown in Tables 5-1 and 5-2 for all runs. Figure 5-1 through figure 5-6 are the graphical results of simulation runs. Each run is presented in 6 consecutive figures a through f and depict the following.

- a. Commanded roll rate (PCMD) and roll rate (P) vs time.
- b. Commanded bank angle (PHICMD) and bank angle (PHI) vs time.
- c. Range, X Range, Y Range and Z Range vs time.
- d. Left and right stabilizers (LSTAB and RSTAB) vs time.
- e. Rudder position vs time.
- f. Map of YMISLE and HMISLE vs XMISLE.

The following matrix indicates the test conditions used to generate each figure:

TABLE 5-1

Baseline Guidance and Control Scheme

Miss Distance (feet)

ECM Blinking Rate	Roll Rate Limit	Burnthrough Ranges				
		400	800	1200	1500	2000
.5 cps	50	19.9	15.7	16	16	6.28
	100	17	11.3	6.95	6.95	18.16
	200	27	30	29	29	26.1
1 cps	50	24	23	11.3	9.8	10.7
	100	12.6	13.7	12.5	11	6.9
	200	5.4	3	4.9	2.9	6.57
2 cps	50	25	20	8.9	6.6	4.34
	100	23.7	15.7	2.2	1.69	6.8
	200	13.3	7.9	1.5	4.2	6.81
0 cps	50	2.5				
	100	4.4				
	200	4.5				

TABLE 5-2

Sea-Skimmer Guidance and Control Scheme

Miss Distance (feet)

ECM Blinking Rates	Roll Rate Limit	Burnthrough Ranges				
		400	800	1200	1500	2000
.5	50	43	37.7	37.7	37.7	2.8
	100	72	61	61	61	1.56
	200	44.64	28.7	37.7	28.7	1.77
1	50	54	54	38.62	28.8	1.48
	100	52	52	20	20.6	3.9
	200	65	63	26	26	3.09
2	50	34.6	31.20	37.7	37.7	2.87
	100	32.9	27.9	61	61	1.56
	200	43.5	37.35	28.8	28.8	1.77
0	50	3.9				
	100	2.7				
	200	2.6				

BASE GUIDANCE SCHEME

- 5-1 (a-f) NO ECM, 100° /sec roll rate
- 5-2 (a-f) ECM (1Hz), 100° /sec roll rate
- 5-3 (a-f) ECM (1Hz), 50° /sec roll rate
- 5-4 (a-f) ECM (1Hz), 200° /sec roll rate

SEA SKIMMER SCHEME

- 5-5 (a-f) NO ECM, 100° /sec roll rate
- 5-6 (a-f) ECM (1Hz), 100° /sec roll rate

1. Analysis of Baseline Scheme Results

a. Varying Burn Through Range

Miss distances generally decrease as the burn through range increases. For runs beyond 1500 feet burn through ranges, the miss distances are close enough to be considered as hits since most of the miss distance is in the Y component of range which has the largest offset (75 feet) applied during ECM.

b. Varying ECM Blinking Frequency

The miss distance decreases as blinking rate increases for the same burn through range. Miss distances for burn through ranges beyond 1200 feet are particularly good for all three roll rates.

c. Varying Roll Rate Limit

Varying roll rate limit results in the largest variation in miss distance. For 200 degree per second roll rate limit and 0.5 Hertz ECM blinking frequency the

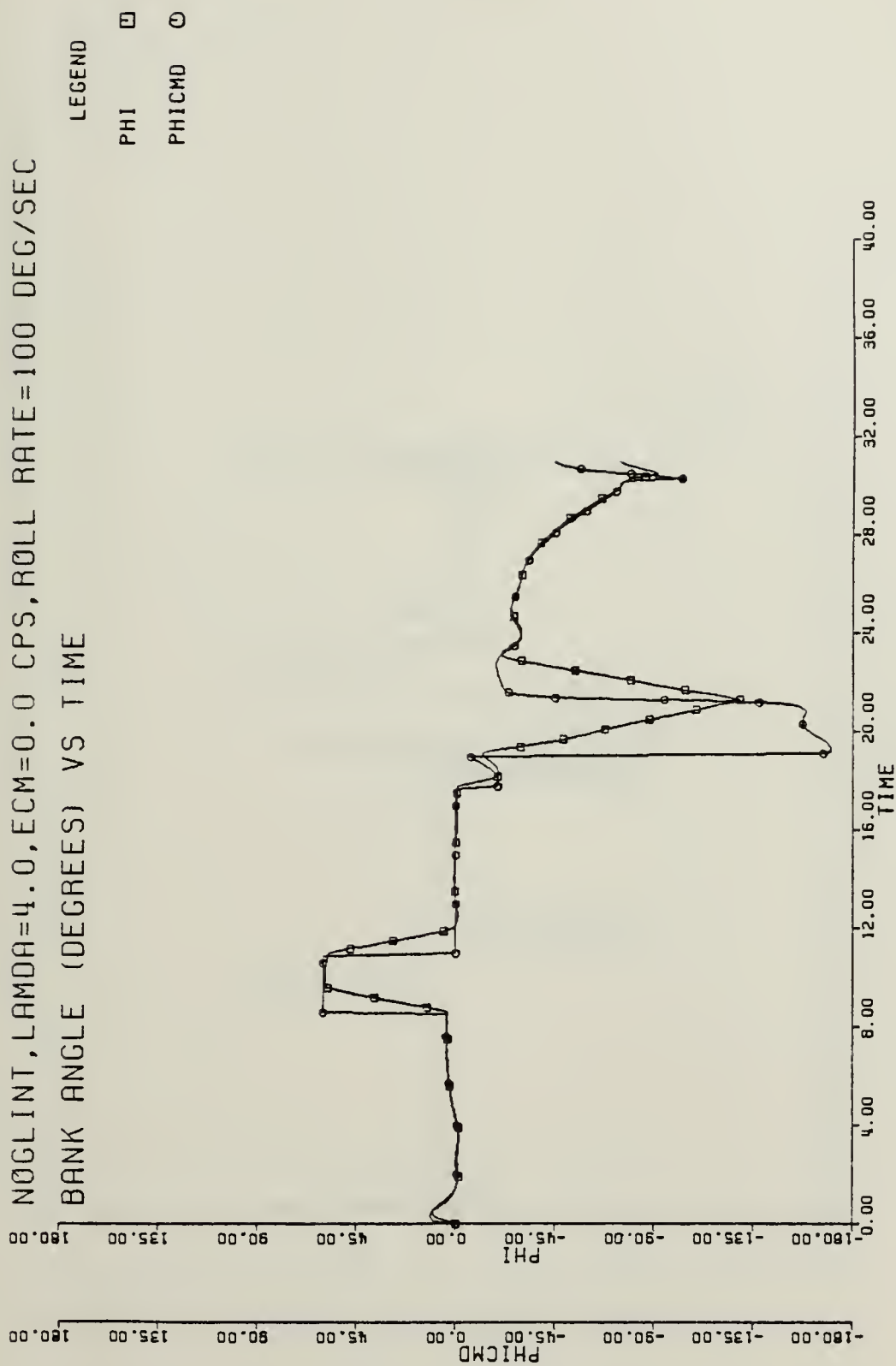


Figure 5-1a Baseline Response for No ECM, Roll Rate Limit 100 deg/sec
(PHICMD, PHI vs TIME)

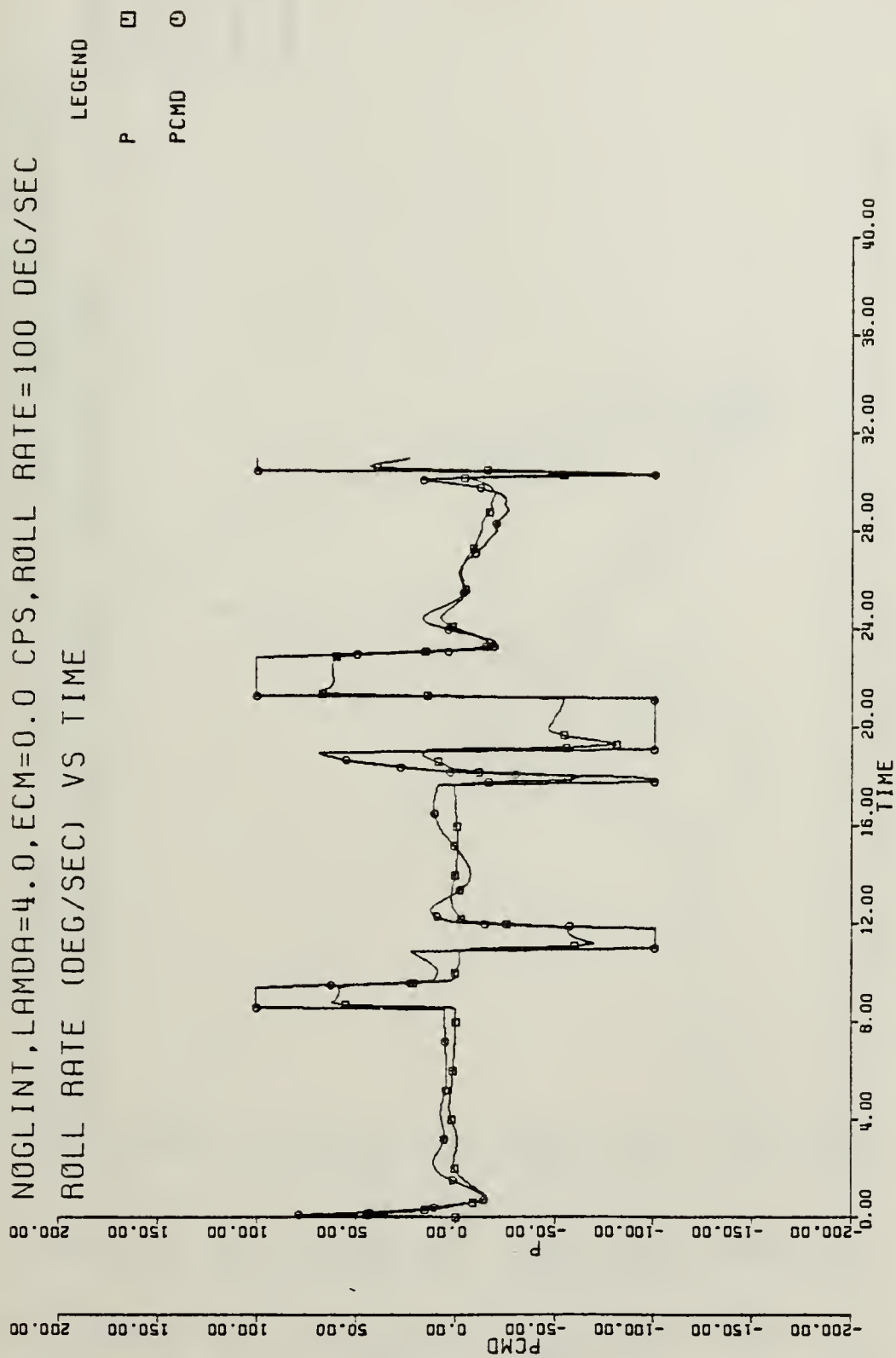


Figure 5-1b Baseline Response for No ECM, Roll Rate Limit 100 deg/sec
 (PCMD, P vs TIME)

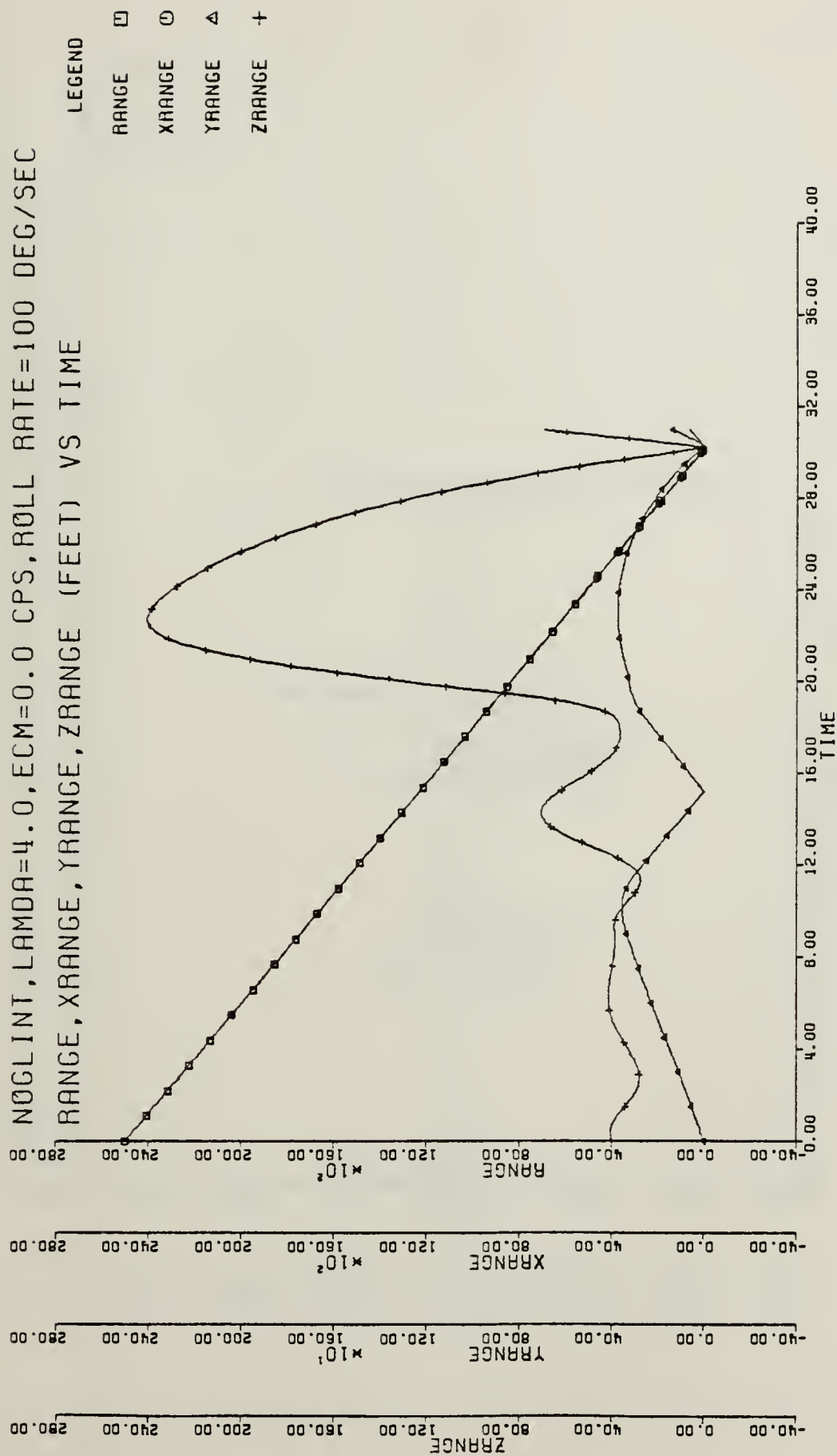


Figure 5-1c Baseline Response for No ECM, Roll Rate Limit 100 deg/sec
 (RANGE, X RANGE, Y RANGE, Z RANGE vs TIME)

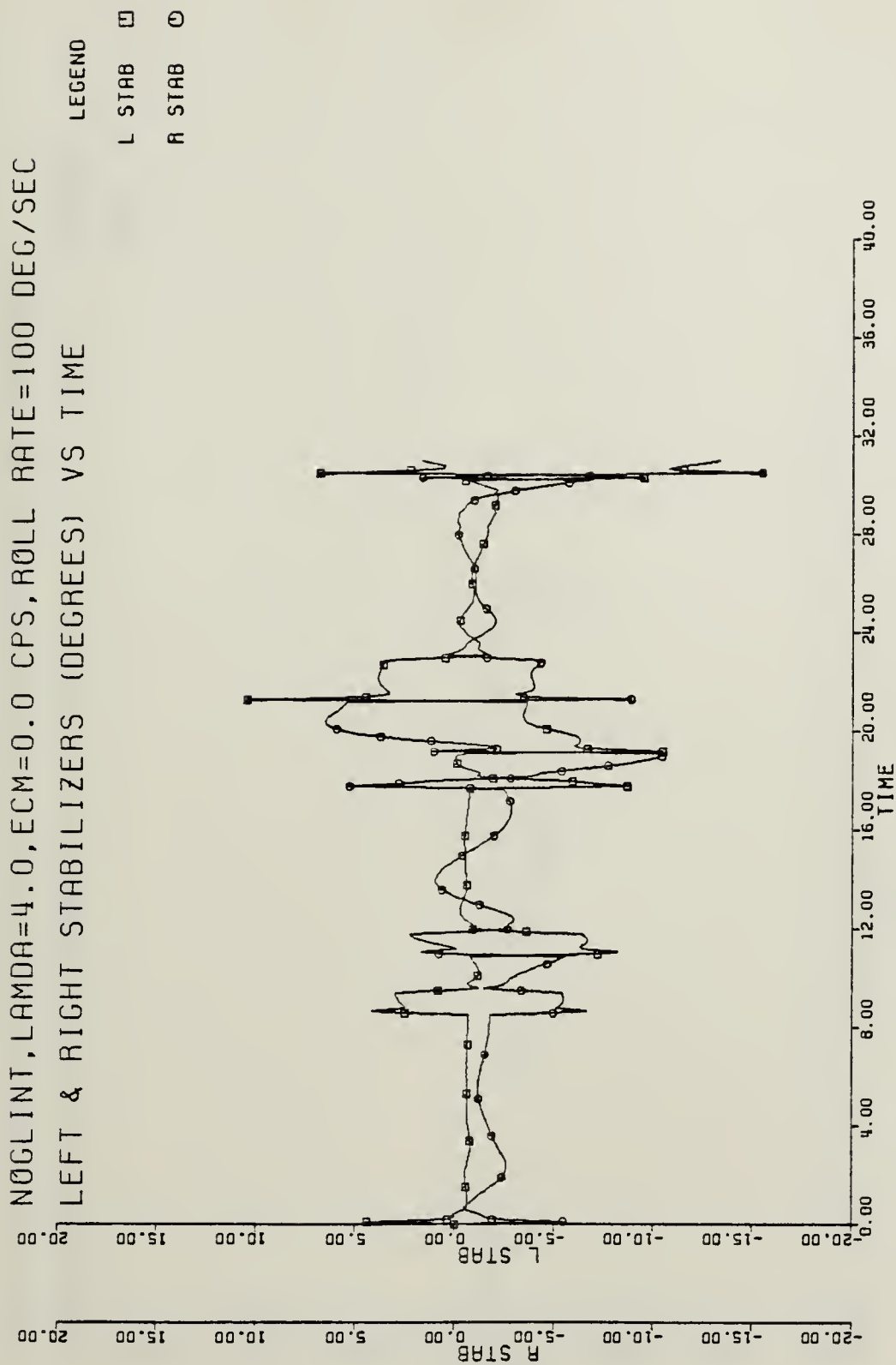



Figure 5-1d Baseline Response for No ECM, Roll Rate Limit 100 deg/sec
(L STAB, R STAB vs TIME)

NOGLINT, LAMDA=4.0, ECM=0.0 CPS, ROLL RATE=100 DEG/SEC
 RUDDER POSITION (DEGREES) VS TIME

LEGEND

RUDDER 

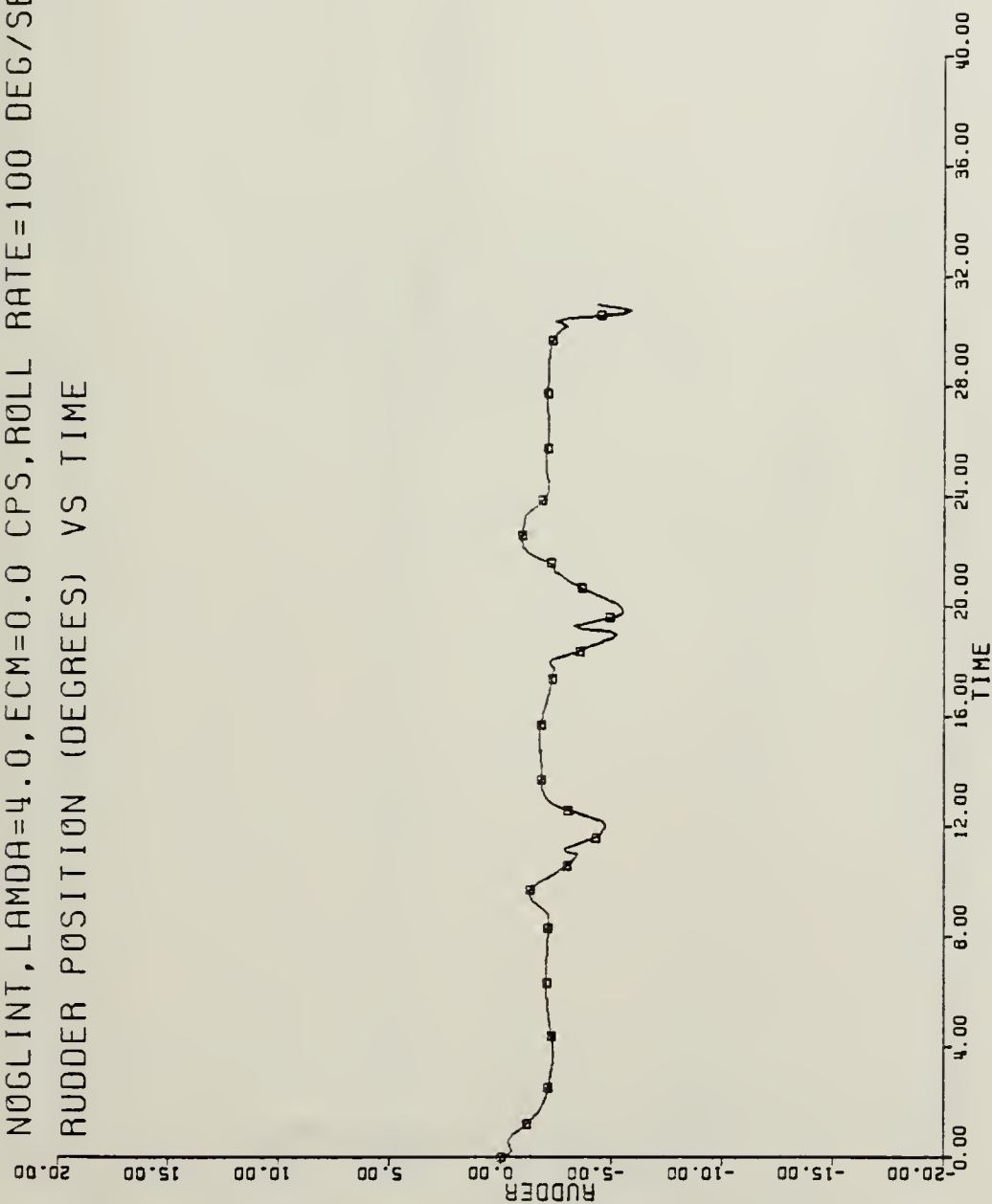


Figure 5-1e Baseline Response for No ECM, Roll Rate Limit 100 deg/sec
 (RUDDER vs TIME)

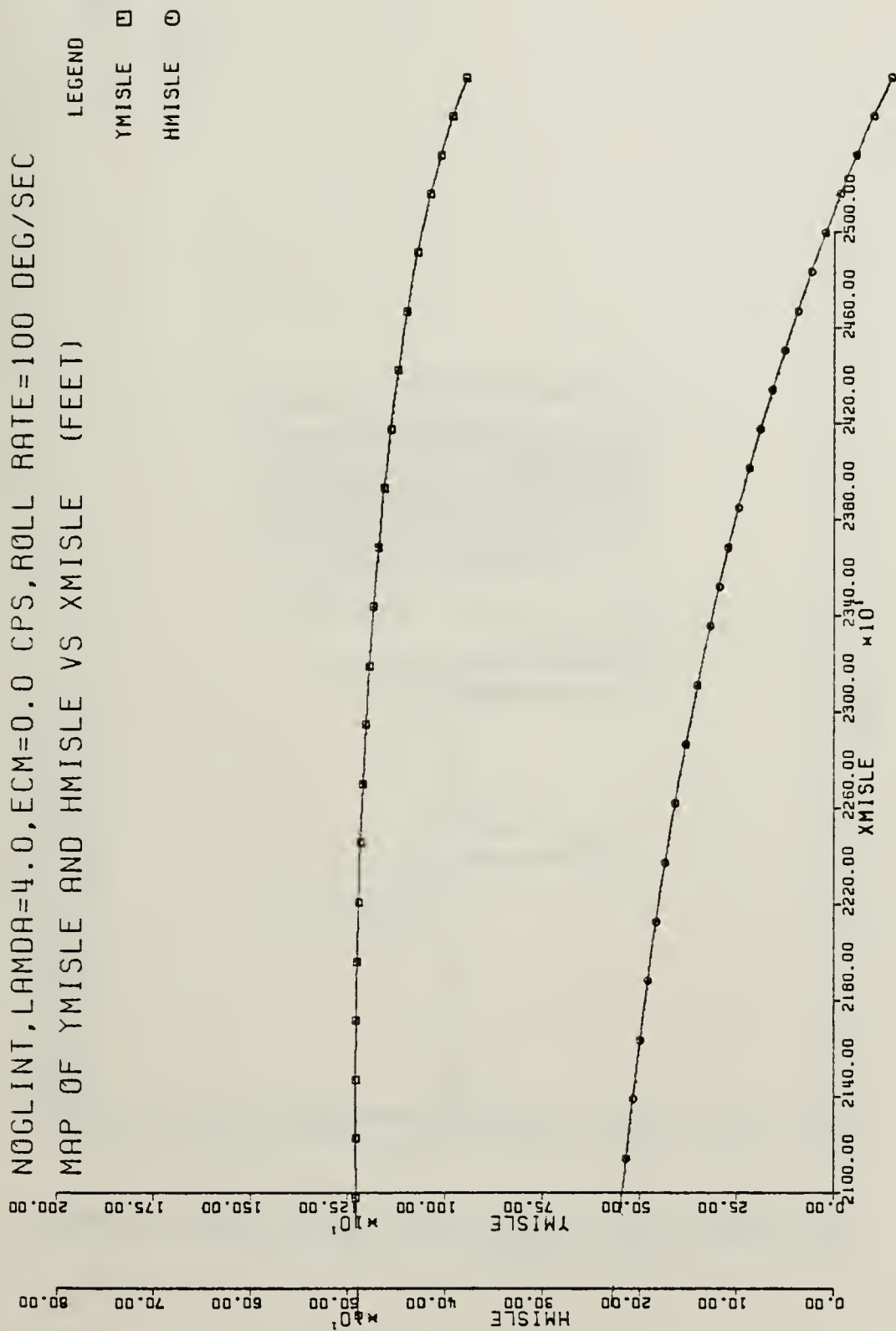


Figure 5-1f Baseline Response for No ECM, Roll Rate Limit 100 deg/sec
YMISLE, HMISLE vs XMISLE)

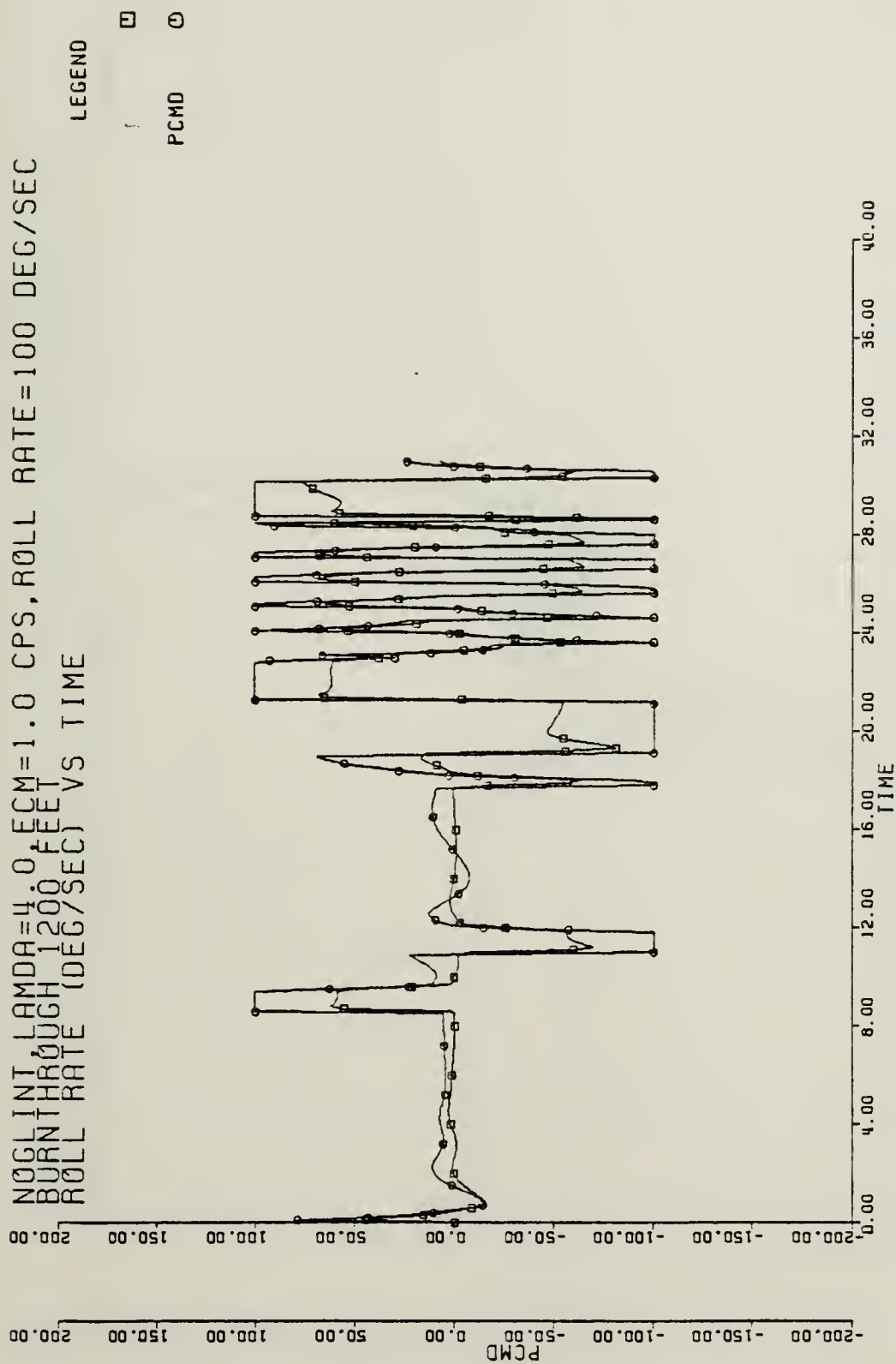


Figure 5-2a Baseline Response for ECM 1 CPS, Roll Rate Limit 100 deg/sec
(PCMD,P vs TIME)

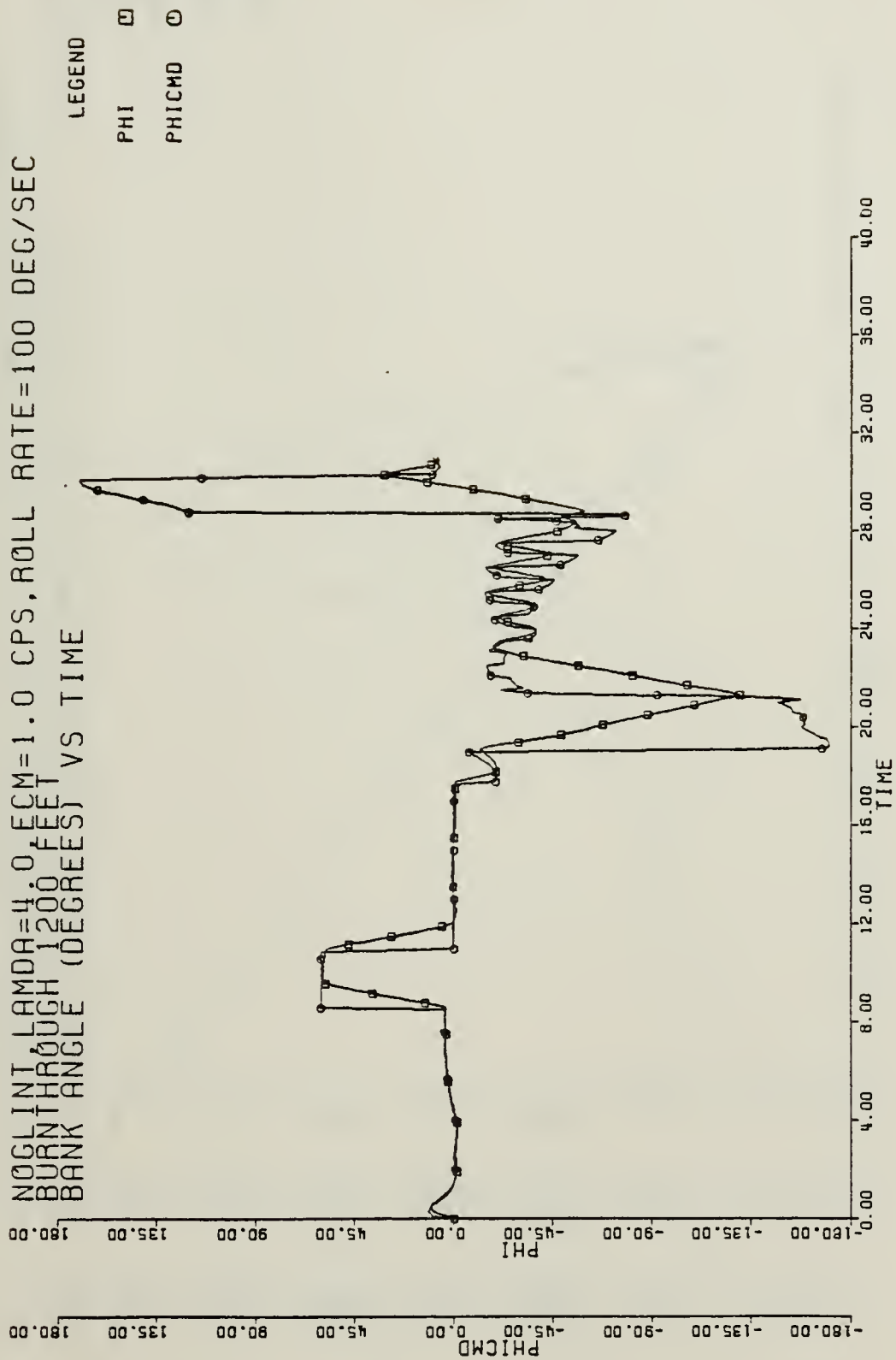


Figure 5-2b Baseline Response for ECM 1 CPS, Roll Rate Limit 100 deg/sec

(PHICMD, PHI vs TIME)

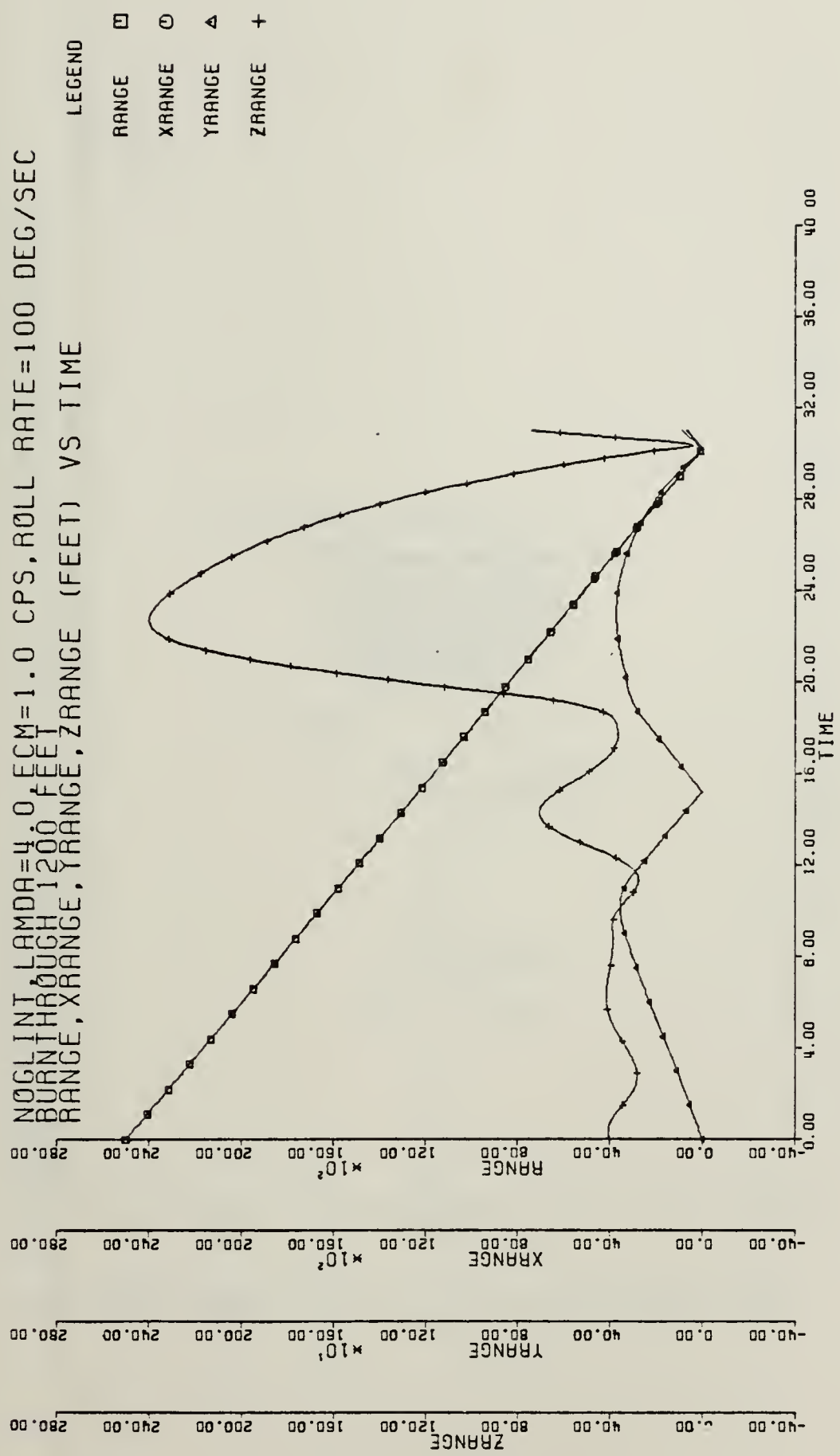


Figure 5-2c Baseline Response for ECM 1 CPS, Roll Rate Limit 100 deg/sec

(RANGE, X RANGE, Y RANGE, Z RANGE vs TIME)

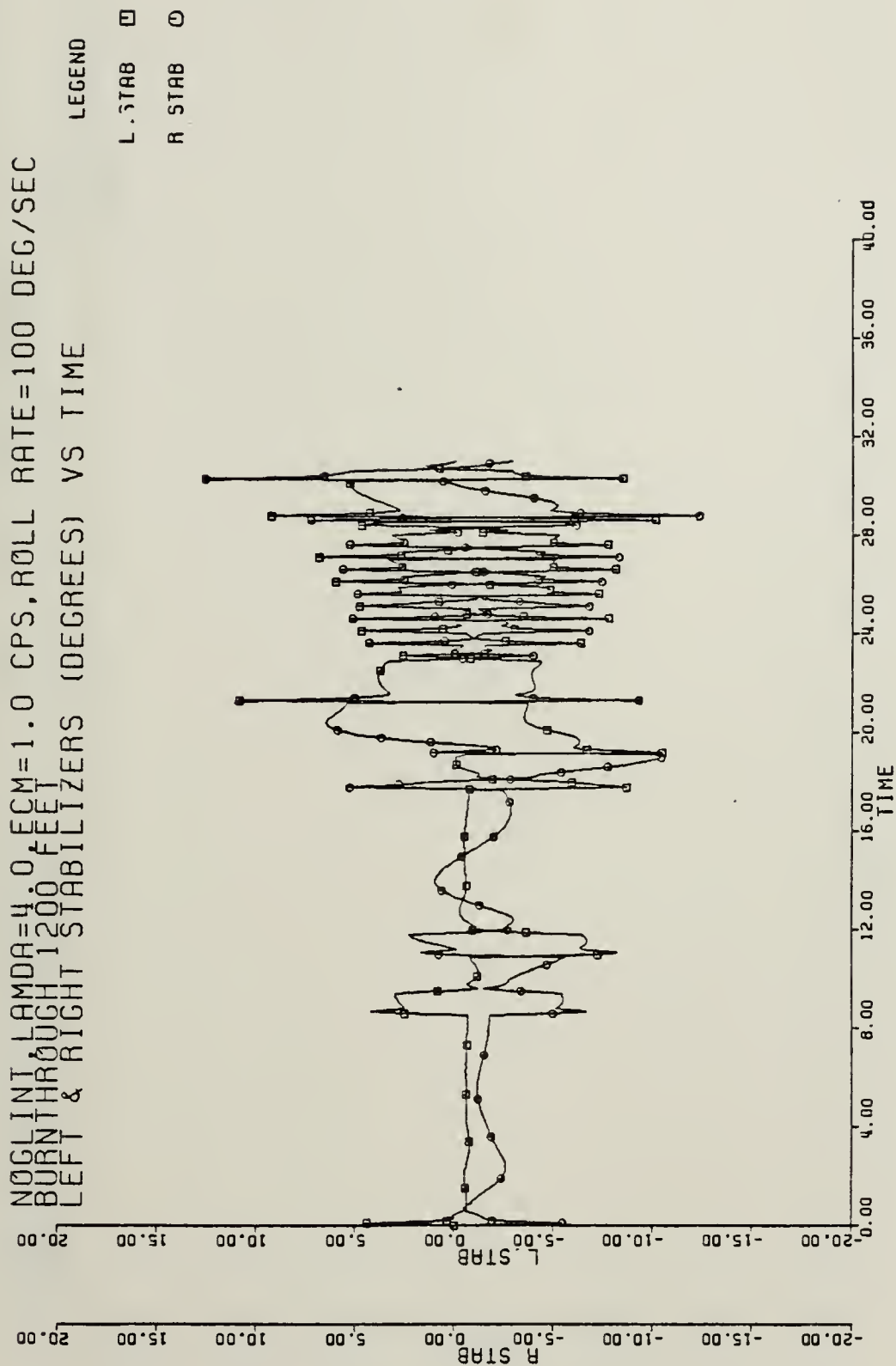



Figure 5-2d Baseline Response for ECM 1 CPS, Roll Rate Limit 100 deg/sec

(L STAB, R STAB vs TIME)

NOGLINT LAMDA=4.0 ECM=1.0 CPS, ROLL RATE=100 DEG/SEC
 BURNTHROUGH 1200 FEET
 RUDDER POSITION (DEGREES) VS TIME

LEGEND

RUDDER 

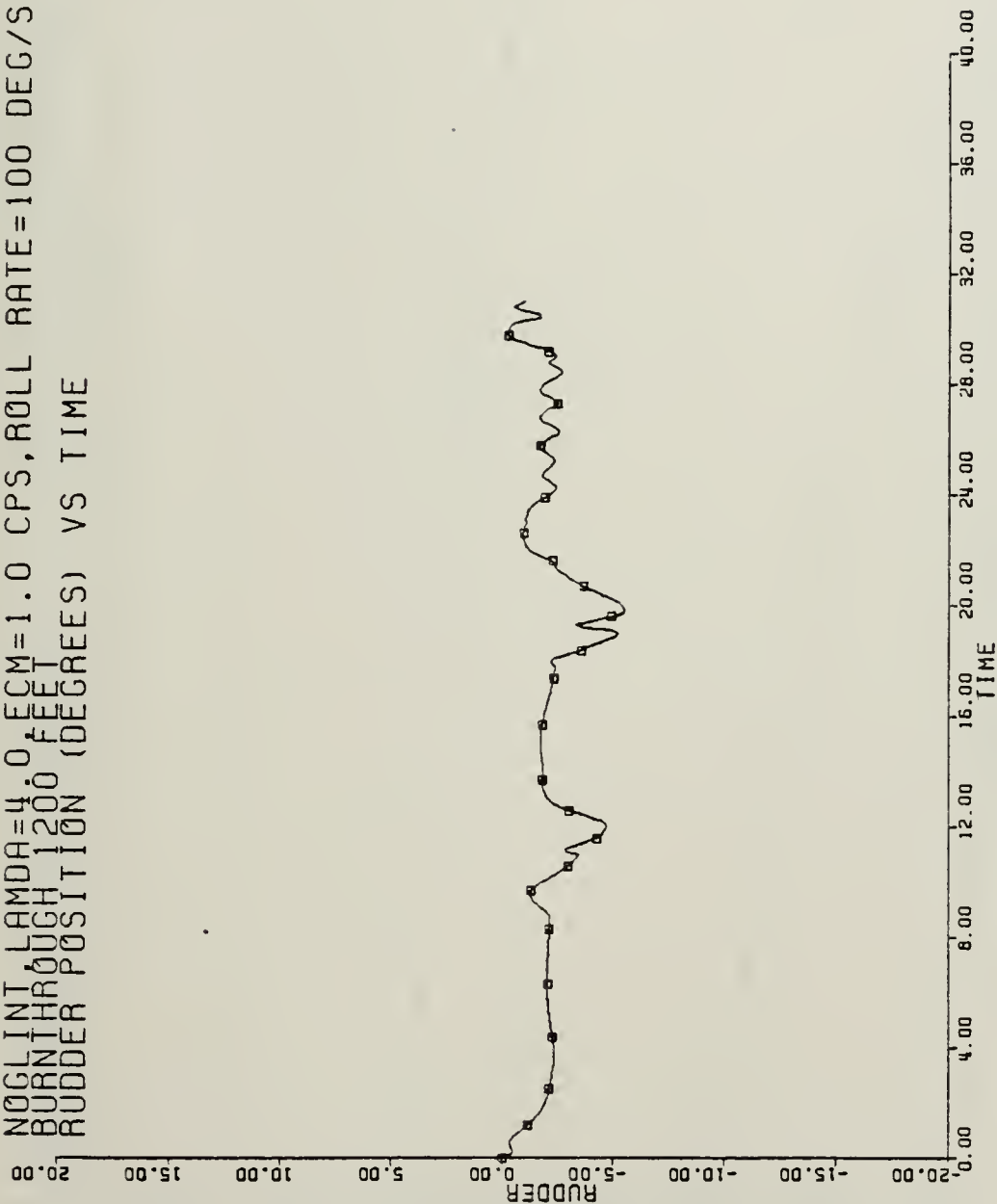


Figure 5-2e Baseline Response for ECM 1 CPS, Roll Rate Limit 100 deg/sec

(RUDDER vs TIME)

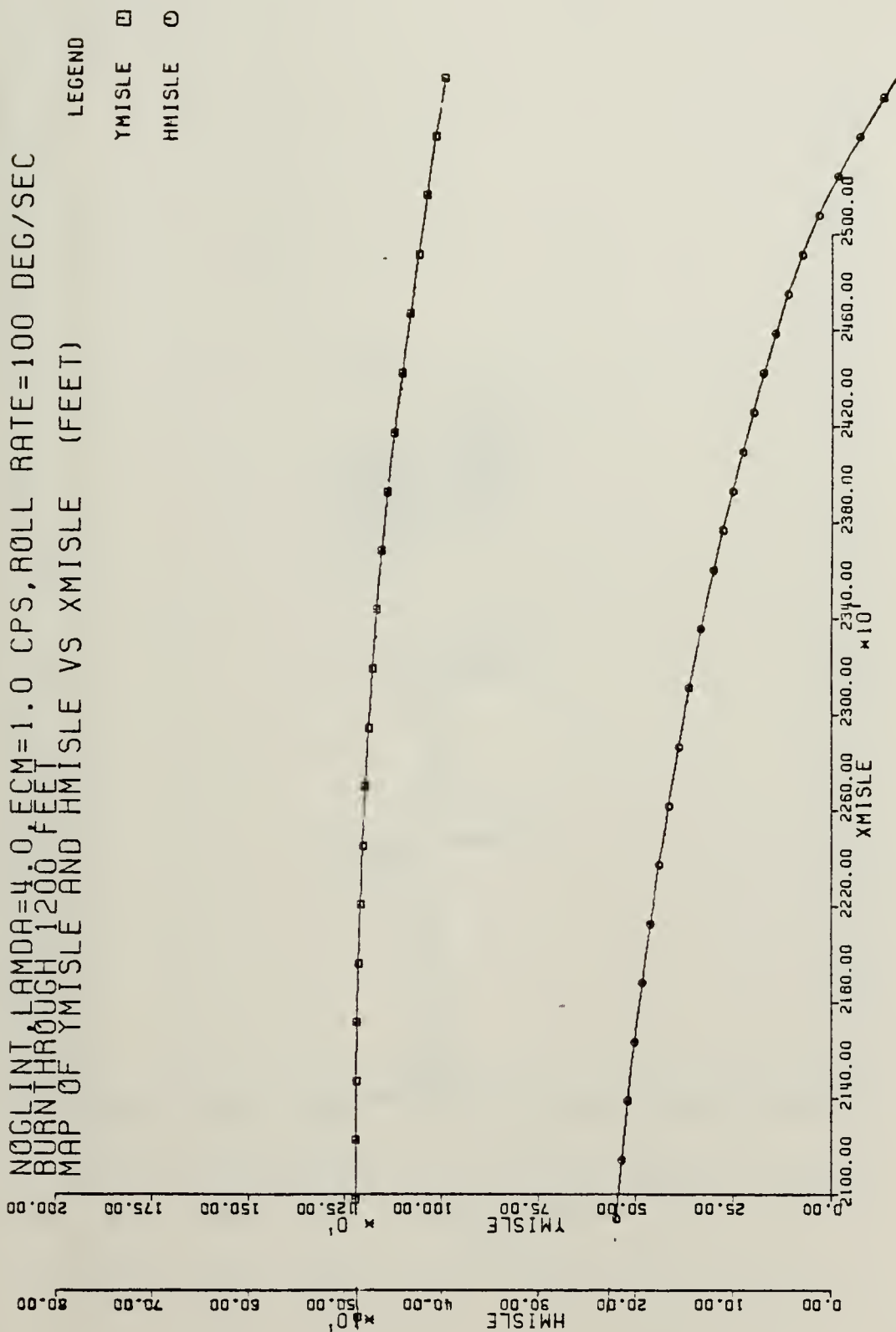


Figure 5-2f Baseline Response for ECM 1 CPS, Roll Rate Limit 100 deg/sec
 (YMISLE, HMISLE vs XMISLE)

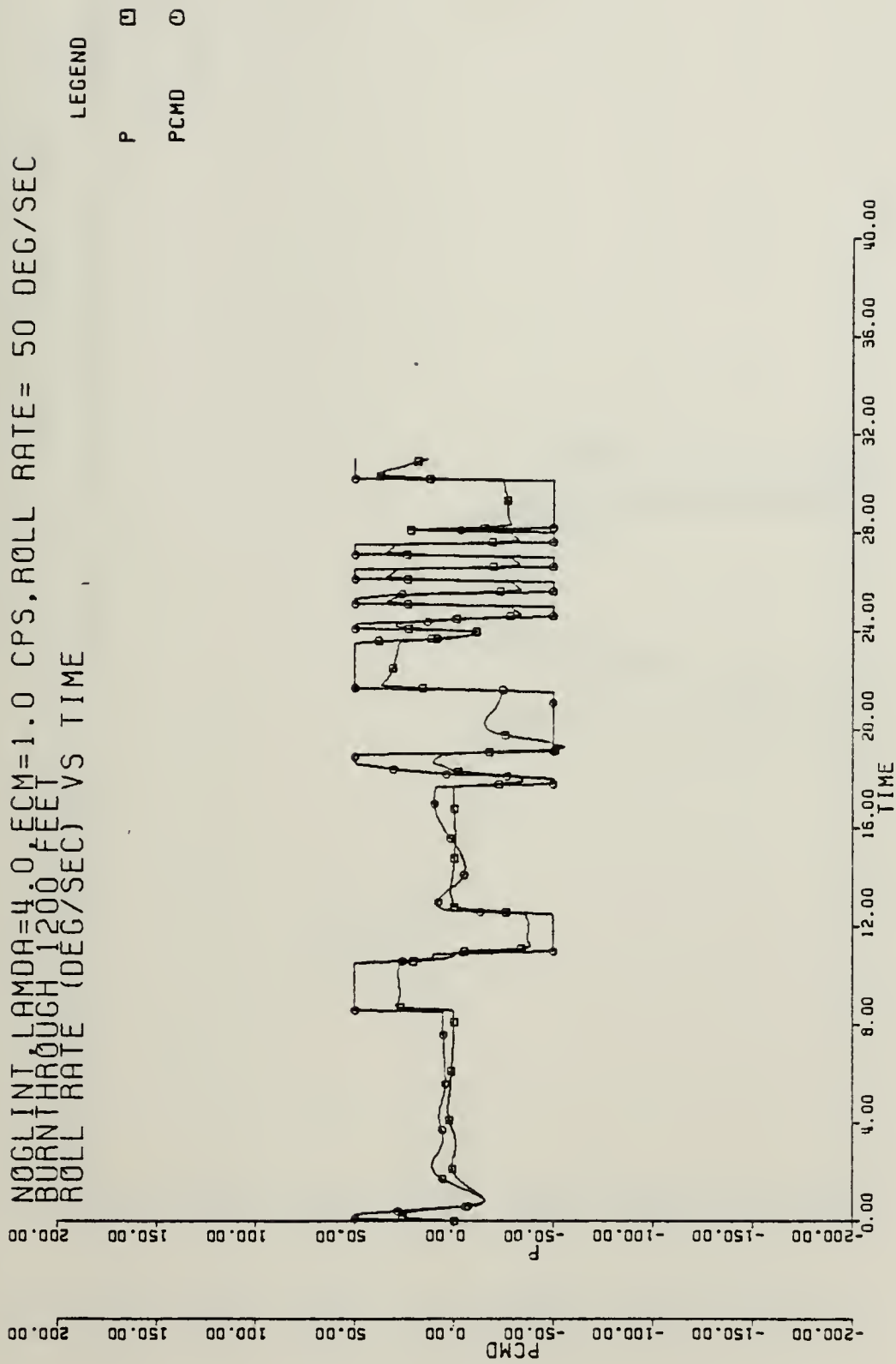


Figure 5-3a Baseline Response for ECM 1 CPS, Roll Rate Limit 50 deg/sec,

(PCMD, P vs TIME)

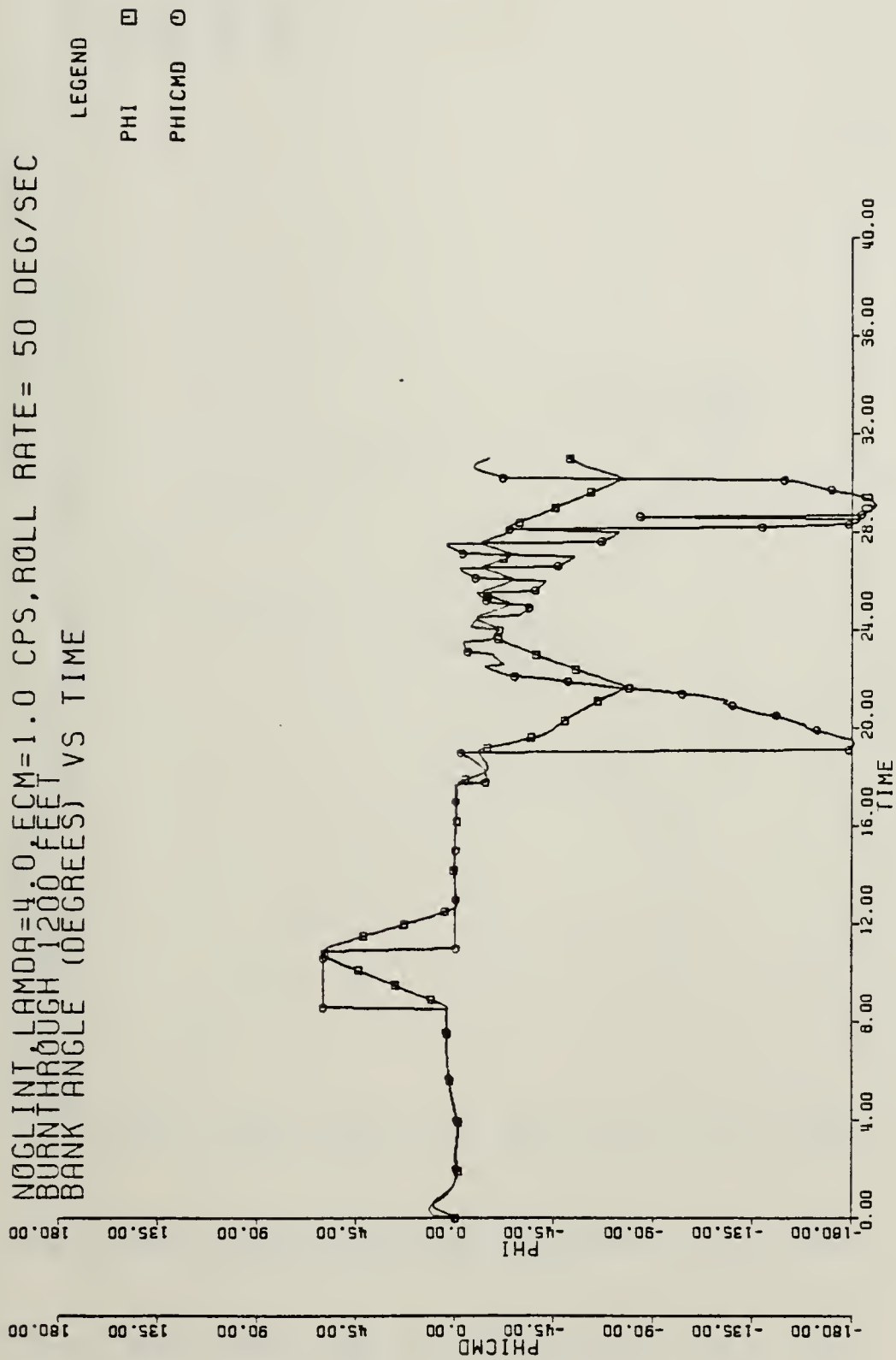


Figure 5-3b Baseline Response for ECM 1 CPS, Roll Rate Limit 50 deg/sec

(PHICMD, PHI vs TIME)

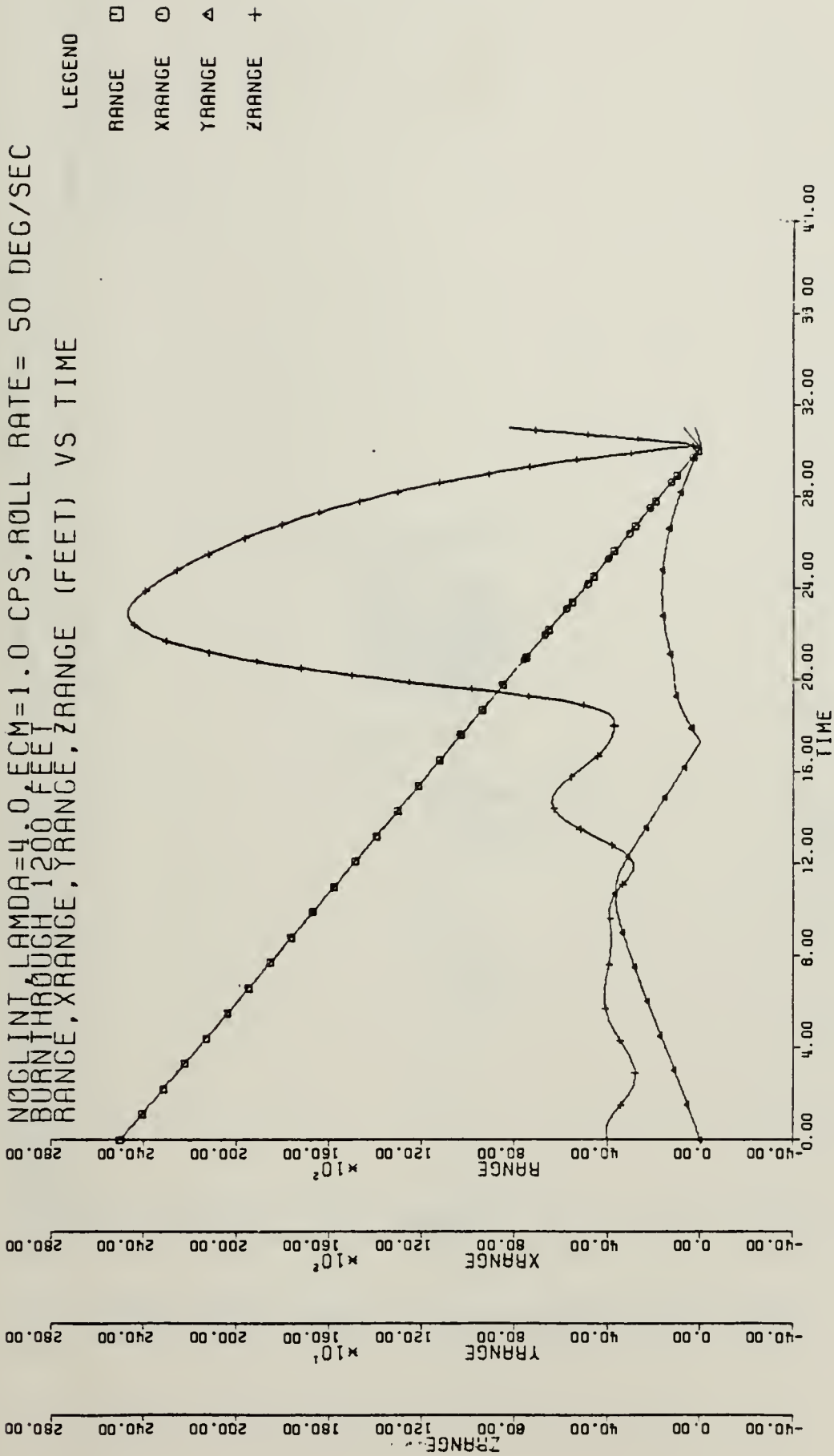


Figure 5-3c Baseline Response for ECM 1 CPS, Roll Rate Limit 50 deg/sec

(RANGE, X RANGE, Y RANGE, Z RANGE vs TIME)

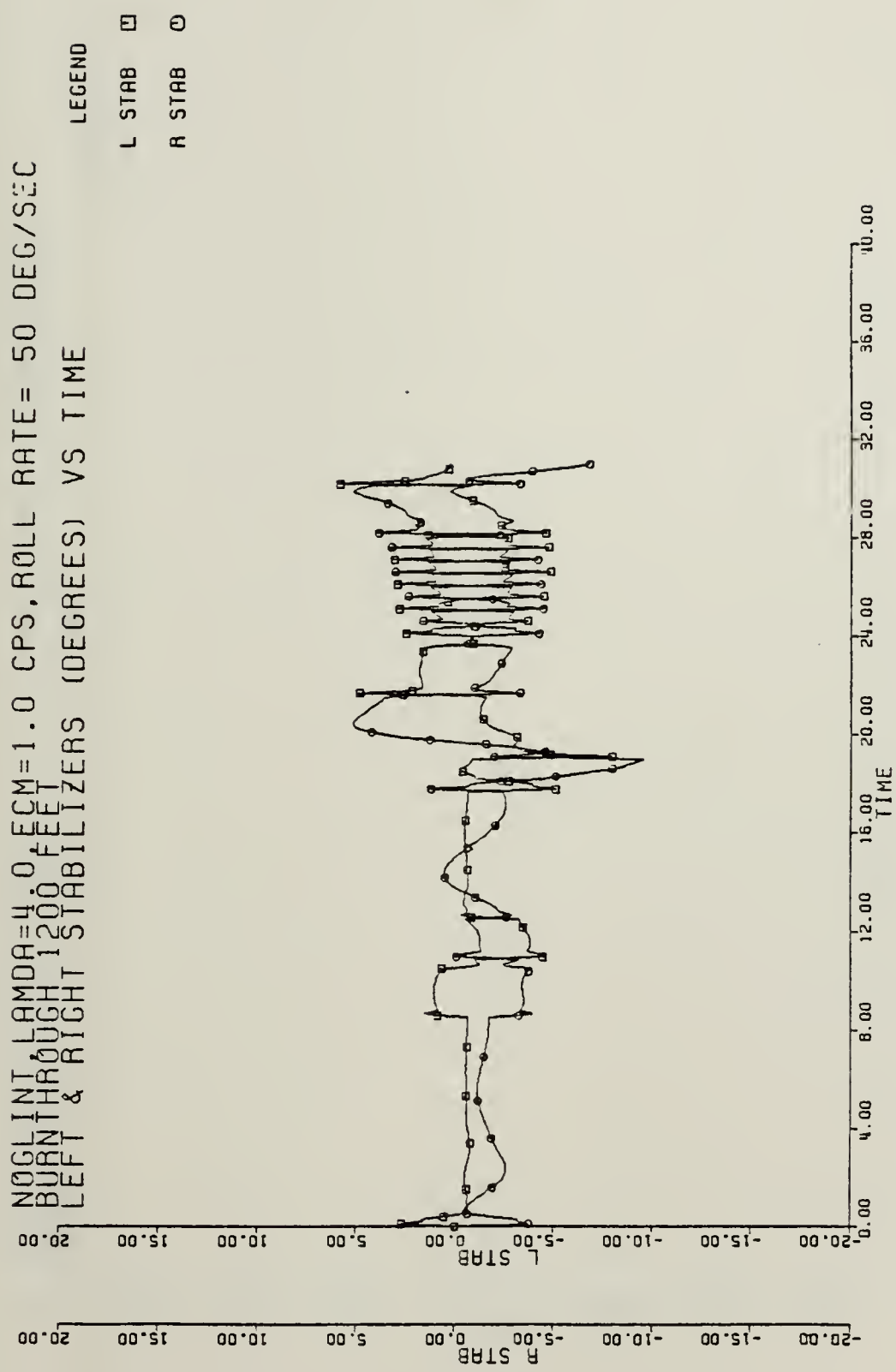


Figure 5-3d Baseline Response for ECM 1 CPS, Roll Rate Limit 50 deg/sec
 (L STAB, R STAB vs TIME)

NOGLINT, LAMDA=4.0, ECM=1.0 CPS, ROLL RATE= 50 DEG/SEC
 BURNTHROUGH 1200 FEET
 RUDDER POSITION (DEGREES) VS TIME

LEGEND

RUDDER

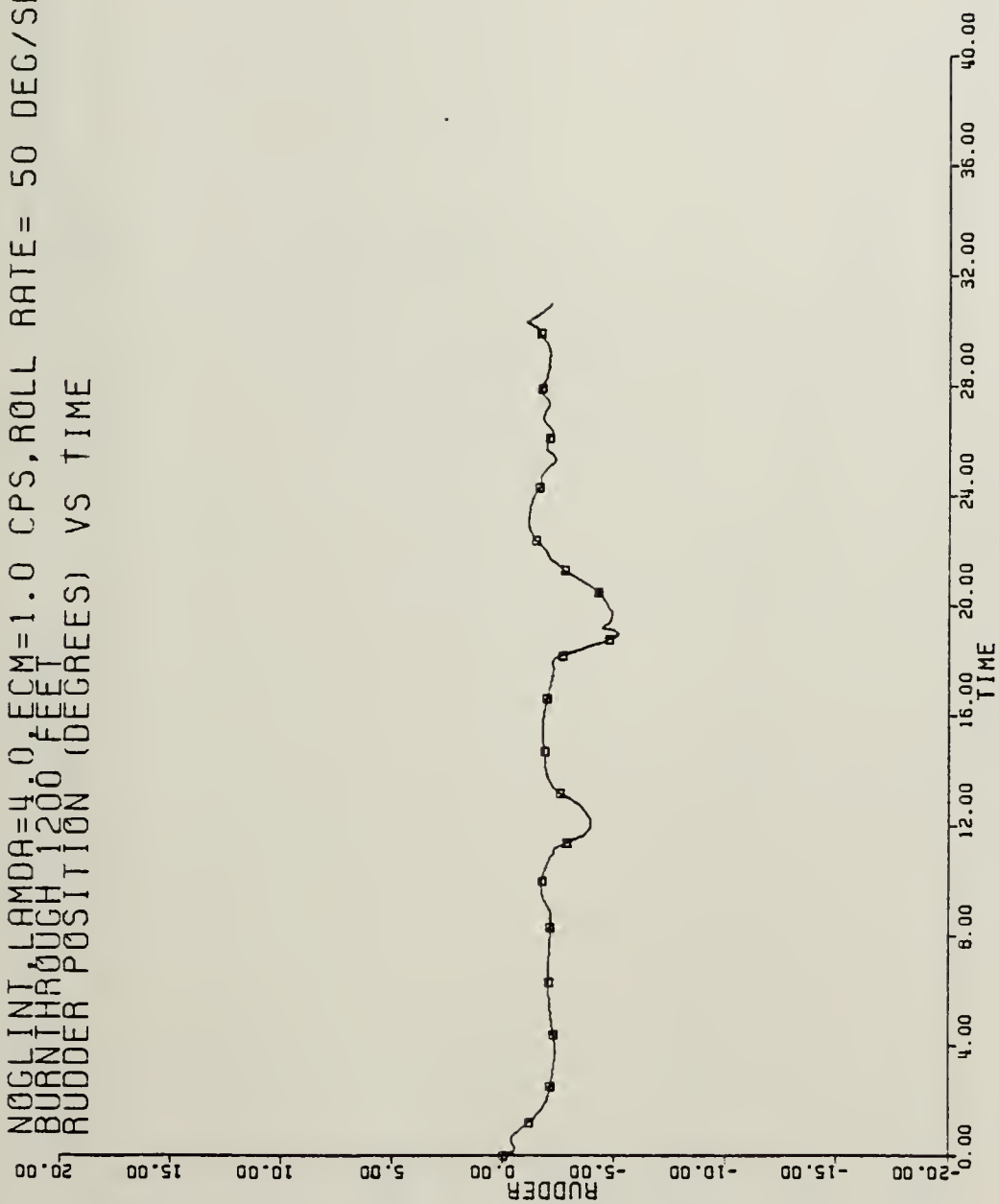


Figure 5-3e Baseline Response for ECM 1 CPS, Roll Rate Limit 50 deg/sec
 (RUDDER vs TIME)

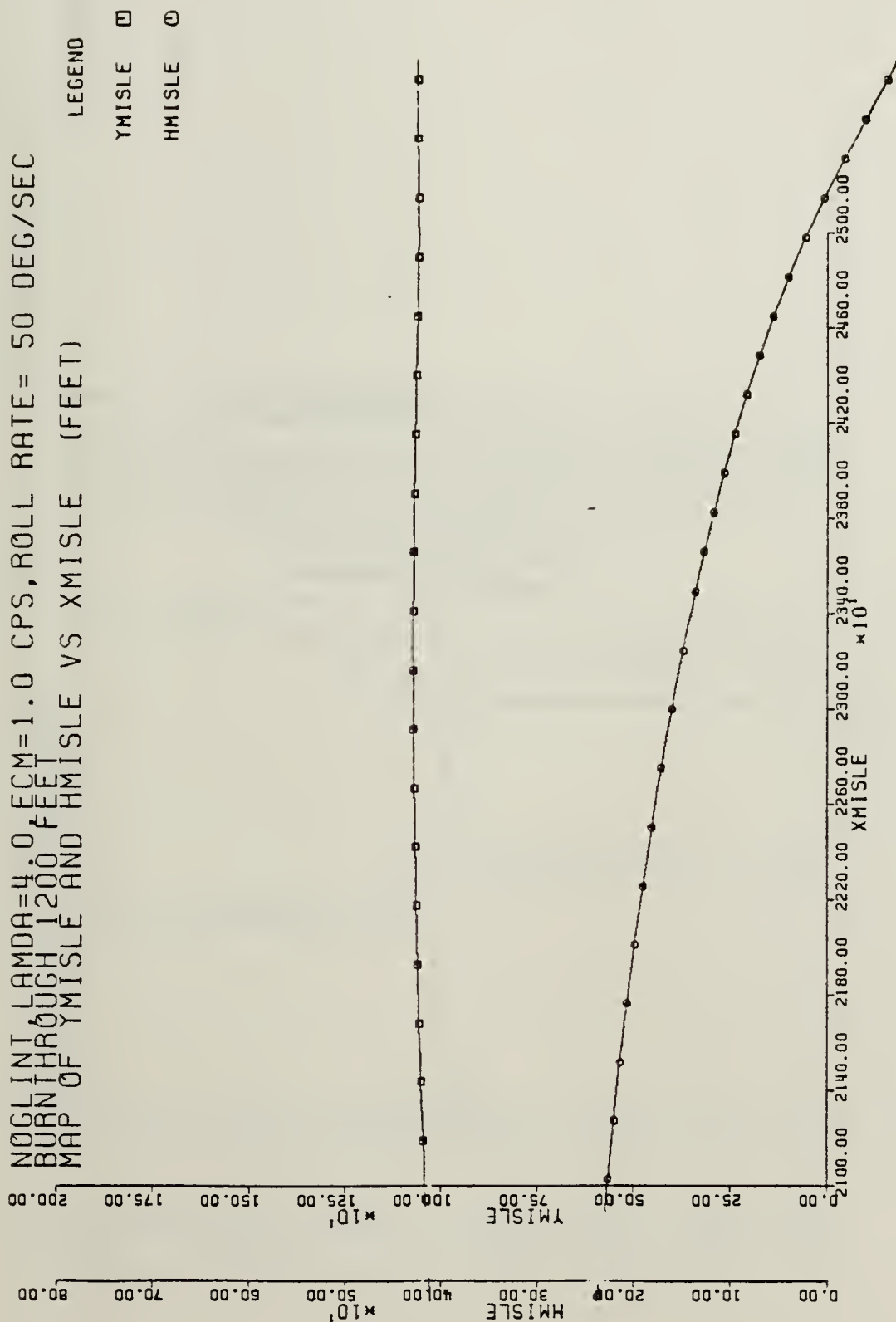


Figure 5-3f Baseline Response for ECM 1 CPS, Roll Rate Limit 50 deg/sec
 (YMISLE, HMISLE vs XMISLE)

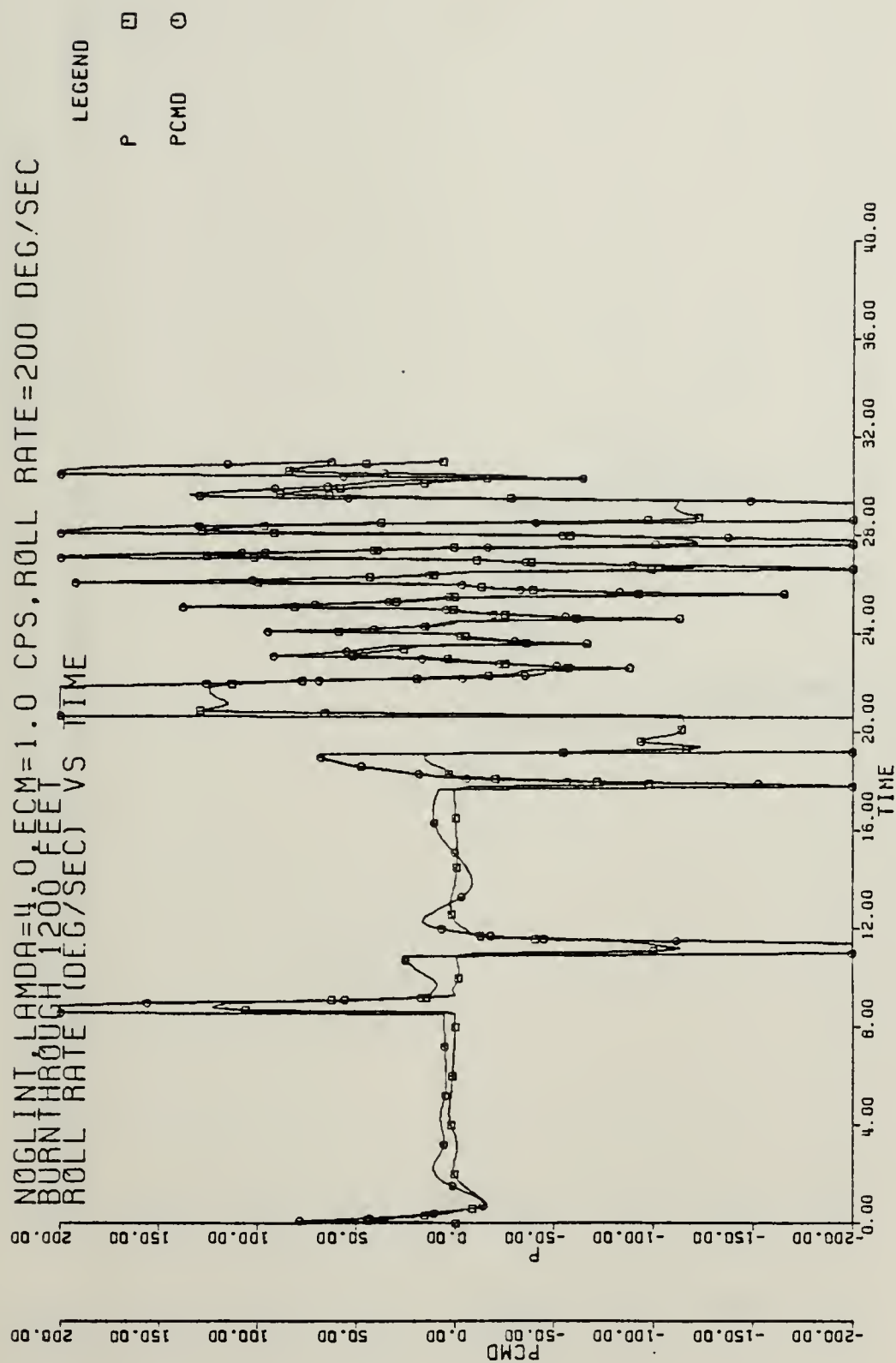


Figure 5-4a Baseline Response for ECM 1 CPS, Roll Rate Limit 200 deg/sec
PCMD, P vs TIME)

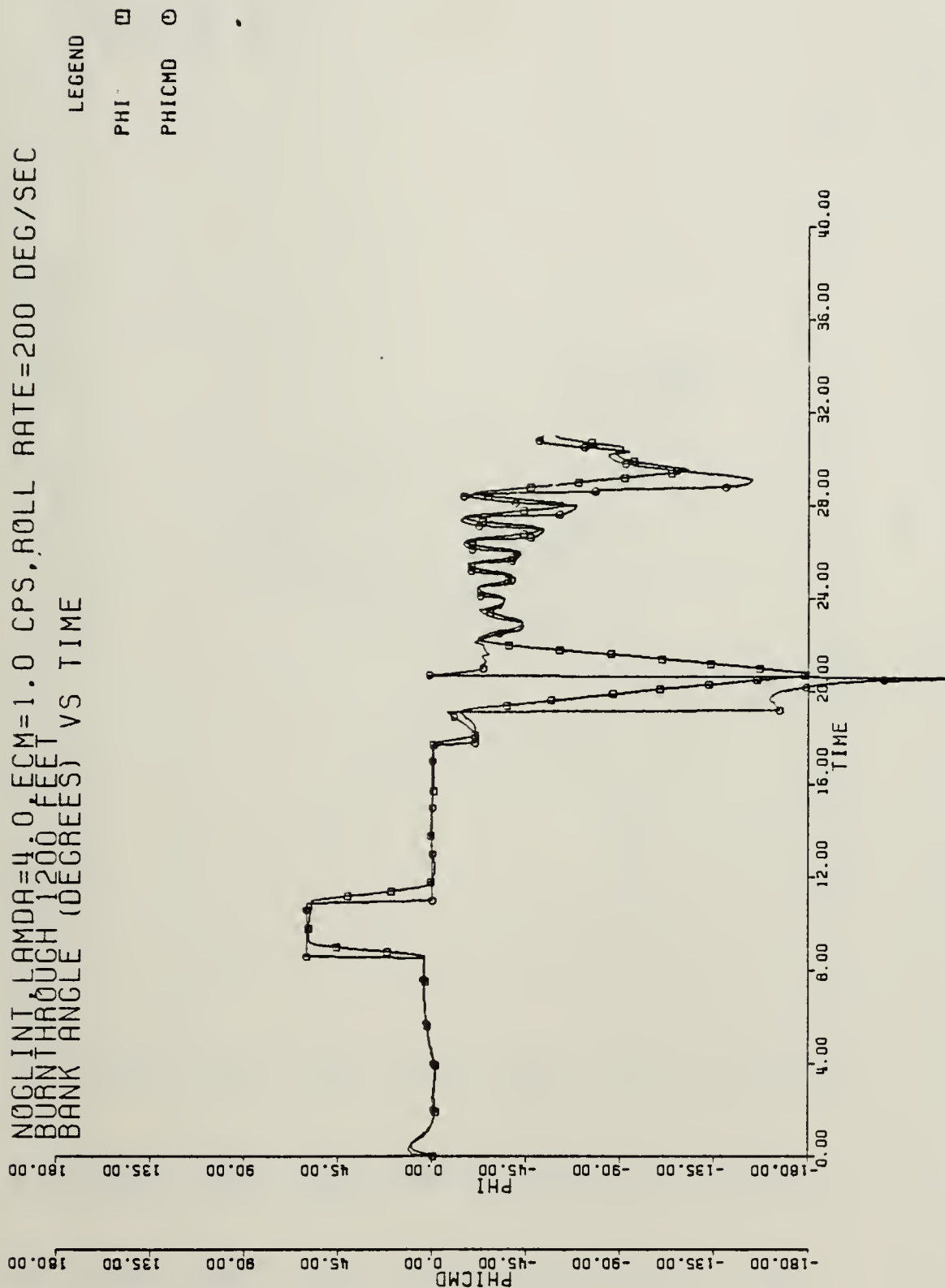


Figure 5-4b Baseline Response for ECM 1 CPS, Roll Rate Limit 200 deg/sec
 (PHICMD, PHI vs TIME)

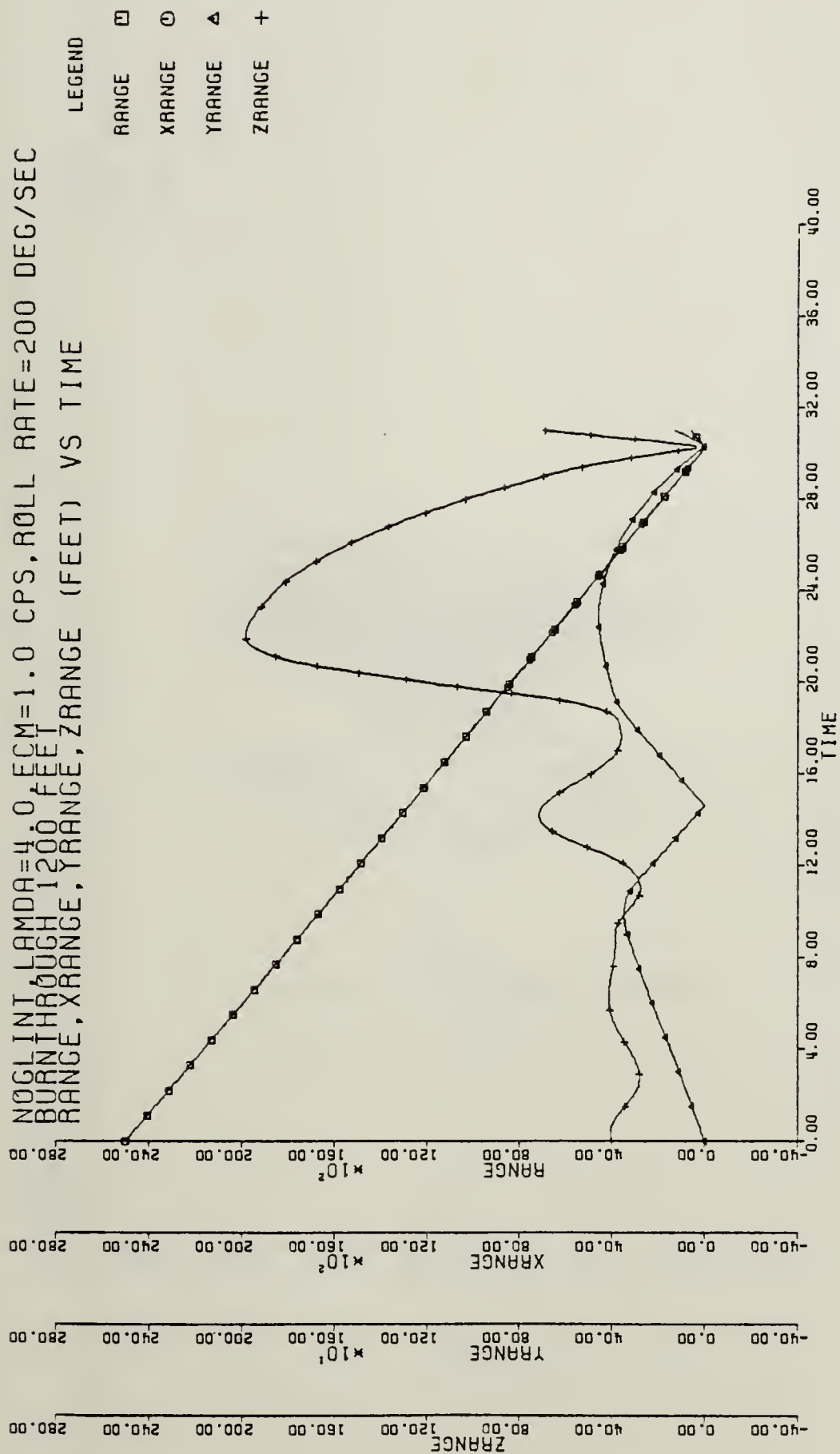


Figure 5-4c Baseline Response for ECM 1 CPS, Roll Rate Limit 200 deg/sec
 (RANGE, X RANGE, Y RANGE, Z RANGE vs TIME)

NOGLINT LAMDA=4.0 ECM=1.0 CPS, ROLL RATE=200 DEG/SEC
 BURNTHROUGH 1200 FEET
 LEFT & RIGHT STABILIZERS (DEGREES) VS TIME

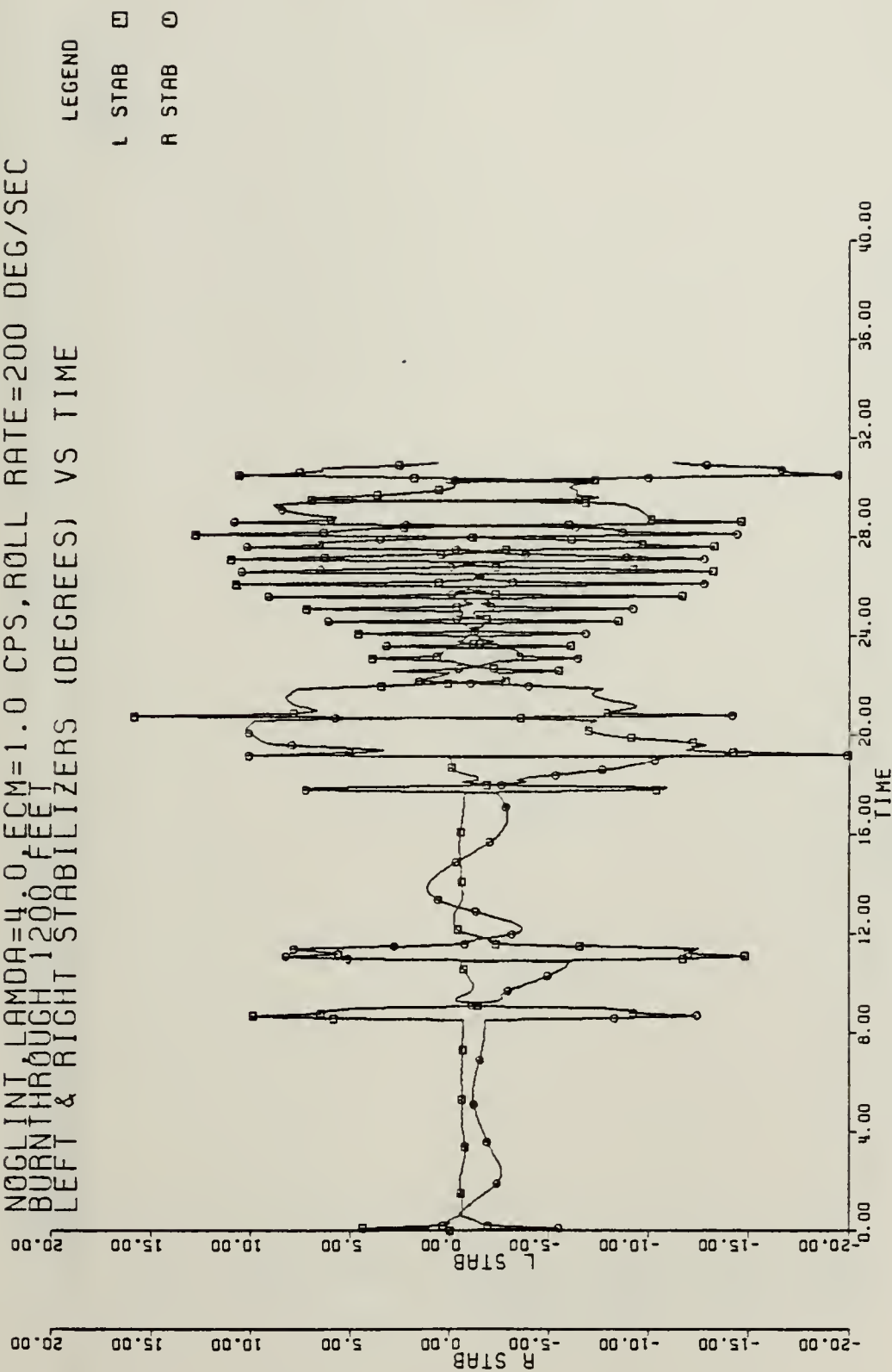


Figure 5-4d Baseline Response for ECM 1 CPS, Roll Rate Limit 200 deg/sec
 (L STAB, R STAB vs TIME)

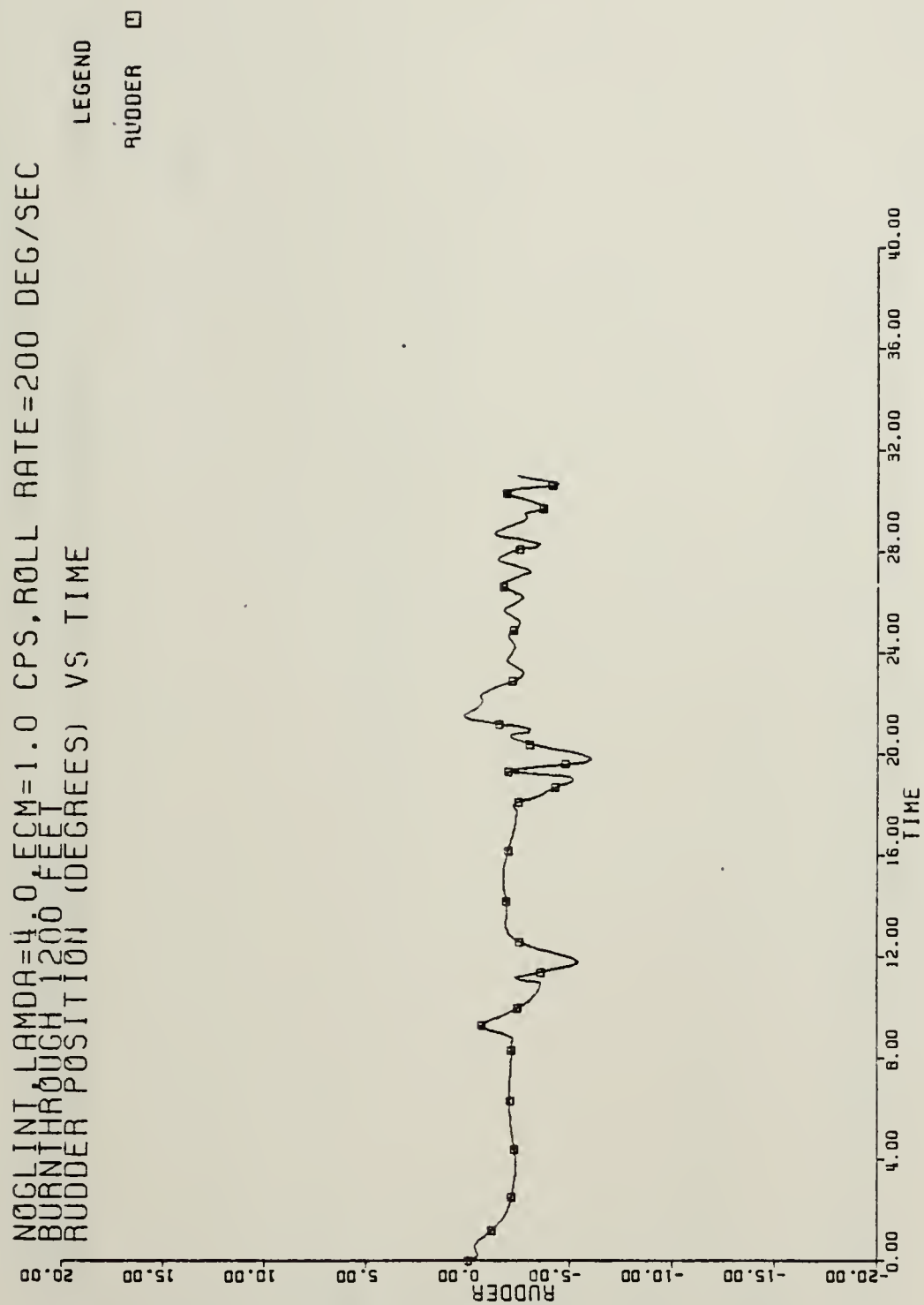


Figure 5-4e Baseline Response for ECM 1 CPS, Roll Rate Limit 200 deg/sec
 (RUDDER vs TIME)

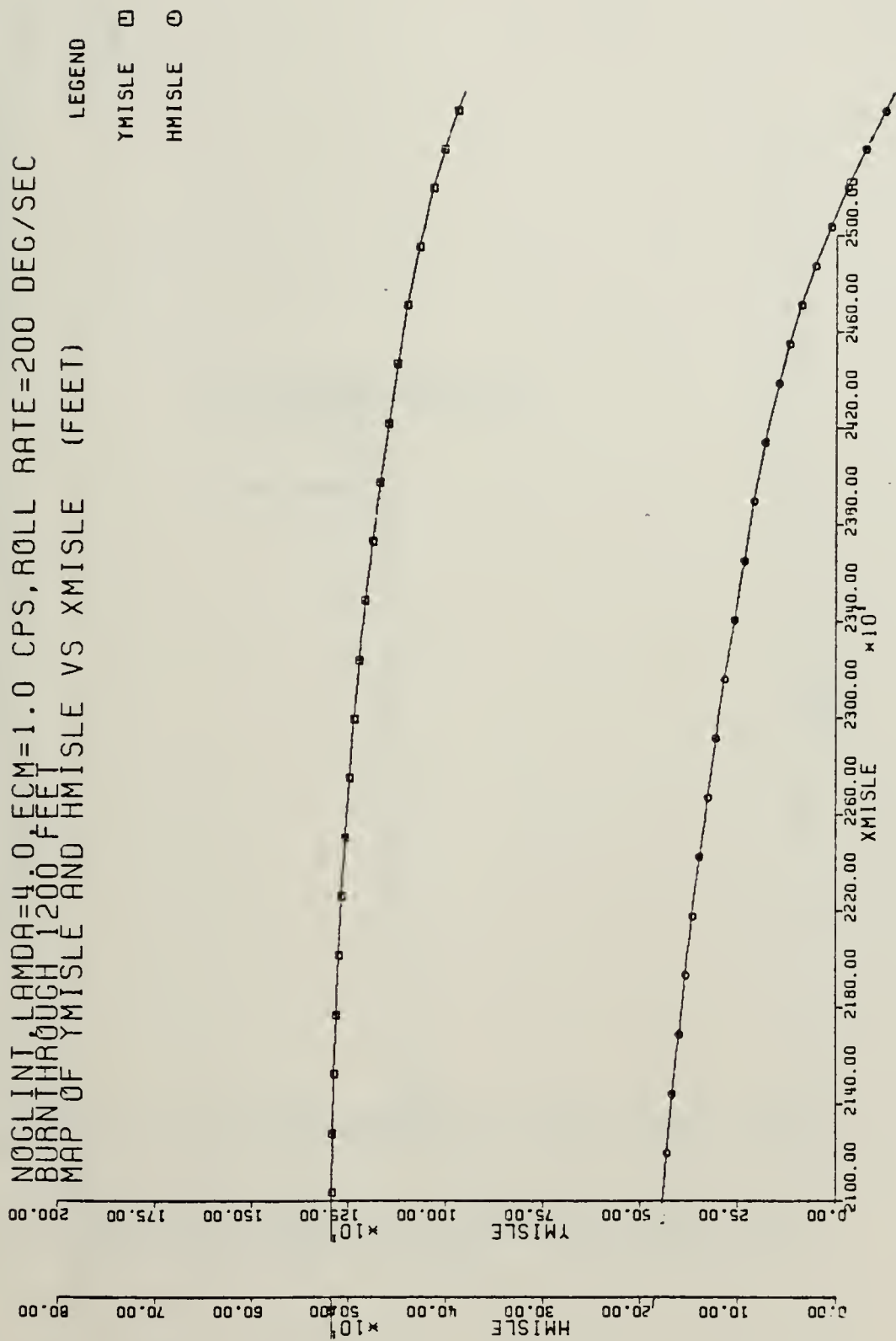


Figure 5-4f Baseline Response for ECM 1 CPS, Roll Rate Limit 200 deg/sec

(YMISLE, HMISLE vs XMISLE)

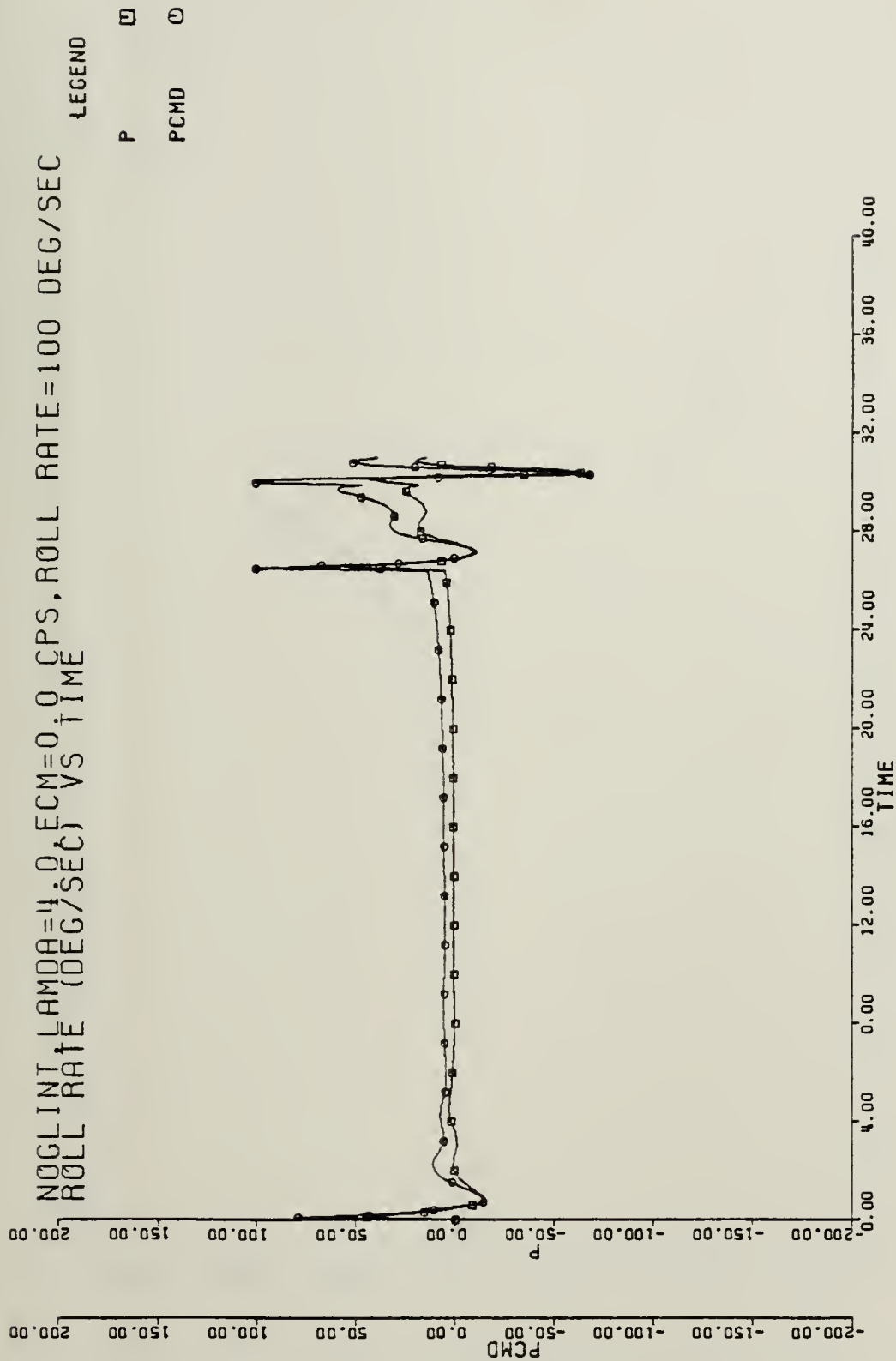


Figure 5-5a Sea Skimmer Response for No ECM, Roll Rate Limit 100 deg/sec
 (PCMD, P vs TIME)

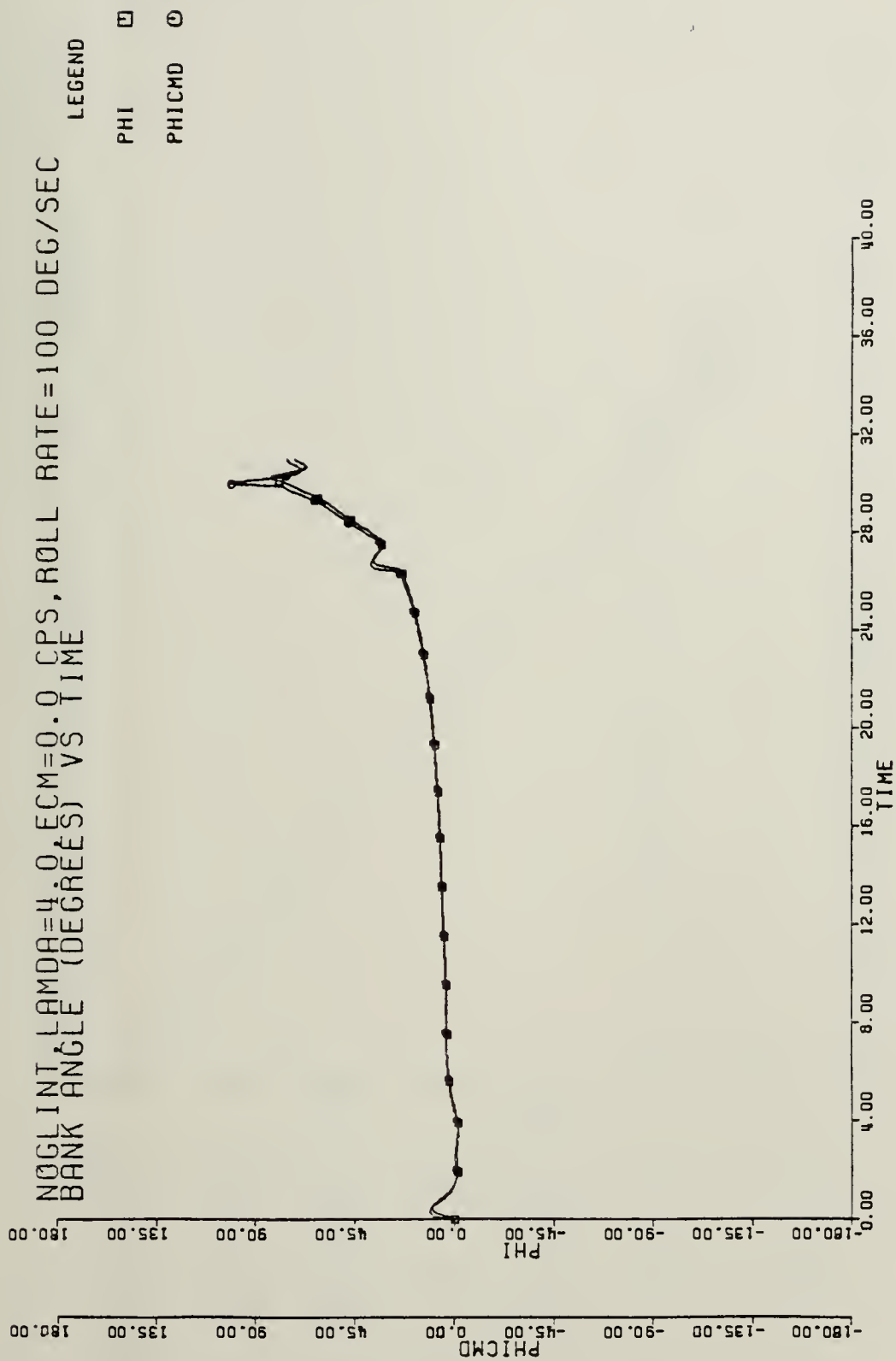


Figure 5-5b Sea Skimmer Response for No ECM, Roll Rate Limit 100 deg/sec

(PHICMD, PHI vs TIME)

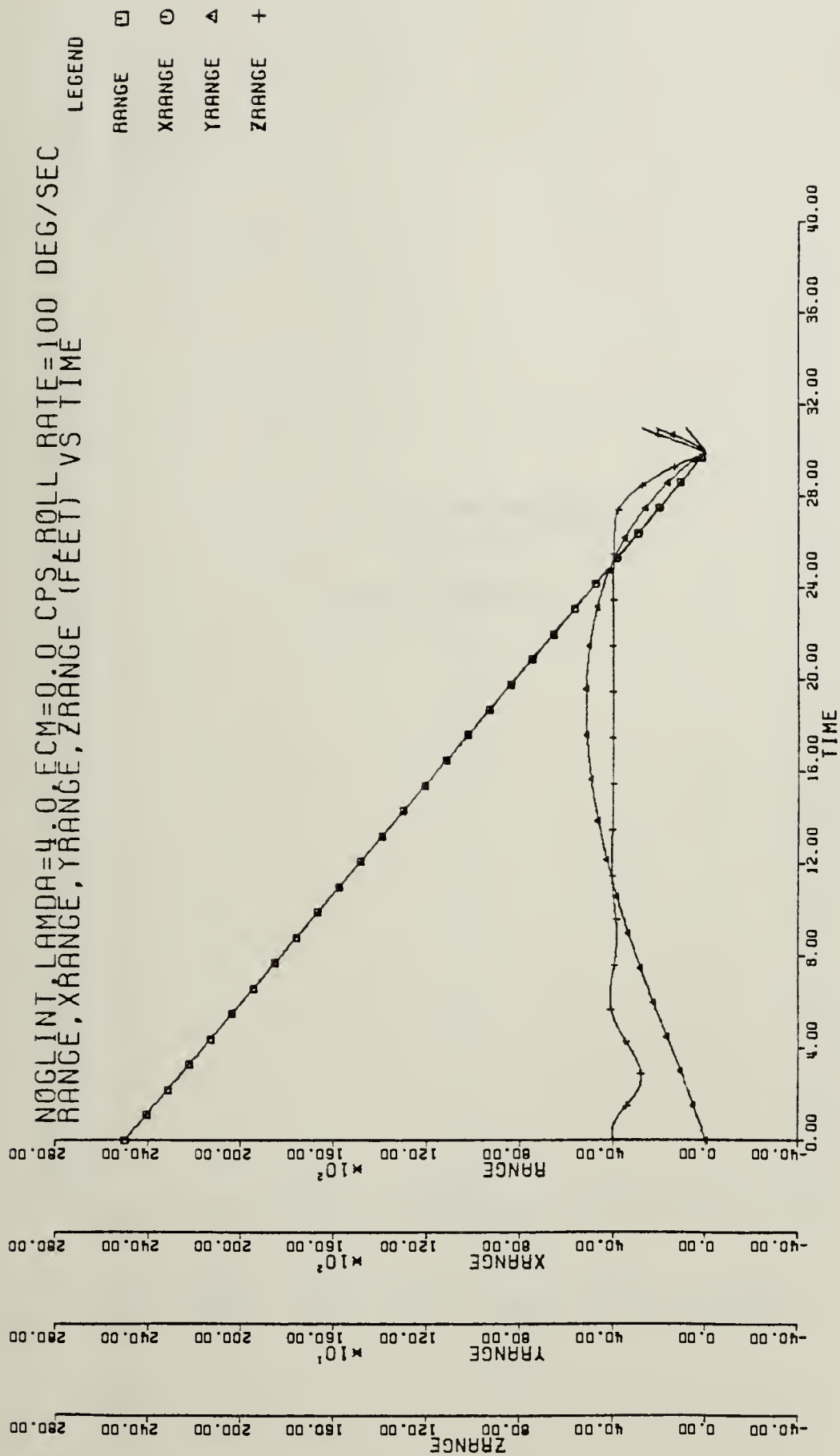


Figure 5-5c Sea Skimmer Response for No ECM, Roll Rate Limit 100 deg/sec
 (RANGE, X RANGE, Y RANGE, Z RANGE vs TIME)

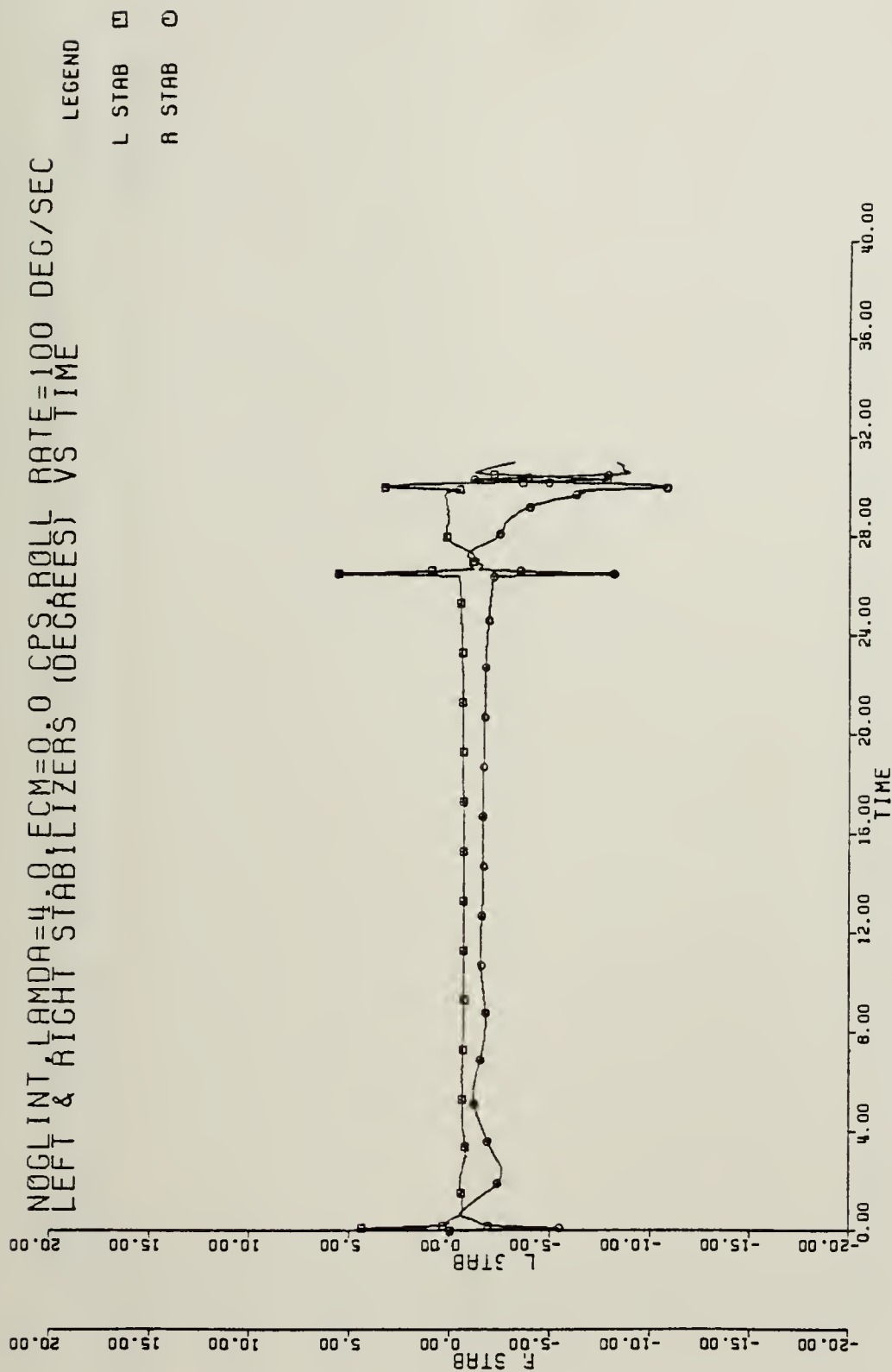


Figure 5-5d Sea Skimmer Response for No ECM, Roll Rate Limit 100 deg/sec
(L STAB, R STAB vs TIME)

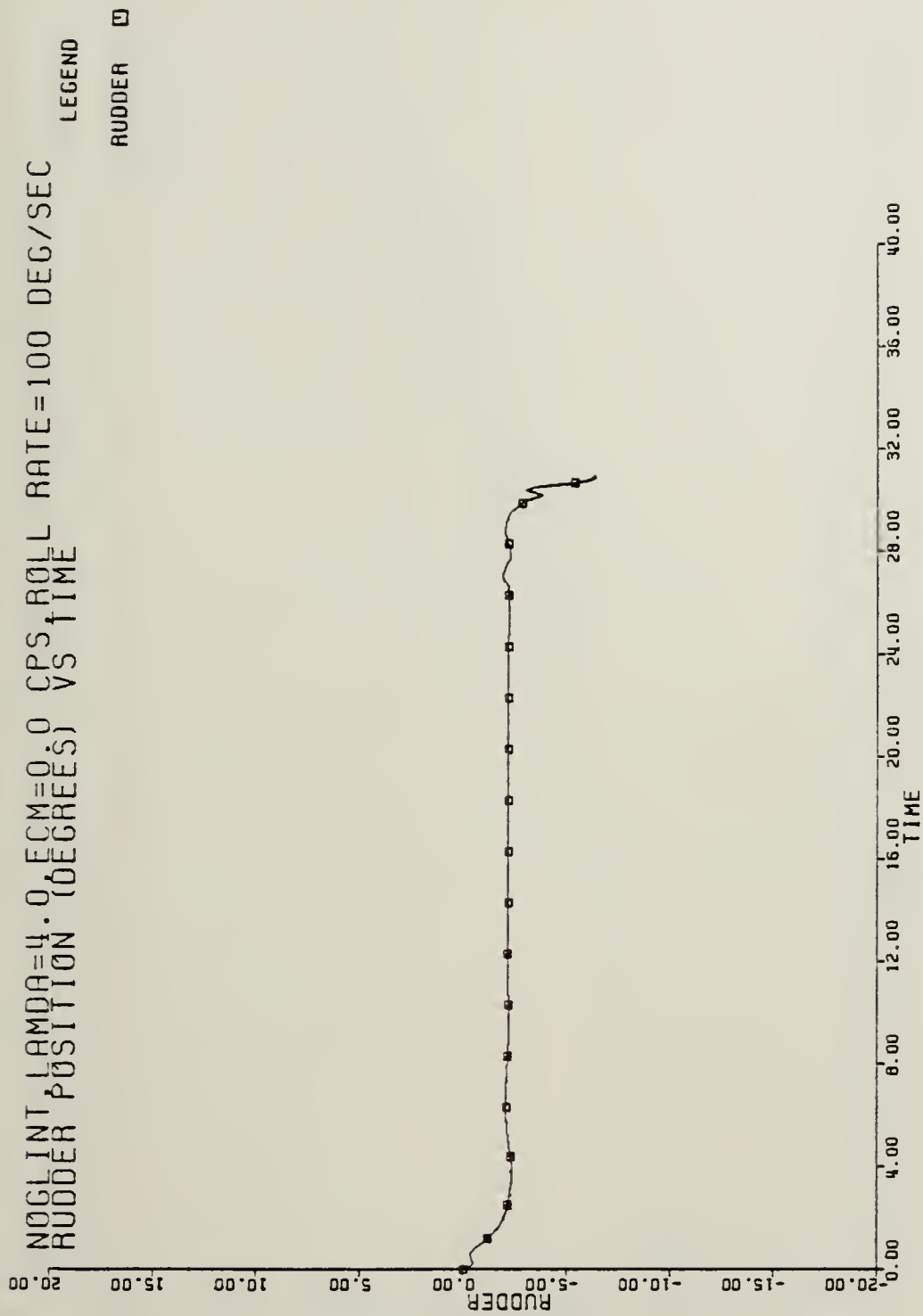


Figure 5-5e Sea Skimmer Response for No ECM, Roll Rate Limit 100 deg/sec
 RUDDER vs TIME)

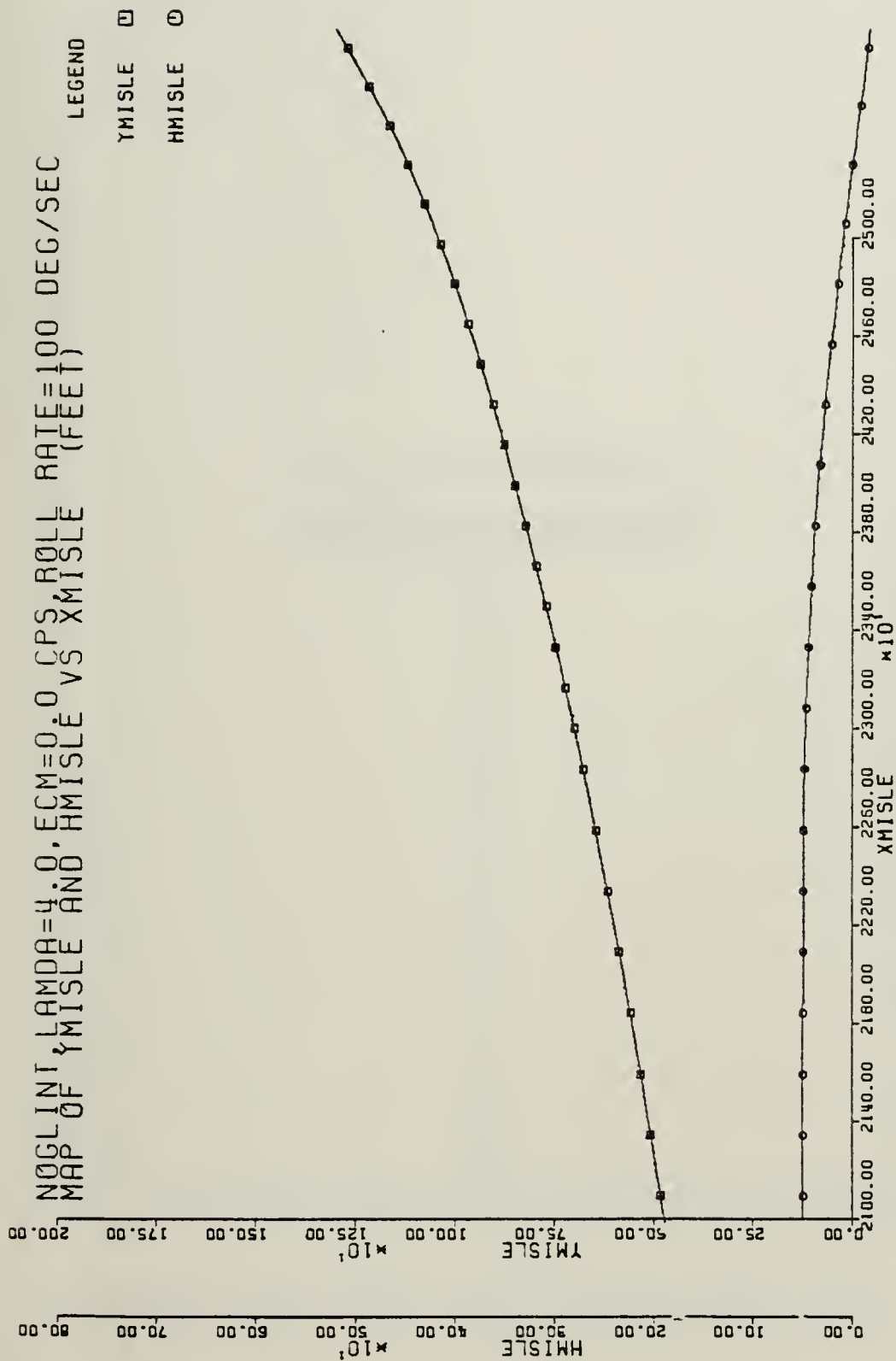


Figure 5-5f Sea Skimmer Response for No ECM, Roll Rate Limit 100 deg/sec
YMISLE, HMISLE vs XMISLE)

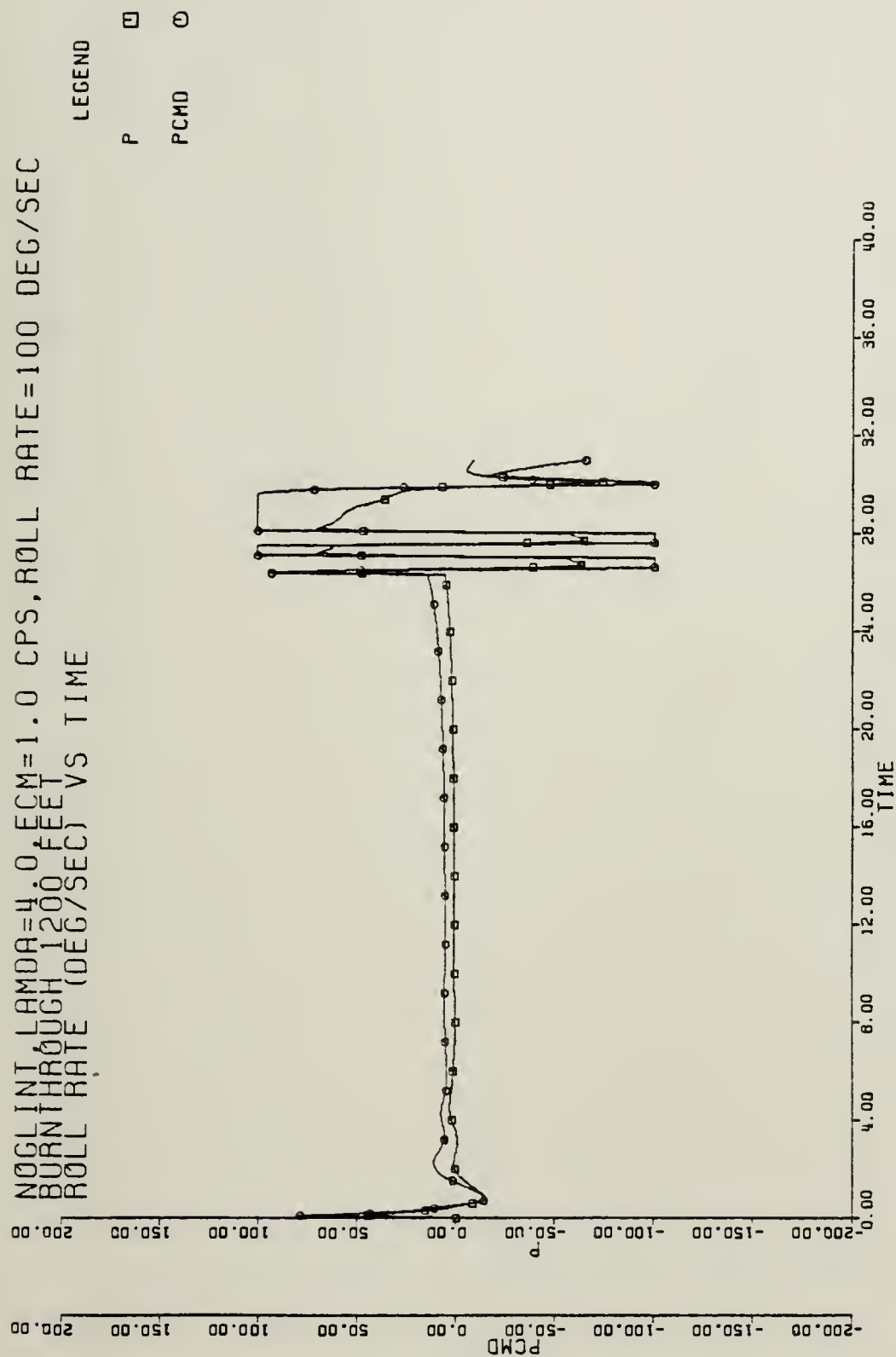


Figure 5-6a Sea Skimmer Response for ECM 1 CPS, Roll Rate Limit 100 deg/sec

... (PCMD, P vs TIME)

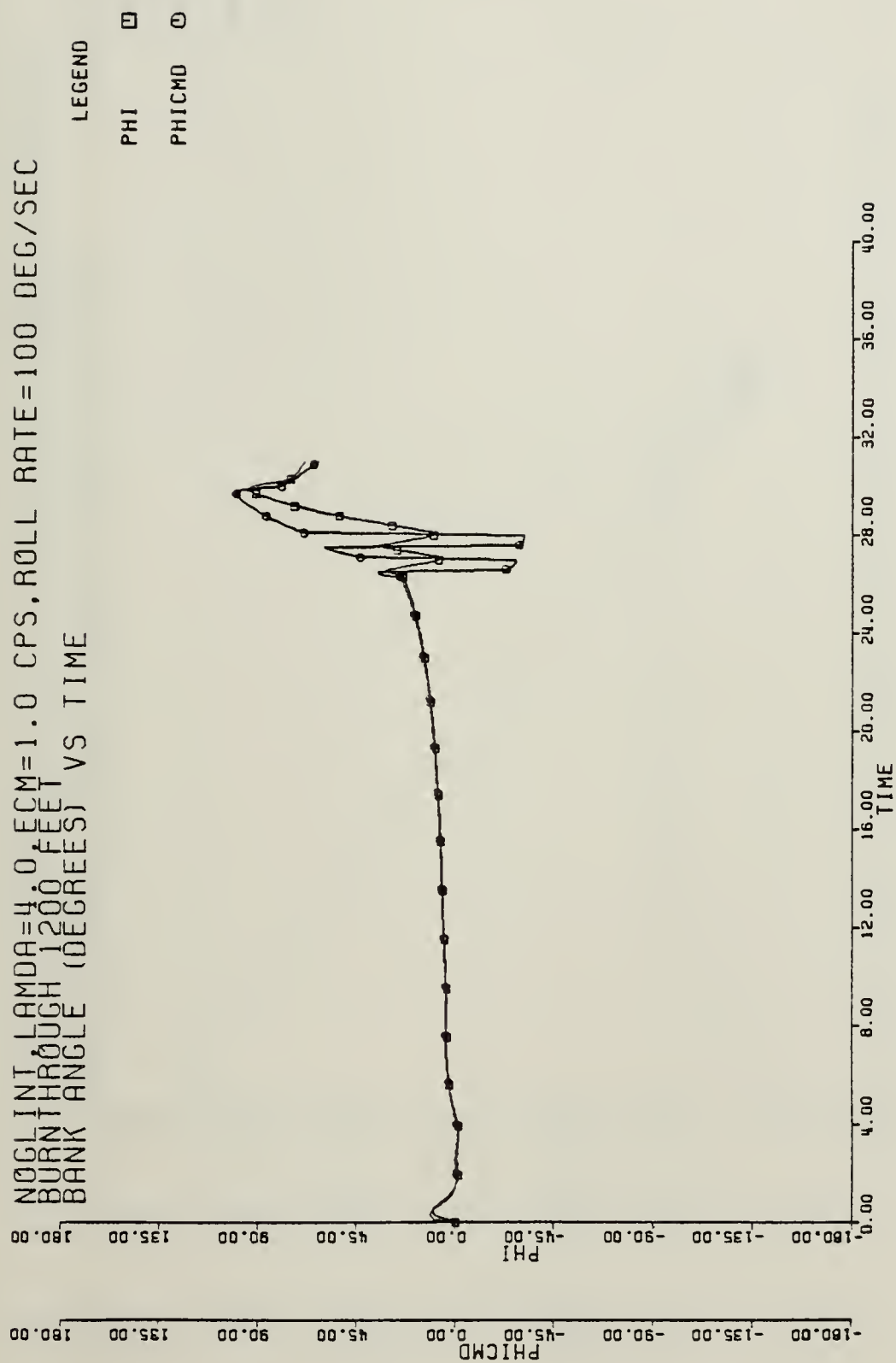


Figure 5-6b Sea Skimmer Response for ECM 1 CPS, Roll Rate Limit 100 deg/sec

(PHICMD, PHI vs TIME)

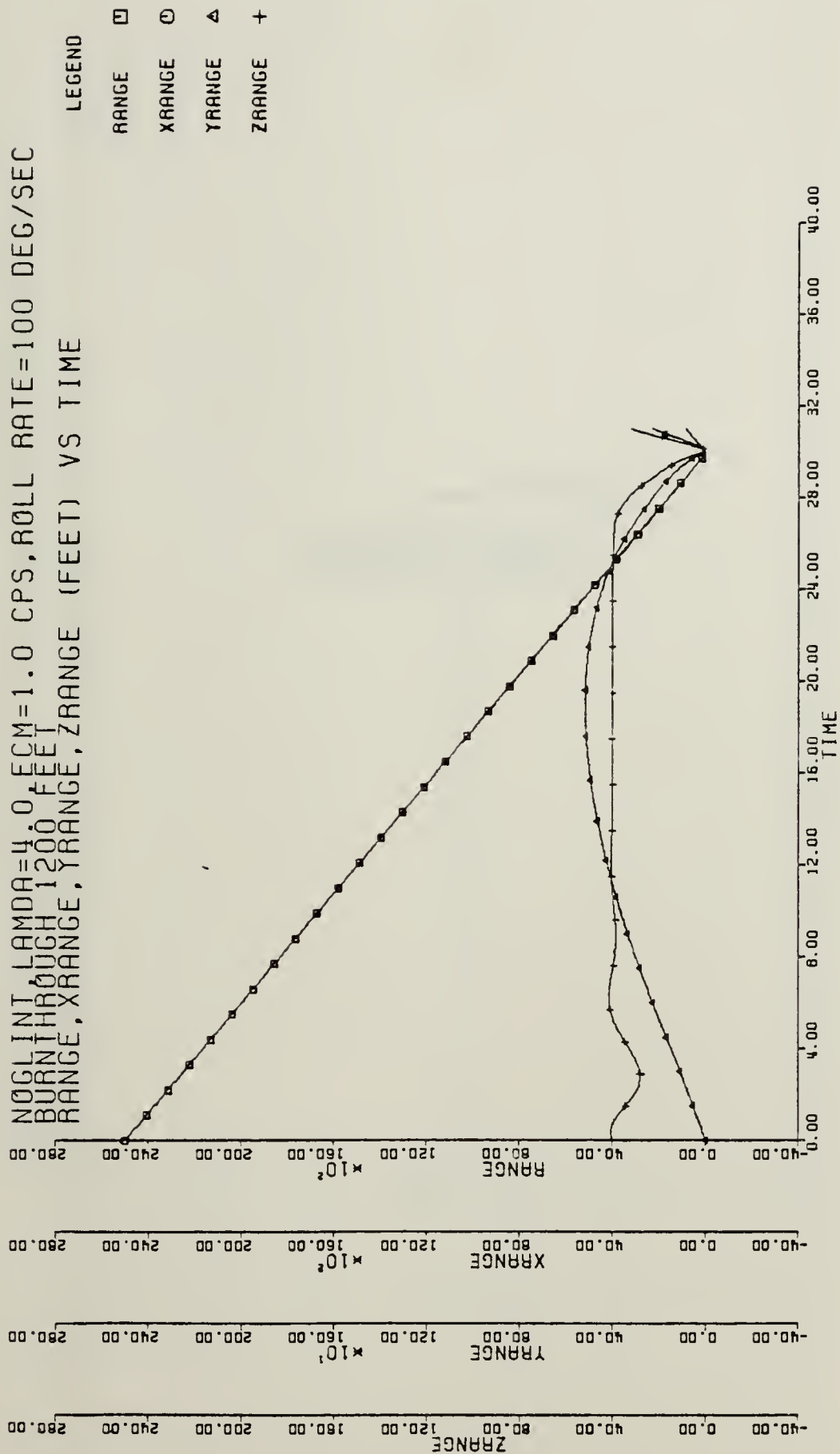


Figure 5-6c Sea Skimmer Response for ECM 1 CPS, Roll Rate Limit 100 deg/sec
 (RANGE, X RANGE, Y RANGE, Z RANGE vs TIME)

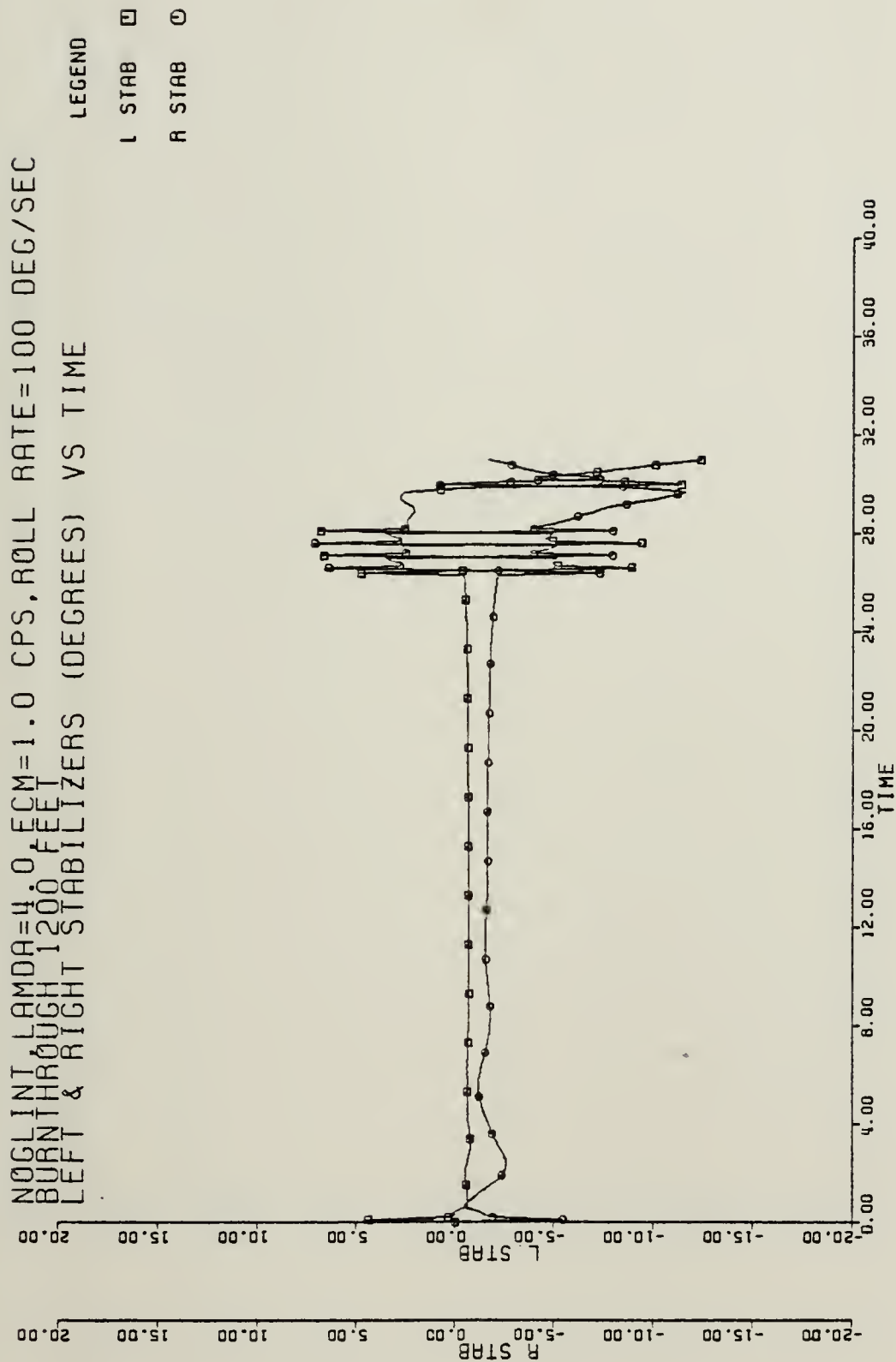


Figure 5-6d Sea Skimmer Response for ECM 1 CPS, Roll rate Limit 100 deg/sec
 (L STAB, R STAB vs TIME)

NOCLINT LAMDA=4.0 ECM=1.0 CPS, ROLL RATE=100 DEG/SEC
 BURNTHROUGH 1200 FEET
 RUDDER POSITION (DEGREES) VS TIME

LEGEND

RUDDER □

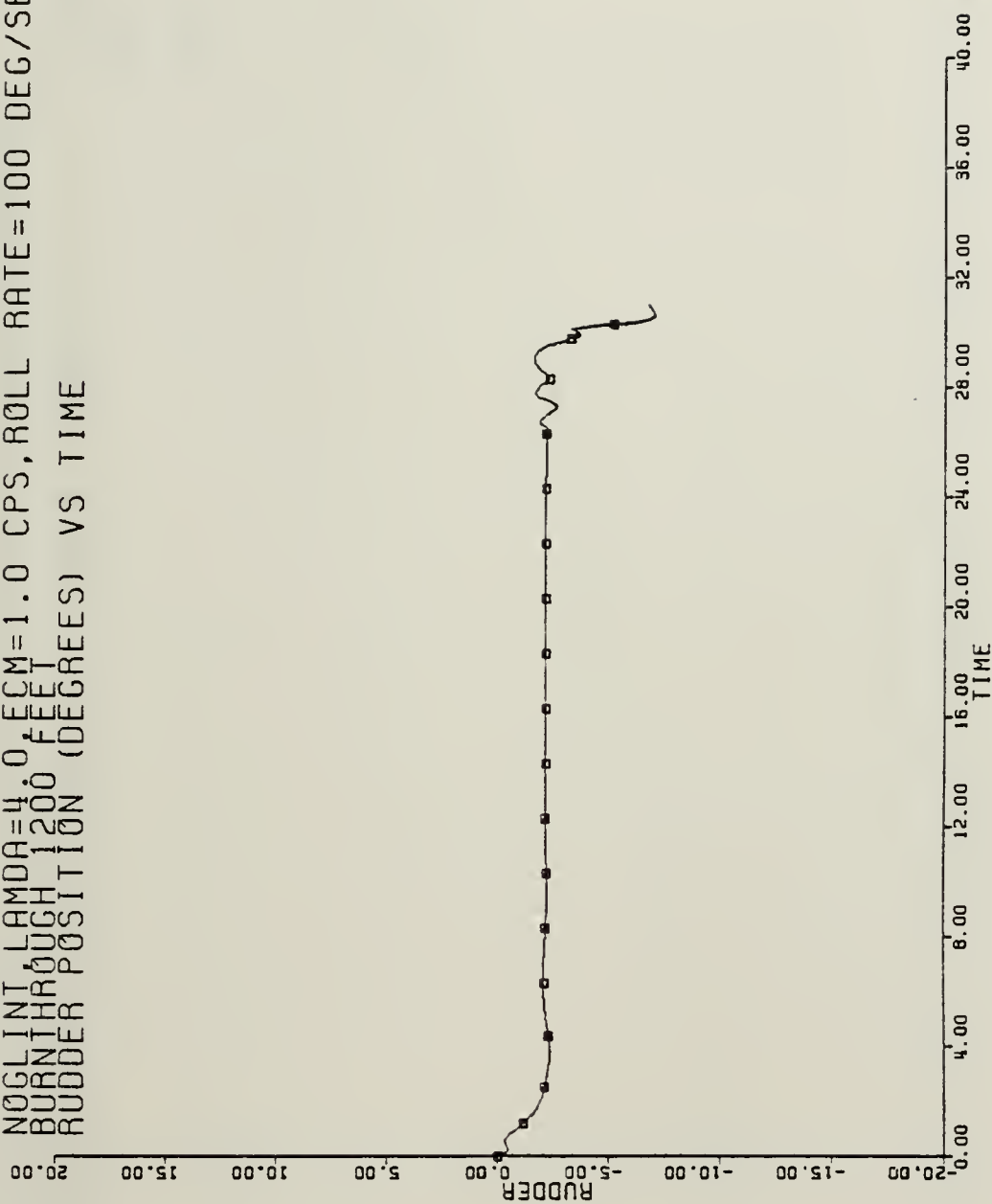


Figure 5-6e Sea Skimmer Response for ECM 1 CPS, Roll Rate Limit 100 deg/sec
 (RUDDER vs TIME)

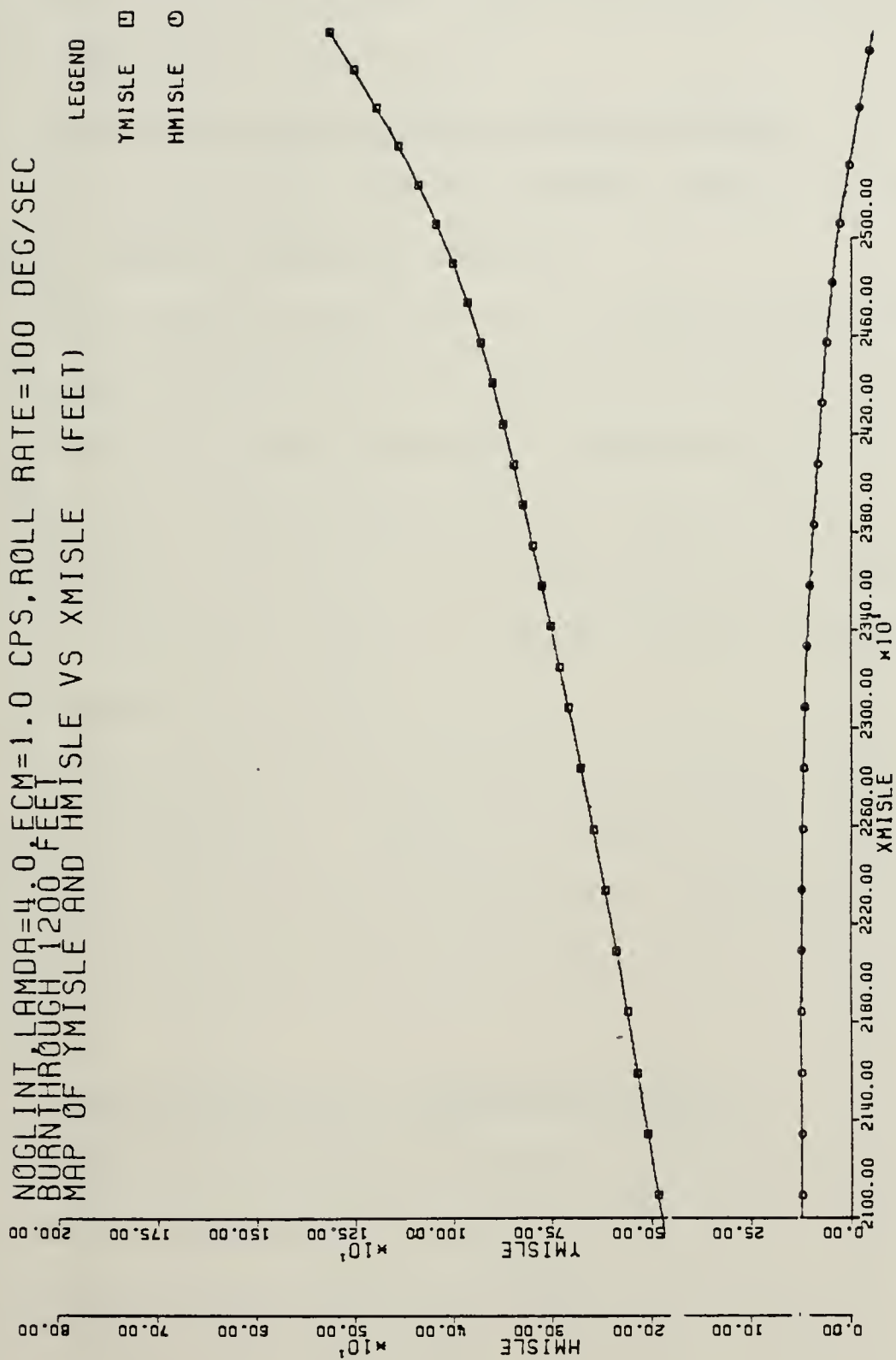


Figure 5-6f Sea Skimmer Response for ECM 1 CPS, Roll Rate Limit 100 deg/sec
 (YMISLE, HMISLE vs XMISLE)

miss distance remains high for all burn through ranges out to 2000 feet. But, for the remaining blinking frequencies and burn through ranges the miss distances improve significantly for increasing roll rate limits. A miss distance of 7.9 feet for a burn through range of 800 feet and 2 Hertz blinking frequency is excellent.

2. Analysis of Sea Skimmer Scheme Results

The results for the sea skimmer scheme are quite different than the baseline scheme.

Burn through range seems to be the single most controlling variable. Miss distances for a burn through range of 1500 feet are marginally satisfactory for all roll rate limits and ECM blinking rates. However, at a burn through range of 2000 feet, miss distances for varying roll rate limits and ECM blinking frequencies are extremely low and considered quite good.

Varying the ECM blinking rate produces little effect on the miss distances. However, a unique roll rate limit of 100 degrees per second produces miss distances double the miss distances for roll rate limits of 50 or 200 degrees per second.

3. Analysis of Glint Simulation Results

Figure 5-7 shows the random introduction of glint in the target position and line of sight rate. The miss distance for the run in this figure is 15 feet, but analysis from other runs show that glint increases the miss distance 30 to 50 percent.

TEST RUN WITH TARGET 25000XOX-40FT FROM MISSILE.
 MISSILE INITIAL HEADING TRUE NORTH, GLINT,
 SYT, THETAT

LEGEND

SYT □
 THETAT ○

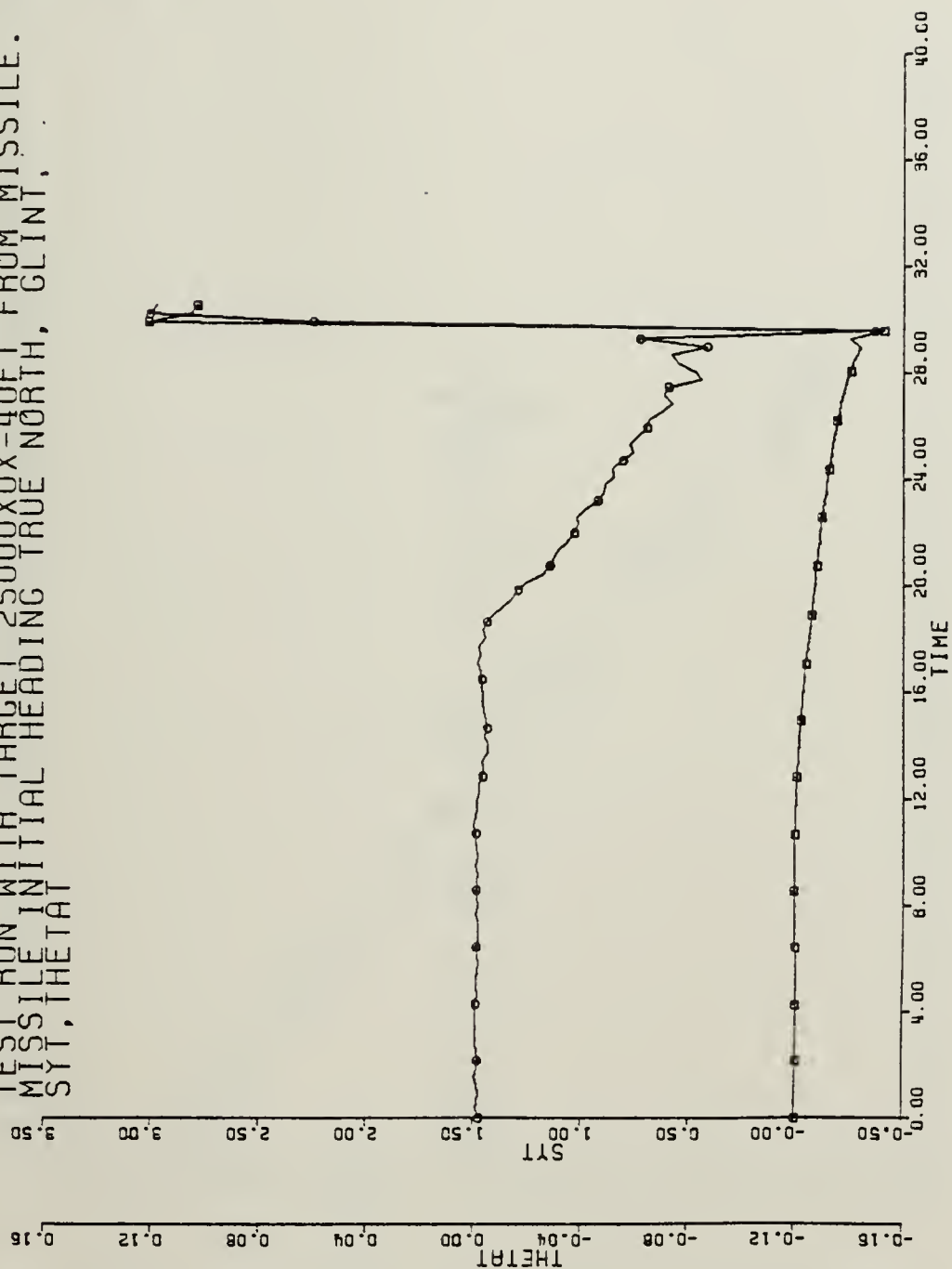


Figure 5-7a Baseline Response with Glint
 (SYT, THEATAT vs TIME)

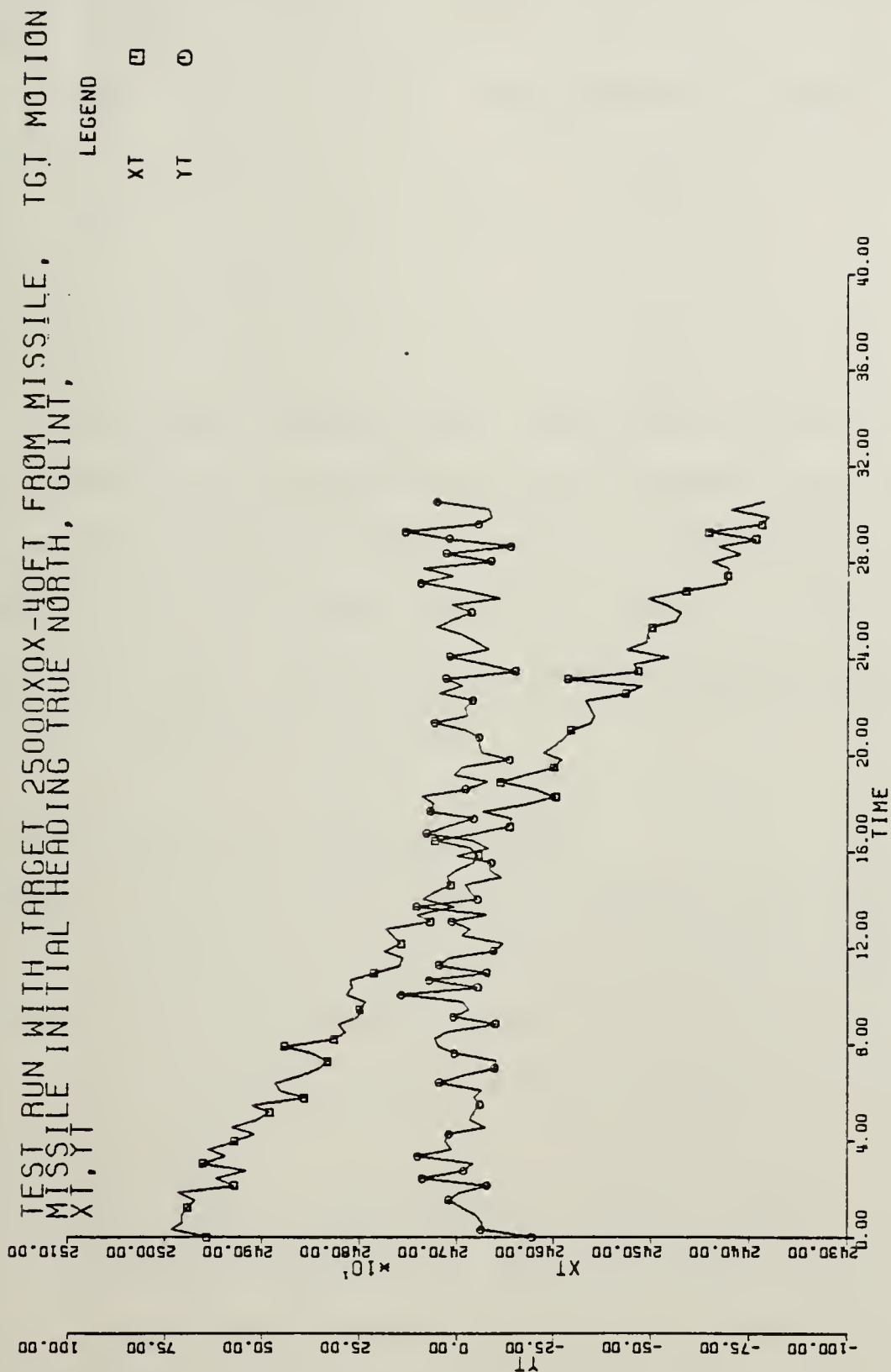


Figure 5-7b Baseline Response with Glint
 (XT, YT vs Time)

4. Proportional Navigation Ratio Selection

The following matrix shows the result of miss distance in a no ECM environment for varying proportional navigation constant (PN).

PN	Miss Distance (feet)
3	10.6
3.5	6.9
4	4.4
4.5	3.2

Although a proportional navigation constant (PN) of 4.5 results in the smallest miss distance excessive overshoot to step inputs results in this proportional navigation constant as being an unsatisfactory choice. A PN of 4.0 was chosen based upon satisfactory system responses and the small miss distance achieved.

C. CONCLUSIONS AND RECOMMENDATIONS

Based upon the results of this study it can be concluded that miss distance is a function of roll rate limit, ECM blinking rate, burn through range, and the guidance scheme chosen. The guidance scheme chosen is most significant of these factors.

For the baseline guidance and control scheme, roll rate limit is the most significant variable affecting miss distance. One exception to this is the 0.5 Hertz blinking

rate set of runs which shows a miss distance improvement when roll rate is increased from 50 to 100 degrees per second, but yields poor miss distances for 200 degrees per second.

The most significant variable affecting miss distance for the sea-skimmer scheme is burn through range. Nevertheless, a 100-degree-per-second roll rate limit appears to be unacceptable at all burn through ranges simulated.

In summary, given that the target controls ECM blinking frequency and burn through range, the optimum selections are:

Baseline Scheme - Roll rate limit = 200 degrees per second
Sea-Skimmer - Roll rate limit = 50 or 200 degrees per second

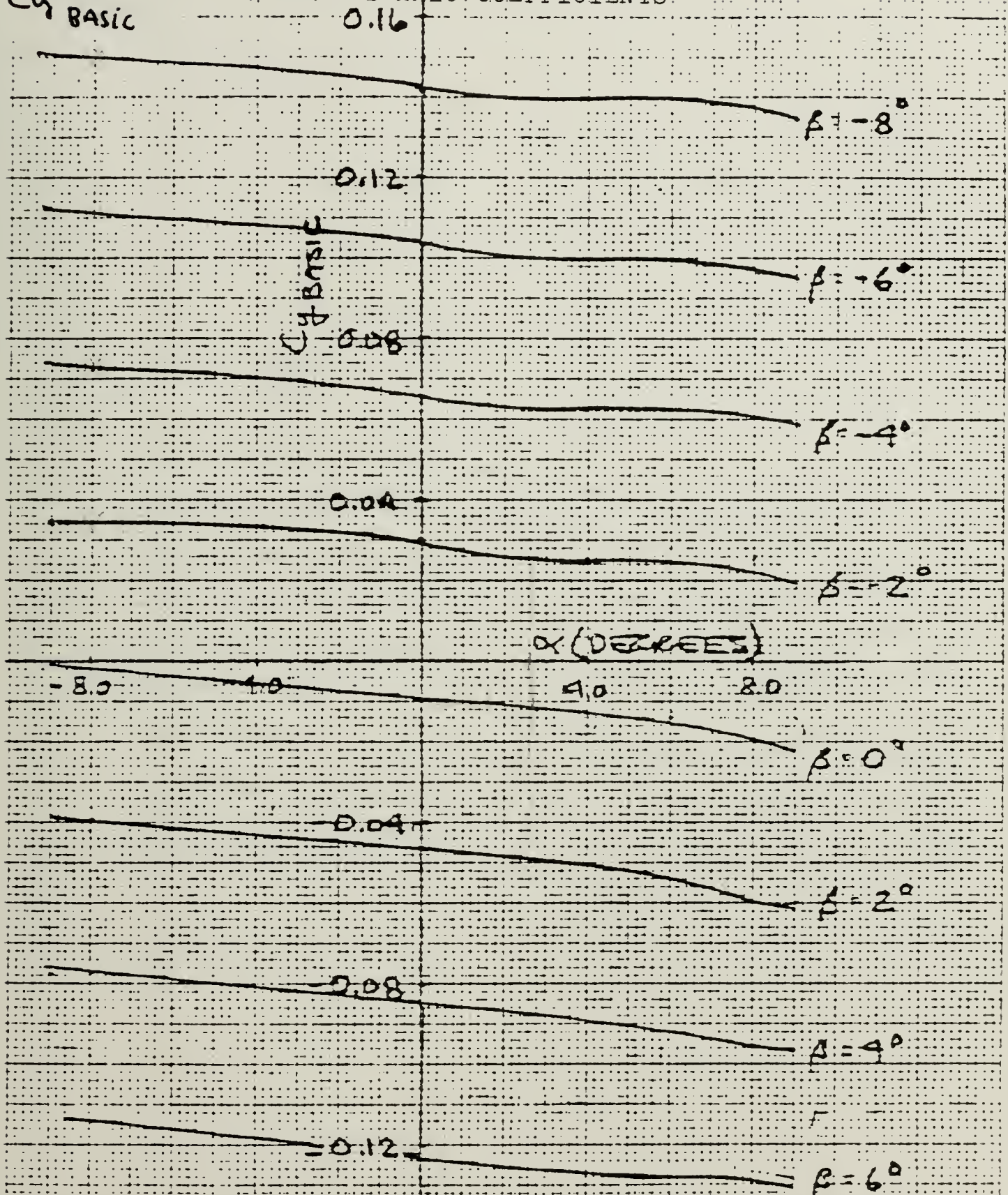
The following additional studies are recommended:

- a. Further modeling with glint.
- b. Variation of the direction and magnitude of the ECM shift.
- c. Alteration of the decision variable used in the simulation to switch phases from range to line of sight rate.
- d. Variations in flight path geometry.
- e. Comparison of control laws using skid-to-turn with control laws using bank-to-turn maneuvering.

APPENDIX A

AERODYNAMIC COEFFICIENTS

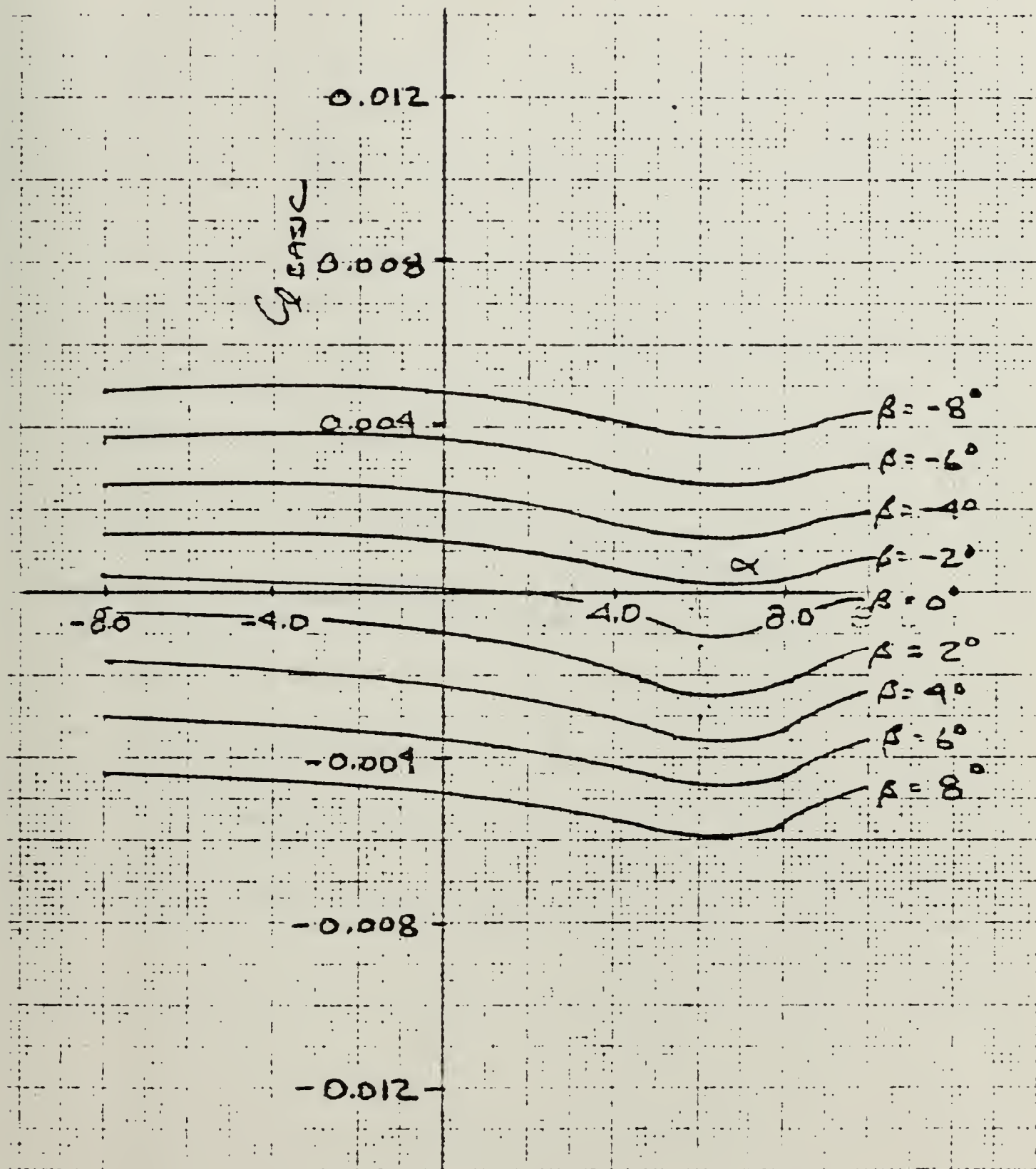
$C_{Y \text{ BASIC}}$



Side Slip Characteristics

α vs β vs $C_{Y \text{ BASIC}}$

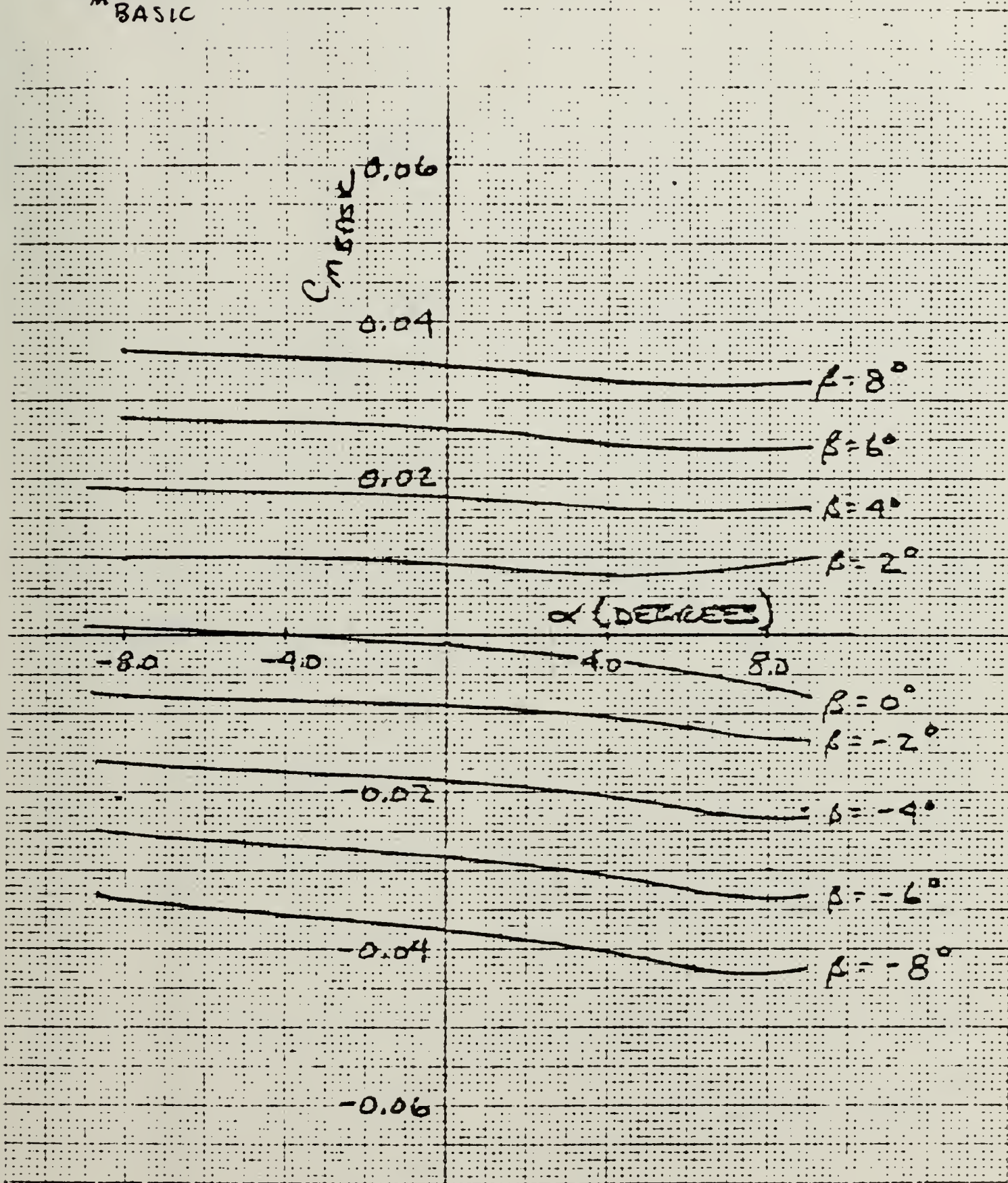
$C_{l \text{ BASIC}}$



Side Slip Characteristic

α vs β vs $C_{l \text{ basic}}$

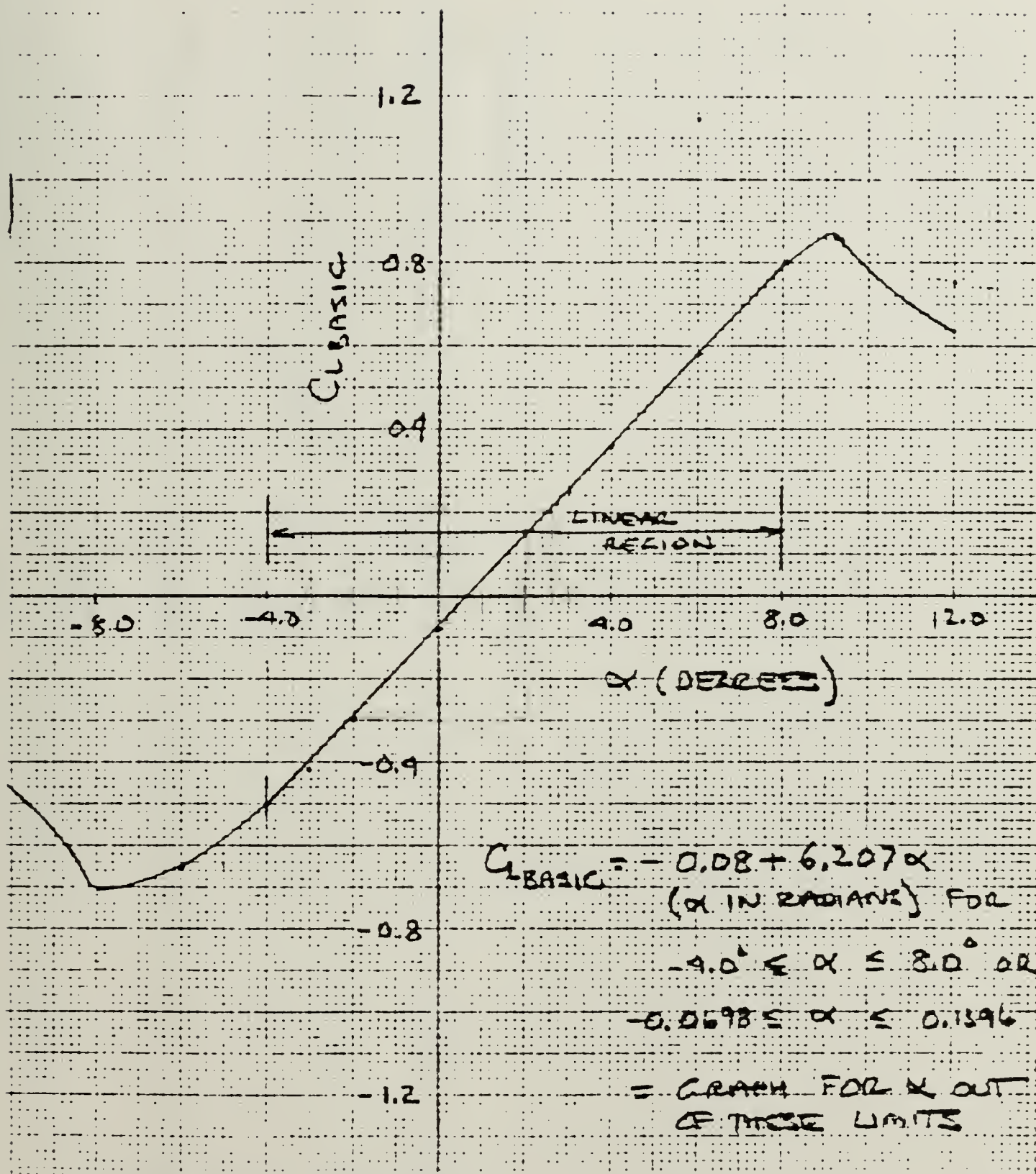
$C_{m \text{ BASIC}}$



Side Slip Characteristics

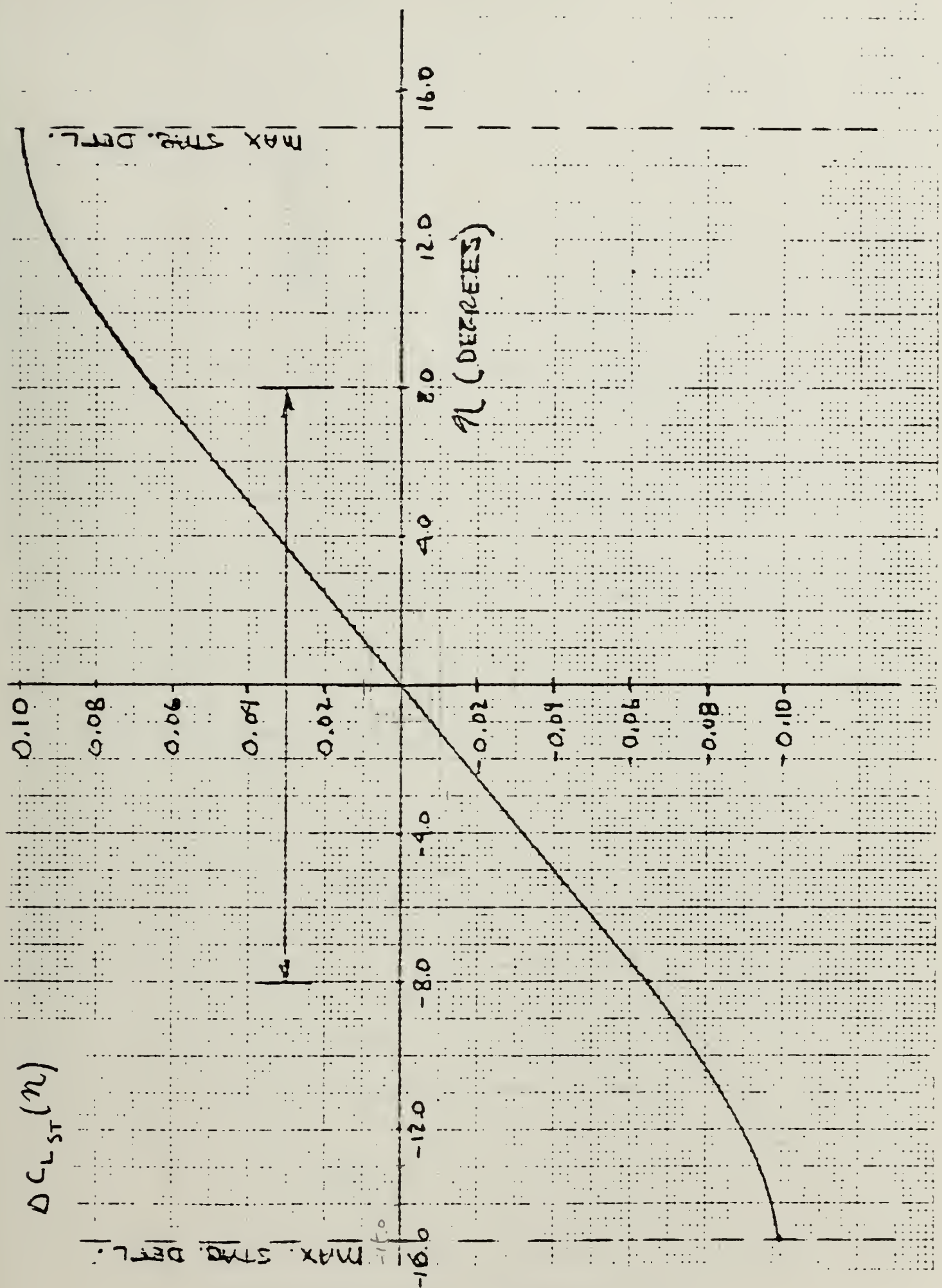
α vs β vs $C_{n \text{ basic}}$

C_LBASIC



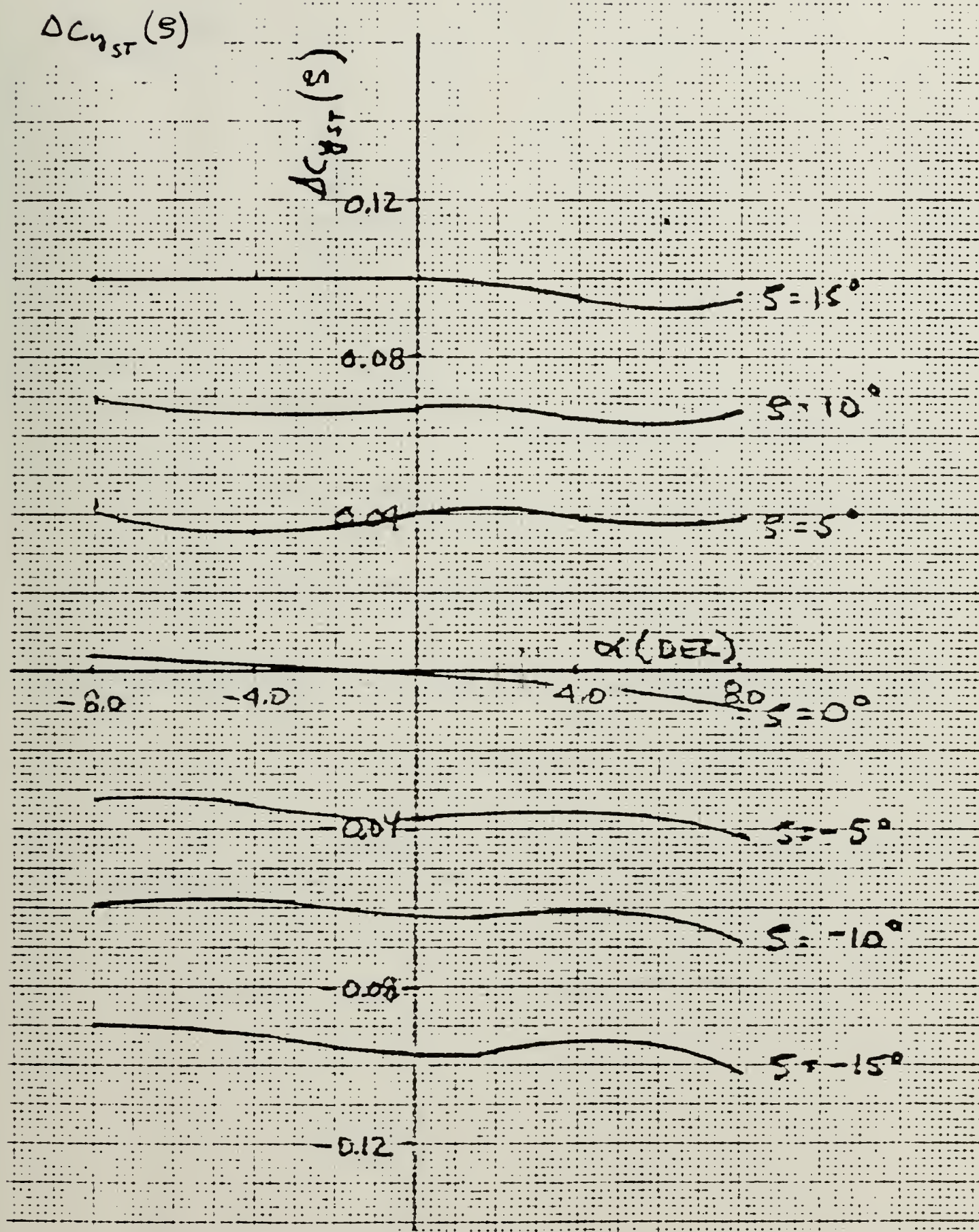
Lift Characteristics

α vs $C_{L \text{ basic}}$



Lift Characteristics

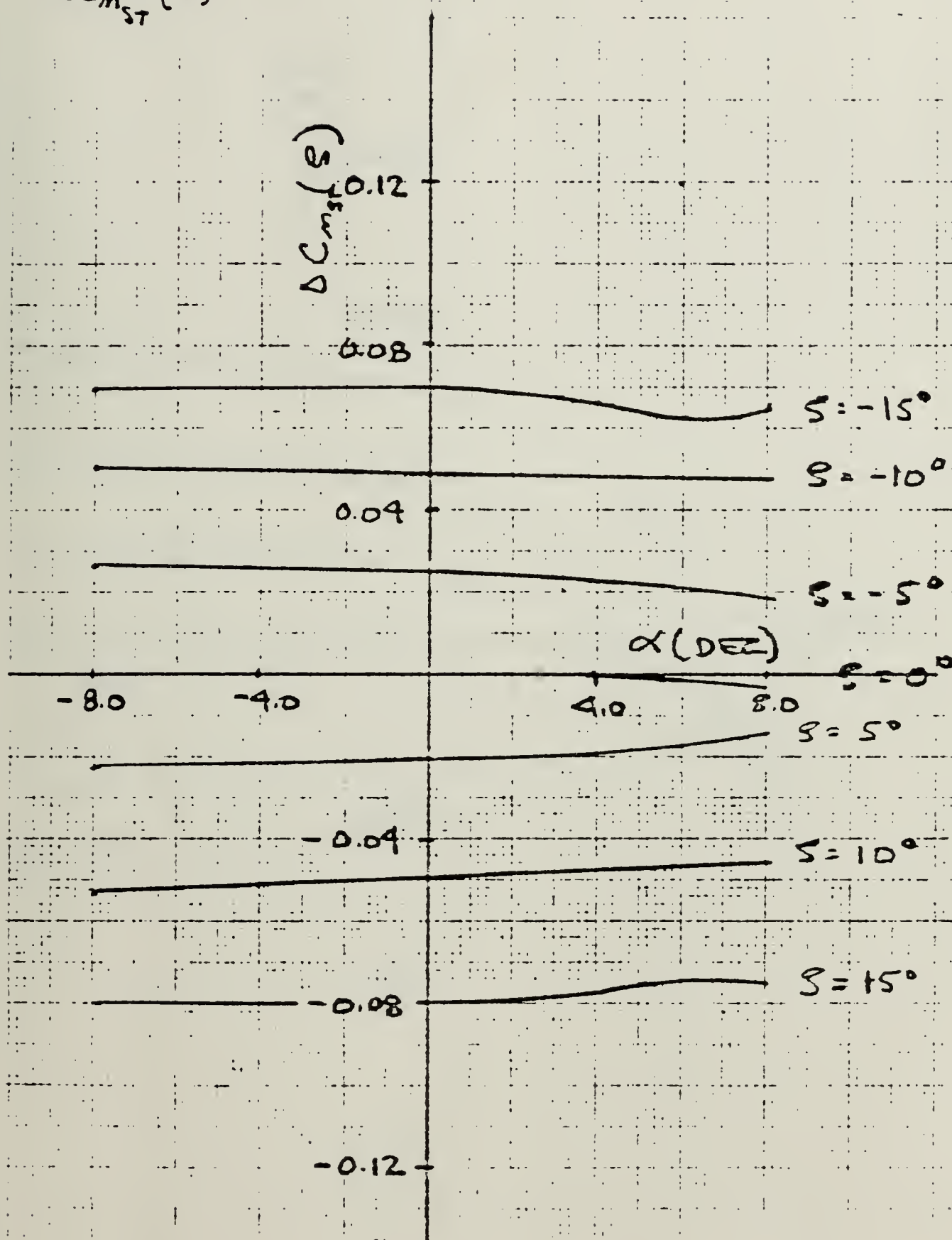
n vs $\Delta C_{L_{ST}}(n)$



Directional Control Characteristics

α vs ζ vs $\Delta C_{Y_{ST}}(\zeta)$

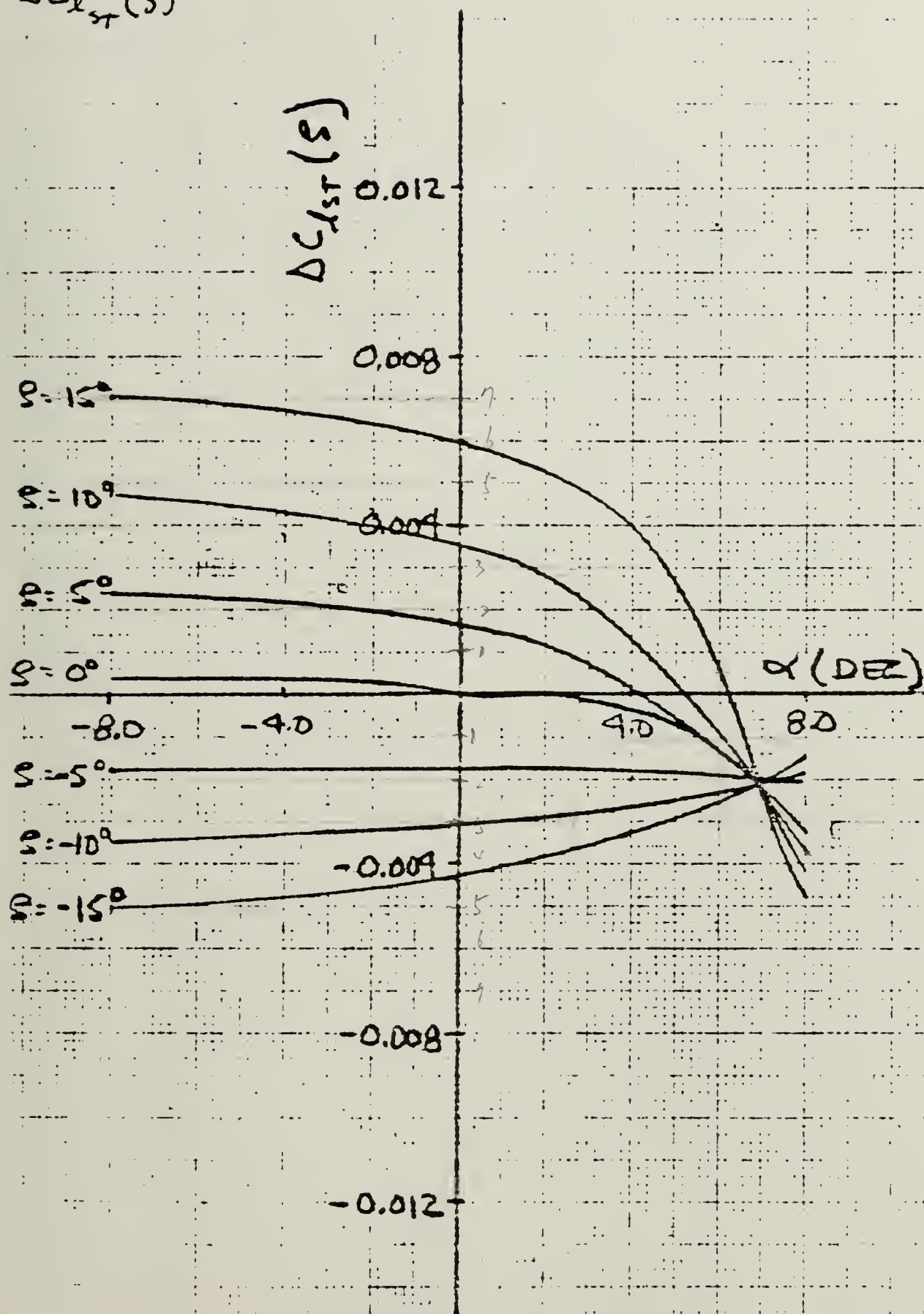
$\Delta C_{m_{ST}}(\xi)$



Directional Control Characteristics

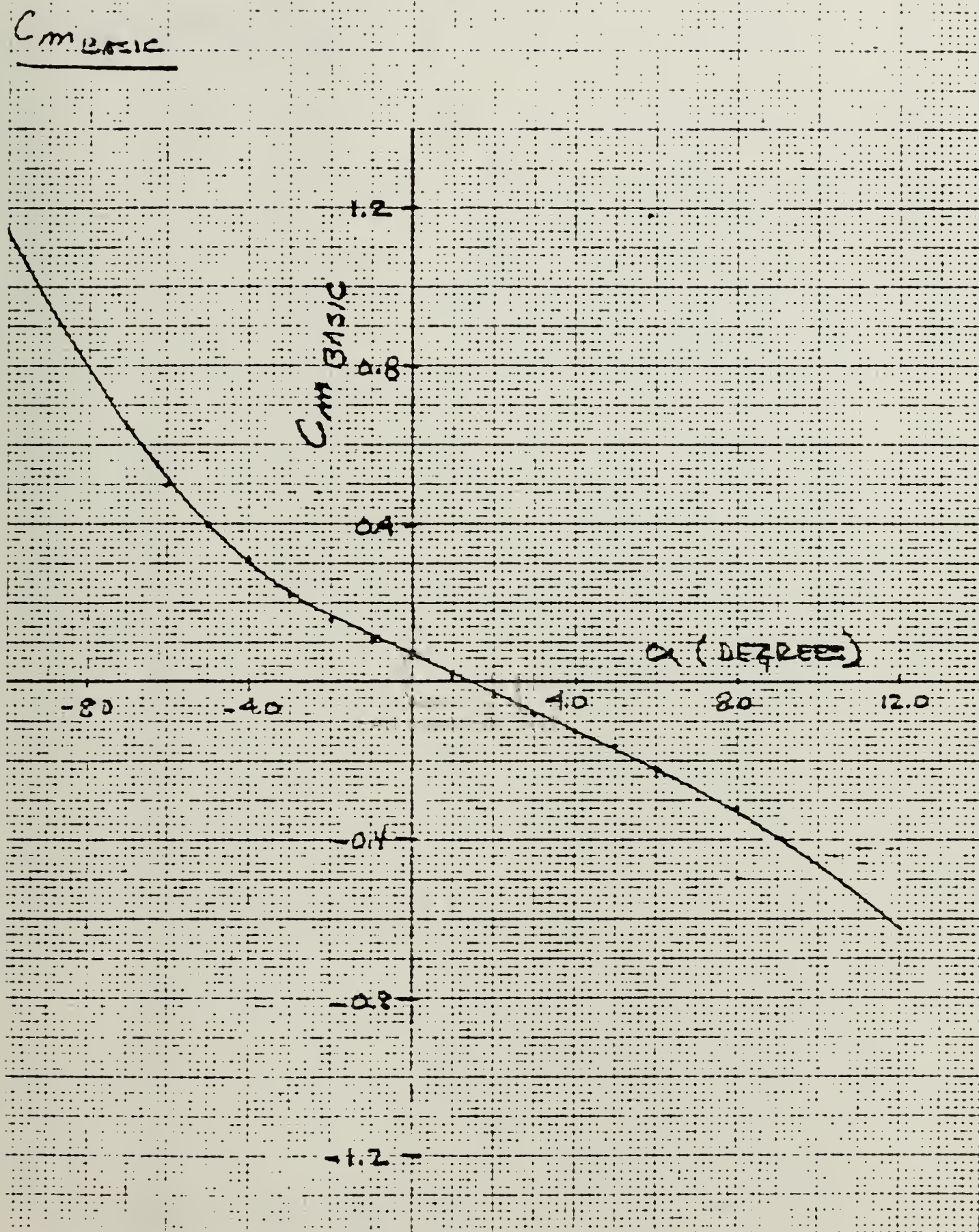
α vs ξ vs $\Delta C_{n_{ST}}(\xi)$

$\Delta C_{LST}(\beta)$

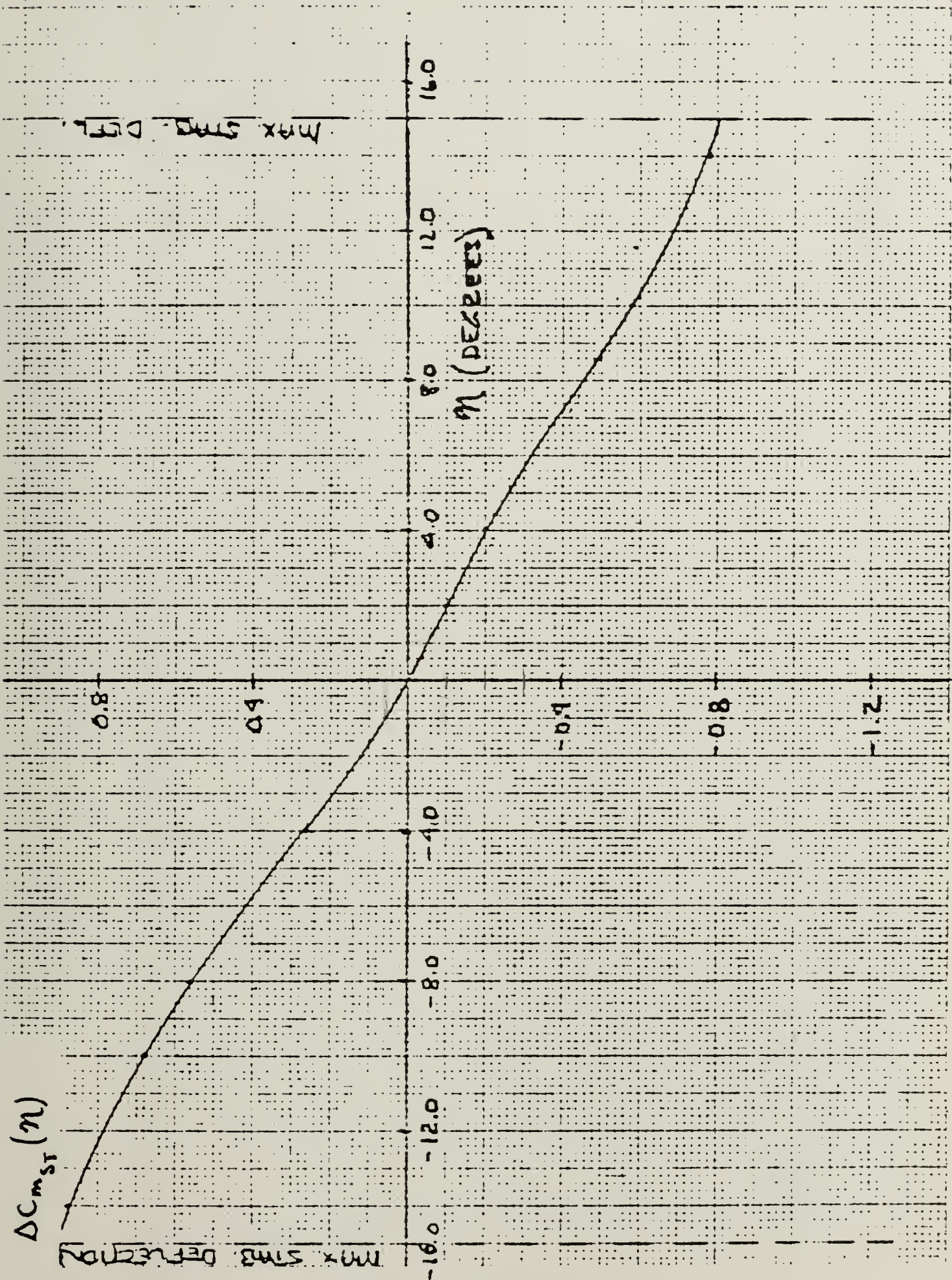


Directional Control Characteristics

α vs β vs $\Delta C_{LST}(\beta)$

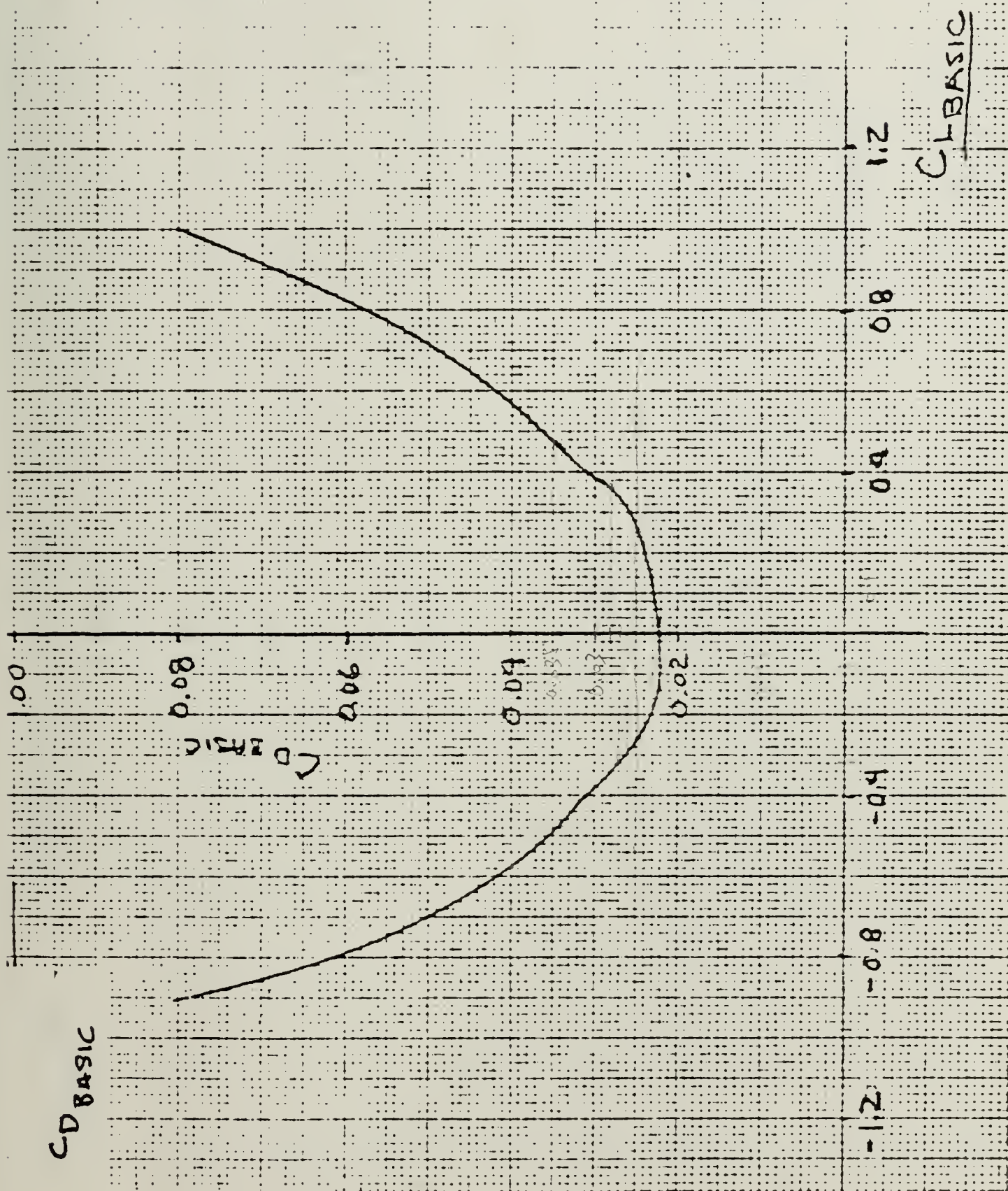


Pitching Moment Characteristics
 α vs $C_{M\text{ basic}}$



Pitching Moment Characteristics

η vs $\Delta C_{m_{ST}}(\eta)$



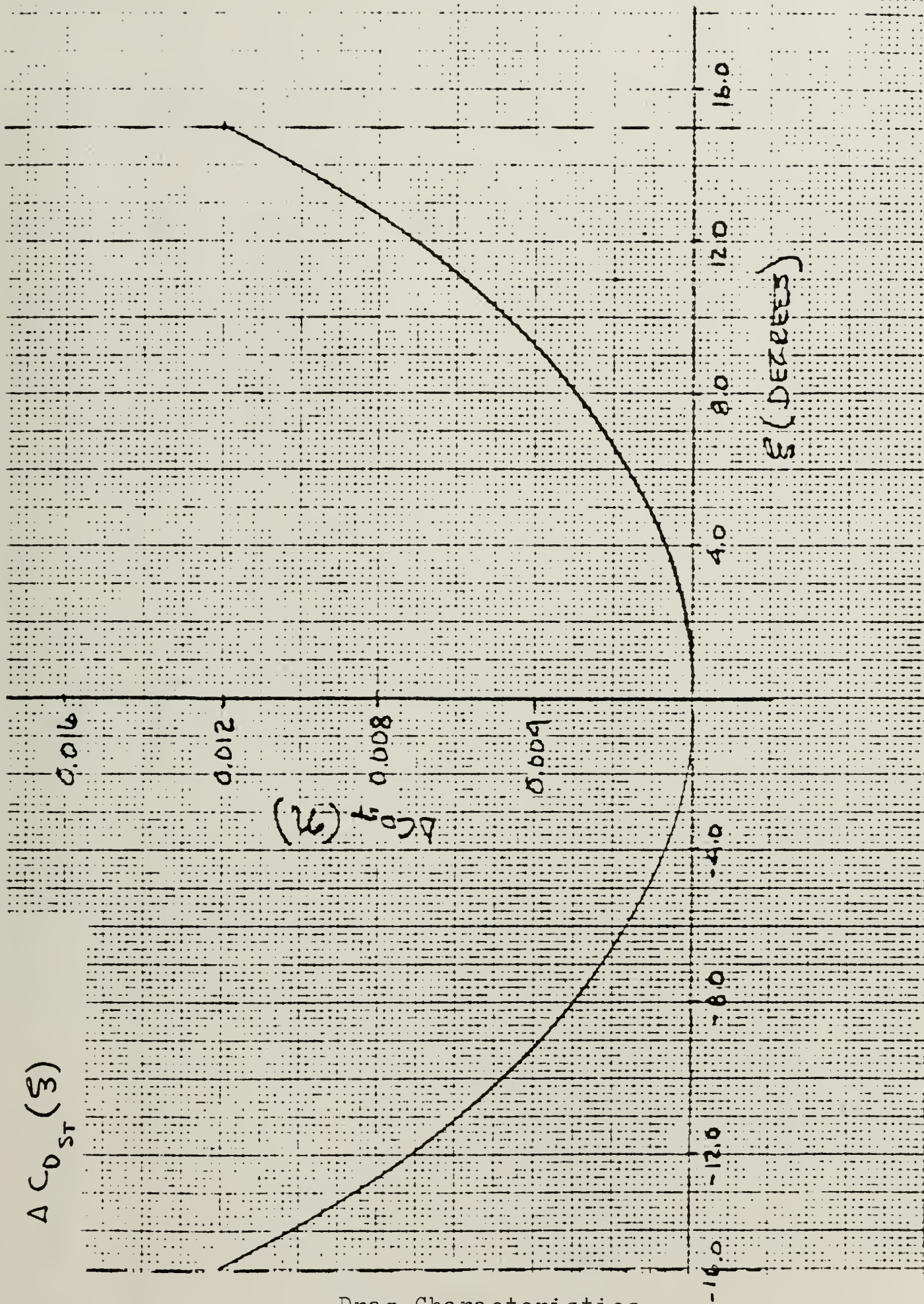
Drag Characteristics

$C_{L\text{BASIC}}$ vs $C_{D\text{BASIC}}$



Drag Characteristics

η vs $\Delta C_{DST} (\eta)$



Drag Characteristics

ξ vs $\Delta C_{D_{ST}} (\xi)$

$\Delta C_{D_{ST}}(\zeta)$

0.016

0.012

0.008

0.004

$\Delta C_{D_{ST}}(\zeta)$

-12.0

-8.0

-4.0

0.0

4.0

8.0

12.0

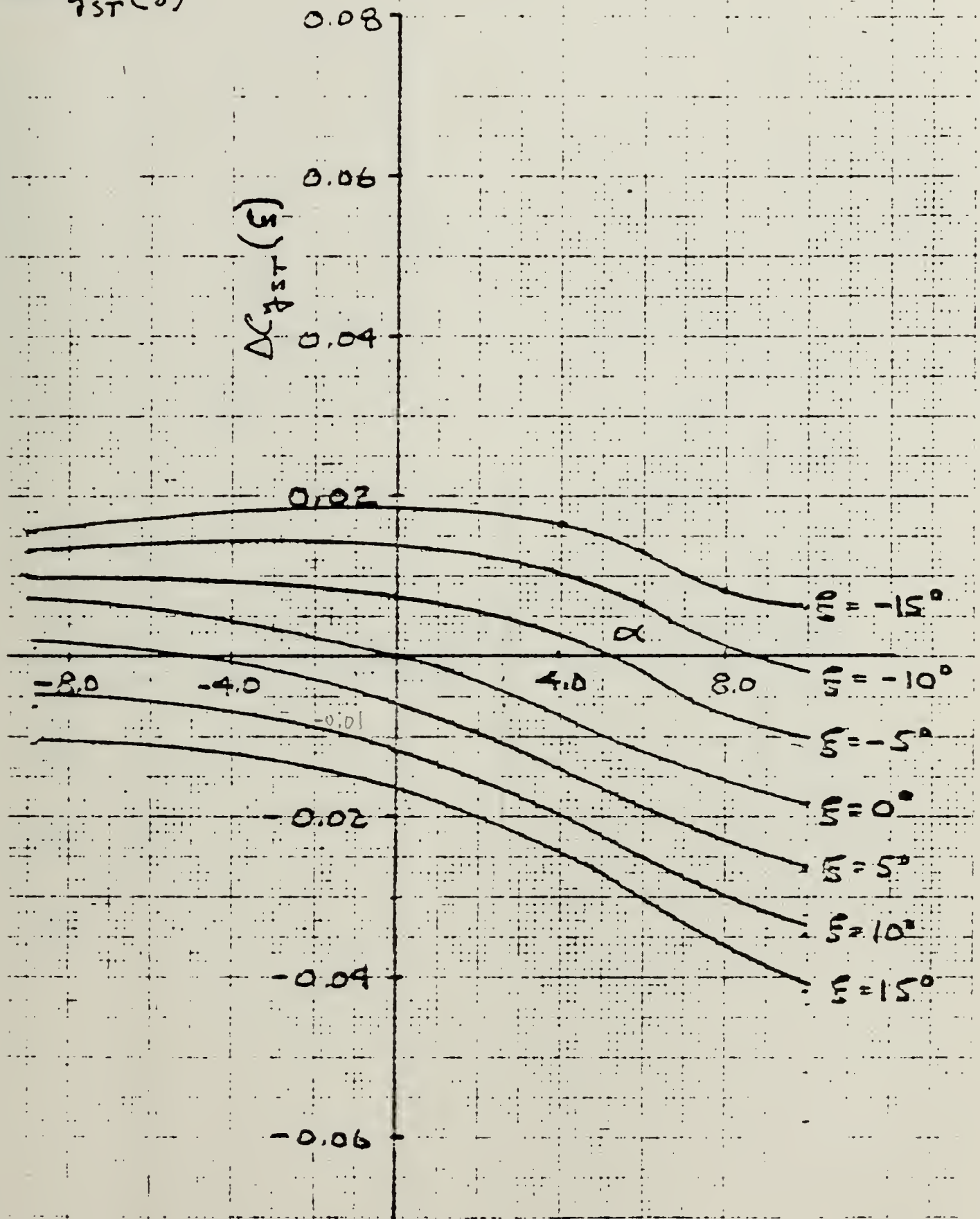
16.0

ζ (DEGREES)

Drag Characteristics

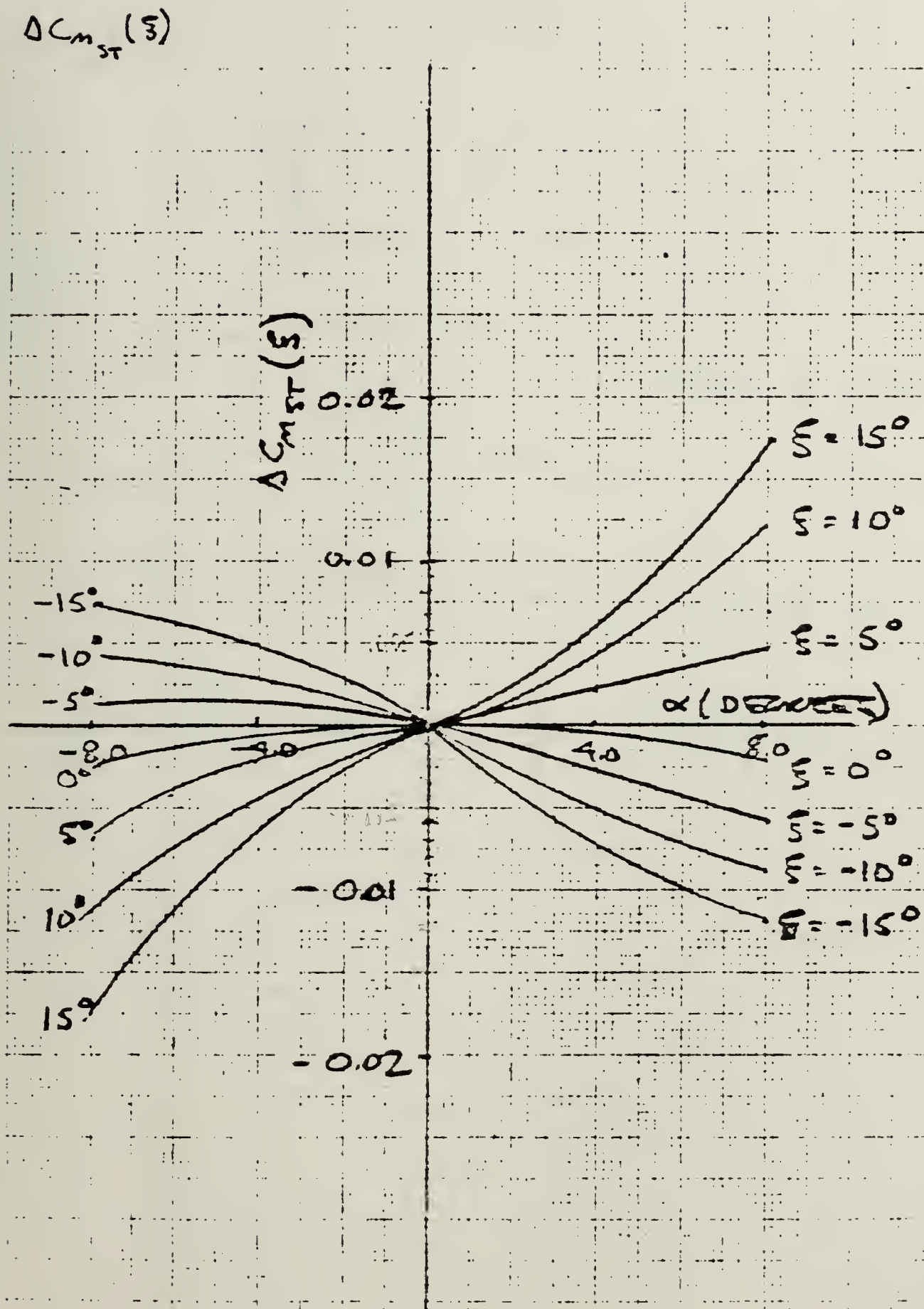
ζ vs $\Delta C_{D_{ST}}(\zeta)$

$\Delta C_{YST}(\xi)$



Lateral Control Characteristics

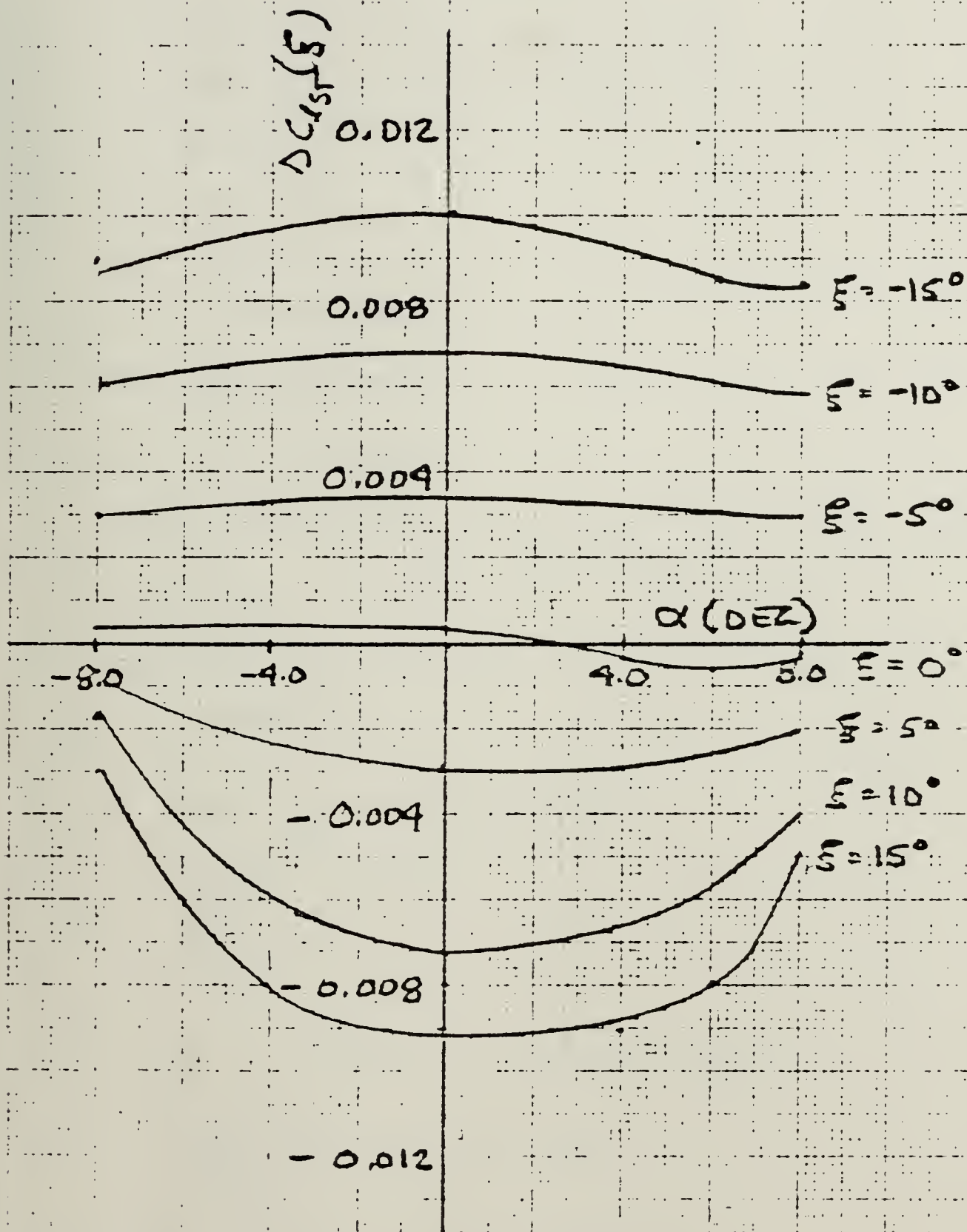
α vs ξ vs $\Delta C_{YST}(\xi)$



Lateral Control Characteristics

α vs ξ vs $\Delta C_{n_{ST}}(\xi)$

$\Delta C_{l_{ST}}(\xi)$



Lateral Control Characteristics

α vs ξ vs $\Delta C_{l_{ST}}(\xi)$

APPENDIX B
STEADY STATE DATA

$$\begin{aligned}
 W &= 2200 \text{ LBS (At end of cruise flight)} = 2200 \times 0.454 \text{ kg} = 998.8 \\
 m &= 68.38 \text{ Slugs} = 68.38 \times 14.18 \text{ kg} = 999.6 \text{ kg} \\
 S &= 12 \text{ feet}^2 \\
 \bar{b} &= 8.485 \text{ Feet} \\
 \bar{c} &= 1.414 \text{ Feet} \\
 I_{xx} &= 27.8 \text{ Slug feet}^2 \\
 I_{yy} &= 1507 \text{ Slug feet}^2 \\
 I_{zz} &= 1512 \text{ Slug feet}^2 \\
 I_{xz} &= 11.7 \text{ Slug feet}^2 \\
 T_x = T &= 600 \text{ LBS} = 500 \text{ lbf} = 500 \times 0.454 \text{ kg} \times 9.81 \text{ m/s}^2 = 2412 \text{ N} \\
 M &= 0.75 \\
 V_{T_{SS}} &= 839 \text{ Feet/Sec} \\
 \bar{q}_{SS} &= \frac{1}{2} \rho S V_{T_{SS}}^2 = 837 \text{ LBS/feet}^2 \\
 C_{L_{SS}} &= \frac{W}{\bar{q}_{SS} S} = 0.219 \\
 C_{D_{SS}} &= 0.0242 \\
 \alpha_{SS} &= \theta_{SS} = 2.65^\circ = 0.04625 \text{ Radian} \\
 T_{SS} &= \frac{C_{D_{SS}} \bar{q}_{SS} S}{\cos \alpha_{SS}} = 243.3 \text{ LBS} \\
 W_{SS} &= V_{T_{SS}} \sin \alpha_{SS} = 38.79 \text{ Feet/sec}
 \end{aligned}$$

$$U_{SS} = V_{T_{SS}} \cos \alpha_{SS} = 838.1 \text{ Feet/sec}$$

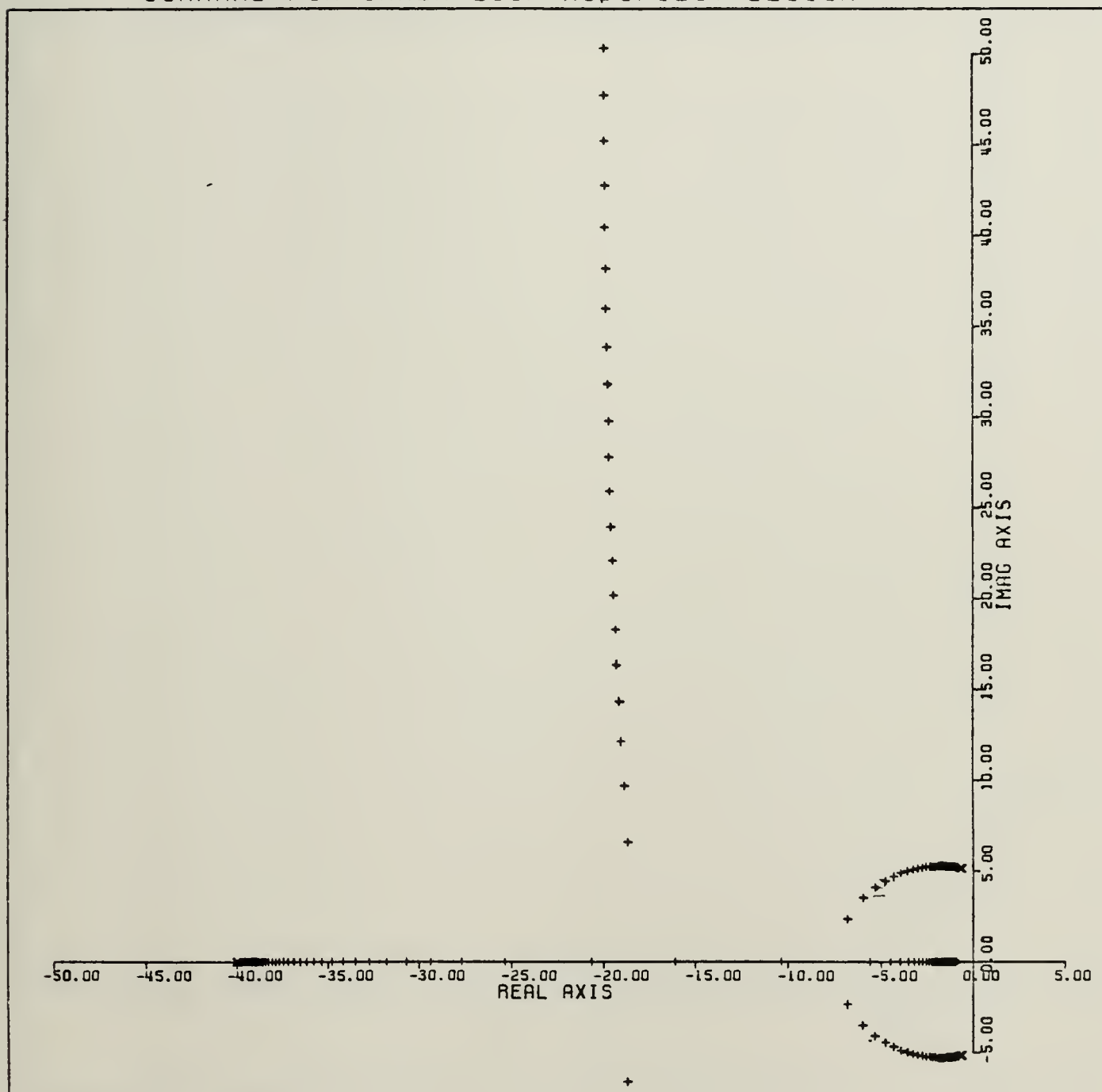
$$C_{m_{basic_{SS}}} = -0.06$$

$$C_{m_{ST_{SS}}} = 0$$

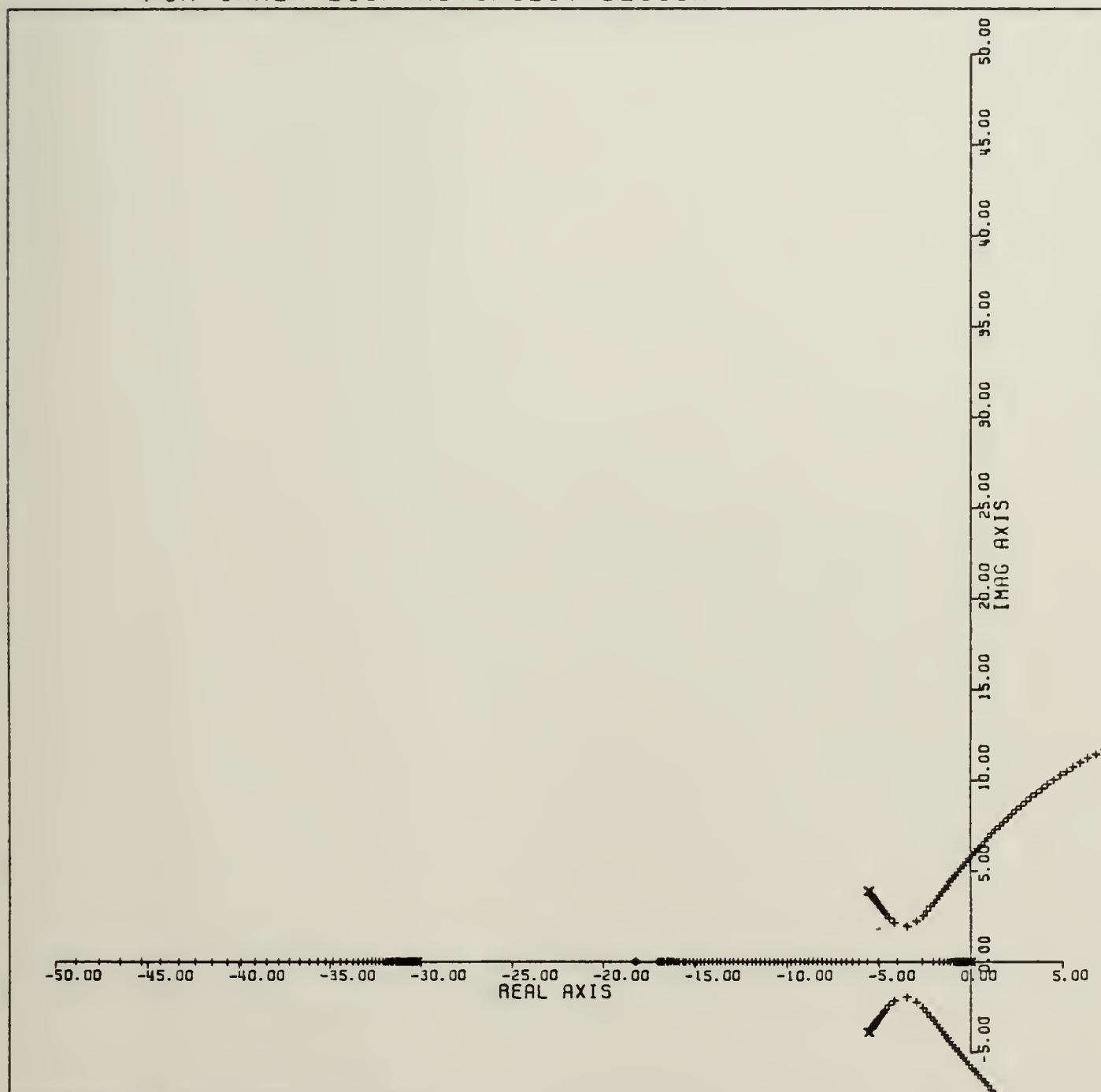
$$\eta_{SS} = -1.0^{\circ} = 0.01745 \text{ Radian}$$

APPENDIX C
AUTOPILOT ROOT LOCUS PLOTS

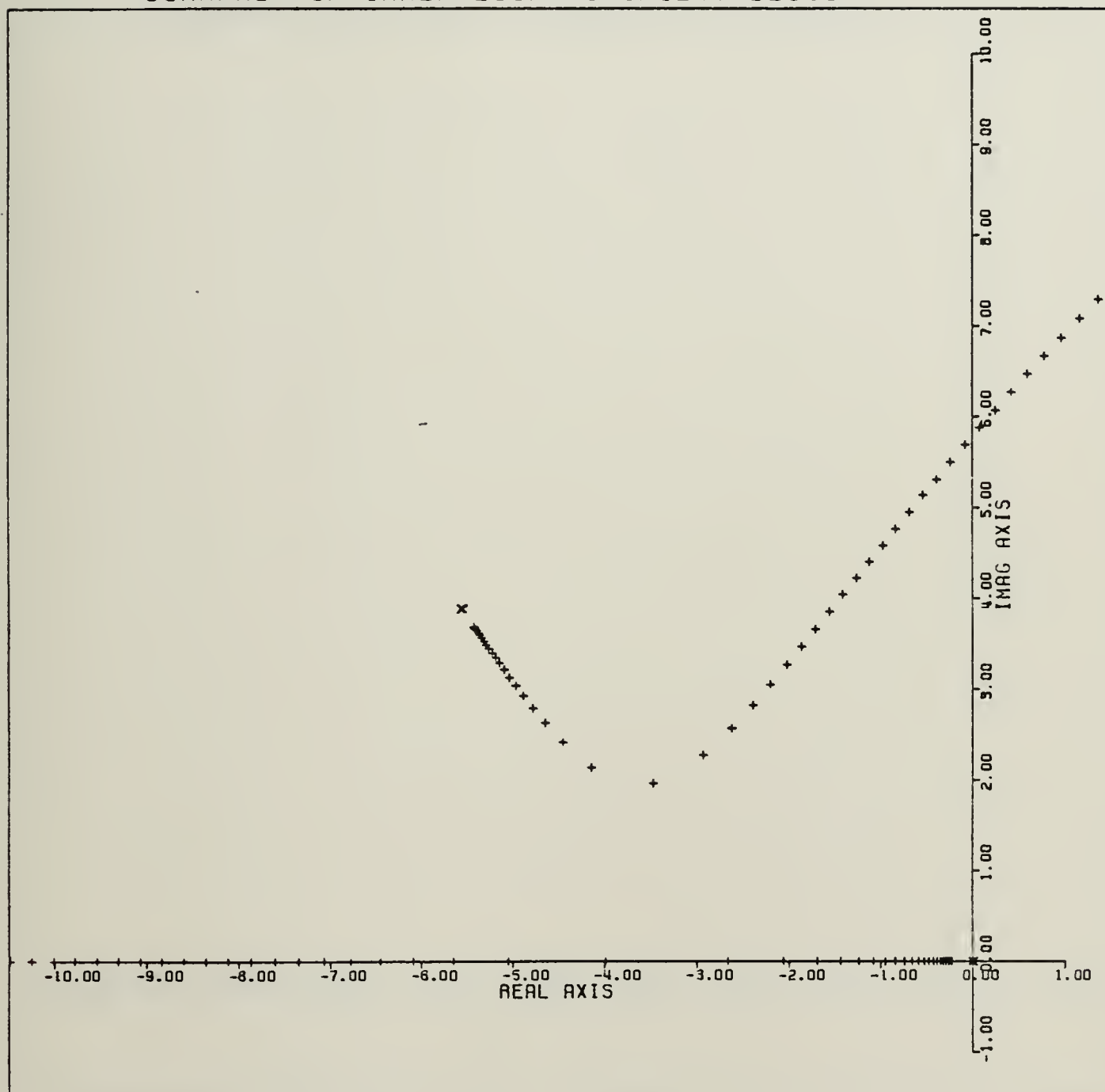
REAL AXIS (UNITS PER INCH) = 5.0000
IMAG AXIS (UNITS PER INCH) = 5.0000
ROOT LOCUS OF PITCH RATE LOOP OF NORMAL ACCEL
COMMAND FOR INNER LOOP AUTOPILOT DESIGN



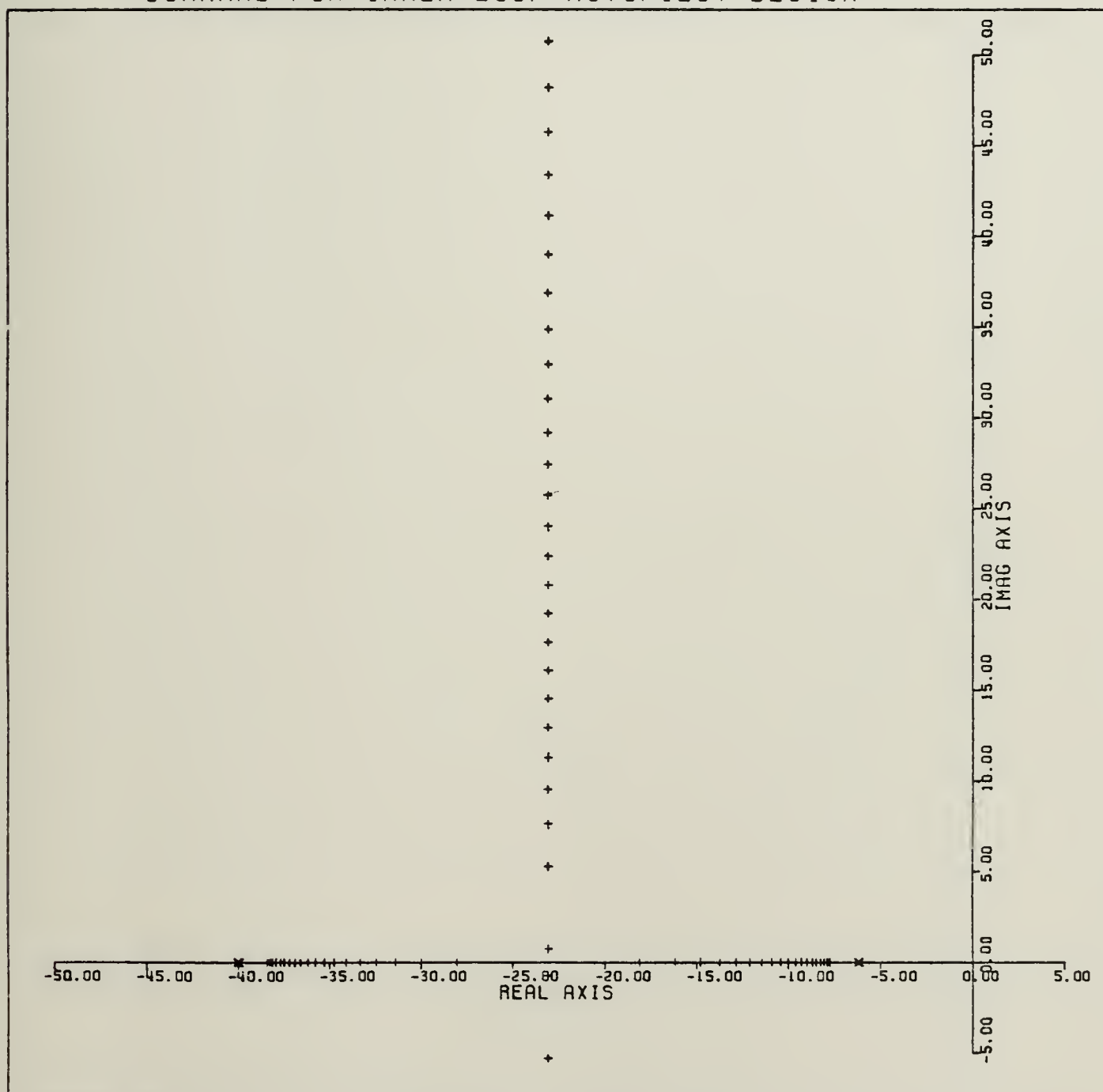
REAL AXIS (UNITS PER INCH) = 5.0000
IMAG AXIS (UNITS PER INCH) = 5.0000
ROOT LOCUS OF NORMAL ACCELERATION COMMAND
FOR INNER LOOP AUTOPILOT DESIGN



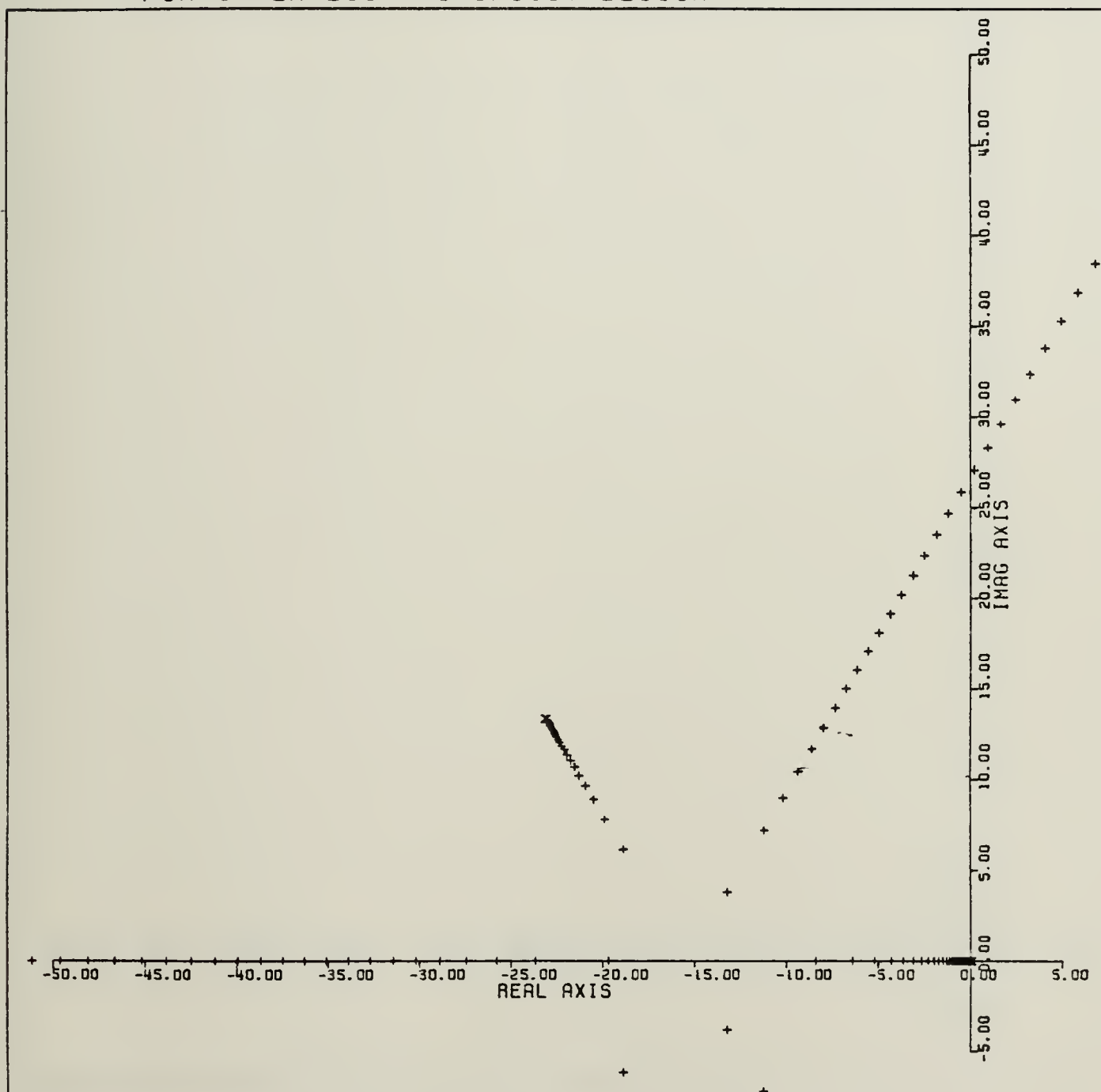
REAL AXIS (UNITS PER INCH) = 1.0000
IMAG AXIS (UNITS PER INCH) = 1.0000
ROOT LOCUS OF NORMAL ACCELERATION
COMMAND FOR INNER LOOP AUTOPILOT DESIGN



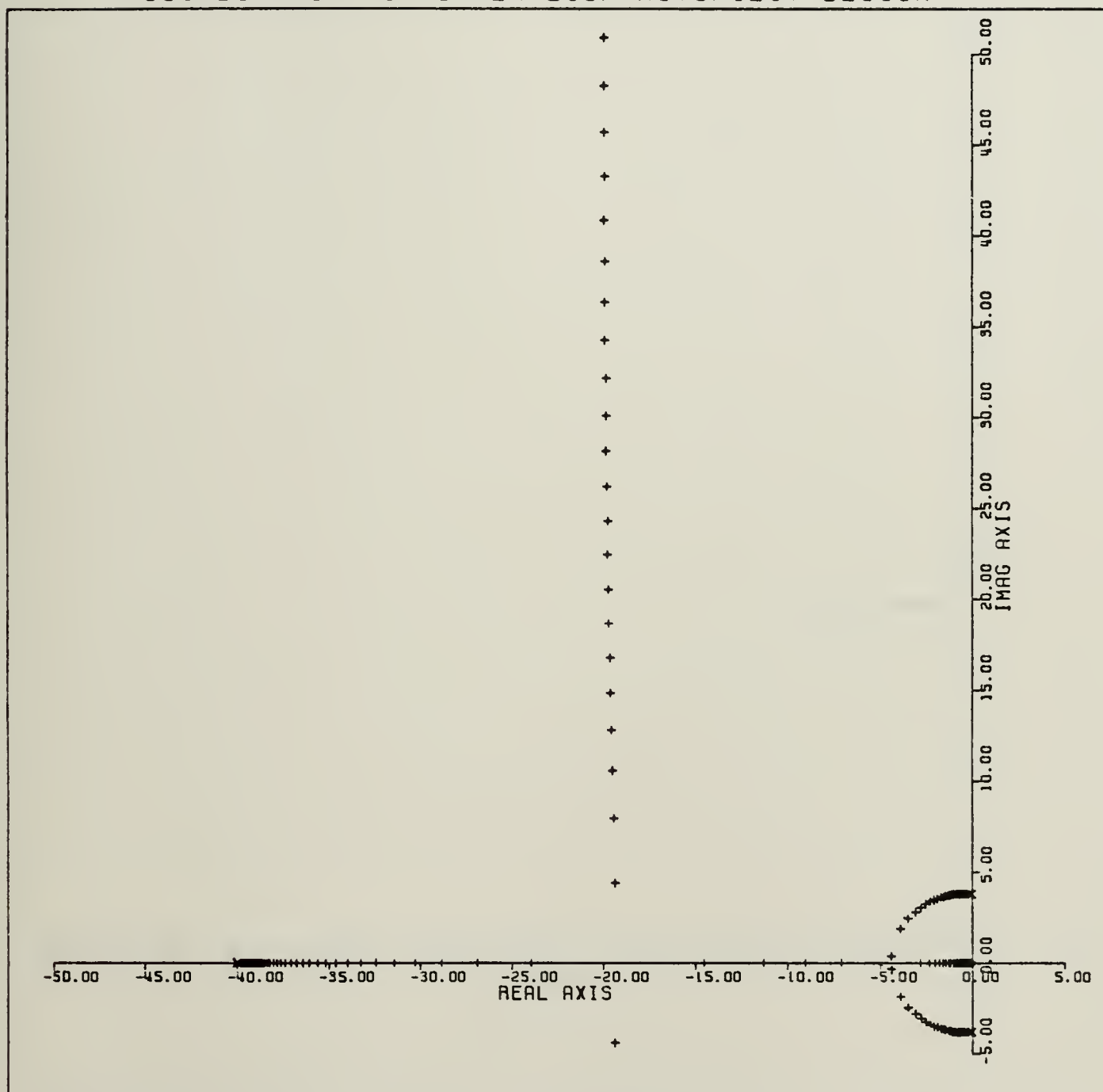
REAL AXIS (UNITS PER INCH) = 5.0000
 IMAG AXIS (UNITS PER INCH) = 5.0000
 ROOT LOCUS OF ROLL RATE LOOP OF BANK ANGLE
 COMMAND FOR INNER LOOP AUTOPILOT DESIGN



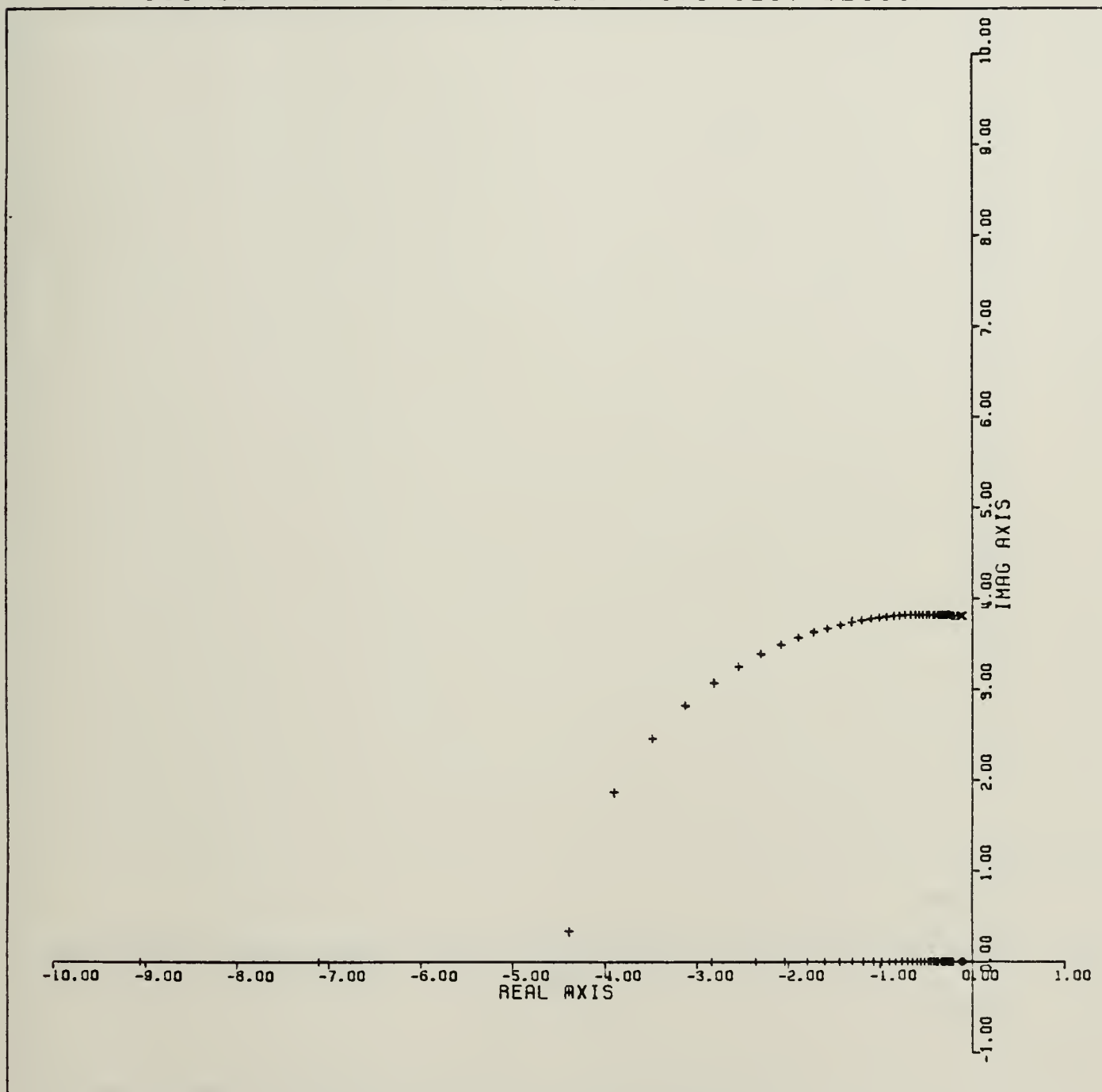
REAL AXIS (UNITS PER INCH) = 5.0000
 IMAG AXIS (UNITS PER INCH) = 5.0000
 ROOT LOCUS OF BANK ANGLE COMMAND
 FOR INNER LOOP AUTOPILOT DESIGN



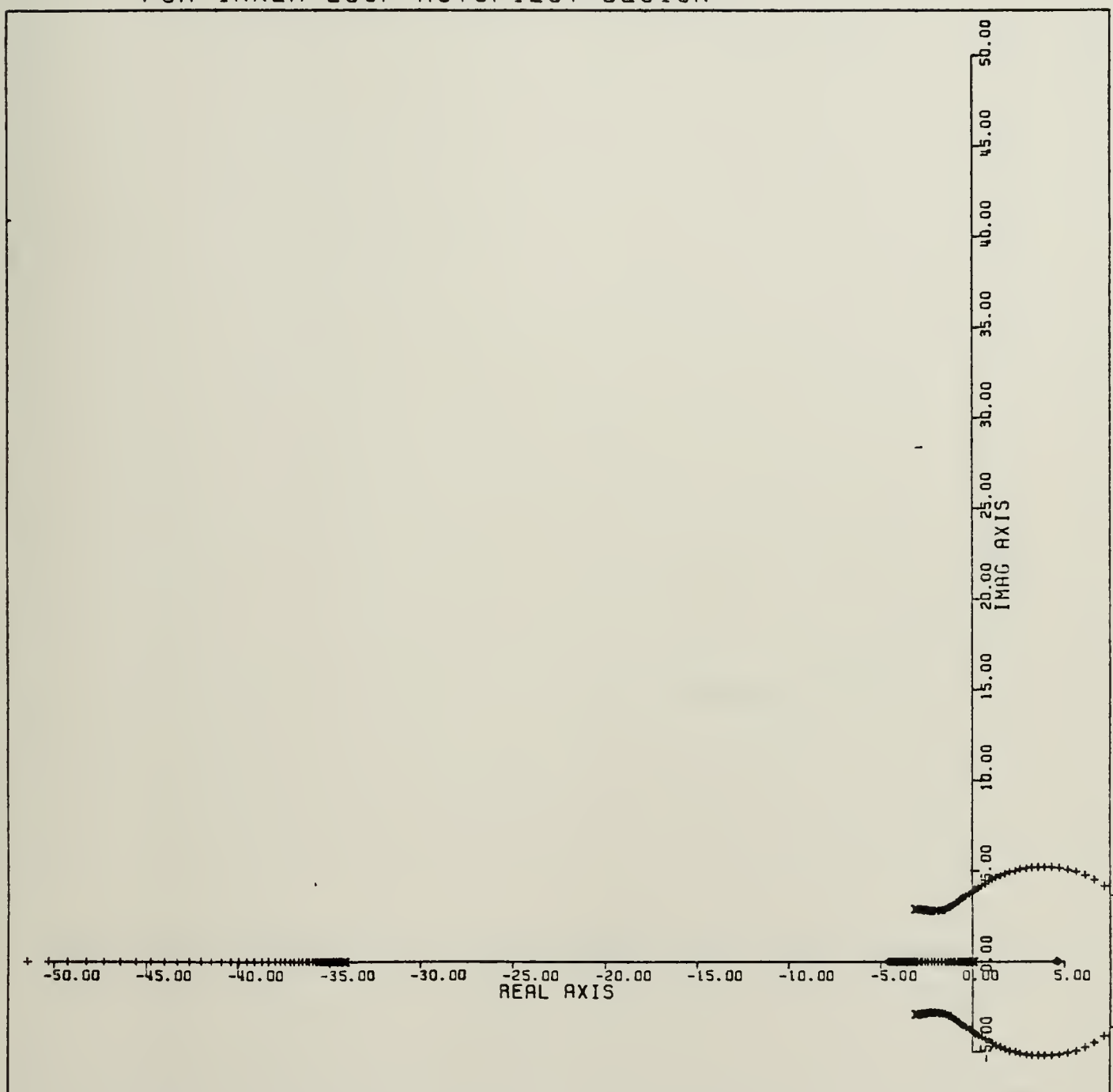
REAL AXIS (UNITS PER INCH) = 5.0000
 IMAG AXIS (UNITS PER INCH) = 5.0000
 ROOT LOCUS OF YAW RATE LOOP OF TURN
 COORDINATOR FOR INNER LOOP AUTOPILOT DESIGN



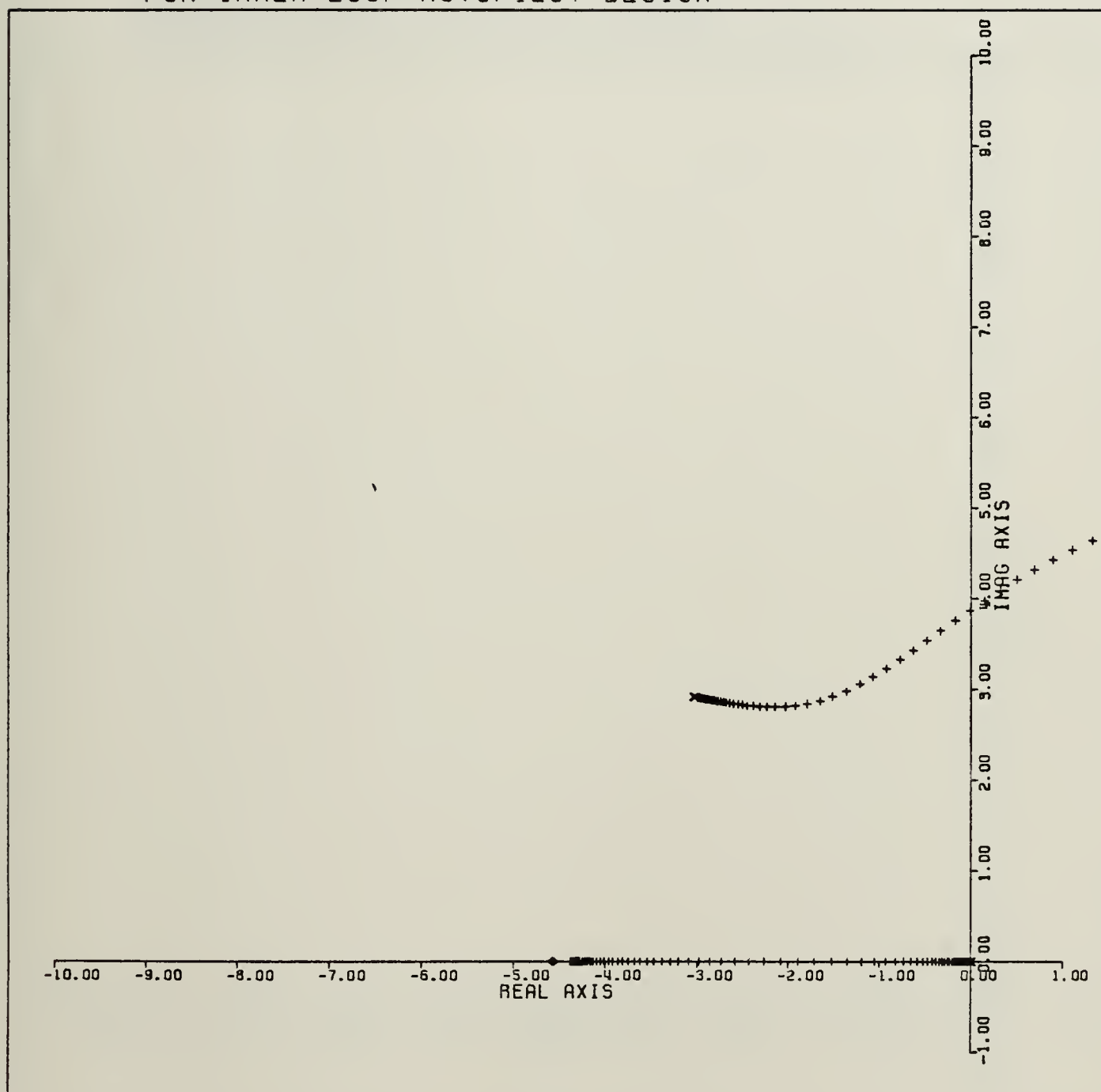
REAL AXIS (UNITS PER INCH) = 1.0000
IMAG AXIS (UNITS PER INCH) = 1.0000
ROOT LOCUS OF YAW RATE LOOP OF TURN
COORDINATOR FOR INNER LOOP AUTOPILOT DESIGN



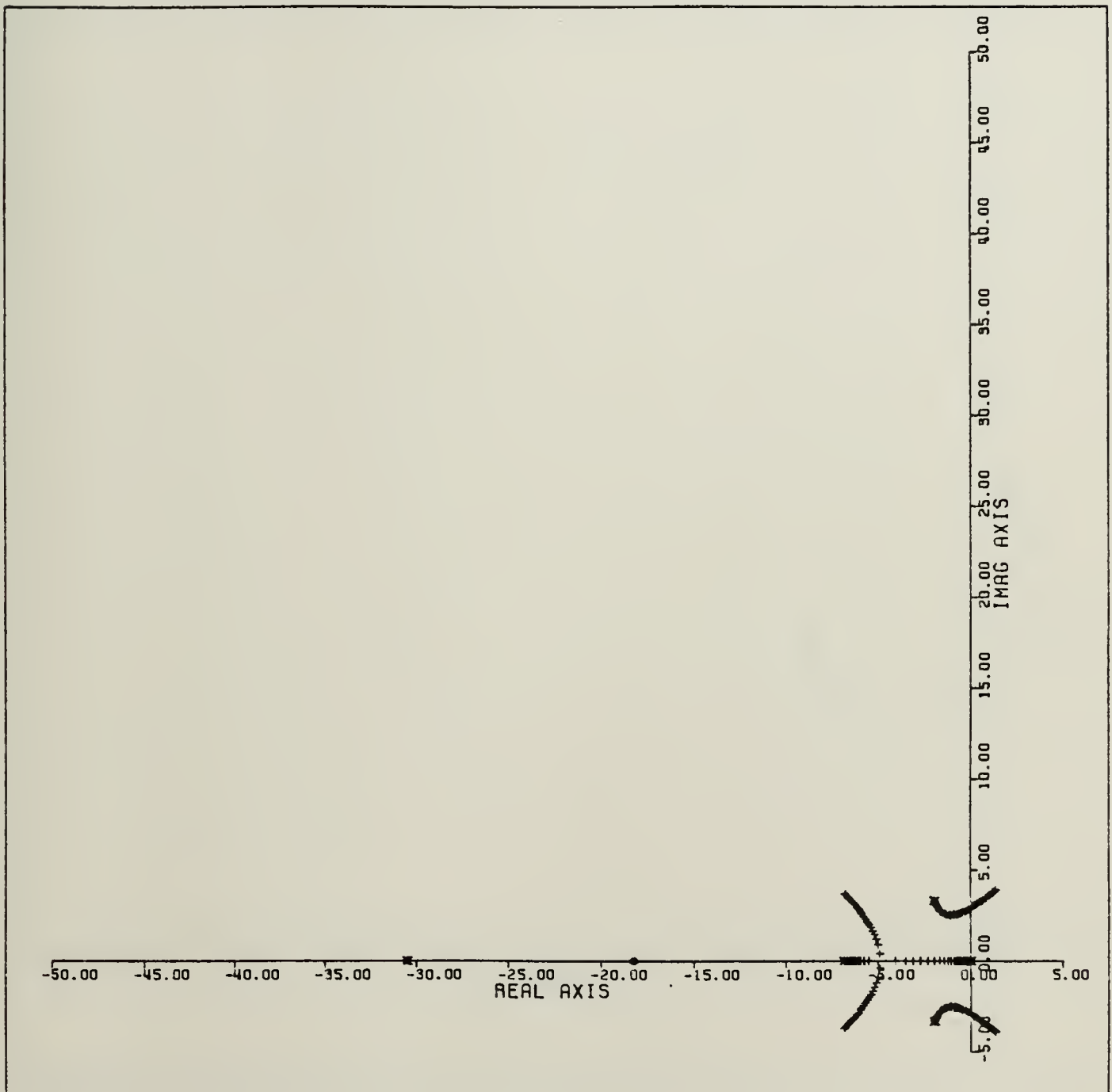
REAL AXIS (UNITS PER INCH) = 5.0000
IMAG AXIS (UNITS PER INCH) = 5.0000
ROOT LOCUS OF TURN COORDINATOR
FOR INNER LOOP AUTOPILOT DESIGN



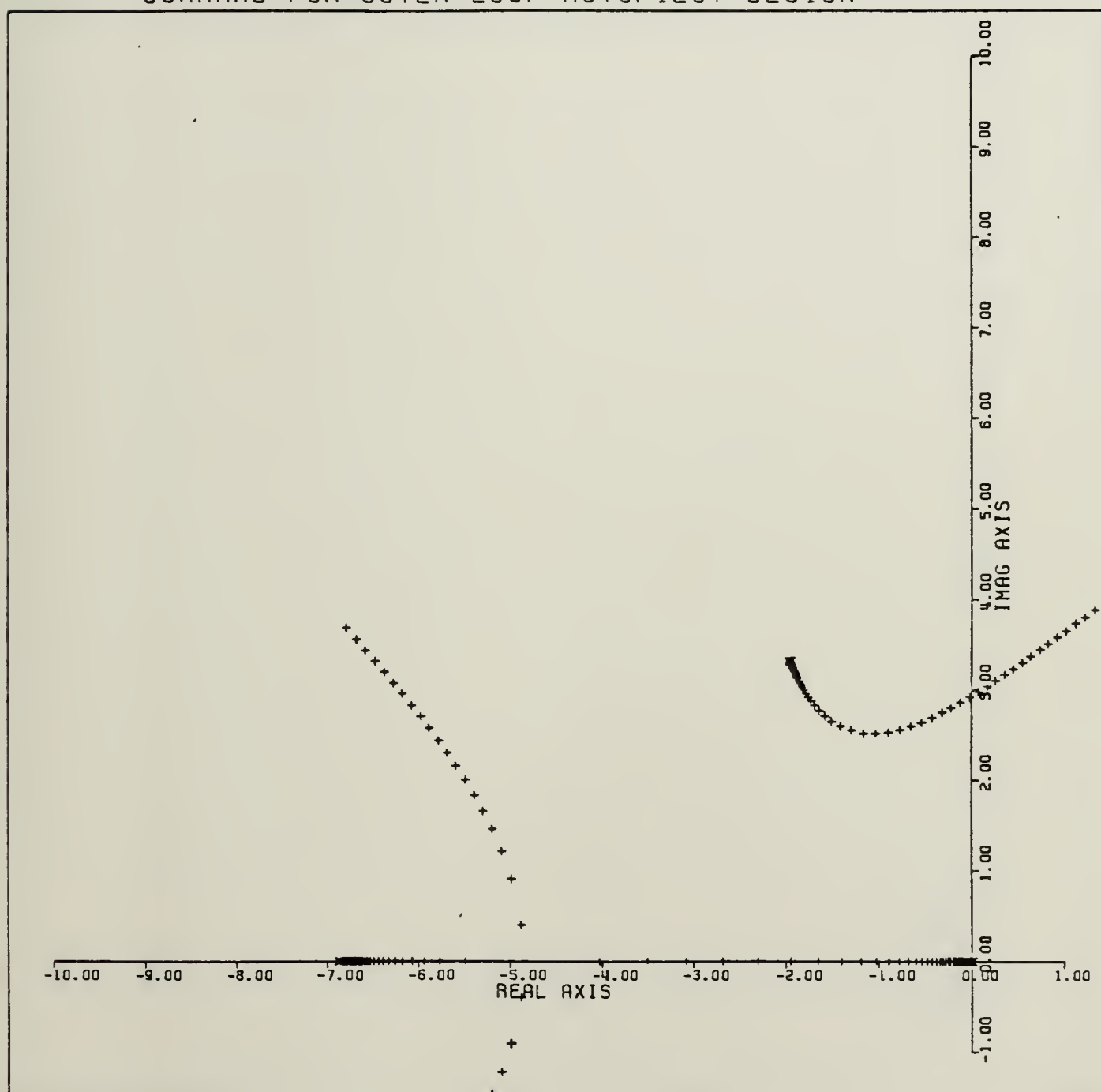
REAL AXIS (UNITS PER INCH) = 1.0000
IMAG AXIS (UNITS PER INCH) = 1.0000
ROOT LOCUS OF TURN COORDINATOR
FOR INNER LOOP AUTOPILOT DESIGN



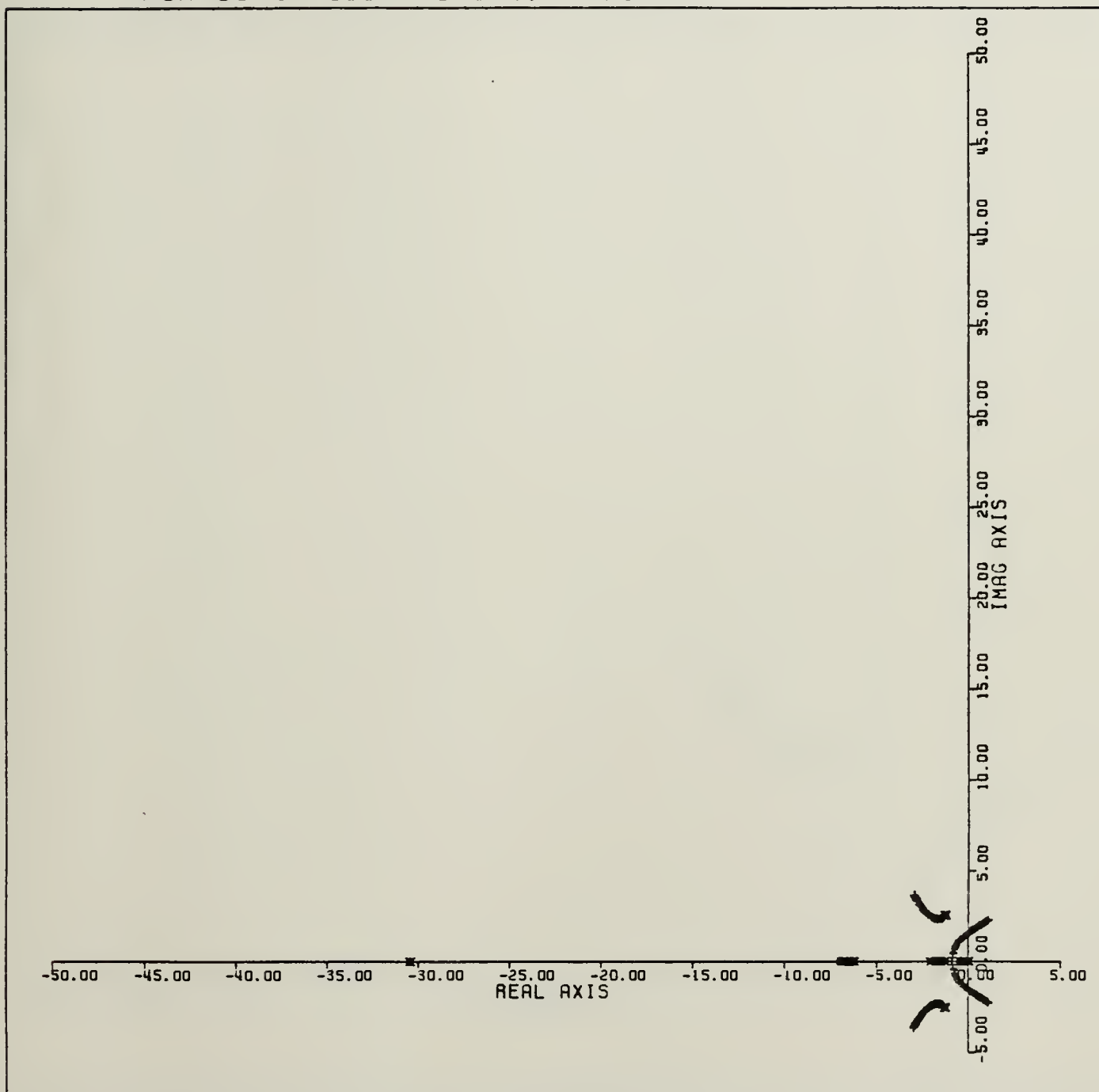
REAL AXIS (UNITS PER INCH) = 5.0000
IMAG AXIS (UNITS PER INCH) = 5.0000
ROOT LOCUS OF FLIGHT PATH ANGLE
COMMAND FOR OUTER LOOP AUTOPILOT DESIGN



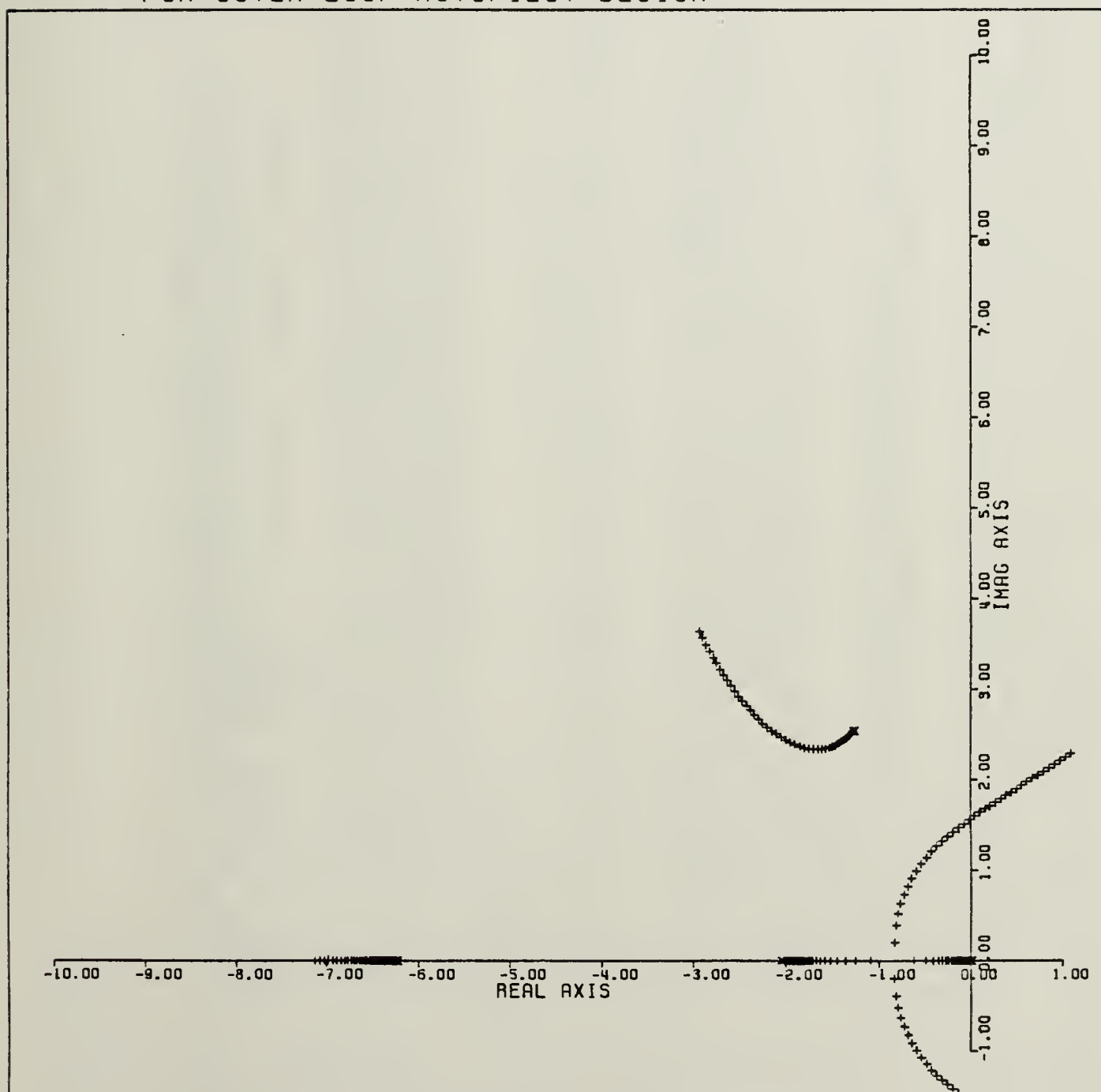
REAL AXIS (UNITS PER INCH) = 1.0000
 IMAG AXIS (UNITS PER INCH) = 1.0000
 ROOT LOCUS OF FLIGHT PATH ANGLE
 COMMAND FOR OUTER LOOP AUTOPILOT DESIGN



REAL AXIS (UNITS PER INCH) = 5.0000
IMAG AXIS (UNITS PER INCH) = 5.0000
ROOT LOCUS OF ALTITUDE HOLD COMMAND
FOR OUTER LOOP AUTOPILOT DESIGN



REAL AXIS (UNITS PER INCH) = 1.0000
IMAG AXIS (UNITS PER INCH) = 1.0000
ROOT LOCUS OF ALTITUDE HOLD COMMAND
FOR OUTER LOOP AUTOPILOT DESIGN



BASELINE GUIDANCE LAW SIMULATION

166


```

(0.0,-.0010),(5.0,-.0030),(10.0,-.0045),(15.0,-.0070)
FUNCTION LAIRL2,(10.0,-.0015),(15.0,-.0030),(20.0,-.0050),...
(5.0,-.0010),(10.0,-.0015),(15.0,-.0020),(20.0,-.0025),...
FUNCTION LAIRL2,(10.0,-.0015),(15.0,-.0020),(20.0,-.0025),...
(0.0,-.0008),(5.0,-.0025),(10.0,-.0040),(15.0,-.0070),...
FUNCTION LAIRL2,(10.0,-.0015),(15.0,-.0020),(20.0,-.0025),...
(0.0,-.0020),(5.0,-.0050),(10.0,-.0120),(15.0,-.0175),...
ALFA VS AILERON VS DELTA CROLL ST(AIL),
FUNCTION LAIRL3,(10.0,-.0008),(15.0,-.0018),(20.0,-.0030),...
(0.0,-.0004),(5.0,-.0015),(10.0,-.0036),(15.0,-.0033),...
FUNCTION LAIRL3,(10.0,-.0023),(15.0,-.0059),(20.0,-.0080),...
(0.0,-.0004),(5.0,-.0023),(10.0,-.0059),(15.0,-.0034),...
FUNCTION LAIRL3,(10.0,-.0030),(15.0,-.0092),(20.0,-.0092),...
(0.0,-.0004),(5.0,-.0030),(10.0,-.0046),(15.0,-.0088),...
FUNCTION LAIRL3,(10.0,-.0030),(15.0,-.0084),(20.0,-.0058),...
(0.0,-.0004),(5.0,-.0020),(10.0,-.0040),(15.0,-.0050),...
DYNAMIC
NO SORT ME.EQ.0.0) RANGE = 100.0
IF (RNGMIN = RANGE) GO TO 10
IF (RNGMIN = TIME
  CXITGT = DXTGT
  DYTGT = DZTGT
  CZTGT =
CONTINUE
ALGORITHM THAT PROCEEDS FROM INGRESS TO 3000, THEN ATTACK UNTIL
HIT. IF (RANGE.GT.3000.0) GO TO 20
  IF (RANGE.GT.3000.0) GO TO 60
  INGRESS INTIC = XT-XEARTH
  DXTGT = YI-YEARTH
  DZTGT = HT-ALTITUDE
  AYC = LMDAZ*VT*SIGDZ1/5
  ANC = AZC*CS(PHI)+AYC*SIN(PHI)
  IF (AYC.EQ.0.0) PHIC = 0.0
  IF (AYC.NE.0.0) PHIC=ATAN2(AYC,AZC)
  PHIC1 = LIMIT(-1.047,1.047,PHIC)
  GO TO 20
ATTACK PHASE INTO THE TARGET
  IF (RANGE.GT.2900.0) GO TO 65
  IF (RANGE.LT.400.0) GO TO 65
  ALLOW ECM TC OCCUR BETWEEN 2900 AND BURN THROUGH RANGE

```



```

*      PUT ECM BLINKING OF 75FT HORIZONTAL SHIFT AT FREQ(.5,1,2 CPS)
YI = SIN(2*PI*FREQ*TIME)
YY = IN$W(Y1,SHIFTY,0.0)
YIT = YI-YY
*      PUT ECM BLINKING OF 15FT VERTICAL SHIFT AT FREQ(.5,1,2 CPS)
HI = SIN(2*PI*FREQ*TIME)
HH = IN$W(H1,SHIFTH,0.0)
HIT = HI-HH
*      XT-XEARTH
DXTGT = XT-XEARTH
DYTGT = YT-YEARTH
DZTGT = ZT-ZEARTH
GO TGT = 6
*      XT-XEARTH
DXTGT = XT-XEARTH
DYTGT = YT-YEARTH
DZTGT = ZT-ZEARTH
*      PROPORTIONAL ELEVATION
PNEI = LAMDEL*VT*SIGDEL/G
AZCPR3 = PNEI + 1.0
AYC = LAMDAZ*VT*SIGDZ1/G
ANC = AZCPR3*COS(PHI)+AYC*SIN(PHI)
PHIC1 = ATAN2(AYC,AZCPR3)
THIS ROUTINE KEEPS PHIC1 FROM RCTATING 360 DEG WHEN
TAN FUNCTION PASSES THROUGH 180 DEG.
DELTA1 = PHIC1-PHI
DELTA1 = ABS(DELTA1)
IF (DELTA1.LT.3.141592654) GO TO 200
IF (PHIC1.GE.0.0) GO TO 70
PHIC1 = PHIC1 + 6.2831853
GO TO 200
PHIC1 = PHIC1 - 6.2831853
CONTINUE
SORT = 12.0*0.02377*(VT*.2)/2
PHIDOT = P+TAN(THETA)*(Q*SIN(PHI)+R*COS(PHI))
THETAD = Q*COS(PHI)-R*SIN(PHI)
SYDCT = (Q*SIN(PHI)+R*COS(PHI))/COS(THETA)
PHI = INTGRL(0.0,PHIDOT)
THETA = INTGRL(0.0,THETAD)
SY = INTGRL(0.0,SYDCT)
UDOT = -G*SIN(THETA)+V*R-W*Q+X/M+I/M
VDOT = G*SIN(PHI)*COS(THETA)-U*R+W*P+Y/M
WDOT = G*COS(PHI)*COS(THETA)
U = INTGRL(0.0,UDOT)
V = INTGRL(0.0,VDOT)
W = INTGRL(0.0,WDOT)
XEDCT = U*SY)*COS(THETA)+V*(COS(SY)*SIN(THETA)*SIN(PHI)...
-SIN(SY)*COS(PHI))+W*(COS(SY)*SIN(THETA)*COS(PHI)+...
SIN(SY)*SIN(PHI))

```



```

YEDDT=U*SIN(SY)*COS(THETA)+V*(SIN(SY)*SIN(THETA)*SIN(PHI)...
+COS(SY)*COS(PHI))+W*(SIN(SY)*SIN(THETA)*COS(PHI))-...
COS(SY)*SIN(PHI))
ZEDDT=L*SIN(THETA)-V*COS(THETA)*SIN(PHI)-W*COS(THETA)*COS(PHI)
XEARTH=INTGRL(0.0,XEDDT)
YEARTH=INTGRL(0.0,YEDDT)
NOTE: ALTITUDE AND Z FUNCTIONS ARE DEFINED AS POSITIVE GOING UP
ALTUDE=INTGRL(50.,ZEDDT)
PDDT=C.036089*LA+C.000279*NA+C.009160*P*Q-C.183711*K*Q
RDDT=C.000279*LA+C.000664*NA-C.978236*P*Q-C.009160*R*Q
QDDT=(MA+1484.2*P-R-11.7*(P**2-R**2))/1507.0
P=INTGRL(C.0,PDDT)
Q=INTGRL(C.0,QDDT)
R=INTGRL(C.0,RDDT)
ALFA=ATAN(W/U)
BETA=ASIN(V/VT)
ALFADT=CERIV(0.0,BETA) (4880,ALFA)
BETADT=CERIV(0.0,W**2)
VT=SQRT(U**2+V**2)
CLCBAS=FUNGEN(LIFT1,1,ALFA1)
DCLBSTE=FUNGEN(LIFT2,1,ELE1)
DCDBAS=FUNGEN(DRAG1,1,CLCBAS)
DCDSTE=FUNGEN(DRAG2,1,ELE1)
DCDSTA=FUNGEN(DRAG3,1,AILI)
DCDSTR=FUNGEN(DRAG4,1,RUDI)
CMBAS=FUNGEN(PITCH1,1,ALFA1)
DCMSTE=FUNGEN(PITCH2,1,ELE1)
CYBAS=TWQVAR(SIDE1,BETA1,ALFA1)
CRBAS=TWQVAR(SIDE2,BETA1,ALFA1)
CNBYSTR=TWQVAR(SIDE3,BETA1,ALFA1)
DCNSTR=TWQVAR(DIREC1,ALFA1)
DCNSTR=TWQVAR(DIREC2,RUDI,ALFA1)
DCNSTR=TWQVAR(DIREC3,RUDI,ALFA1)
DCYSTA=TWQVAR(LATRL1,AILI,ALFA1)
DCNSTA=TWQVAR(LATRL2,AILI,ALFA1)
DCNSTA=TWQVAR(LATRL3,AILI,ALFA1)
CL=CLCBAS+DCCLSTE+.707/VT*(2.0*ALFADT+5.0*Q)*ALFADT+0.1*Q)
CD=CDBBAS+DCCLSTE+DCYSTA+4.24/VT*(0.4C*R-C.10*P-0.10*BETADT)
CY=CYBAS+DCCNSTE+DCYSTA+4.24/VT*(0.4C*R-C.10*P-0.10*BETADT)
CM=CNBAS+DCCNSTE+DCNSTA+4.24/VT*(0.15*BETADT-0.20*R-0.01*P)
CNOLL=QS
L=CD*QS
D=CD*QS
LA=8.485*CRCLL*CS
MA=1.414*CM*QS
NA=8.485*CN*QS
X=L*SIN(ALFA)-D*COS(ALFA)

```

```

THE02410
THE02420
THE02430
THE02440
THE02450
THE02460
THE02470
THE02480
THE02490
THE02500
THE02510
THE02520
THE02530
THE02540
THE02550
THE02560
THE02570
THE02580
THE02590
THE02600
THE02610
THE02620
THE02630
THE02640
THE02650
THE02660
THE02670
THE02680
THE02690
THE02700
THE02710
THE02720
THE02730
THE02740
THE02750
THE02760
THE02770
THE02780
THE02790
THE02800
THE02810
THE02820
THE02830
THE02840
THE02850
THE02860
THE02870
THE02880

```

*


```

Y=C*Q*CCS(ALFA)-D* SIN(ALFA)
Z=-L*CCD=-Z/(M*G)
NYLCCAD=Y/(M*G)
ALFA1=ALFA*K2
BETA1=BETA*K2
PHI1=PHI*K2
THETA1=THETA*K2
P1=P*K2
Q1=C*K2
R1=R*K2
SY1=SY*K2
ELE1=ELE*K2
RUD1=RUD*K2
AIL1=AIL*K2
GAMMA1=GAMMA*K2

INNER LCOP AUTOPILOT
NORMAL ACCELERATION COMMAND
ANCL = LIMIT(-2.0,4.0,ANC)
ERRCRN = ANCL-(NZLOAD+C*QDOT/G)
NSERVI = -1.0*(KA1*INTGRL(0.0,ERRCRN)-KR1*Q)
NSERVO = REALPL(0.0,0.025,NSERVI)
ELE = LIMIT(-0.262,0.262,NSERVO)

BANK ANGLE COMMAND SYSTEM
60 DEGREE LIMIT ON BANK ANGLE = 1.047 RADIANS(DONE IN ALGORITHM)
ROLL RATE (PCL) IS VARIED AS 50,100,8200 DEG/SEC
50=.87, 100=1.75, 200=3.49
ERRBAL = (PHIC1-PHI)*KD
PCL = LIMIT(-1.75,1.75,ERRBAL)
PCL1 = PCL*K2
PHIC2 = PHIC1*K2
BASRVI = -1.0*KR2*(PCL-P)
BASRVO = REALPL(0.0,0.025,BASRVI)
AIL = LIMIT(-0.262,0.262,BASRVO)

TURN COORDINATOR
ALC = 0.0
EN = ALC-(C*RDOT/G+NYLOAD)
EN1=KA2*(INTGRL(0.0,EN))
TSERVI = -1.0*(EN1-KR3*R)
TSERVO = REALPL(0.0,0.025,TSERVI)
RUD = LIMIT(-0.262,0.262,TSERVO)

```

```

GUIDANCE.
GUIDANCE SCHEME IS DIVIDED INTO TWO PHASES-INGRESS AND ATTACK,
PROPORTIONAL NAVIGATION IS USED FOR HEADING CONTROL DURING INGRESS
(WITH BANK ANGLE LIMITED).
(BANK ANGLE UNLIMITED).
AN ALTITUDE HOLD OF 50 FEET IS USED FOR INGRESS PHASE.
PROPORTIONAL NAVIGATION IN ELEVATION IS USED DURING ATTACK PHASE.

OUTER LOCP AUTOPILOT

FLIGHT PATH ANGLE
AZC = 1.0+KGAMMA*VT/G*(GAMMAC-GAMMA)
GAMMA = ASIN(ZEDOT/VT)
ALTITUDE HOLD
ALTCMD = 50.0
GAMMAC = KALT/VT*(ALTCMD-ALTUDE)

SEEKER EQUATIONS

YT2 = YTI+35.0*TIME
RANGE = SQRT((XTI-XEARTH)**2+(YT2-YEARTH)**2+(HTI-ALTUDE)**2)
SIGDZB = -SIGDEL* SIN(PHI)+SIGDAZ* COS(THETA)*COS(PHI)
SIGDEB = SIGDEL* COS(PHI)+SIGDAZ* COS(THETA)*SIN(PHI)
SIGDZ1 = SIGDZB* COS(PHI)+SIGDEB* SIN(PHI)
SIGDE1 = -SIGDZB* SIN(PHI)+SIGDEB* COS(PHI)
THIS SECTION CHANGES PROGRAM VARIABLES TO MORE COMMON NAMES
XRANGE = ABS(XTI-XEARTH)
ZRANGE = ABS(YT2-YEARTH)
PCMD = FCL1
PHICMD = PHIC2
XMISSLE = XEARTH
YMISSLE = YEARTH
HMISSLE = ALTUDE
XTGT = XTI
YTGT = YT2
HTGT = HTI
VECM = FTT
RUCC1 = FTT
RUCC1-AI11
R1STAB = ELE1-AI11
R1STAB = ELE1-AI11
NZ = NZLCAD
NZ1CMD = ANCL
NY = NYLCAD
NY1CMD = ALCL

```

*

*


```

*****
      OUTPUT TIME,XMISLE(0.,32000.0),XTGT(0.,32000.0)
      LABEL MISSILE AND TARGET X COORDINATE (FEET) VS TIME
      PAGE
      OUTPUT TIME,XMISLE(-400.,2800.),YTGT(-400.,2800.),YECM(-400.,2800.)
      LABEL MISSILE AND TARGET Y COORDINATE (FEET) VS TIME
      PAGE
      OUTPUT TIME,HMISLE(-40.,280.),HGT(-40.,280.),HECM(-40.,280.)
      LABEL MISSILE AND TARGET ALTITUDE (FEET) VS TIME
      PAGE
      OUTPUT TIME,L1STAB(-20.,20.),R1STAB(-20.,20.)
      LABEL LEFT & RIGHT STABILIZERS (DEGREES) VS TIME
      PAGE
      OUTPUT TIME,RUDDER(-20.,20.)
      LABEL RUDDER POSITION (DEGREES) VS TIME
      PAGE
      OUTPUT TIME,NZ(-3.,5.),NZ1CMD(-3.,5.)
      LABEL VERTICAL ACCELERATION (G.S) VS TIME
      PAGE
      OUTPUT TIME,NY(-2.,2.),NY1CMD(-2.,2.)
      LABEL HORIZONTAL ACCELERATION (G.S) VS TIME
      PAGE
      OUTPUT TIME,ELLOSR,AZLCSR
      LABEL SEEKER EARTH LINE OF SIGHT RATES (DEG/SEC) VS TIME
      PAGE
      OUTPUT TIME,XMISLE(21000.,25000.),YMISLE(0.,2000.),HMISLE(0.,800.)
      LABEL MAP OF YMISLE AND HMISLE VS XMISLE (FEET)
      PAGE
      END
      STOP
      ENDJGB
*****

```

```

THE04330
THE04340
THE04350
THE04360
THE04370
THE04380
THE04390
THE04400
THE04410
THE04420
THE04430
THE04440
THE04450
THE04460
THE04470
THE04480
THE04490
THE04500
THE04510
THE04520
THE04530
THE04540
THE04550
THE04560
THE04570
THE04580
THE04590
THE04600
THE04610
THE04620

```


SEA SKIMMER GUIDANCE LAW SIMULATION

176


```

-1.0, .0048, -9. .0038, -8. .0030, -7. .0023, -6. .0016, -5. .0011, ...
-4. .0007, -3. .0003, -2. .0001, -1. .0000, 0. .0000, 1. .0001, 2. .0001, 3. .0001, ...
.0003, 4. .0007, 5. .0011, 6. .0017, 7. .0023, 8. .0030, 9. .0038, ...
10. .0048, 11. .0059, 12. .0071, 13. .0085, 14. .0100, 15. .0120
RUDDER VS DELTA CDSI(RUD)
FUNCTION CN DRAG4=-15. .0059, -14. .0054, -13. .0048, -12. .0043, ...
-10. .0032, -9. .0027, -8. .0022, -7. .0017, -6. .0013, -5. .0009, ...
-4. .0006, -3. .0003, -2. .0002, -1. .0001, 0. .0000, 1. .0001, 2. .0001, ...
.0001, 4. .0006, 5. .0009, 6. .0013, 7. .0017, 8. .0022, 9. .0027, ...
10. .0048, 11. .0059, 12. .0071, 13. .0085, 14. .0099, 15. .0120
PITCHING MOMENT CHARACTERISTICS
ALFA VS CMBASIC
FUNCTION CN PITCH1=-10. .013, -8. .008, -6. .005, -4. .003, -2. .016, ...
0. .008, 2. .013, 4. .022, 6. .032, 8. .046, 10. .062
ELE VS CMST(ELE)
FUNCTION CN PITCH2=-15. .090, -14. .088, -12. .078, -10. .068, -8. .056, ...
-6. .042, -4. .027, -2. .014, 0. .000, 2. .010, 4. .020, 6. .032, 8. .045, ...
10. .058, 12. .078, 14. .090
THREE VARIABLE COEFFICIENT TABLES
SIDESLIP CHARACTERISTICS
ALFA VS BETA VS CYBASIC
FUNCTION CN SICE1, -8. .000, (-8. .0148), (-6. .0111), (-4. .0073), (-2. .0151)
.034), (0. .002), (2. .0040), (4. .0077), (6. .0114), (8. .0151)
FUNCTION CN SICE1, -6. .000, (-6. .0149), (-4. .0110), (-2. .0072), (-2. .0153)
.034), (0. .003), (2. .0042), (4. .0078), (6. .0116), (8. .0153)
FUNCTION CN SICE1, 4. .000, (-4. .0140), (-2. .0100), (-2. .0063), (-2. .0162)
.025), (0. .013), (2. .0050), (4. .0089), (6. .0127), (8. .0162)
FUNCTION CN SICE1, 8. .000, (-8. .0137), (-6. .0096), (-4. .0060), (-2. .0162)
.022), (0. .020), (2. .0060), (4. .0096), (6. .0129), (8. .0162)
ALFA VS CROLLBASIC
FUNCTION CN SICE2, -8. .000, (-8. .0048), (-6. .0038), (-4. .0020), (-2. .0000)
.0014), (0. .0004), (2. .0005), (4. .0016), (6. .0030), (8. .0044)
.0044)
FUNCTION CN SICE2, 2. .000, (-2. .0040), (-4. .0026), (-6. .0013), (-8. .0000)
.0010), (0. .0004), (2. .0014), (4. .0026), (6. .0036), (8. .0044)
.0052)
FUNCTION CN SICE2, 6. .000, (-6. .0038), (-4. .0026), (-2. .0013), (-2. .0000)
.0002), (0. .0001), (2. .0025), (4. .0036), (6. .0047), (8. .0059)
.0059)
FUNCTION CN SICE2, 10. .000, (-10. .0044), (-8. .0030), (-6. .0020), (-4. .0000)
.0008), (0. .0002), (2. .0014), (4. .0025), (6. .0036), (8. .0044)
.0048)
ALFA VS CNBASIC
FUNCTION CN SICE3, -8. .000, (-8. .0034), (-6. .0025), (-4. .0016), (-2. .0000)
.0007), (0. .0001), (2. .0019), (4. .0028), (6. .0036)
FUNCTION CN SICE3, 0. .000, (-8. .0037), (-6. .0028), (-4. .0019), (-2. .0000)
.0009), (0. .0001), (2. .0009), (4. .0018), (6. .0026), (8. .0034)

```

*

**

*

*

*

THE000490
THE000500
THE000510
THE000520
THE000530
THE000540
THE000550
THE000560
THE000570
THE000580
THE000590
THE000600
THE000610
THE000620
THE000630
THE000640
THE000650
THE000660
THE000670
THE000680
THE000690
THE000700
THE000710
THE000720
THE000730
THE000740
THE000750
THE000760
THE000770
THE000780
THE000790
THE000800
THE000810
THE000820
THE000830
THE000840
THE000850
THE000860
THE000870
THE000880
THE000890
THE000900
THE000910
THE000920
THE000930
THE000940
THE000950
THE000960


```

FUNCT ICA SI CE3, 6.005, (-8.000, -0.042), (-6.000, -0.033), (-4.000, -0.022), (...
(-2.000, -0.005), (2.000, -0.042), (4.000, -0.016), (6.000, -0.024), (8.000, -0.032),
FUNCT ICA SI CE3, 8.000, (-8.000, -0.042), (-6.000, -0.033), (-4.000, -0.023), (...
(-2.000, -0.008), (2.000, -0.010), (4.000, -0.016), (6.000, -0.024), (8.000, -0.032),
DIRECT ICA L CHARACTERISTICS
ALFA VS RUDELTA CYST(RUD),
FUNCT ICA SI CE3, 6.000, (-15.000, -0.090), (-10.000, -0.060), (-5.000, -0.032), (...
(0.000, -0.040), (10.000, -0.070), (15.000, -0.100),
FUNCT ICA SI CE3, 2.000, (-15.000, -0.097), (-10.000, -0.062), (-5.000, -0.036), (...
(0.000, -0.042), (10.000, -0.066), (15.000, -0.098),
FUNCT ICA SI CE3, 6.000, (-15.000, -0.095), (-10.000, -0.062), (-5.000, -0.037), (...
(0.000, -0.038), (10.000, -0.062), (15.000, -0.092),
FUNCT ICA SI CE3, 8.000, (-15.000, -0.102), (-10.000, -0.069), (-5.000, -0.042), (...
(0.000, -0.040), (10.000, -0.066), (15.000, -0.096),
ALFA VS RUDELTA CYST(RUD),
FUNCT ICA SI CE3, 6.000, (-15.000, -0.070), (-10.000, -0.050), (-5.000, -0.026), (...
(0.000, -0.022), (10.000, -0.052), (15.000, -0.080),
FUNCT ICA SI CE3, 2.000, (-15.000, -0.068), (-10.000, -0.049), (-5.000, -0.024), (...
(0.000, -0.020), (10.000, -0.048), (15.000, -0.079),
FUNCT ICA SI CE3, 6.000, (-15.000, -0.047), (-10.000, -0.048), (-5.000, -0.022), (...
(0.000, -0.018), (10.000, -0.047), (15.000, -0.074),
FUNCT ICA SI CE3, 8.000, (-15.000, -0.065), (-10.000, -0.048), (-5.000, -0.018), (...
(0.000, -0.014), (10.000, -0.046), (15.000, -0.075),
ALFA VS RUDELTA CYST(RUD),
FUNCT ICA SI CE3, 6.000, (-15.000, -0.050), (-10.000, -0.034), (-5.000, -0.018), (...
(0.000, -0.024), (10.000, -0.048), (15.000, -0.070),
FUNCT ICA SI CE3, 2.000, (-15.000, -0.038), (-10.000, -0.029), (-5.000, -0.018), (...
(0.000, -0.012), (10.000, -0.028), (15.000, -0.053),
FUNCT ICA SI CE3, 4.000, (-15.000, -0.033), (-10.000, -0.027), (-5.000, -0.018), (...
(0.000, -0.004), (10.000, -0.012), (15.000, -0.040),
FUNCT ICA SI CE3, 7.000, (-15.000, -0.022), (-10.000, -0.022), (-5.000, -0.002), (...
(0.000, -0.002), (10.000, -0.002), (15.000, -0.002),
FUNCT ICA SI CE3, 8.000, (-15.000, -0.014), (-10.000, -0.018), (-5.000, -0.020), (...
(0.000, -0.0038), (10.000, -0.0041), (15.000, -0.0048),
LATERAL CONTROL CHARACTERISTICS
ALFA VS AILERON VS DELTA CYST(AIL),
FUNCT ICA SI CE3, 6.000, (-15.000, -0.015), (-10.000, -0.013), (-5.000, -0.010), (...
(0.000, -0.007), (10.000, -0.005), (15.000, -0.010),
FUNCT ICA SI CE3, 2.000, (-15.000, -0.019), (-10.000, -0.014), (-5.000, -0.009), (...
(0.000, -0.003), (10.000, -0.009), (15.000, -0.014),
FUNCT ICA SI CE3, 4.000, (-15.000, -0.017), (-10.000, -0.010), (-5.000, -0.002), (...
(0.000, -0.014), (10.000, -0.020), (15.000, -0.025),
FUNCT ICA SI CE3, 7.000, (-15.000, -0.006), (-10.000, -0.002), (-5.000, -0.010), (...
(0.000, -0.026), (10.000, -0.033), (15.000, -0.042),
ALFA VS AILERON VS DELTA CYST(AIL),
FUNCT ICA SI CE3, 6.000, (-15.000, -0.075), (-10.000, -0.040), (-5.000, -0.015), (...
(0.000, -0.070), (10.000, -0.012), (15.000, -0.0175),
FUNCT ICA SI CE3, 2.000, (-15.000, -0.050), (-10.000, -0.030), (-5.000, -0.020), (...

```

**

*

*

**

*


```

(0.,-0010),(5,-0030),(10.,-0045),(15.,-0070)
FUNCTION LAIRL2,(0.0=(-15.,0.),(-10.,0.),(-5.,0.),0.,0.),...
(5.,0.),(10.,0.),(15.,0.)
FUNCTION LAIRL2,(4.0=(-15.,-0075),(-10.,-0050),(-5.,-0025),...
(0.0,-008),{5.,-0025},{10.,-0040},{15.,-0070},...
FUNCTION LAIRL2,(8.C=(-15.,-0120),(-10.,-0085),(-5.,-0060),...
(0.0,-0020),(5.,-0050),(10.,-0120),(15.,-0175)
ALFA VS AILERON VS DELTA CROLLST(AIL)
FUNCTION LAIRL3,-8.0=(-15.,-0087),(-10.,-0060),(-5.,-0030),...
(0.,-0004),(5.,-0008),(10.,-0018),(15.,-0030)
FUNCTION LAIRL3,-4.0=(-15.,-0096),(-10.,-0066),(-5.,-0033),...
(0.,-0004),(5.,-0023),(10.,-0059),(15.,-0080)
FUNCTION LAIRL3,0.0=(-15.,-0100),(-10.,-0068),(-5.,-0034),...
(0.0,-0004),(5.,-0030),(10.,-0072),(15.,-0092)
FUNCTION LAIRL3,4.0=(-15.,-0092),(-10.,-0064),(-5.,-0036),...
(0.0,-0004),(5.,-0030),(10.,-0046),(15.,-0088)
FUNCTION LAIRL3,-8.0=(-15.,-0084),(-10.,-0058),(-5.,-0030),...
(0.0,-0004),(5.,-0020),(10.,-0040),(15.,-0050)
DYNAMIC
NDSORT ME=EQ.0.0,RNGMIN=100.0
IF (TIMGIN=LE.RANGE) GO TO 10
IF (RNGMIN=TIME
TIMMIN=DXTGTT
DYTGTT=DZTGT
CUNTINLE
ALGCRITFM TEL OFF TO 10200,POP UP TC 178CO,RIGHT OFFSET TO
15600,IF(RANGE.GT.17800.0)GO TO 20
IF(RANGE.GT.15800.0)GO TO 30
IF(RANGE.GT.10200.0)GO TO 40
IF(RANGE.GT.9100.0)GO TO 50
INGRES INTCT 17800.0GC TO 60
DCYIGT=XI-XEARTH
DCYTGT=YI-YEARTH
DZTGT=HI-ALTITUDE
AIRC=LAMDZ#VT#SIGDZI/G
ANC=COS(PHI)+AYC*SIN(PHI)PHIC=C.O
IF(AYC.EQ.0.0)AND.AZC.EQ.0.0)PHIC=ATAN2(AYC,AZC)
IF(AYC.NE.0.0)OR.AZC.NE.0.0)PHIC=ATAN2(PHIC)
PHIC1=LIMIT(-1.047,1.047,PHIC)
TURN TO RIGHT UNTIL TARGET AZIMUTH ANGLE = 12 DEGREES(SIGA2)
CXTGT=XI-XEARTH

```


THE01930
THE01940
THE01950
THE01960
THE01970
THE01980
THE01990
THE02000
THE02010
THE02020
THE02030
THE02040
THE02050
THE02060
THE02070
THE02080
THE02090
THE02100
THE02110
THE02120
THE02130
THE02140
THE02150
THE02160
THE02170
THE02180
THE02190
THE02200
THE02210
THE02220
THE02230
THE02240
THE02250
THE02260
THE02270
THE02280
THE02290
THE02300
THE02310
THE02320
THE02330
THE02340
THE02350
THE02360
THE02370
THE02380
THE02390
THE02400

```

DYTGT = YT-YEARTH
DZTGT = HT-ALTUDE
ANC PHIC1 = 1.047
GC TO 200
COMMAND ZERC DEGREES BANK ANGLE UNTIL START OF POP UP
DXTGT = XT-XEARTH
DYTGT = YT-YEARTH
DZTGT = HT-ALTUDE
ANC PHIC1 = 0.0
GC TO 200
POP UP UNTIL ALTUDE = 250 FEET
DXTGT = XT-XEARTH
DYTGT = YT-YEARTH
DZTGT = HT-ALTUDE
AYC = LAMDZ*VT*SIGDZ1/G
ANC = AZCP*CS(PHI)+AYC*SIN(PHI)
PHIC1 = AZCP*CS(PHI)+AYC*AZCP
PHIC1 = LIMIT(-1.047,1.047,PHIC)
TC ZOC
GO ATTACK PHASE INIC THE TARGET
IF (RANGE.GT.9000.0) GC TO 65
IF (RANGE.LT.2000.0) GO TO 65
ALLCW ECM TANK OCCUR BETWEEN 9000 AND 2000 FT RANGE
PUT ECM BLINKING OF 75FT HORIZONTAL SHIFT AT FREQ(.5,1,2 CPS)
YI = SIN(2*PI*FREQ*TIME)
YY = INSW(YI,SHIFTY,0.0)
YTT = YI-Y
YTCM = BLINKING OF 15FT VERTICAL SHIFT AT FREQ(.5,1,2 CPS)
H1 = SIN(2*PI*FREQ*TIME)
HH = INSW(H1,SHIFTH,0.0)
HTT = HT+HH
DXTGT = XT-XEARTH
DYTGT = YT-YEARTH
DZTGT = HT-ALTUDE
GO DZTGT 66
DXTGT = XT-XEARTH
DYTGT = YT-YEARTH
DZTGT = HT-ALTUDE
PROPORTIONAL ELEVATION
PNE1 = LAMDEL*VT*SIGDEL/G
AZCP3 = LAMDEL1 + 1.0
AYC = LAMDZ*VT*SIGDZ1/G
ANC = LAMDZ*CS(PHI)+AYC*SIN(PHI)
PHIC1 = AZCP3*CS(PHI)+AYC*AZCP3
THIS FUNCTION KEEPS PHIC FROM ROLATING 360 DEG WHEN
TAN FUNCTION PASSES THROUGH 18C DEG.

```



```

DELTA = PHIC1-PHI
DELTA1 = ABS(DELTA)
IF (DELTA1.LT.3.141592654) GO TO 200
IF (PHIC1.GE.0.0) GO TO 70
PHIC1 = PHIC1 + 6.2831853
GO TO 200
PHIC1 = PHIC1 - 6.2831853

```

70
200

```

CONTINUE
SORT = 12.C*0.C2377*(VT**2)/2
PHIDOT = P+IAN(THETA)*(Q*SIN(PHI)+R*COS(PHI))
THETAD = Q*COS(PHI)-R*SIN(PHI)
SYDCT = (Q*SIN(PHI)+R*COS(PHI))/COS(THETA)
PHI = INTGRL(0.0,PHIDOT)
THETA = INTGRL(0.04880,THETAD)
SY = INTGRL(0.0,SYDCT)
UDOT = -G*SIN(THETA)+V*R-W*Q+X/M+T/M
VDOT = G*SIN(PHI)*COS(THETA)-U*R+W*P+Y/M
WDOT = G*COS(PHI)*COS(THETA)+U*Q-V*P+Z/M
U = INTGRL(0.0,UDOT)
V = INTGRL(0.0,VDOT)
W = INTGRL(0.0,WDOT)
XEDOT = U*COS(SY)*COS(THETA)+V*(COS(SY)*SIN(THETA)*SIN(PHI)...
-SIN(SY)*COS(PHI))+W*(COS(SY)*SIN(THETA)*COS(PHI)+...
SIN(SY)*SIN(PHI))
YEDOT = U*SIN(SY)*COS(THETA)+V*(SIN(SY)*SIN(THETA)*SIN(PHI)...
+COS(SY)*COS(PHI))+W*(SIN(SY)*SIN(THETA)*COS(PHI)-...
COS(SY)*SIN(PHI))
ZEDCT = L*SIN(THETA)-V*COS(THETA)*SIN(PHI)-W*COS(THETA)*COS(PHI)
XEARTH = INTGRL(0.0,XEDOT)
YEARTH = INTGRL(0.0,YEDOT)
NOTE: ALTITUDE AND Z FUNCTIONS ARE DEFINED AS POSITIVE GOING UP
ALTITUDE = INTGRL(50.,ZEDCT)
PDOT = 0.036089*LA+0.000279*NA+0.009160*P*Q-0.18371*0K*Q
RDOT = C.000279*LA+0.000664*NA-0.978236*P*Q-0.009160*0K*Q
QDOT = (MA+1484.2*P*R-11.7*(P**2-R**2))/1507.0
P = INTGRL(0.0,QDOT)
Q = INTGRL(0.0,RDOT)
R = INTGRL(0.0,PDOT)
ALFA = ASIN(V/VT)
BETAD = ASIN(W/VT)
ALFA1 = 0.04880,ALFA)
BETAD1 = 0.0,BETAD)
BETADT = DERIV(0.0,BETAD**2)
VT = SQRT(U**2+V**2+W**2)
CLBAS = FLNGEN(LIFT1,1,ALFA1)
DCCLBAS = FLNGEN(LIFT2,1,ELE1)
CDBBAS = FLNGEN(DRAG1,1,CLBAS)
DCDBAS = FLNGEN(DRAG2,1,ELE1)

```

*

THE02410
THE02420
THE02430
THE02440
THE02450
THE02460
THE02470
THE02480
THE02490
THE02500
THE02510
THE02520
THE02530
THE02540
THE02550
THE02560
THE02570
THE02580
THE02590
THE02600
THE02610
THE02620
THE02630
THE02640
THE02650
THE02660
THE02670
THE02680
THE02690
THE02700
THE02710
THE02720
THE02730
THE02740
THE02750
THE02760
THE02770
THE02780
THE02790
THE02800
THE02810
THE02820
THE02830
THE02840
THE02850
THE02860
THE02870
THE02880


```

DCDSTA=FUNGEN(DRAG3,1,AI11)
DCDSTR=FUNGEN(DRAG4,1,RUDI1)
CMBAS=FUNGEN(PITCH1,1,ALFA1)
DCMSTE=FUNGEN(PITCH2,1,EL1)
CYBAS=TWCVAR(SIDE1,BETA1,ALFA1)
CRBAS=TWCVAR(SIDE2,BETA1,ALFA1)
CNBAS=TWCVAR(SIDE3,BETA1,ALFA1)
DCYSTR=TWVVAR(DIREC1,RUDI1,ALFA1)
DCRSTR=TWVVAR(DIREC2,RUDI1,ALFA1)
DCYSTA=TWVVAR(LAIRL1,AI11,ALFA1)
DCNSTA=TWVVAR(LAIRL2,AI11,ALFA1)
DCRSTA=TWVVAR(LAIRL3,AI11,ALFA1)
CL=CLBAS+DCLSTE+.707/VI*(2.0*ALFADT+5.0*Q)
CD=CDBAS+DCCSTE+DCDSTA+DCDSTR+.707/VI*(C.1*ALFADT+0.1*Q)
CY=CYBAS+DCCYSTR+DCYSTA+4.24/VI*(0.4C*R-0.10*P-0.10*BETACT)
CM=CMBAS+DCCNSTE+0.707/VI*(-10.0*ALFADT-15.0*Q)
CN=CNBAS+DCCNSTR+DCNSTA+4.24/VI*(0.15*BETADT-0.20*K-0.001*P)
CROLL=QS
L=CCL*QS
D=CCL*QS
LA=8.485*CRCLL*QS
MA=1.414*CM*QS
NA=8.485*CN*QS
X=L*SQ SIN(ALFA)-D*COS(ALFA)
Y=L*SQ COS(ALFA)-D*SIN(ALFA)
Z=-L*SQ SIN(ALFA)-D*SQ SIN(ALFA)
NZLCA=-Z/(M*G)
NYLCA=Y/(M*G)
ALFA1=ALFA*K2
BETA1=BETA*K2
PHI1=PHI*K2
THETA1=THETA*K2
PI=P*K2
WI=W*K2
RI=R*K2
SY1=SY*K2
ELE1=ELE*K2
RUDI1=RUDI*K2
AI11=AI1*K2
GAMMA1=GAMMA*K2
INNER LCCP AUTOPILOT
NORMAL ACCELERATION COMMAND
ANCL1=LIMIT(-2.0,4.0,ANC1)
ERRCRN=ANCL1-(NZLCA+D*QDCT/G)

```

```

NSERVI = -1.0*(KAL*INTGRL(0.0,ERRKN)-KRI*Q)
NSERVO = REALPL(0.0,0.025,NSERVI)
ELE = LIMIT(-0.262,0.262,NSERVO)

```

```

BANK ANGLE COMMAND SYSTEM
60 DEGREE LIMIT ON BANK ANGLE = 1.047 RADIAN(S/DONE IN ALGORITHM)
ROLL RATE (FCL) IS VARIED AS 50,100,&200 DEG/SEC
50=.87, 100=1.75, 200=3.49

```

```

ERRBAL = (PHIC1-PHI)*KD
PCL = LIMIT(-1.75,1.75,ERRBAL)
PCL1 = PCL*K2
PHIC2 = PHIC1*K2
BASRVI = -1.0*KR2*(FCL-P)
BASRVO = REALPL(0.0,0.025,BASRVI)
AIL = LIMIT(-0.262,0.262,BASRVO)

```

TURN COORDINATOR

```

ALC = G.C
EN = ALC-(C*RDOT/G+NYLOAD)
EN1 = KA2*(INTGRL(0.0,EN))
TSERVI = -1.0*(EN1-KR3*R)
TSERVO = REALPL(0.0,0.025,TSERVI)
RUD = LIMIT(-0.262,0.262,TSERVO)

```

GUIDANCE.

GUIDANCE SCHEME IS DIVIDED INTO FOUR PHASES-INGRESS,TURN,POP UP,
AND ATTACK. PROPORTIONAL NAVIGATION IS USED FOR HEADING CONTROL
DURING INGRESS AND POP UP (BOTH WITH BANK ANGLE LIMITED TO 60 DEG)
AND DURING ATTACK PHASE (BANK ANGLE UNLIMITED). DURING THE TURN
PHASE THE HEADING COMMANDS ARE ACHIEVED WITH FIXED BANK ANGLES.
AN ALTITUDE HOLD OF 50 FEET IS USED FOR INGRESS AND TURN PHASES.
VERTICAL FLIGHT PATH ANGLE CONTROL (CONSTANT RATE OF CLIMB OF 8.6
DEGREES IS USED FOR THE POP UP MANEUVER).

```

GUTER LCCP AUTOPILOT
FLIGHT PATH ANGLE
AZC = 1.0+KGAMMA*VT/G*(GAMMAC-GAMMA)
GAMMA = ASIN(ZEDOT/VT)
ALTITUDE HOLD
ALTCMD = 50.0
GAMMAC = KALT/VT*(ALTCMD-ALTUDE)
POP UP MANEUVER (CLIMB ANGLE=CLIMBA=8.6 DEGREES)
AZCP = 1.0+KGAMMA*VT/G*(CLIMBA-GAMMA)

```

SEEKER EQUATIONS

*

*

*

```
YT2 = YTI+35.0*TIME  
RANGE = SQR((XTI-XEARTH)**2+(YTI2-YEARTH)**2+(HTI-ALTUDE)**2)  
SIGDZB = -SIGDEL*CSIN(PHI)+SIGDAZ*CS(THETA)*COS(PHI)  
SIGDCZ1 = -SIGDEL*CSIN(PHI)+SIGDEB*CS(THETA)*SIN(PHI)  
SIGDEI = -SIGDZB*CSIN(PHI)+SIGDEB*CS(PHI)  
THIS SECTION CHANGES PROGRAM VARIABLES TO MORE COMMON NAMES  
XCHANGE = ABS(XTI-XEARTH)  
YRANGE = ABS(YTI2-YEARTH)  
ZRANGE = ABS(HTI-ALTUDE)  
PCMD = PCL1  
PHICMD = PHIC2  
XMISSLE = XEARTH  
YMISSLE = YEARTH  
HMISSLE = ALTUDE  
XTGT = XTI  
YTGT = YTI  
HTGT = HTI  
HECM = FTT  
RUDDER = FTT  
LISTAB = ELE1-AILI  
R1STAB = ELE1+AILI  
NZ = NZLCAD  
NZ1CMD = ANCI  
NY1CMD = NYLCAD  
NYLCMD = ALLC  
ELLCMD = ALLC  
AZLCMD = SIGDEL*K2  
SIGDZB = SIGDAZ*K2
```

*

*

```
THETDT = (-ZEDDT*(DXTGT**2+DYTGT**2)-DZTGT*(-XEDDT*DXTGT+...  
(35.0-YEDDT)*DYTGT))/((RANGE**2)*SQR(1+(DXTGT**2+DYTGT**2)))  
THEIDF = REALPL(0.0,10.,THETAD)  
SIGDEL = THEIDT-THETDF  
SYDDTT = (XEDDT*LYTGT+(35.-YEDDT)*DXTGT)/(DXTGT**2+DYTGT**2)  
SYDDTF = REALPL(0.0,10.0,SYDDT)  
SIGDAZ = SYDDT-SYDDTF
```

```
TARGET GLINT FACTOR WITH SHIP MOVING AT 21 KNOTS TO EAST  
YTR = GAUSS(5,0.0,20.0)  
XTR = GAUSS(3,0.0,6.0)  
XTI = XTI+XTR  
YTI = YTI+YTR  
HTI = HTI+HTR  
XTI2 = XTI  
YTI2 = YTI
```



```

HT = HTI
NOSCR T
CALL DEBUG(1,30.16)
CALL DEBUG(1,30.17)
CALL DEBUG(1,30.18)
CALL DEBUG(1,30.19)
CALL DEBUG(1,30.20)
CALL DEBUG(1,30.21)
CALL DEBUG(1,30.22)
CALL DEBUG(1,30.23)
CALL DEBUG(1,30.24)
CALL DEBUG(1,30.25)
CALL DEBUG(1,30.26)
TERMINAL
TIMMIN,RAGMIN,DXIGTM,DYIGTM,CZIGTM
OUTPUT MINUT=
LABEL MPLCT=
PAGE NPLCT=
TIMER FINTIM=31.00, OUTDEL=0.100, DELT=0.01525
OUTPUT TIME,PI(-200.0,200.0),PCMD(-200.0,200.0)
LABEL RCLLGT
PAGE XYFLGT
OUTPUT XYTIME,PHI1(-180.0,180.0),PHICMD(-180.0,180.0)
LABEL BANK
PAGE XYFLGT
OUTPUT XYTIME,RANGE(-4000.0,28000.0),XRange(-4000.0,28000.0),...
YRange(-4000.0,28000.0),ZRange(-40.0,280.0)
LABEL RANGE
PAGE XYFLGT
OUTPUT XYTIME,(29.5,30.5),RANGE(0.0,800.0),XRange(0.0,80.0),...
YRange(0.0,80.0),ZRange(0.0,80.0)
LABEL RANGE
PAGE XYFLGT
OUTPUT XYTIME,XMISLE(0.0,32000.0),XTGT(0.0,32000.0)
LE AND TARGET X COORDINATE (FEET) VS TIME
PAGE XYFLGT
OUTPUT XYTIME,MISLE(-400.0,2800.0),YGT(-400.0,2800.0),YECM(-400.0,2800.0)
LE AND TARGET Y COORDINATE (FEET) VS TIME
PAGE XYFLGT
OUTPUT XYTIME,HMISLE(-40.0,280.0),HTGT(-40.0,280.0),HECM(-40.0,280.0)
LE AND TARGET ALTITUDE (FEET) VS TIME
PAGE XYFLGT
OUTPUT XYTIME,L1STAB(-20.0,20.0),R1STAB(-20.0,20.0)
LE AND TARGET STABILIZERS (DEGREES) VS TIME
PAGE XYFLGT
OUTPUT XYTIME,RUDDER(-20.0,20.0)
LE AND TARGET RUDDER POSITION (DEGREES) VS TIME
PAGE XYFLGT

```

```

THE04330
THE04340
THE04350
THE04360
THE04370
THE04380
THE04390
THE04400
THE04410
THE04420
THE04430
THE04440
THE04450
THE04460
THE04470
THE04480
THE04490
THE04500
THE04510
THE04520
THE04530
THE04540
THE04550
THE04560
THE04570
THE04580
THE04590
THE04600
THE04610
THE04620
THE04630
THE04640
THE04650
THE04660
THE04670
THE04680
THE04690
THE04700
THE04710
THE04720
THE04730
THE04740
THE04750
THE04760
THE04770
THE04780
THE04790
THE04800

```

*

```

THE04810
THE04820
THE04830
THE04840
THE04850
THE04860
THE04870
THE04880
THE04890
THE04900
THE04910
THE04920
THE04930
THE04940
THE04950

```

```

*****
OUTPUT TIME,NZ(-3.,5.),NZ1CMD(-3.,5.)
LABEL VERTICAL ACCELERATION (G'S) VS TIME
PAGE XYFLOT
OUTPUT TIME,NY(-2.,2.),NY1CMD(-2.,2.)
LABEL HORIZONTAL ACCELERATION (G'S) VS TIME
PAGE XYFLOT
OUTPUT TIME,ELLCSR,AZLGSR
LABEL SEEKER EARTH LINE OF SIGHT RATES (DEG/SEC) VS TIME
PAGE XYFLOT
OUTPUT TIME,21000.,25000.,YMISLE(0.,2000.),HMISLE(0.,800.)
LABEL MAP OF YMISLE AND HMISLE VS XMISLE (FEET)
PAGE XYFLOT
END
STOP
ENDJCB

```


LIST OF REFERENCES

1. Gonzalez, J., New Methods in the Terminal Guidance and Control of Tactical Missiles, AGARD Lecture Series No. 101, 1979.
2. Hewett, M.D., Guidance and Control Systems Course (Class Notes), 1982.
3. Hoisington, D.B., Introduction to Electronic Warfare Notes, 1980.
4. Speclchart, F.H., and Green, W.L., A Guide to Using CSMP-The Continuous System Modeling Program, Prentice-Hall, 1976.

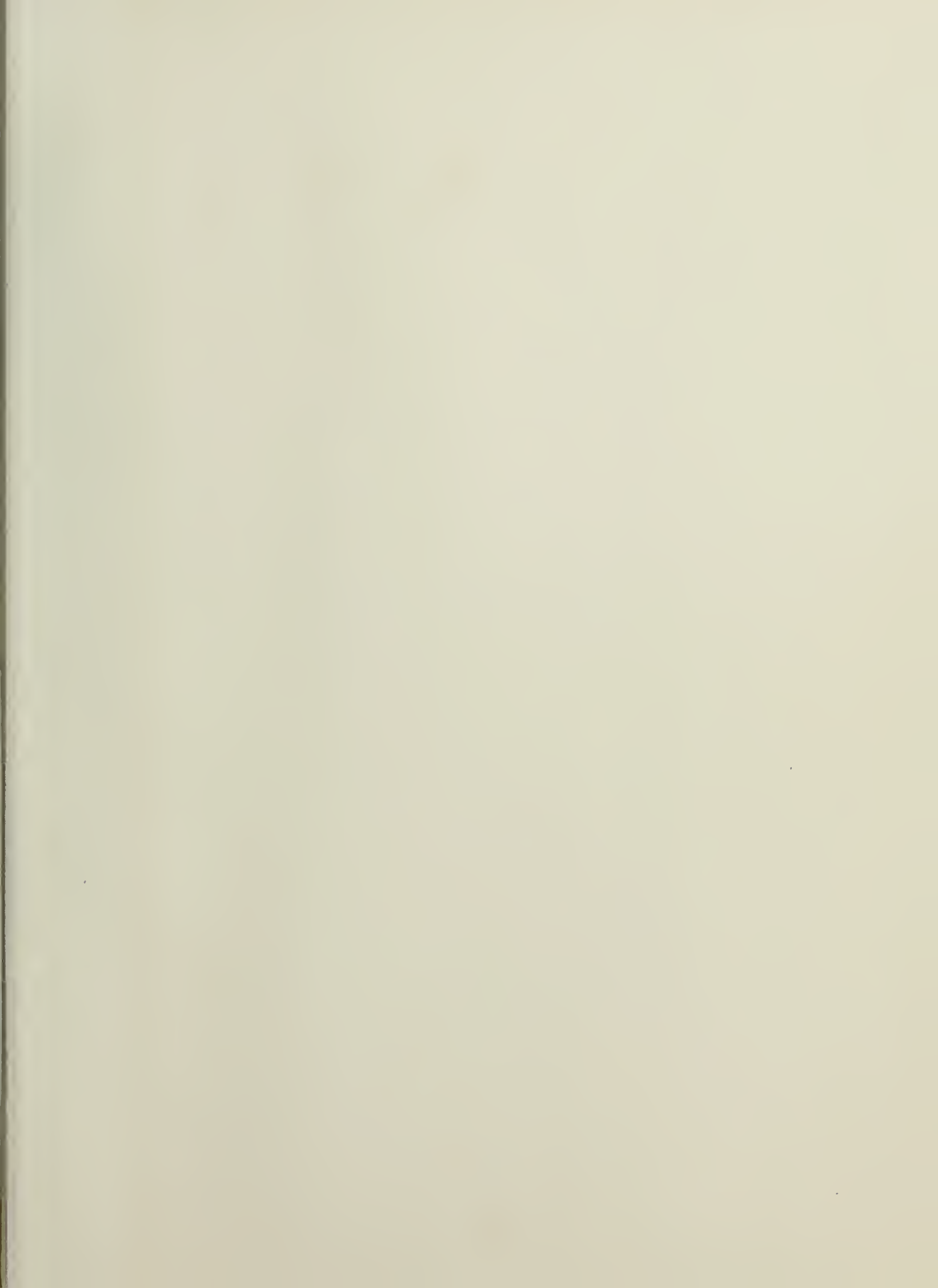
INITIAL DISTRIBUTION LIST

No. Copies

1. Library, Code 0142 2
Naval Postgraduate School
Monterey, California 93940
2. Department Chairman, Code 62 1
Department of Electrical Engineering
Naval Postgraduate School
Monterey, California 93940
3. Professor M.D. Hewett, Code 67Hj 5
Department of Aeronautics
Naval Postgraduate School
Monterey, California 93940
4. Professor H. A. Titus, Code 62Ts 1
Department of Electrical Engineering
Naval Postgraduate School
Monterey, California 93940
5. Professor G. Thaler, Code 62Tr 1
Department of Electrical Engineering
Naval Postgraduate School
Monterey, California 93940
6. Director 1
Attention: CDR Richard Fessenden
JCM 531
Joint Cruise Missile Programs
Bldg. NC-1
Washington, D.C. 20360
7. Professor D. J. Collins, Code 67Co 1
Department of Aeronautics
Naval Postgraduate School
Monterey, California 93940
8. LCDR Kent B. Watterson 5
Naval Sea Systems Command (SEA-62Y1F)
Department of the Navy
Washington, D.C. 20362
9. LT Daniel A. Forkel 1
Naval Postgraduate School
SMC 2088
Monterey, California 93940

10. Defense Technical Information Center
Cameron Station
Alexandria, Virginia 22314

2



201745

Thesis

W2825

Watterson

c.1

Bank-to-turn cruise
missile terminal guid-
ance and control law
comparison.

thesW2825

Bank-to-turn cruise missile terminal gui



3 2768 000 99489 1

DUDLEY KNOX LIBRARY